NOVEL PROPERTIES OF HNRNP-UL1: ITS POSSIBLE ROLE IN THE PATHOGENESIS OF ALS.

By

KENNY MATTHEW PRATT

A thesis submitted to the

University of Birmingham

for the degree of

DOCTOR OF PHILOSOPHY

Institute of Cancer and Genomic Sciences

The Medical School

University of Birmingham

October 2015

ABSTRACT

Heterogeneous nuclear ribonucleoprotein-U like 1 (hnRNP-UL1) is a protein with numerous roles within the cell, including RNA processing and responses to DNA damage. Within this study two novel aspects of the protein are explored: the role of a putative nucleotide-binding domain and the protein's possible involvement in amyotrophic lateral sclerosis (ALS).

hnRNP-UL1 is known to have a putative nucleotide-binding domain within its central region containing both a Walker A and Walker B motif. This region had not been investigated previously and was therefore of great interest in this study. The Walker A motif was shown to bind adenosine triphosphate (ATP) and the region appears to possess protein kinase activity. A biological substrate and function for these activities were not established, but these observations suggest that there are still layers of complexity to hnRNP-UL1's cellular roles to be elucidated.

ALS is a late-onset neurodegenerative disease with limited treatment strategies and poor patient outcomes. Many of the proteins involved in its pathogenesis have two properties in common: they have roles in RNA-processing and possess prion-like domains (PrLDs). The properties of hnRNP-UL1 appertain to both of these and therefore it was of great interest when ALS patients were discovered with heterozygous hnRNP-UL1 mutations. Results showed that cells possessing the ALS patient mutations (R639C and R468C) had no DNA damage response (DDR) defects or mislocalisation of the protein, but their ssDNA/RNA-binding capability was markedly reduced. Whilst no direct causative links to ALS pathogenesis were shown with the hnRNP-UL1 patient mutations in this study, growing evidence implies good reason for the protein to have involvement in the disease.

ACKNOWLEDGEMENTS

I am extremely grateful to my supervisor, Roger, for his continued help and advice in all aspects of the work I have undertaken as part of my PhD. He is responsible for me coming to Birmingham to pursue working in science and I am very glad to have completed my research under his experienced and nurturing tutorage.

There are also many other members of staff that I would like to thank for their help and friendship. Andy provided good advice and guidance on the project, as well as daily sport-related chats. I am also thankful to Grant for his advice and knowledge, plus reagents and equipment. I must thank Elizabeth, Sally, Ruth, Helen, Kirsty, Alex, Tom, John, Martin, Phil and Rob for help along the way, and particularly Ruth and Elizabeth for technical help with certain procedures. I also thank the whole IBR 1st floor who are a great bunch of people and it is a welcoming and friendly place to work.

I am also thankful for the financial support given to me by the University of Birmingham Medical School and the Medical Research Council.

Finally, I would like to thank every single member of my family for supporting me from when I was young right up until this point, especially my Ma and Pa. I started my own family whilst doing this PhD and nothing has kept me happier during this time in my life than my wife Hannah and son Henry. Coming home to play with Henry helped to relieve stress and put in to perspective a failed experiment. Finally, thank you Hannah for all the love, commitment and sacrifices made in the past four years.

TABLE OF CONTENTS

I INTRODUCTION 1

1.1 The DNA molecule 2

1.2 The DNA damage response (DDR) 4

1.2.1 Single strand break (SSB) repair 8

1.2.2 Base excision repair (BER) 10

1.2.3 Nucleotide excision repair (NER) 11

1.2.4 Non-homologous end joining (NHEJ) 11

1.2.5 Homologous recombination (HR) 13

1.2.6 Diseases associated with malfunction of the DDR 16

1.3 Heteronuclear ribonucleoproteins (hnRNPs) 24

1.3.1 hnRNPs 24

1.3.2 hnRNP-UL1 26

1.3.3 hnRNPs in the DDR 30

1.3.4 hnRNP-UL1 in the DDR 33

1.3.5 hnRNP-UL1's Walker A motif and activity of PNKP 36

1.4 Amyotrophic lateral sclerosis (ALS) 42

1.4.1 ALS aetiology and pathogenesis 43

1.4.2 RNA processing and ALS 49

1.4.3 Prion-like domain (PrLD) proteins and ALS 53

1.4.4 ALS and the DDR 57

1.5 Aims 62

II MATERIALS AND METHODS 63

2.1 Cell biology techniques 64

2.1.1 Cell lines 64

2.1.2 Cell culture media 64
2.1.3 Maintenance and passage of cell lines 64
2.1.4 Cryopreservation of cell lines 65
2.1.5 IR and UV irradiation 65
2.1.6 Drug treatments 66
2.1.6.1 Camptothecin 66
2.1.6.2 Kinase inhibitors 66
2.1.6.3 Tert-butylhydroquinone 67
2.1.7 RNA interference (RNAi) 67
2.1.8 Transfection of plasmid DNA 68
2.2 Molecular biology techniques 69
2.2.1 Preparation of media and plates 69
2.2.2 Bacterial transformations 69
2.2.3 Large scale preparation of DNA plasmids 70
2.2.4 Agarose gel electrophoresis 71
2.2.5 Site-directed mutagenesis PCR 72
2.2.6 DNA sequencing 73
2.2.7 Cloning 74
2.3 Protein and DNA biochemistry techniques 75
2.3.1 Preparation of total cell lysates 75
2.3.2 Preparation of lysates from cells for co-immunoprecipitation 76
2.3.3 Determination of protein concentration 76
2.3.4 SDS-polyacrylamide gel electrophoresis (SDS-PAGE) 76
2.3.5 Urea-polyacrylamide gel electrophoresis (Urea-PAGE) 77
2.3.6 Visualisation of protein on nitrocellulose membranes 77
2.3.7 Detection of radioactively labelled protein and DNA by autoradiography 78

2.3.8 ^{32}Phosphorous radioactive assays 78
2.3.8.1 *α-^{32}P-ATP binding assay* 78
2.3.8.2 γ-^{32}P-ATP kinase assay 79
2.3.9 Preparation of samples for mass spectrometry 80
2.3.10 ssDNA-binding assays 81
2.3.11 ssRNA-binding assays 81
2.4 Immunochemistry techniques 82
2.4.1 Antibodies 82
2.4.2 Co-immunoprecipitation 84
2.4.3 Western blotting 84
2.4.4 Immunofluorescence microscopy 85
III HNRNP-UL1 AS A KINASE 86
3.1 Introduction 87
3.2 Results 88
3.2.1 hnRNP-UL1 shares significant homology to PNKP 88
3.2.2 ATP-binding by hnRNP-UL1 91
3.2.3 hnRNP-UL1 shows no activity as a DNA kinase 91
3.2.4 hnRNP-UL1 shows activity as a protein kinase 94
3.2.5 hnRNP-U and –UL2 ATP-binding and kinase activity 97
3.2.6 Validation of hnRNP-UL1 kinase activity by use of kinase inhibitors 97
3.3 Discussion 104
IV HNRNP-UL1 AND ALS 109
4.1 Introduction 110
4.2 Results 111
4.2.1 ALS patient mutations 111
4.2.2 Protein expression levels are not affected by mutations 111

4.2.3 The DNA damage response was unaffected in ALS LCLs 114
4.2.4 Localisation of hnRNP-UL1 is unaffected by the mutations present in the ALS patient cells 114
4.2.5 Mutant hnRNP-UL1 proteins R639C and R468C do not induce oxidative stress 118
4.3 Discussion 121
V PROFILING THE HNRNP-UL1 MUTATIONS 127
5.1 Introduction 128
5.2 Results 129
5.2.1 The Walker A mutant does not bind ATP and lacks protein kinase activity .. 129
5.2.2 The R639C and R468C mutants exhibit normal ATP-binding and kinase activity 129
5.2.3 Single stranded DNA-binding deficiencies of mutants 133
5.2.4 Single stranded RNA-binding deficiencies of mutants 133
5.2.5 The DNA damage response of the mutants 139
5.2.6 Protein interactions of the mutants with XRCC1, NBS1 and PARP-1 143
5.3 Discussion 148
VI FINAL DISCUSSION AND FUTURE WORK 157
6.1 Nucleotide-binding of hnRNP-UL1 158
6.2 Kinase acitivity of hnRNP-UL1 160
6.2 ALS and hnRNP-UL1 163
6.3 The role of hnRNP-UL1 in early response to DNA damage 170
VII REFERENCES 177

LIST OF FIGURES

Figure 1.1 Schematic of anti-parallel pairing between complementary DNA strands 3

Figure 1.2 DNA damage and the methods of repair 5

Figure 1.3 The cell cycle checkpoints 7

Figure 1.4 Model for the core NER reaction 12

Figure 1.5 The early responses to DSBs resulting in the highly hierarchical assembly of IRIF 15

Figure 1.6 The DNA formations and processing during DSB repair by HR..... 17

Figure 1.7 Structure of hnRNP-UL1 and -UL2 and their domains 27

Figure 1.8 Crystal structure of yeast adenylate kinase (pale green) bound to the ATP-mimic, bi-substrate inhibitor bis(adenosine)-5'-pentaphosphate (Ap5A), and Mg^{2+} at 1.96A° resolution 37

Figure 1.9 Ribbon diagram of mouse PNKP 39

Figure 1.10 The mouse PNKP active site cleft permitting ATP and DNA binding..... 41

Figure 1.11 Overview of events in the pathogenesis of amyotrophic lateral sclerosis ... 44

Figure 1.12 RNA dysfunction in ALS 52

Figure 1.13 PrLD assessment of hnRNP-UL1, -U and –UL2 using PLAAC 58-59

Figure 3.1 Sequence comparison of human hnRNP-U, -UL1, -UL2, PNKP and *drosophila* hnRNP-UL1 89

Figure 3.2 A secondary structure prediction of human hnRNP-UL1 based on the known structure of mouse PNKP 90

Figure 3.3 hnRNP-UL1 binds ATP 92

Figure 3.4 hnRNP-UL1 does not exhibit activity as a DNA kinase..... 93

Figure 3.5 hnRNP-UL1 possesses activity as a protein kinase 95-96

Figure 3.6 hnRNP-UL2 and hnRNP-U fail to bind ATP, but when immunoprecipitated exhibit protein kinase activity 98

Figure 3.7 An interaction network for hnRNP-UL1 based on mass spectrometry data following co-immunoprecipitation 99
Figure 3.8 Phosphorylation of the MBP and PLC substrates is not due to the presence of PI3Ks 100
Figure 3.9 hnRNP-UL1 co-immunoprecipitates with p70S6K, although the observed phosphorylation is probably not due to p70S6K 102-103
Figure 4.1 The expression levels of hnRNP-UL1, hnRNP-UL2 and TDP43 are normal in all the patient LCLs 113
Figure 4.2 ALS patient cell lines exhibited no significant differences in their DDR to ionizing radiation (IR) compared to non-patient controls 115
Figure 4.3 ALS patient cell lines exhibited no significant differences in their DDR to camptothecin (CPT) treatment compared to non-patient controls 116
Figure 4.4 Localisation of hnRNPUL1 is unaffected by the mutations present in the ALS patient cells 117
Figure 4.5 Localisation of hnRNP-UL1 is unaffected by the mutations present in the ALS patient cells 119
Figure 4.6 Expression of the ALS patient proteins harbouring the mutations R639C and R468C causes no increase in oxidative stress 120
Figure 5.1 The Walker A mutant (MWA) does not bind ATP 130
Figure 5.2 The Walker A mutant (MWA) has reduced kinase activity 131
Figure 5.3 WT-WT and WT-MWA hnRNP-UL1 proteins homerdimerize 132
Figure 5.4 Binding of ATP by the hnRNP-UL1 mutants 134
Figure 5.5 The R639C and R468C mutants exhibit kinase activity 135
Figure 5.6 Reduced ssDNA-binding of hnRNP-UL1 mutants 136
Figure 5.7 Reduced ssRNA-binding of hnRNP-UL1 mutants 137-138
Figure 5.8 Wild-type and mutant proteins restore DDR defects seen in response to IR

after knockdown of endogenous hnRNP-UL1 140
Figure 5.9 Wild-type and mutant proteins restore DDR defects seen in response to CPT after knockdown of endogenous hnRNP-UL1 141
Figure 5.10 Wild-type and mutant proteins restore DDR defects seen in response to UV after knockdown of endogenous hnRNP-UL1 142
Figure 5.11 γH2AX foci form normally in response to IR in hnRNP-UL1 depleted cells and in cells expressing the various mutated forms 144
Figure 5.12 53BP1 foci are cleared at a normal rate in hnRNP-UL1 depleted cells and in cells expressing the various mutated forms 145
Figure 5.13 5.13 hnRNP-UL1 variants restored pRPA foci following endogenous protein depletion. 146
Figure 5.14 Interaction with XRCC1 is unaffected with mutant hnRNP-UL1 protein 147
Figure 5.15 Binding of NBS1 is unaffected with mutant hnRNP-UL1 proteins 149
Figure 5.16 Interaction with PARP-1 is affected with the Walker A mutant but not the ALS variants 150
Figure 6.1 The effect of the hnRNP-UL1 patient mutations on potential steric zipper formation 166

LIST OF TABLES

Table 1.1 Selected human genetic diseases associated with DDR defects 19-20

Table 2.1 Cell lines used in this study..... 64

Table 2.2 Kinase inhibitors used in kinase assays 66-67

Table 2.3 siRNAs used in this study 67-68

Table 2.4 Plasmids used in this study 70-71

Table 2.5 Primer sequences used to generate mutated forms of HA-hnRNPUL1 72

Table 2.6 Cloning primers used in this study..... 74

Table 2.7 DNA substrates used for γ-^{32}P-ATP kinase assay..... 80

Table 2.8 Primary antibodies used in this study..... 82-83

Table 2.9 Secondary antibodies used in this study..... 83

Table 4.1 Details of the patient derived lymphoblastoid cell lines 112

ABBREVIATIONS

53BP1	p53-binding protein 1
9-1-1	Rad9-Hus1-Rad1
A	adenine
AD	Alzheimer's disease
ADP	adenosine diphosphate
AOA1	ataxia with oculomotor apraxin 1
AOA2	ataxia with oculomotor apraxin 2
APE1	apurinic-apyrimidinic endonuclease 1
APS	ammonium persulphate
APTX	aprataxin
AT	ataxia telangiectasia
ATLD	ataxia telangiectasia-like disorder
ATM	ataxia telangiectasia mutated
ATP	adenosine triphosphate
ATR	ATM and Rad3-related
ATRIP	ATR-interacting protein
Bdnf	brain derived neurotrophic factor
BER	base excision repair
BLM	Bloom syndrome protein
BRCA1	breast cancer susceptibility gene 1
BRCT1	BRCA1 C-terminus
BRD7	bromodomain-containing protein 7
BSA	bovine serum albumin
C	cytosine
C9ORF72	chromosome 9 open reading frame 72
C-terminal	carboxy-terminal
CDK	cyclin-dependent kinase
Chk1	checkpoint kinase 1
Chk2	checkpoint kinase 2
CIN	chromosomal instability
CJD	Creutzfeldt-Jakob disease
COFS	cerebro-oculo-facio-skeletal syndrome
co-IP	co-immunoprecipitation
CPT	camptothecin
Cs	caesium
CS	Cockayne syndrome
CSA	Cockayne syndrome group A protein
CSB	Cockayne syndrome group B protein
CSF	cerebrospinal fluid
CtIP	CtBP-interacting protein

DAPI	4’,6-diamidino-2-phenylindole
DDR	DNA damage response
DDSR1	DNA damage-sensitive RNA1
DMEM	Dulbecco’s modified Eagle’s medium
DMSO	dimethyl sulphoxide
DNA	deoxyribonucleic acid
DNA-PK	DNA-dependent kinase
DNA-PKcs	DNA-PK catalytic subunit
DLSM	digital light-sheet microscopy
dNTP	deoxynucleotide triphosphate
DSB	double strand break
dsDNA	double strand DNA
DTT	dithiothretiol
E1B-55K	early region 1B 55-kDa protein
E1B-AP5	E1B-55K-associated protein 5
EDTA	ethylenediaminetetraacetic acid
EWSR1	Ewing sarcoma breakpoint region 1
FA	Fanconi anaemia
fALS	familial ALS
FCS	foetal calf serum
FHA	forkhead-associated
FTD	frontotemporal dementia
FUS	fused in sarcoma
g	gravitational force
G	guanine
GG-NER	global genomic-NER
GST	glutathione S-transferase
GTP	guanosine triphosphate
H2AX	histone 2A family member X
H_2O_2	hydrogen peroxide
HA	hemagglutinin
HDAC	histone deacetylase
HJ	Holliday junction
HNPCC	hereditary nonpolyposis colorectal cancer
hnRNP	heteronuclear ribonucleoprotein
hnRNP-UL1	heteronuclear ribonucleoprotein U-like 1
hnRNP-UL2	heteronuclear ribonucleoprotein U-like 2
HR	homologous recombination
ID	intellectual disability
IF	immunofluorescence
IgG	immunoglobulin G
IP	immunoprecipitation

IR	ionizing radiation
IRIF	Ionising Radiation-Induced Foci
JNK	c-Jun N-terminal kinase
K	kilodalton
kDa	kilodalton
Keap1	Kelch-like ECH-associated protein 1
LB	Luria broth
LCL	lymphoblastoid cell line
LF	lipofectamine
LIG	ligase
LMN	lower motor neuron
lncRNA	long non-coding RNA
MBP	myelin basic protein
MCM	minichromosome maintenance
MDC1	mediator of DNA damage checkpoint protein 1
min	minute
miRNA	microRNA
MMR	mismatch repair
MRE11	meiotic recombination 11
MRN	MRE11-Rad50-NBS1
mRNA	messenger RNA
mtDNA	mitochondrial DNA
mTOR	mammalian target of rapamycin
MWA	mutated Walker A
N-terminal	amino-terminal
NBS	Nijmegen breakage syndrome
NBSLD	NBS-like disorder
NER	nucleotide excision repair
NHEJ	non-homologous end-joining
NK	nucleotide kinase
NLS	nuclear localisation signal
Nrf2	nuclear erythroid 2-related factor 2
NTP	nucleotide triphosphate
OF	oligofectamine
OPTN	optineurin
p	phosphorylated
P	phosphate
p70S6K	ribosomal protein S6 kinase
PAGE	polyacrylamide gel electrophoresis
PAR	poly(ADP-ribose)
PARP-1	poly(ADP-ribose) polymerase 1
PBS	phosphate-buffered saline

PCNT	proliferating cell nuclear antigen
PCR	polymerase chain reaction
PD	Parkinson's disease
PFA	paraformaldehyde
PI3K	phosphatidylinositol 3-kinase-like kinase
PIAS	protein inhibitor of activated STAT
PLC	myosin phosphorylatable light chain
PLK1	polo-like kinase 1
PNKP	polynucleotide kinase phosphatase
pol	polymerase
PP	proline-rich region
PrLD	prion-like domain
PRMT1	protein arginine methyl transferase 1
Rad	radiation sensitivity gene
RAG1	recombination activating gene 1
RAG2	recombination activating gene 2
RAN	repeat associated non-AUG translation
RGG	Arg-Gly-Gly
RNA	ribonucleic acid
RNAi	RNA interference
RNF8	RING-finger 8
RNF168	RING-finger 168
RNP	ribonucleoprotein
ROS	reactive oxygen species
RPA	replication protein A
RPMI	Roswell Park Memorial Institute
RT	room temperature
S6K	ribosomal protein S6 kinase
SAF	scaffold attachment factor
sALS	sporadic ALS
SAP	SAF-A/B, Acinus and PIAS
SCID	severe combined immunodeficiency
SDS	sodium dodecyl sulphate
sec	second
SETX	senataxin
siRES	siRNA resistant
SOD1	superoxide dismutase 1
SPRY	spore lysis A/ryanodine receptor
SS	Seckel syndrome
SSB	single strand break
SSBR	single strand break repair
ssDNA	single stranded DNA

SV40	simian virus 40
TAF15	TATA-box binding protein-associated factor 15
T	thymine
TBHQ	*tert*-butylhydroquinone
TBE	Tris-borate-EDTA
TBS	Tris-buffered saline
TBST	TBS containing Tween 20
TC-NER	transcription-coupled NER
TDP1	tyrosyl-DNA phosphodiesterase 1
TDP43/TARDBP	transactive response element DNA/RNA binding protein of 43 kDa
TEMED	N, N, N', N'-Tetramethylethylenediamine
TOPBP1	topoisomerase-binding protein 1
TRIM5α	tripartite motif-containing protein 5
Tris	trishydroxymethylaminomethane
TTD	trichotiodystrophy
UBQLN2	ubiquilin 2
UMN	upper motor neuron
UV	ultraviolet
VCP	vasolin-containing protein
V(D)J	variable (diversity) joining
WB	western blot
WRN	Werner protein
WS	Werner syndrome
WT	wild-type
XAB2	XPA binding protein 2
XLF	XRCC4-like factor
XP	xeroderma pigmentosum
XPA	xeroderma pigmentosum group A protein
XPC	xeroderma pigmentosum group C protein
XRCC	x-ray repair cross-complemetary protein

CHAPTER I

INTRODUCTION

1.1 The DNA molecule

Deoxyribonucleic acid (DNA) lies at the heart of the central dogma of molecular biology. Its genetic instructions allow the co-ordination of cellular life in virtually all organisms. To comprehend how it is damaged and subsequently repaired within the cell, the structure of the macromolecule must firstly be understood. DNA is a polymer of a subunit known as a nucleotide, each of which contain a five-carbon sugar residue (deoxyribose), a phosphate group and an aromatic nitrogenous base. Alternating sugar and phosphate residues form the backbone of the DNA polymer and are linked by phosphodiester bonds between the 3' carbon atom of one deoxyribose and the 5' carbon atom of the next adjacent deoxyribose (Figure 1.1). Four different bases [guanine (G), cytosine (C), adenine (A), and thymine (T)] can be covalently linked by a β-N-glycosidic bond to the first carbon atom of the deoxyribose residue. T and C are aromatic compounds known as pyrimidines, whilst A and G are purines with an additional imidazole ring.

Watson and Crick first described the double helix structure which DNA commonly forms *in vivo* in 1953 (Watson and Crick, 1953). The complementary base-pairing of A to T and G and C (via hydrogen bonds) allows two DNA polymers (strands) to lie anti-parallel to one another. The two strands curl within the helix structure around a central axis and form a major groove and a minor groove. The larger space within the major groove means the bases are more accessible and permits interaction with DNA-binding proteins.

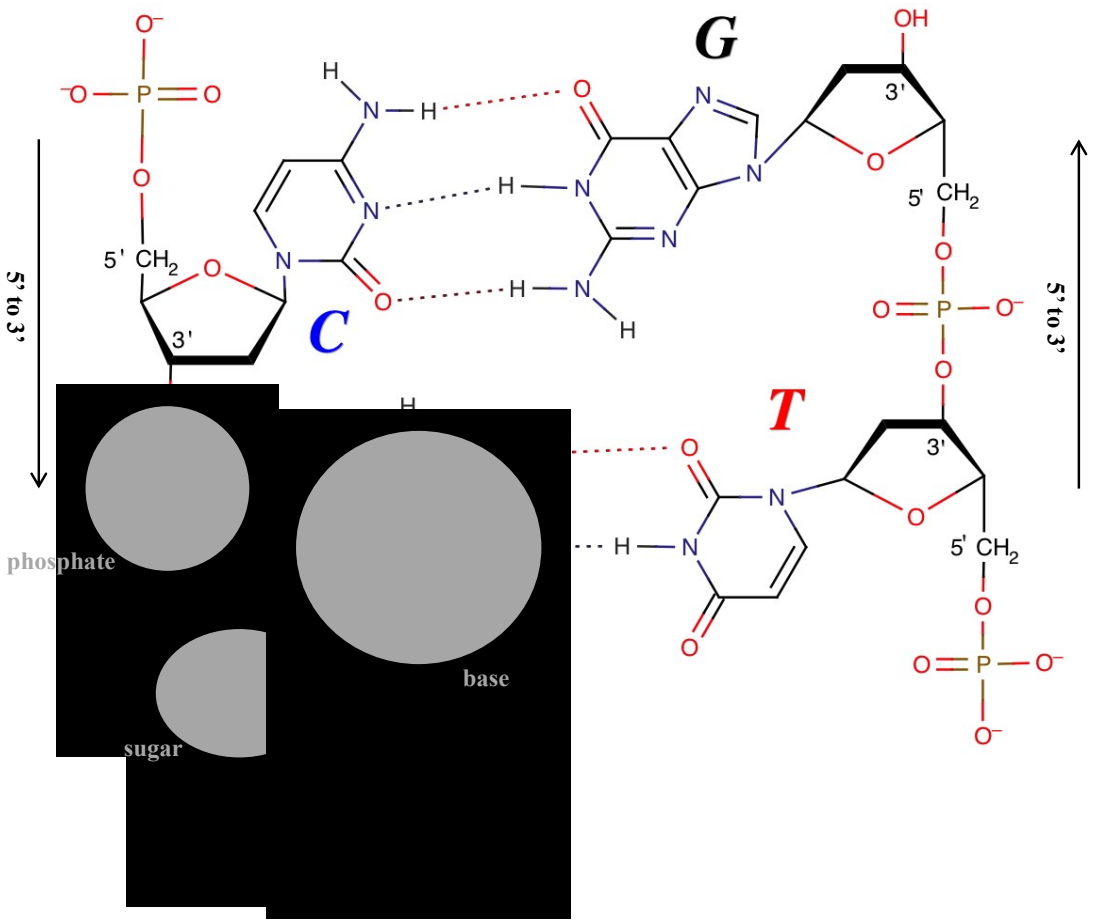

Figure 1.1 Schematic of anti-parallel pairing between complementary DNA strands. The nitrogenous bases cytosine (C), guanine (G), thymine (T) and adenine (A) are shown. The phosphate group, deoxyribose and base of one nucleotide are indicated. 5' phosphate and 3' hydroxyl groups are also indicated.

1.2 The DNA damage response (DDR)

The primary objective for every life form is to pass on information through its genetic code, which should remain intact and unaltered, to the next generation. Each of the human body's ~10^{13} cells must combat tens of thousands of DNA lesions every day and replicate its DNA accurately when division is necessary (Lindahl and Barnes, 2000). The means by which cells detect damage to their DNA and initiate repair is collectively known as the cellular DNA damage response (DDR). This term encompasses a number of different pathways which, generally speaking, are designed to deal with specific forms of damage, which tend to be caused by different agents.

The agents that cause damage to DNA derive from both endogenous and exogenous sources. There are many different types, including reactive oxygen species, ionising and ultraviolet radiation, replicative stress, infectious pathogens and inflammation that can cause various types of DNA lesions (Figure 1.2). For cells to counter the continual attack on their DNA they have evolved a complex set of DNA detection and repair systems. Given their importance and links with so many diseases (explored in section *1.2.6*) it is unsurprising that so much research is focussed within this area.

Cell cycle and the DDR

Before describing the details of the various DDR pathways it is important to consider the wider cellular processes affected during the response to DNA damage, and in particular, cell cycle regulation. Cell cycle regulation is critical to maintain the required proliferation rate of any particular cell, and the mammalian cell has evolved a series of checkpoints to ensure the integrity of the DNA and accurate replication from mother to daughter cells during division.

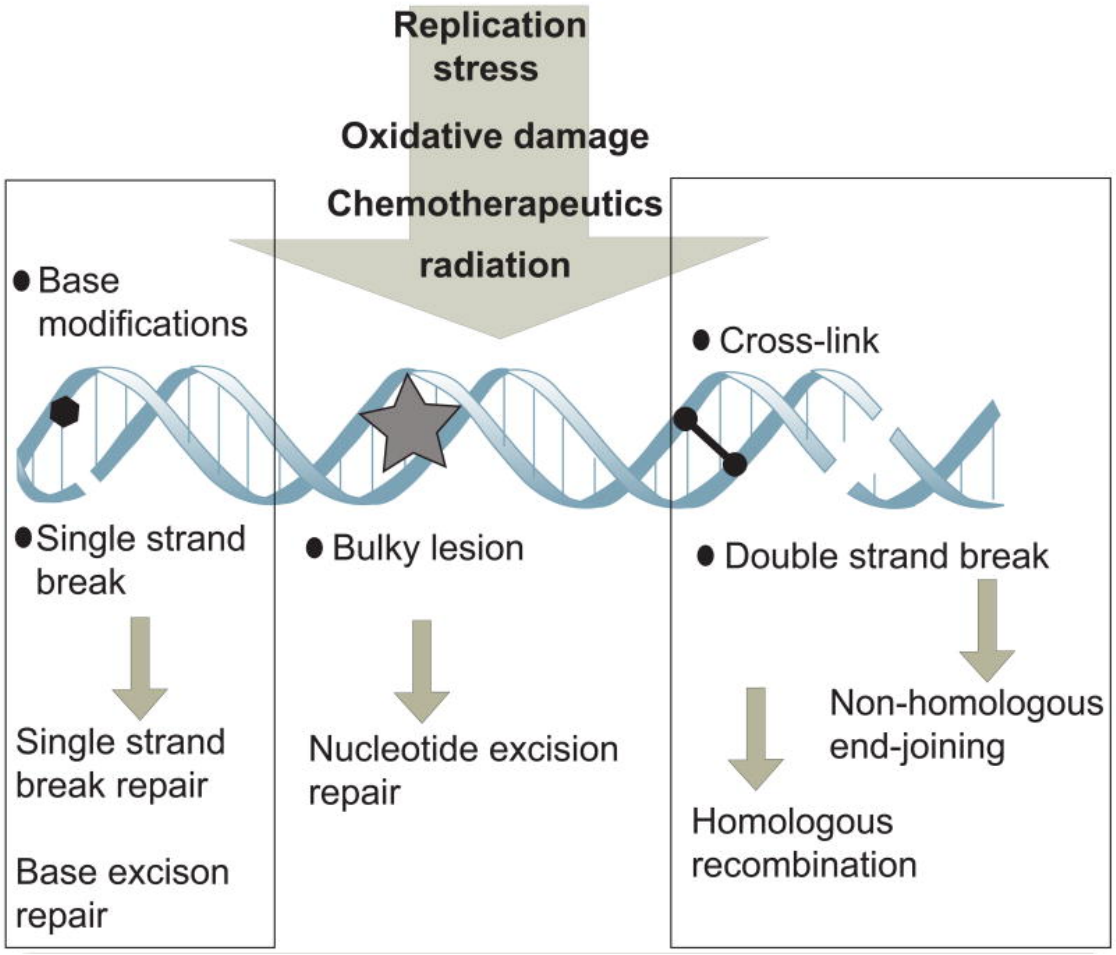

Figure 1.2 DNA damage and the methods of repair. Various endogenous (replication stress and oxidative damage) and exogenous (chemotherapeutic agents and radiation) can cause different types of DNA lesions. These include single-strand breaks (SSBs), double-strand breaks (DSBs), base modifications, bulky adducts and crosslinks of the DNA strands. Differing and specific DNA repair pathways are employed to correct each type of damage. (Adapted from McKinnon, 2009).

The most significant DDR-signalling enzymes in mammalian cells are the PI3K (phosphatidylinositol 3 kinase) proteins; ATM (ataxia telangiectasia), ATR (ataxia telangiectasia and RAD3-related) and DNA-PK (DNA-dependent protein kinase). Once activated, they have the potential to phosphorylate hundreds of substrates with a preference for serine and threonine residues that are followed by glutamines (S/TQ) (Nam and Cortez, 2011). Their activation can trigger activities such as cell cycle inhibition, DNA repair or apoptosis, depending on the severity of the DNA damage. Two main targets of ATM and ATR for phosphorylation are Chk2 and Chk1 in response to DSBs and single-strand breaks (SSBs), respectively. These proteins collectively act to reduce activity of cyclin-dependent kinases (CDKs), which along with cyclins are the principle drivers of the cell cycle. Chk2 and Chk1 mediate this through the inhibition of Cdc25 family members, which drive cell cycle progression by removing inhibitory phosphates on CDK/cyclin complexes (e.g. Tyr15 on CDK 1 and 2). Chk1 also activates the kinase, Wee1, which is responsible for phosphorylating the Tyr15 residue (Reinhardt and Yaffe, 2009).

Arresting the progression of the cell cycle at either the G1-S, intra-S, or G2-M cell-cycle checkpoints is critical in allowing the DDR pathways time to repair lesions before replication or mitosis (Figure 1.3) (Jackson and Bartek, 2009). Activation of the G1 checkpoint prevents progression to S phase before replication begins, to ensure DNA damage is repaired. If damage has occurred during replication in S phase or replication is incomplete, the intra-S and G2 checkpoints are activated prior to cell division. The final checkpoint in M phase (mitosis) is activated in response to misalignment of sister chromatids on the mitotic spindle (Cooper, 2006).

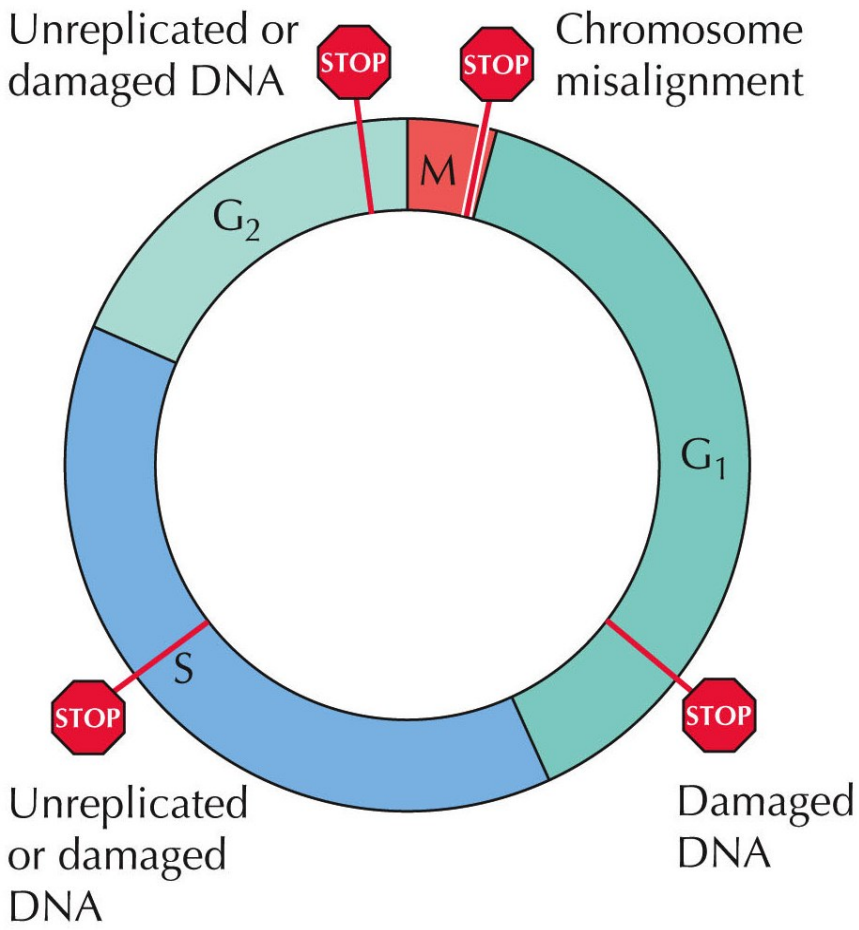

Figure 1.3 The cell cycle checkpoints. To ensure the genetic material is intact before progression through to the next phase of the cell cycle several checkpoints exist. The G1 checkpoint is activated if DNA damage is identified. If damage has occurred during replication in S phase or replication is incomplete, the intra-S and G2 checkpoints are activated prior to cell division. The final checkpoint in M phase (mitosis) is activated in response to misalignment of sister chromosomes on the mitotic spindle (Cooper, 2006).

DNA damage repair

As well as cell cycle inhibition, ATM/ATR signalling induces repair of DNA damage by recruitment of repair factors to sites of damage. These signalling pathways are explored in greater detail in the following sections. If DNA repair is successful, the DDR is inactivated and the cell cycle begins to proceed once again. However, if the damage is too great to repair, death of the cell via apoptosis, mitotic catastrophe or autophagy can be triggered. Evolution has considered the death of a single cell in response to significant unrepaired DNA damage as a reasonable solution because continued cycles of replication increase the risk of greater genetic instability and subsequently carcinogenesis.

1.2.1 Single strand break (SSB) repair

Single strand DNA breaks (SSBs) are the most common form of DNA damage and are estimated to occur in tens of thousands per cell every day (Caldecott, 2008). SSBs arise from a number of types of DNA attack, including ultraviolet (UV) radiation, stalled replication forks and oxidation by reactive oxygen species (ROS) and subsequent disintegration of the deoxyribose sugar in the DNA molecule. The intermediate abasic site created during base excision repair (BER, see section *1.2.2*) is another source of SSBs, as is the abortive intermediates of TOP1 (DNA topoisomerase 1) activity during the relaxation of chromatin (Caldecott, 2008). Repair of SSBs follows a basic four step process: SSB detection, DNA end processing, DNA gap filling and DNA ligation. Detection is by PARP-1 (poly(ADP-ribose) polymerase 1), a key protein in response to nearly all DNA breaks. It is rapidly and transiently recruited to break sites, subsequently activated and poly(ADP)-ribosylates itself and a number of other proteins (Krishnakumar and Kraus, 2010). Perhaps the most important of its targets is

the scaffold protein XRCC1 (X-ray repair cross-complementing protein 1). This acts as an attachment, stabilisation and stimulation factor for a host of proteins involved in the SSBR process (Krishnakumar and Kraus, 2010). DNA end processing follows and involves the conversion of damaged ends back to the conventional 3'-hydroxyl and 5'-phosphate. This involves a number of proteins depending on the type of damage, including APE1 (apurinic–apyrimidinic endonuclease 1), TDP1 (tyrosyl-DNA phosphodiesterase 1), DNA polymerase (pol) β, APTX (aprataxin) and PNKP (polynucleotide kinase phosphatase), of which the latter three directly interact with XRCC1 (Caldecott, 2008). The majority of SSBs are repaired by base excision repair (BER) during which one nucleotide is removed during repair, often termed short-patch repair. Nucleotide excision repair (NER) requires the removal of a long-patch of nucleotides (24-32). Subsequently, gap filling by a DNA polymerase (typically β) and end ligation by a DNA ligase (typically LIG3 for short-patch and LIG1 for long-patch) occurs (Caldecott, 2008).

As already mentioned, the PI3K protein ATR, plays an important role in response to SSBs. It plays a vital role during S-phase when MCM helicase continues to unwind the DNA template after replication forks stall. This exposes long stretches of ssDNA, which is bound by replication protein A (RPA). Canonical ATR signalling involves recruitment of ATR to ssDNA-RPA sites via its partner ATRIP (ATR-interacting protein). The RAD9-HUS1-RAD1 (9-1-1) complex is independently recruited to these sites along with TOPBP1 (topoisomerase-binding protein 1), which activates ATR allowing phosphorylation of downstream targets, such as Chk1 (Nam and Cortez, 2011). ATR signalling occurs wherever ssDNA-RPA complexes form, including those resulting from resection of one strand during double strand break repair by homologous recombination (Nam and Cortez, 2011).

It is important to note that if SSBs cannot be dealt with efficiently, for example in the blockage of replication in proliferating cells, collapse can occur resulting in the formation of a double strand break (DSB) which are more deleterious to the cell (see sections *1.2.4* and *1.2.5*).

1.2.2 Base excision repair (BER)

Base excision repair (BER) deals with the small alterations to bases, such as 8-oxoguanine, formamidopyrimidines and 5-hydroxyuracil, caused mainly by endogenous mechanisms (Maynard et al., 2009). Oxidative respiration and lipid peroxidation generates thousands of reactive oxygen species (ROS) in each cell every day, which can produce oxidised DNA products (of which 8-oxoguanine is the most common), also seen in exposure to radiation (e.g. gamma rays, and alpha and beta particles) (Pecorino, 2008). The alterations do not interfere with replication or transcription but if left unrepaired will cause a point mutation.

DNA glycosylases check for lesions at a rate of millions of base pairs per second. Upon finding one, they dissociate the lesion from the DNA-helix by cleavage of the N-glycosyl bond linking the sugar and the base creating an abasic site. An endonuclease then cleaves the DNA strand at the abasic site, DNA polymerase β replaces the nucleotide and a ligase ligates the DNA ends back together (Pecorino, 2008).

1.2.3 Nucleotide excision repair (NER)

Ionising radiation can damage DNA directly or indirectly by generating further ROS. Ultraviolet (UV) radiation from the sun is an obvious environmental DNA-damaging agent, with UVB (290-320 nm) being the most deleterious carcinogenic wavelength causing cyclobutane pyrimidine dimers and pyrimidine-pyrimidone photoproducts. Pyrimidine dimers result in a distortion in the DNA helix which, during replication, is unreadable such that DNA polymerases preferentially incorporate an adenine residue commonly resulting in transition mutations (Melis et al., 2005). The repair of such bulky DNA adducts, such as pyrimidine dimers, is carried out by the nucleotide excision repair (NER) pathway. NER occurs in two forms; global genomic-NER (GG-NER) and transcription-coupled NER (TC-NER), which differ in their method of mutation recognition. GG-NER continually scans the genome for bulky DNA adducts and requires XPC-RAD23B for their recognition, whilst TC-NER employs RNA polymerase to identify damage interfering with on-going transcription with the help of the TC-NER specific proteins CSA, CSB, and XAB2 (Schärer, 2013). Both forms then employ the core NER reaction for repair of the lesion (Figure 1.4). Both methods result in a 24-32 nucleotide section surrounding the lesion being excised and DNA polymerase δ/ε/κ filling in the gap using the complementary strand as a template (Shuck et al., 2008).

1.2.4 Non-homologous end joining (NHEJ)

DSBs are particularly dangerous DNA lesions that can lead to potentially oncogenic genome rearrangements or cell death (Mao et al., 2008). It is interesting to note, however, that DSBs are necessary for critical processes in the cell such as meiotic recombination and V(D)J recombination in immune system development (Jackson and Bartek, 2009). DSBs may result

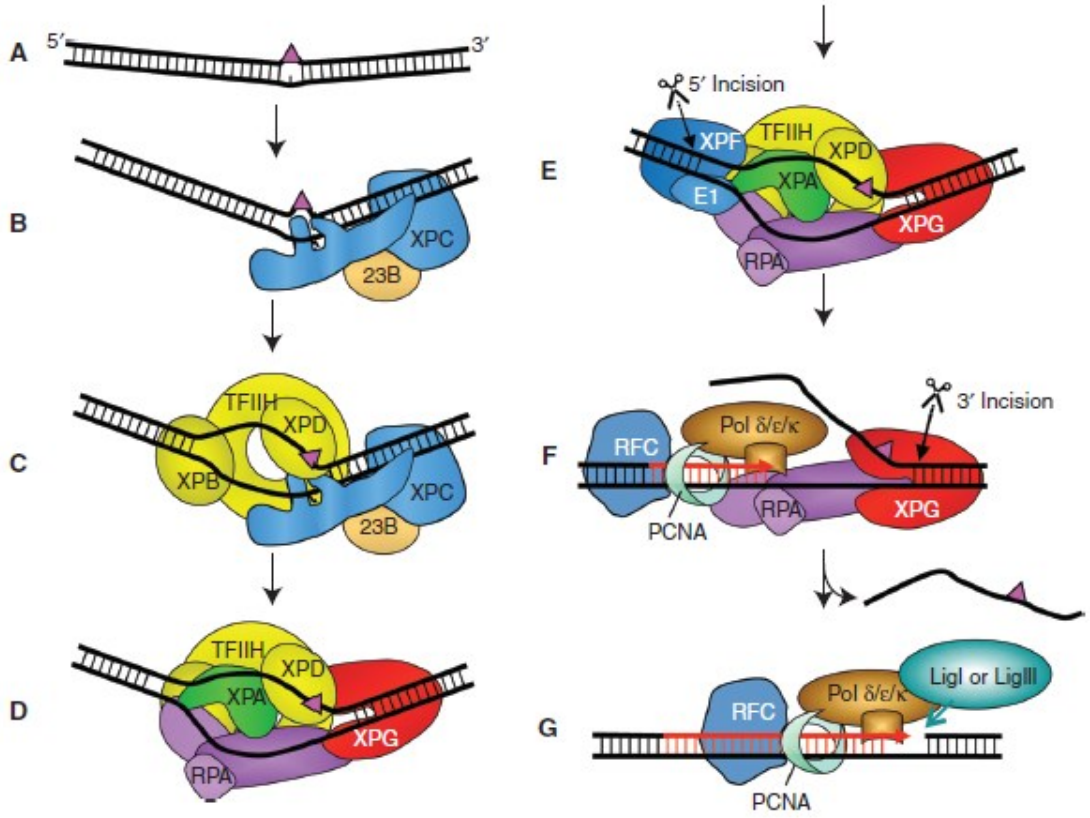

Figure 1.4 Model for the core NER reaction. (A) Bulky DNA lesions that destabilise duplex DNA are induced by a number of damaging agents. (B) In global genome NER, strongly distorting lesions are directly recognised by XPC-RAD23B, which binds the non-damaged strand opposite the lesion. (C) TFIIH interacts with XPC-RAD23B and pries the DNA open with its XPB subunit allowing XPD to track along DNA until stalls at the damage and verifies the chemical modification (bulkiness) of the lesion. (D) Stalling of XPD at the lesion allows for the formation of the pre-incision complex by recruitment of XPA, RPA, and XPG. The endonuclease XPG does not make an incision at this point. (E) Recruitment of ERCC1-XPF by interaction with XPA to the complex leads to incision 5' to the lesion. (F) Initiation of repair synthesis by Pol δ and Pol κ or Pol ε and associated factors, followed by 3' incision by XPG. (G) Completion of repair synthesis and sealing of the nick by DNA ligase IIIa/XRCC1 or DNA ligase I completes the process (Schärer, 2013).

from a number of factors, including the collapse of stalled replication forks, ionising radiation or certain anti-cancer drugs (Chapman et al., 2012).

DSBs are most commonly repaired by two mechanisms; homologous recombination (HR) and non-homologous end joining (NHEJ). The cell's choice of repair pathway in response to a DSB is determined by the stage of cell cycle in which the cell exists at that point. HR requires a section of homologous DNA in order to complete error-free repair and the sister chromatids on which this relies exist only during replication (i.e. the S and G2 phases of the cell cycle). When not available the cell employs the simpler mechanism of NHEJ; however, this process is error-prone, often resulting in an altered DNA sequence (Shrivastav et al., 2008). Ku, a heterodimer consisting of Ku70 and Ku80, has an extremely high affinity for DNA ends and initiates NHEJ by binding DNA ends and recruiting DNA-dependent protein kinase catalytic subunit (DNA-PKcs) forming the active DNA-PK holoenzyme (Meek et al, 2004). DNA-PK phosphorylates itself, as well as many other proteins involved in the repair pathway, including RPA, WRN, XLF, Artemis, DNA ligase IV (LigIV), and XRCC4. DNA-PKcs autophosphorylation causes a structural shift allowing DNA-end processing by PNKP, nucleotide addition by DNA pol λ and μ where required and finally ligation by the LigIV/XRCC4/XLF complex. This describes the classical-NHEJ pathway; however, an alternative exists which is promoted by PARP-1 and involves a PARP-1/XRCC1/LIGIII complex (Mladenov and Iliakis, 2011).

1.2.5 Homologous recombination (HR)

Efficient repair by HR requires a cascade of tightly controlled protein signalling pathways. This involves recognition of the DSB, the recruitment of repair factors and

execution of accurate repair, before deactivation of the response and disassembly of the proteins involved. Within the initial response to a DSB by HR, a distinct focal point around the location of the break is created and is often referred to as an Ionising Radiation-Induced Foci (IRIF) (Figure 1.5); this will stretch many megabases from the actual site of the break (Bekker-Jensen and Mailand, 2010). The MRN (MRE11-RAD50-NBS1) complex is the initial sensor and has an intrinsic capacity to bind DNA, before recruiting and stimulating ATM. ATM is activated through autophosphorylation at S1981 and also phosphorylates a number of other substrates. One of which is the histone H2AX, whose phosphorylation mediates interaction with the scaffold protein MDC1. MDC1 acts as a hub for many proteins involved in the DDR to attach and form repair foci, including the ubiquitin ligases RNF8, RNF168 and BRCA1 (Stewart et al., 2009).

The interplay of DDR proteins within IRIF is extremely complex and highly regulated. The early response ultimately serves to bring about the recruitment of necessary factors to begin repair and the generation of a pre-synaptic filament to begin a homology search. DNA ends are resected to produce long, 3'-single-stranded DNA (ssDNA) tails.

DNA end resection serves as a critical regulatory step in the choice of repair pathway for DSBs (Symington et al., 2011). During NHEJ, Ku binds DNA ends and prevents any resection. Conversely, resection of one strand at a DSB site prevents Ku binding obstructing repair by classical NHEJ and guiding the repair to be made via the HR mechanism. HR requires the resection of the 5' strand to reveal a 3'-single stranded length of DNA, which then acts to locate a homologous strand of DNA on the sister chromatid (Mao et al., 2008).

DNA end resection is carried out by a series of enzymes including nucleases and helicases. The MRN complex was alluded to earlier for its role as the initial sensor of DNA

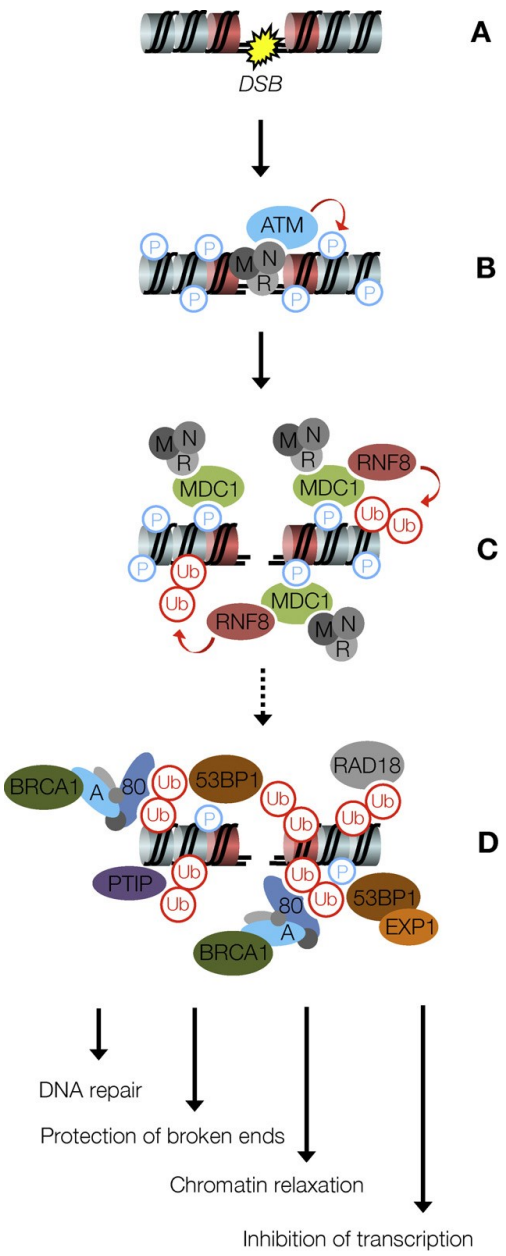

Figure 1.5 The early responses to DSBs resulting in the highly hierarchical assembly of IRIF. The DSB (A) is sensed by the MRN (MRE11-RAD50-NBS1) complex, which recruits the ATM kinase (B) resulting in turn in the recruitment of the scaffold protein MDC1 via phosphorylation of the histone H2AX. MDC1 recruits many proteins including the ubiquitin ligase RNF8, which ubiquitylates histones (C) to further recruit a second wave of repair factors such as 53BP1, the BRCA1 A complex and so on (D). The assembly of these repair proteins controls various DNA and chromatin transactions, ultimately leading to repair of the DSB. P: phosphate, M: MRE11, N: NBS1, R: RAD50, Ub: Ubiquitin, A: Abraxas (ABRA1), 80: Rap80, EXP1: EXPAND1 (Bekker-Jensen and Mailand, 2010).

damage and recruitment of ATM. It also acts as the major regulator of 5'-3' resection and the MRE11 component of the complex exhibits a 3'-5' dsDNA exonuclease activity and an ssDNA endonuclease activity (Mimetou and Symington, 2009; Paull and Gellert, 1998; Stracker and Petrini, 2011; Trujillo et al., 1998). CtIP is recruited to DSB sites through its interaction with BRCA1 and NBS1 to control the G2/M DNA damage checkpoint and direct the choice of repair pathway (Yun and Hiom, 2009). However, it also interacts with MRN to help mediate resection through its endonuclease activity and subsequently promoting HR (Sartori et al., 2007). The Bloom Syndrome protein (BLM) is also central to resection and recombination. It is a member of the RecQ family of DNA helicases and unwinds dsDNA in the 3' to 5' direction. It exhibits an affinity for recombination intermediates, such as D-loops and Holliday junctions, and co-localises with γ-H2AX (Wu et al., 2006; Bugreev et al., 2007).

The ssDNA is initially coated with RPA, which is subsequently replaced by Rad51. This creates a nucleoprotein filament capable of homology searching and mediating strand-exchange. This forms a D-loop structure and the 3'-end of the invading strand is extended by DNA polymerase. It can then dissociate and anneal to the other resected end, the ends joined by a DNA ligase and finally, the intermediate HJ structures (Holliday junctions) are resolved (Figure 1.6) (Mimetou and Symington, 2009).

1.2.6 Diseases associated with malfunction of the DDR

An effective DDR is crucial for the prevention of a number of diseases. Many syndromes and disorders result from mutations in DDR genes. They result in cancer predisposition, premature aging and affect the nervous, immune and reproductive systems (Ciccia and Elledge, 2010).

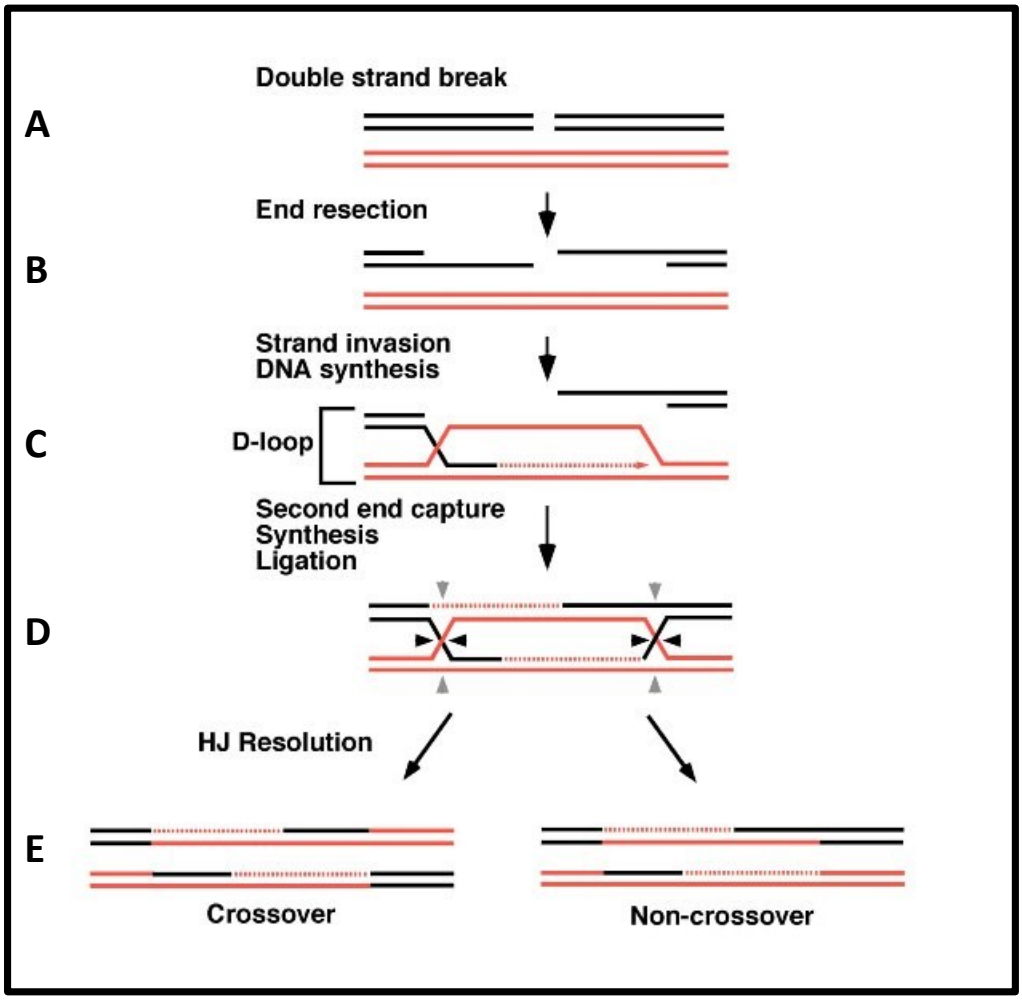

Figure 1.6 The DNA formations and processing during DSB repair by HR. A DSB occurs and repair foci form (A), followed by end resection (B) and the strand invasion by the recruited complementary sister DNA strand. DNA synthesis follows creating D-loop structures (C). Ligation of the DNA ends causes the formation of Holliday junctions (HJ) (D). Finally, these are junctions are resolved, which can result in the exchange (crossover) of DNA between sister chromatids (E) (adapted from Filippo et al., 2008).

Xeroderma pigmentosum (XP) was one of the first described DDR defect syndromes. Mutations in *XPA-G* and *POLH* result in inefficient NER of UV lesions greatly increasing the risk of skin cancer and melanoma (Hoeijmakers, 2009). Hereditary nonpolyposis colorectal cancer (HNPCC) results from mutations in the mismatch repair (MMR) genes *MLH1*, *MSH2* and *MSH6*, resulting in highly repeated short sequences of DNA (MIN) leading to a predisposition to colorectal cancer (Spry et al., 2007). Many other disorders caused by mutations in DDR genes result in cancer-prone phenotypes, a selection of which are shown in Table 1.1, along with some other DDR syndromes causing neuronal, immune, aging and fertility diseases.

DDR disorders, neuronal disorders and premature aging

Many neuronal cells must function for very long periods without renewal making them particularly vulnerable to DNA damage. Their high metabolic rate and oxygen consumption by mitochondrial respiration also generates large amounts of oxidative stress. Such factors aid development of neurodegenerative disorders such as Parkinson's disease (PD), Alzheimer's disease (AD) and amyotrophic lateral sclerosis (ALS), which are explored in greater detail in section *1.4.4* (Coppedé and Migliore, 2015). Many neuronal congenital disorders resulting in early life symptoms are caused by mutations in DDR genes. Ataxia telangiectasia (A-T) is a classical and extensively studied DDR disorder which results in severe movement and co-ordination problems in early life, as well as, immunodeficiency and predisposition to leukaemias and lymphomas (Biton et al., 2008). The disorder gave its name to the causative mutated gene, ATM (ataxia telangiectasia mutated). MRE11 (part of the MRN complex) is responsible for activating ATM in the DSB response. Mutations in the gene encoding MRE11 result in a similar phenotype to A-T (the syndrome is termed ataxia telangiectasia-like disorder (A-TLD)) and are reflective of the roles they have within the DDR

Table 1.1 – Selected human genetic diseases associated with DDR defects. (Adapted from Ciccia and Elledge, 2010).

Syndrome	**Mutated genes**	**DDR defect**	**Phenotype**
Cerebro-oculo-facio-skeletal syndrome (COFS)	*CSB, XPD, XPG, ERCC1*	TC-NER	Brain calcification, hypomyelination, microcephaly, neurodegeneration, cataracts, hearing loss, optic atrophy, osteopororsis, facial dysmorphism, joint contractures, photosensitivity, growth defects
Cockayne syndrome (CS)	*CSA, CSB XPB, XPD, XPG*	TC-NER	Microcephaly, neurodegeneration, neuronal demyelination, cachexia, cataracts, hearing loss, retinopathy, photosensitivity, growth defects
Trichotiodystrophy (TTD)	*CPB, XPD, TTDA*	TC-NER	Hypomyelination, neurodegeneration, cachexia, cataracts, osteopororsis, brittle hair and nails, photosensitivity, scaly skin
Xeroderma pigmentosum (XP)	*XPA-G, POLH*	NER	Microcephaly, neurodegeneration, squamous and basal cell carcinoma, melanoma photosensitivity, scaly skin
Fanconi anemia (FA)	*FANCA-C, FANCD1, D2 FANCE-G, FANCI,J,L-N*	ICL repair, HR	Microcephaly, pancytopenia, bone marrow failure, AML, myelodysplasia, squamous cell carcinoma, abnormal skin pigmentation, infertility, limb deformities renal dysfunction
Familial breast cancer	*ATM, BRCA1, BRCA2, BRIP1, CHK2, NBS1, PALB2, RAD50, RAD51C*	HR, damage signalling	Breast cancer, ovarian cancer
Werner syndrome (WS)	*WRN*	HR, BER, telomere maintenance	Atherosclerosis, cataracts, grey hair, osteosarcoma, skin cancers, skin and skeletal abnormalities, growth defects
Hereditary nonpolyposis colorectal cancer (HNPCC)	*MSH2, MSH6, MLH1, PMS2*	MMR	Colorectal cancer, carcinomas

Ataxia telangiectasia (A-T)	*ATM*	Damage signalling, DAB repair, oxidative stress	Ataxia, cerebellar degeneration, oculomotor apraxia, immunodeficiency, lymphomas, leukemias, breast cancer, dilated blood vessels, infertility, metabolic defects, growth defects
Ataxia telangiectasia-like disorder (A-TLD)	*MRE11*	Damage signalling, DAB repair, oxidative stress	Ataxia, cerebellar degeneration, oculomotor apraxia, immunodeficiency
Nijmegen breakage syndrome (NBS)	*NBS1*	Damage signalling, DAB repair, replication fork repair	Microcephaly, immunodeficiency, B cell lymphoma, facial dysmorphism, growth defects
Nijmegen break syndrome-like disorder (NBSLD)	*RAD50*	Damage signalling, DAB repair, replication fork repair	Microcephaly, facial dysmorphism, growth defects
Seckel syndrome (SS)	*ATR, PCTN, SCKL2, SCKL3*	Damage signalling, DAB repair, replication fork repair	Microcephaly, mental retardation, AML?, facial dysmorphism, growth defects
Primary microcephaly 1	*MCPH1*	Damage signalling, DAB repair, replication fork repair	Microcephaly, mental retardation,
Amyotrophic lateral sclerosis (ALS)	*SOD1, SETX, FUS,*	Oxidative stress, SSB repair?	Degeneration of motor neurons, muscular atrophy, dementia in some cases

(Stewart et al., 1999). Consistent with the importance of the DDR during brain development many patients with DDR syndromes display microcephaly, a reduced head circumference caused by lack of neuroprogenitor cell proliferation (O'Driscoll and Jeggo, 2008). A number of the genes mutated have roles in the ATR pathway (primarily involved in the response to SSBs), including ATR and PCNA (proliferating cell nuclear antigen) (Seckel syndrome - SS), MCPH1 (primary microcephaly), RPA1 (Miller-Dieker lissencephaly syndrome) and RCF2 (Williams-Beuren syndrome) (Kerzendorfer and O'Driscoll, 2009; O'Driscoll and Jeggo, 2008). Furthermore, mutations in NBS1 and RAD50 cause Nijmegen breakage syndrome (NBS) and Nijmegen break syndrome-like disorder (NBSLD), respectively. They result in microcephaly and "bird-like" features, but with other symptoms very different from A-T and A-TLD patients, despite NBS1 and RAD50 being the other two components of the MRN complex (Katyal and McKinnon, 2008; Waltes et al., 2009). This can probably be attributed to the complex regulation of ATM and ATR activation by MRN confirming that different mutations in DDR genes cause different and distinct phenotypes (Ciccia and Elledge, 2010).

Accumulation of DNA damage contributes to the aging process and numerous DDR syndromes exhibit premature aging. Werner syndrome (WS) causes symptoms astoundingly like those of normal aging but with significant acceleration and is caused by mutations in the RecQ helicase WRN, which functions in BER, HR and telomere maintenance (Bohr, 2008; Chu and Hickson, 2009). Cockayne syndrome (CS), trichotiodystrophy (TTD) and cerebro-oculo-facio-skeletal syndrome (COFS) patients all display premature aging symptoms that result from mutations in genes involved in NER (Table 1.1) (Ciccia and Elledge, 2010).

The DDR and cancer

Cancer is a disease characterised and ultimately defined by genetic instability. The majority of cancers display chromosomal instability (CIN), characterised by changes in chromosome number or structure, whilst base mutations and microsatellite instability (MIN) (variation in the number of repeats of small microsatellite sequences) are also common. Such genomic instability leads to the uncontrolled division of the cell (Ciccia and Elledge, 2010). Hanahan and Weinberg, 2011, describe genomic instability as an enabling characteristic of cancer, whilst eight cellular abilities termed 'hallmarks' are required for a malignant tumour to develop. These are: resisting cell death, sustaining proliferative signalling, evading growth suppressors, activating invasion and metastasis, enabling replicative immortality, inducing angiogenesis, deregulating cellular energetics and avoiding immune destruction. However, it is important to note that not all cells within a tumour may exhibit these properties as cancer cell populations are heterogeneous in nature.

The clinical rationale for studying the DDR in relation to cancer is twofold. Firstly, mutations in DDR genes/proteins incapacitate one or more of the detection and repair pathways, such that DNA damage is not rectified. This damage may go on to produce a tumour. Secondly, many cancer cells have defects in their damage response pathways making them more susceptible to DNA damage than healthy cells. This observation has led to the use of DNA-damaging agents, such as irradiation and platinum-based derivatives, as anti-cancer therapies, despite inevitable side effects on healthy cells, resulting in hair loss, immune suppression, gastrointestinal problems and rather ironically, secondary tumour development (Kastan and Bartek, 2004). For example, cisplatin, a platinum-based drug, is used in the treatment of ovarian cancer. The drug crosslinks DNA, which is repaired by a combination of nucleotide excision repair (NER) and homologous recombination (HR). As many ovarian

cancers harbour mutations in BRCA1 or BRCA2 – crucial in HR – this makes the cancer cells more vulnerable to this treatment than normal cells (Lord and Ashworth, 2012). The development and use of PARP inhibitors in recent years to treat BRCA-1 and -2 deficient tumours works by the similar principle of 'synthetic lethality'. Inhibition of PARP leads to stalled replication forks collapsing, resulting in DSBs. These require repair by HR, but the tumour cells are deficient in this mechanism of repair triggering cell death (Bryant et al., 2005). The exploitation of a cancer cell's DDR deficiencies for treatment is an exciting avenue of current research and a paradoxically interesting one considering such defects help drive initial tumourigenesis.

DDR, fertility and the immune system

Fertility also relies on an effective DDR. This is due to the generation of gametes during meiosis requiring exchange of DNA between homologous chromosomes via DSBs and subsequent repair by HR. Patients with the DDR syndromes, A-T, BS and FA, exhibit aberrant meiosis resulting in infertility (Biton et al., 2008; Bohr, 2008; Matzuk and Lamb, 2008). Furthermore, the immune system depends on the creation of thousands of immunoglobulins and T cell receptors for antigen recognition. This occurs by V(D)J recombination facilitated by DSB formation by the nucleases RAG1, RAG2 and Artemis. Patients with mutations in any of these three genes display severe combined immunodeficiency (SCID) due to insufficient immunoglobulin production (Corneo et al., 2007; Sobacchi et al., 2006; Gennery, 2006).

1.3 Heteronuclear ribonucleoproteins (hnRNPs)

1.3.1 hnRNPs

mRNAs are the product of gene transcription and post-transcriptional processing by an extensive network of ribonucleoproteins (RNPs). Primary transcripts from DNA are termed pre-mRNAs and require processing to become mature mRNA, involving packaging, processing, nuclear export and cellular localisation to production sites in the cytoplasm. Such regulation by RNPs is complex and requires these proteins to recognise specific RNA sites. As well as protein-RNA interaction, RNPs exhibit protein-DNA and protein-protein interactions that connect them to the major regulatory networks of the cell (Haley et al., 2009).

Only 2-3% of all primary transcriptional output is protein-coding. Protein coding regions are termed exons and non-protein coding are termed introns. Introns must be spliced from pre-mRNA and disposed of by the exosome (Mattick, 2003). However, intronic sequences have important roles in the regulation of chromatin architecture, transcription and alternative splicing. MicroRNAs (miRNAs) are also non-coding RNA sequences, typically 21-25 nucleotides in length, that are coded by intergenic regions and are now being shown to have major regulatory roles in RNA silencing and post-transcriptional regulation of gene expression (Mattick, 2003). Therefore, post-transcriptional regulation of gene expression is complex and it appears that both RNA and RNPs co-operate to process pre-mRNA effectively.

Eukaryotic mRNA usually requires guidance to distinct cellular locations. It is RNPs which direct this considerable RNA traffic. This requirement for transcript processing, signalling and localisation has led to the evolution of a diversity of RNPs with many

structural conformations, binding specificities and isoforms (Haley et al., 2009). Heterogeneous nuclear ribonucleoproteins (hnRNPs) constitute a large class of RNPs. They are characterised by their RNA-binding specificity and their association with one another within a large complex. However, this complex is highly dynamic and very readily remodelled through the loss or gain of hnRNPs due to the requirement for specific processes. There are at least 20 known hnRNPs with additions still being made in recent years due to the re-classification of some relatively well-studied proteins (Chaudhury et al., 2010). The most abundant of the hnRNPs are designated hnRNPA1 through to hnRNP-U and have molecular weights ranging from 34K to 120K. It is these members that are said to form 'core hnRNPs' (Dreyfuss et al., 1993). There are a number of other hnRNPs, which are not considered to be 'core hnRNPs' as they do not co-immunoprecipitate as readily with core hnRNPs (Krecic and Swanson, 1999).

Whilst hnRNPs exhibit overlapping structure and function, they do not necessarily exhibit extensive amino acid homology to one another (Haley et al., 2009). Each individual hnRNP consists of both protein and RNA. The RNA component is critical for the facilitation of mRNA-binding through complementary nucleotide interactions. hnRNPs contain one or more RNA-binding motifs and at least one auxiliary domain that regulates protein-protein interactions and subcellular localisation (Chaudhury et al., 2010).

Alongside histones, hnRNPs are some of the most abundant cellular proteins. They reside largely in the nucleus, but are known to shuttle between the nucleus and cytoplasm in transporting mRNA through nuclear pores to ribosomes. Indeed, the majority of their functions are still thought to principally involve mRNA metabolism (Chaudhury et al., 2010). However, in recent years they have been implicated in a far wider range of cellular activities, including the DNA damage response (DDR), which is a major focus of this study (Haley et

al., 2009). Extended involvement in a broader range of activities has led to more of hnRNPs' protein-protein interactions being characterised.

1.3.2 hnRNP-UL1

Screening of a human expression library to look for proteins that interacted with adenovirus 5 early protein E1B-55K allowed identification of hnRNP-UL1 (heterogeneous nuclear protein-U like 1), which was originally named adenovirus early region 1B-associated proteins 5 (E1B-AP5) (Gabler et al., 1998). However, subsequent revelation of sequence similarity to hnRNP-U (SAF-A) resulted in recognition of it together with hnRNP-UL2, as new members of the hnRNP family. In addition, a number of groups have isolated hnRNP-UL1 as a component of large dynamic mRNA-RNP complexes (Hartmuth et al., 2002; Rappsilber et al., 2002; Chen et al., 2007) that form during RNA regulation and processing (Singh and Valcárel, 2005). Indeed, hnRNP-UL1 and –UL2 were shown to co-immunoprecipitate with hnRNP-H, -K and –U (Pratt, 2012).

hnRNP-UL1 and –UL2 are approximately of 96 K and 85 K in molecular weight, respectively, and share 43% homology, with a significant amount shared across their conserved domains (Figure 1.7). Both contain an N-terminal SAP (after SAF-A/B, Acinus and PIAS) motif, which has DNA-binding capability and is found in many proteins with diverse functions, such as transcriptional regulation, DNA repair, RNA processing and chromosomal organisation (Aravind et al., 2000; Hong et al., 2013). The SPRY domain is present in about 700 eukaryotic proteins, of which 150 are human. Until recently it was considered to have no known function; however, studies have now revealed that it has importance in protein-protein interactions. Studies of TRIM5α and Pyrin showed that the

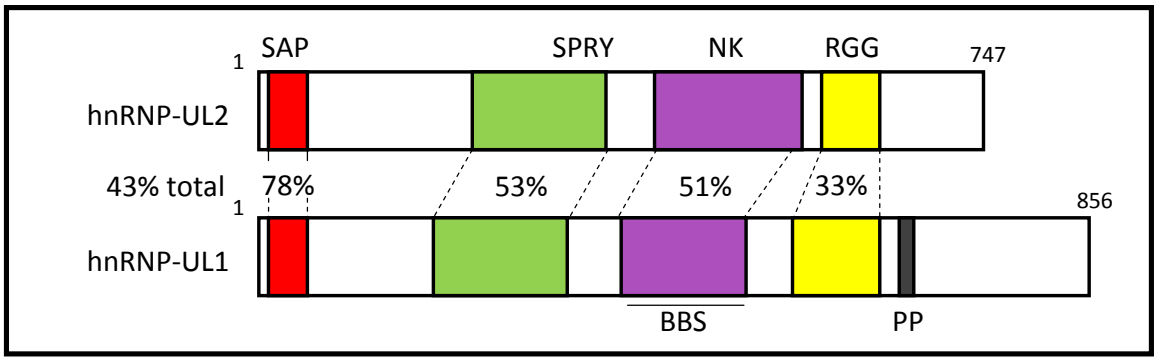

Figure 1.7 Structure of hnRNP-UL1 and -UL2 and their domains. A schematic representation of the hnRNP-U-like proteins and their domains with shared homology. SAP, SAF-A/B, Acinus and PIAS motif; SPRY, SPIa/Ryanodine receptor domain; NK, putative nucleoside/nucleotide kinase domain; BBS, BRD7-binding site; RGG, arginine and glycine-rich region, RNA and ssDNA binding; PP, proline-rich region. (Adapted from Polo et al., 2012).

amino acids lining the ligand-binding surface of the SPRY domain are highly variable and therefore, it is thought that each SPRY domain recognises its own specific partner protein rather than a consensus sequence motif (Woo et al., 2006). This suggests why SPRY domains are found within such a large number of proteins with hugely diverse functions in different biological processes. The RGG box was originally described in hnRNP-U and is characterised by closely spaced clusters of Arg-Gly-Gly (RGG) tripeptide repeats with interspersed aromatic (Phe, Tyr) residues (Chaudhury et al., 2010). Its major function is in facilitating RNA-binding, but it is also involved in protein-protein interactions, transcriptional activation and nuclear localisation (Hong et al., 2013). Methylation of arginine residues within the RGG box was first observed in 2001 and the BBS domain was shown to be involved in bromodomian-containing protein 7 (BRD7) binding (Kzhyshkowska et al., 2001). Proximal to the RGG box in hnRNP-UL1, but not hnRNP-UL2 there is a proline-rich region (PP) which has also been implicated in transcriptional regulation and in protein-protein interactions (Polo et al., 2012).

Of greater interest to this study, is a previously undescribed region within both hnRNP-U, –UL1 and –UL2, which shows significant homology to human PNKP (polynucleotide kinase phosphatase). This region was identified as a putative nucleotide kinase domain (labelled NK in Figure 1.7) by Gabler et al. (1998). Details of this region and its significance to this study will be considered in section *1.3.5*. A C-terminal region of hnRNP-UL1 and also hnRNP-U have been confirmed as being "prion-like" meaning they have a similar amino acid composition to yeast prion proteins enabling the proteins to take on an alternative form and convert native isoforms by self-templating (Li et al., 2013). This domain and its consequence are explored in detail in section *1.4.3*.

Many of hnRNP-UL1 and –UL2's functions are within mRNA metabolism. Gabler et al. (1998) described the adenovirus E1B-55K protein's interaction with hnRNP-UL1 as critical for the viral control of the host cell's mRNA transport and processing. This alluded to the already suspected roles of the U-like proteins in mRNA processing. hnRNP-UL1 was found to bind TAP (nuclear RNA export factor 1), a protein involved in RNA export from the nucleus further supporting its proposed role in mRNA processing (Bachi et al., 2000). hnRNP-UL1 has also been implicated in the regulation of RNA transcription by interaction with the transcription factors p53, BRD7 and SMAD2 (small and mothers against decaplentapegic-related 2) (Barral et al., 2005; Kzhyshkowska et al., 2001; Luo et al., 2006). Through interaction with U7 small nuclear ribonucleoprotein (U7 snRNP) hnRNP-UL1 also represses the transcription of histone genes outside of the S phase (Ideue et al., 2012).

Apart from these RNA regulatory roles, the extent of hnRNP-UL1's functions continue to grow with further study. A genetic variant of hnRNP-UL1, defined by an intronic single nucleotide polymorphism (SNP) (ID rs11881940), was identified in two separate studies as a genetic risk factor for the closely associated diseases myocardial infarction (MI) (Shiffman et al., 2006) and coronary heart disease (CHD) (van der Net et al., 2009). A replication study using different sample data confirmed the association between the SNP and CHD in a high risk population with familial hypercholesterolemia (van der Net et al., 2008). It remains unclear whether the mutation causes the encoding of a dysfunctional hnRNP-UL1 protein leading to pathogenesis or that the SNP simply marks an inherited region of chromosome 19 which is associated with these diseases.

There are a number of studies which have shown hnRNP-UL1 to have quite significant roles within the DNA damage response (DDR). Such roles included direct binding to p53 and regulation of its transcriptional targets. hnRNP-UL1 is involved in the mediation

of ATR-dependent signalling during adenovirus infection and is responsible for BLM recruitment necessary for DNA end resection. Furthermore, it is recruited specifically to double-strand DNA break sites (DSBs) through interaction with the MRN complex and PARP-1 (Barral et al., 2005; Blackford et al., 2008; Polo et al., 2012; Hong et al., 2013). These roles will be explored in more detail in section *1.6*.

1.3.3 hnRNPs in the DDR

In recent years, more and more evidence has accumulated which implicates hnRNPs in coordinating repair pathways both through protein-protein interactions and the regulation of mRNA transcripts for proteins involved in DNA repair and stress responses (Haley et al., 2009). Given the extensive roles of hnRNPs in mRNA processing it is unsurprising that they play a pivotal role in repair pathways by controlling the expression levels of DNA repair proteins through post-transcriptional control of mRNA stability, splicing and translation (Reinhardt et al., 2011). More unexpected is their regulation by direct interaction with proteins involved in repair processes of which many examples have now been recognised.

hnRNP K has been shown to play an important role as a cofactor of the DNA damage response protein, p53. siRNA knockdown of hnRNP-K inhibited effective recruitment of p53 to the p21 promoter region. The subsequent downregulation of p21 expression led to ineffective cell cycle inhibition (Moumen et al., 2005). hnRNP K levels are controlled in cells by ubiquitin-dependent proteasomal degradation. However, Lee et al. (2012) showed that in response to DNA damage, hnRNP-K was SUMOylated, stabilising the protein and increasing its affinity for p53. This allows p53 to carry out its DDR and cell-cycle inhibition roles more effectively. Additionally, hnRNP-K SUMOylation was found to be ATR-dependent and

hnRNP-K is indeed a phosphorylation substrate of ATM and ATR. p53 was also shown to bind hnRNP-UL1 (the protein of interest to this study). The regulation of p53 activity is thought to be the opposite of that by hnRNP-K. hnRNP-UL1 instead binds to p53 to reduce its activity as a transcription factor for other genes (Barral et al., 2005).

Roles for other hnRNPs in the DDR are shown by hnRNP-B1's interaction and inhibition of DNA-PK, causing the cell to direct its DSB repair towards the HR mechanism (Iwanaga et al., 2005). hnRNP-C1/C2 has been shown to bind Ku and be phosphorylated by DNA-PK suggesting a role in NHEJ (Zhang et al., 2004). The significance of this interaction and modification within the DDR has yet to be revealed. There is also some evidence to suggest a role for hnRNP-A1, -A18, -A2/B1, -C1/C2, -K and -P2 in regulating the choice between HR and NHEJ (Haley et al., 2009).

As stated earlier, hnRNPs are now being recognised as having crucial roles in the DNA damage response through their mRNA processing activities. Unsurprisingly, in response to DNA damage, cells transiently inhibit gene transcription (Rockx et al., 2000; Vichi et al., 1997). The reasons for doing so are obvious. Firstly, the genetic material is damaged and therefore, protein products may be functionally aberrant if produced. Secondly, transcription is very energy intensive (synthesis of an mRNA molecule with *n* bases requires at least *n* NTP molecules) and the cell must initially use its energy to address the repair of the damage. The time required to produce a final protein product from DNA is large in cellular terms and manipulation of specific gene expression is very much a secondary response to DNA damage. Therefore, for cells to accomplish DNA-damage-induced changes in mRNA expression, when transcription activity is globally supressed, is unlikely. It is more efficient to manipulate the mRNA already produced via processing activities. Several recent studies have now implicated hnRNPs as targets of the DDR for this specific purpose (Reinhardt et al., 2011).

Cimprich and colleagues found that depletion of mRNA-binding and processing factors by RNA interference (RNAi) resulted in spontaneous γH2AX formation (Paulsen et al., 2009). Gorospe and colleagues found that over 50% of the observed changes in steady state mRNA levels in H1299 cells treated with UV were due to mRNA turnover, which is a process managed by RNPs (Fan et al., 2002). The mRNA levels of the tumour suppressor DDR protein Gadd45α were found to be stabilised in response to UV or MS exposure (Jackman et al., 1994). A more direct link to the DDR was found through a mass spectrometry-based phospho-proteomic screen for substrates of the DDR kinases ATM, ATR and DNA-PK in response to IR. Of 700 proteins identified in the study with a consensus ATM and ATR phosphorylation motif, 124 were proteins involved in mRNA transcription or processing (Matsuoka et al., 2007). Such phosphorylation would suggest a possible signalling mechanism for the control of these RNP activities in response to DNA damage (Reinhardt et al., 2011).

It should also be noted that whilst there is a global repression of gene expression in cells following DNA damage many of the hnRNPs' expression levels are in fact increased. The specific upregulation of hnRNP gene expression adds further evidence to their significant role in the DNA damage response. For example, γ-irradiation of cells caused hnRNP-A1 transcript expression to increase 2-fold between 2 and 5 hours post-irradiation (Jen and Cheung, 2003). The protein was also found to translocate from the nucleus to cytoplasm in response to ultraviolet irradiation, and other forms of cell stress including heat shock, osmotic stress and oxidative stress (van Oordt et al., 2000). Furthermore, levels of hnRNP-A2/B1 protein decrease 4-fold in response to γ-irradiation and hnRNP-A18 levels increase in response to UV exposure (Gamble et al., 2000; Yang and Carrier, 2001). It appears that

different hnRNPs have very diverse roles within the DDR and their importance is now being increasingly recognised.

1.3.4 hnRNP-UL1 in the DDR

In recent years, there has been much research showing various roles for hnRNP-UL1 in the DDR. The C-terminal region of p53 was shown to interact with a middle region of hnRNP-UL1 incorporating the BBS and RGG regions, suggesting they are important for binding. Reporter assays also indicated that hnRNP-UL1 interacted directly with p53 to reduce its transcriptional activity and subsequently expression levels of p21 were reduced in cells transfected with hnRNP-UL1 after UV irradiation (Barral et al., 2005).

Multiple RPA complexes bind the 3'-single stranded DNA tails exposed due to resection during HR repair of DSBs. Blackford et al., (2008) showed that hnRNP-UL1 binds both RPA70 and RPA32, which are principle components of the RPA complex, as well as the protein ATRIP (ATR-interacting protein). Additionally, during adenovirus infection hnRNP-UL1 is required for ATR-dependent phosphorylation of RPA32 and also contributes to phosphorylation of H2AX (Blackford et al., 2008).

In 2012, work published in conjunction with our laboratory highlighted further interactions of hnRNP-UL1, particularly with DDR proteins involved in DNA resection. The roles of the MRN complex, CtIP and BLM within resection are discussed in section *1.2.5*. Polo et al. (2012) showed the hnRNP-U like proteins to interact with both the MRN complex and BLM, whilst further GST-pulldown and co-immunoprecipitation experiments have shown interactions with CtIP as well. The C-terminal region of NBS1 exhibited affinity for the BBS-RGG region of hnRNP-UL1 and this interaction is crucial for the recruitment of hnRNP-UL1

to damage sites. Indeed, when RNA was depleted in cells to prevent its interaction with the hnRNP-U like proteins, the interdependent recruitment of hnRNP-UL1 and –UL2 to sites of DNA damage was observed (Polo et al., 2012). Furthermore, the NBS1 interaction was shown to be dependent upon arginine methylation in the RGG domain by PRMT1 (protein arginine methyltransferase 1) and this methylation was required for recruitment to laser-microirradiation sites (Gurunathan et al., 2015). At DSB sites caused by either laser-induced or camptothecin (CPT)-induced damage hnRNP-UL1 was shown to promote resection of 5' ends, in an ATR-dependent manner, through the recruitment of BLM (Polo et al., 2012). hnRNP-UL1 depletion causes mild radiosensitivity to DSB-inducing IR and CPT, but not SSB-inducing UV (Polo et al., 2012). Whilst ATR signalling is traditionally linked to SSB responses arising from stalled replication forks, it also has a crucial role in HR repair of DSBs due to the exposure of 3' end tails by resection. hnRNP-UL1's role in stimulating this resection, which is required to initiate RPA binding to the exposed ssDNA and subsequent ATR signalling, may explain the sensitivity to DSBs and not SSBs. Altogether, it appears that the direct protein-protein interactions of hnRNP-UL1 and –UL2 with members of the DDR are critically important in executing responses to particular forms of DNA damage.

An alternative proposal of hnRNP-UL1 recruitment to sites of damage is through interaction with PARP-1 (Hong et al., 2013). PARP-1 is rapidly recruited to sites of DNA damage where single-stranded DNA is exposed, including both SSB sites and DSB sites where resection has occurred. DNA-binding increases its catalytic activity of PARP-1 10- to 500-fold (Rouleau et al., 2010). Its catalytic activity results in the poly ADP-ribosylation of many proteins involved in gene transcription, DNA damage repair, and cell death signalling (Krishnakumar and Kraus, 2010). However, its main substrate is itself and this auto-modification is a method of increasing its own activity. Due to a reliance of many

cancer cells on PARP for DNA repair, PARP inhibitors have become of great clinical interest. Hong et al., (2013) recently showed a close relationship between PARP-1 and hnRNP-UL1. Interestingly, a number of RNA-binding proteins are PAR-dependently recruited in the early phase response to DNA damage and it appears that the electrostatic interactions between positively charged RGG repeats and negatively charged PAR are responsible for the recruitment (Altmeyer et al., 2015). hnRNP-UL1's C-terminal region was shown to directly interact with PARP-1 and help facilitate recruitment to DSB, but not SSB sites. hnRNP-UL1 also undergoes poly ADP-ribosylation and was shown to regulate the expression levels of PARP-1 via mRNA processing (Hong et al. 2013). This rapid recruitment of hnRNP-UL1 to damage sites provides a possible early role in DDR signalling different from that of its promotion of resection, but its precise early-phase role is unclear.

The roles of hnRNP-UL1 in the DDR make it a potential target for cancer therapy as cancer cells commonly have defects in their response pathways. The discussed requirement of hnRNP-UL1 in ATR signalling is interesting as cancer cells are heavily reliant on the ATR pathway to progress through S phase under high levels of replicative stress (Nam and Cortez, 2011). Therefore, inhibition of hnRNP-UL1 could cause cancer cells to be more susceptible to treatment with DNA-damaging agents than healthy cells. However, to design drugs specific for the hnRNP-U like proteins whilst not affecting other hnRNPs would not be straight forward.

1.3.5 hnRNP-UL1's Walker A motif and activity of PNKP

ATP-binding and the Walker A motif

A vast number of proteins of both eukaryotic and prokaryotic organisms bind and utilise the mononucleotides adenosine 5'-triphosphate (ATP) or guanosine 5'-phosphate (GTP) (Matte and Delbaere, 2010). Given that the transfer of the γ-phosphoryl moiety from these molecules can be used in such a wide array of metabolic activities it is unsurprising that so many proteins possess the ability to bind mononucleotides. For example, P-loop NTPases (nucleoside tripohosphatases) represent 10-18% of all proteins in sequenced genomes (Koonin et al., 2000).

Proteins have evolved different methods of binding the ATP or GTP molecule through recognition of the triphosphate, the ribose sugar and/or the adenine base. Evolution has led to conserved motifs which are responsible for this binding, and these contain amino acid sequences or structures facilitating the interaction. With a focus on ATP-binding, the Walker-A motif is the best-known and first-identified such motif. The motif GXXXXGKT/S (X = any residue) was recognised in 1982 by Walker and colleagues as a common sequence required for ATP-binding in F_1-ATPase, myosin and a number of kinases (Walker et al., 1982). Upon structural analysis the sequence was found to form a loop structure sandwiched between an N-terminal β strand and a C-terminal alpha-helix and became known as the Walker loop or P-loop (phosphate-binding loop) (Figure 1.8) (Ramakrishnan et al., 2002). The loop contains a pair of conserved glycine residues which allow for main-chain hydrogen-bonding interactions with the phosphoryl groups of the nucleotide. A conserved serine or threonine residue is found at the C-terminus of the loop co-ordinating interaction with the catalytic Mg^{2+} ion, whilst the lysine residue is involved in phosphoryl transfer (Matte and Delbaere, 2010).

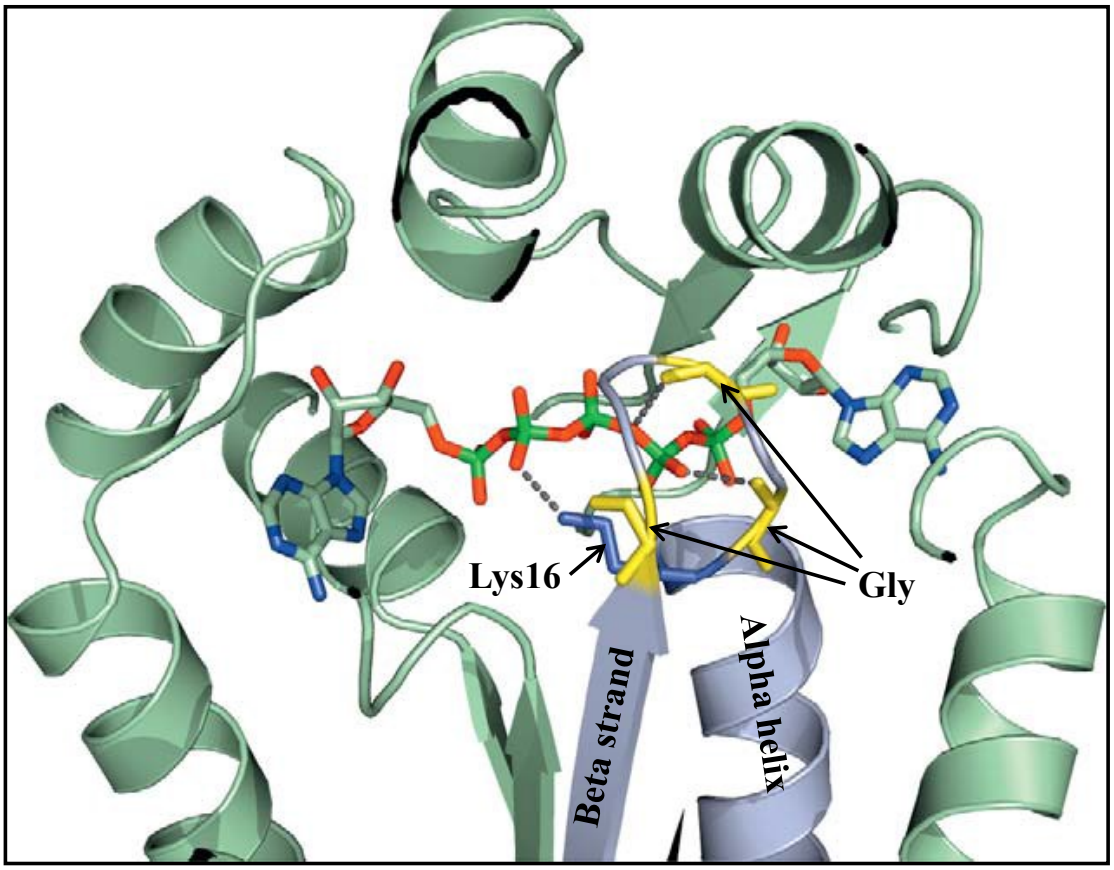

Figure 1.8 Crystal structure of yeast adenylate kinase (pale green) bound to the ATP-mimic, bi-substrate inhibitor bis(adenosine)-5'-pentaphosphate (Ap5A), and Mg^{2+} at 1.96A° resolution. The β-strand-loop-α-helix motif containing the P-loop is coloured grey, with the catalytic Lys16 coloured blue, and the three Gly residues of the P-loop coloured yellow. Hydrogen-bonding interactions with the Ap5A inhibitor (red = oxygen, blue = nitrogen, grey = carbon and green = phosphorous) are indicated as grey dashed lines (Matte and Delbaere, 2010).

DNA end processing by PNKP

As described earlier many different agents can cause various types of DNA damage and they are repaired by various activities of the DDR machinery. For many types of DNA lesion, the effective repair by a number of the pathways requires the DNA ends to be processed before ligation can occur. Human PNKP (polynucleotide kinase phosphatase) contains both 5'-kinase and 3'-phosphatase activity, allowing the creation of 5'-phosphate/3'-hydroxyl termini, which are essential for synthesis by polymerases and ligation of the two strand ends (Schellenberg and Williams, 2011). PNKP has been shown to have crucial roles in SSB repair, DSB repair and BER (Weinfeld et al., 2011). Segal-Raz et al. (2011) demonstrated the phosphorylation of PNKP at residues Ser-114 and Ser-126 by ATM in response to DSBs to be crucial for upregulating PNKP activity and effective accumulation at sites of damage. PNKP has attracted clinical interest due to the discovery that, like many DDR proteins, its inhibition can result in the sensitisation of cancer cells to irradiation or chemotherapeutics (Zhu et al., 2009; Allinson, 2010). In addition, Shen et al. (2010) showed that mutations of PNKP are associated with the severe autosomal recessive disorder MCSZ (debilitating and heritable seizure syndrome).

Towards the C-terminus of PNKP there is a bi-lobed catalytic domain, which contains fused kinase and phosphatase subdomains with separate catalytic activities. These subdomains have significant contact with one another across a relatively large interface such that the domains cannot be separated by proteolysis during crystallographic studies (Bernstein et al., 2005). The catalytic domain is linked to an N-terminal FHA (forkhead-associated) domain by a flexible polypeptide segment (Figure 1.9). The FHA domain permits binding to XRCC1 and XRCC4, which are critical scaffolding proteins in the repair of SSBs and DSBs, respectively (Loizou et al., 2004; Koch et al., 2004).

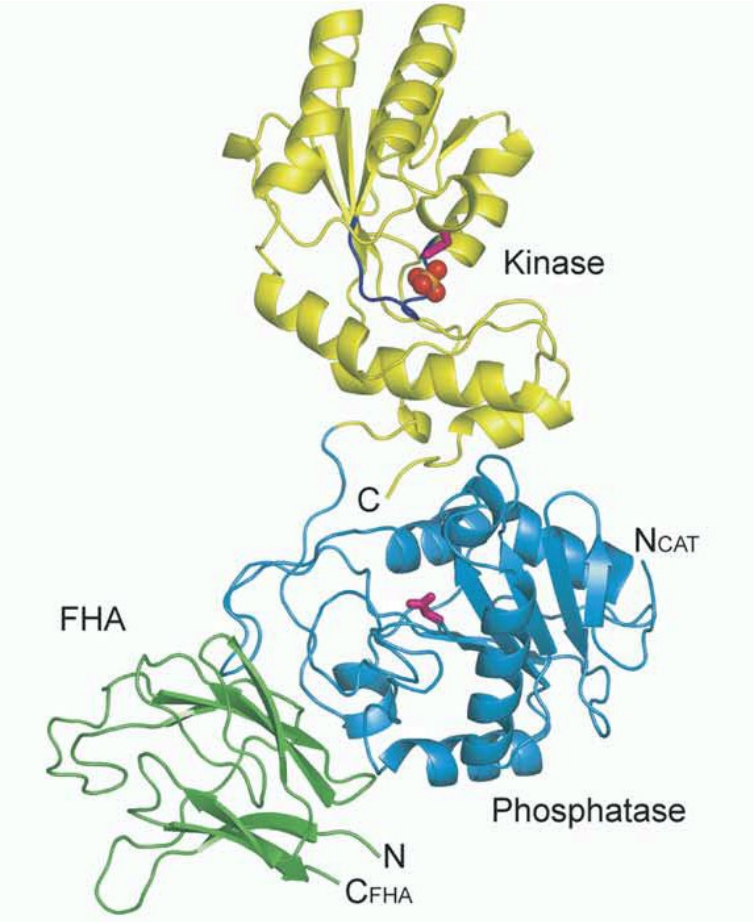

Figure 1.9 Ribbon diagram of mouse PNKP. The kinase domain is in yellow, the phosphatase domain in blue and FHA domain in green. Catalytic side chains (Asp170 and Asp396 in the phosphatase and kinase, respectively) are in pink, the ATP-binding P-loop is in navy blue, and the sulphate bound at the P-loop is in orange and red spheres (Bernstein et al., 2005).

The detailed interaction of PNKP with its DNA substrate was unclear until recently. The crystallographic studies of Coquelle et al. (2011) employed mouse PNKP to look at the phosphatase subdomain's interactions with both ssDNA and dsDNA. In short, single-stranded substrates interact with a narrow active site cleft of the phosphatase domain in a sequence-independent manner. For double-stranded substrates, PNKP is able to destabilise the terminal 2-3 base pairs at the 3'-phosphate end allowing access to the active site. However, another positively charged region of PNKP, distinct from the active site, specifically facilitates double-strand substrate interactions (Coquelle et al., 2011). These interactions are limited to the phosphatase domain.

The kinase domain obviously requires the binding of ATP for its activity and is defined in human PNKP by its Walker-A and –B motifs. The kinase domain belongs to the adenylate kinase family and consists of a 5'-stranded parallel β sheet, which is flanked by helices on both sides. Such an arrangement is common in P-loop kinases (Bernstein et al., 2005). The ATP-binding site and the DNA substrate binding site exist within a long cleft (Figure 1.10). The β- and γ-phosphates of ATP are bound by the Walker-A loop, whilst the Walker-B motif is involved in positioning the motifs and co-ordinating Mg^{2+} (a co-substrate required for activity). Mammalian PNKP shows kinase substrate preference towards a recessed 5'-hydroxyl with a 3' overhang greater than 3 nucleotides (Bernstein et al., 2005). This makes biological sense considering the 5' resection of DNA ends during HR of DSBs. An aspartic acid residue (Asp397 in human PNKP) is also responsible for the activation of the 5'-hydroxyl for attack on the ATP γ-phosphate (Weinfeld et al., 2011).

Of interest to this study is the fact that upon comparison of the hnRNP-U proteins and PNKP some homology can be observed in their respective putative kinase and established kinase domains. This is discussed in detail in section *3.2.1*.

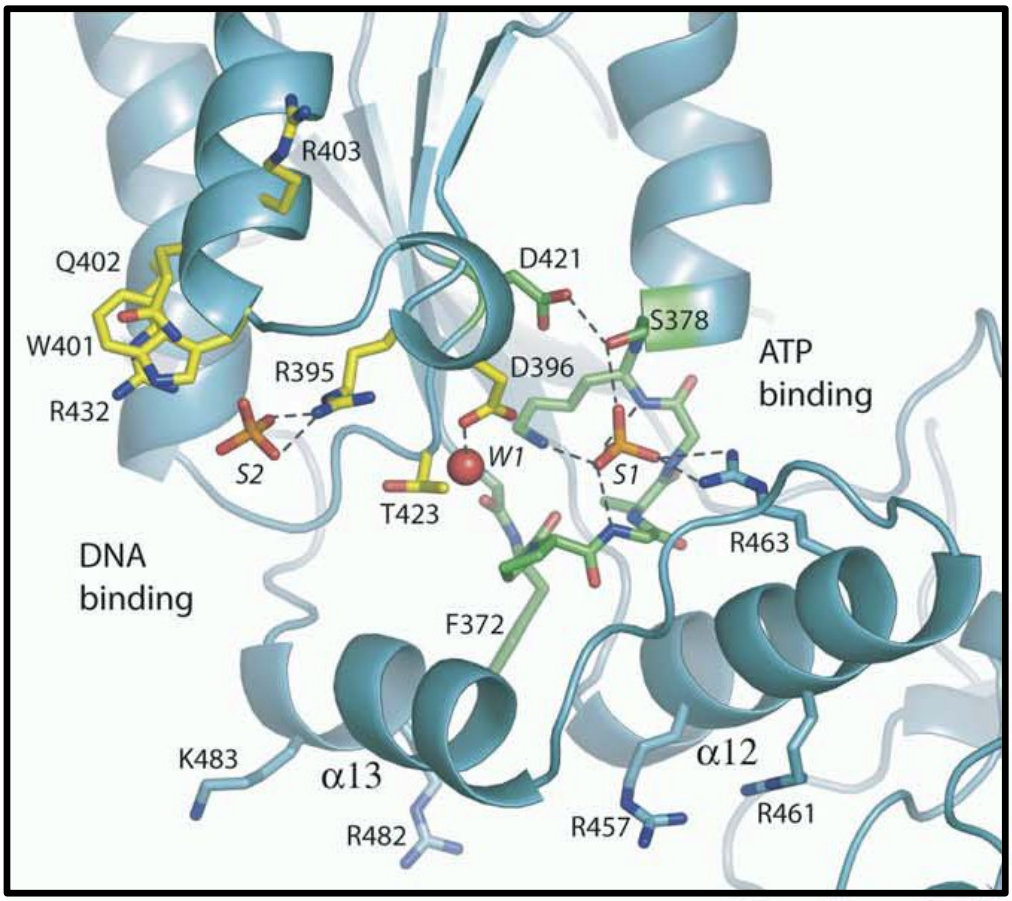

Figure 1.10 The mouse PNKP active site cleft permitting ATP and DNA binding. The Walker-A and –B motifs form the ATP-binding site and are shown in green. Sulphate ions bound at the active site are shown in orange and red. *S1* corresponds to the β-phosphate of ATP, while *S2* mimics the binding of a DNA backbone phosphate. The side chains of residues involved in catalysis or substrate binding are shown in yellow. The red sphere (*W1*) represents the location of the substrate 5'-hydroxyl during binding (Bernstein et al., 2005).

1.4 Amyotrophic lateral sclerosis (ALS)

Amyotrophic lateral sclerosis (ALS) is a hugely debilitating neurodegenerative disease affecting 4-6 people per 100,000 (Dion et al, 2009). Age of onset most commonly occurs between the ages of 45 and 60. The disease is relentlessly progressive with 50% of patients succumbing to death within 30 months and only 20% surviving between 5 and 10 years after initial symptom recognition (Talbot, 2009). It affects the lower motor neurons (LMNs) in the brainstem and spinal cord and the upper motor neurons (UMNs) in the motor cortex (Robberecht and Philips, 2013). As axons die and neuronal connections fail, symptoms and signs emerge with, typically, progressive muscular weakness and finally death resulting from paralysis and respiratory failure. There is also damage to neurons in the prefrontal and temporal cortex of the brain but this varies considerably amongst patients. The degeneration of these neurons results in cognitive defects in as many as 20-50% of ALS patients (Ringholz et al., 2005). In fact, there is an increasingly strong overlap between ALS and frontotemporal dementia (FTD), both clinically and pathogenically. FTD results from degeneration of neurons in the front and temporal lobes causing changes in personality, speech and behaviour (Lee et al, 2013). The genetic links between the two will be explored in detail later on.

Despite efforts, extensive investigations and trials, only one drug (riluzole) has been shown to have any beneficial effect on survival time for ALS patients, and it is a moderate 3-6 months (Bensimon et al., 1994). Unravelling of the disease aetiology is providing avenues for therapeutic agent design. The discovery of C9ORF72 GGGGCC (G_4C_2) repeat expansions has led to the development of small molecules targeting these repeats and decreasing amounts of the disease-causing protein (Su et al., 2014). The often late diagnosis of ALS creates a problem for treatment strategies. Cell replacement and stem cell therapies are a large area of current research, as are the use of siRNAs in an attempt to decrease the production of disease-

causing proteins in neuronal cells (Vuvic et al., 2014). However, the biggest strides in clinical therapy are being made in tackling physical symptoms to improve quality of life. For example, percutaneous gastronomy provides nutrition when oral intake is difficult due to dysphagia and respiratory management including assisting coughing to aid ventilation (Rosenfeld and Strong, 2015).

ALS is classified as familial (fALS) in 5-10% of cases, commonly with hereditary links and an autosomal dominant pattern of inheritance (Sreedharan, 2008). Patients who have no detectable affected relatives are said to have the sporadic form (sALS) of the disease. The two forms mirror one another clinically and in recent years have been shown to have many molecular and cellular commonalities, including genetic factors (Verma and Tandan, 2013).

1.4.1 ALS aetiology and pathogenesis

Large strides have been made in the last 5-10 years in the understanding of the disease's pathogenesis as more genetic causes are discovered. Like many other neurodegenerative diseases, aggregates of disease-causing mutant proteins are hallmarks of ALS (Robberecht and Philips, 2013). These ubiquitylated proteins aggregate in motor neurons and glial cells, primarily of the spinal cord and motor cortex causing an imbalance in normal protein homeostasis resulting in cellular stress (Laferriere and Polymenidou, 2015). Normal cellular functions, such as intracellular transport, cytoskeletal structure and mitochondrial function are disrupted to the point that the neurons become dysfunctional (Figure 1.11). The axons begin to retract, which initially can be countered by new sprouting and re-innervation by the axons of more resistant neurons (Saxena and Caroni, 2011). With time, however, the disease progresses as these compensative methods and the more resistant neurons are

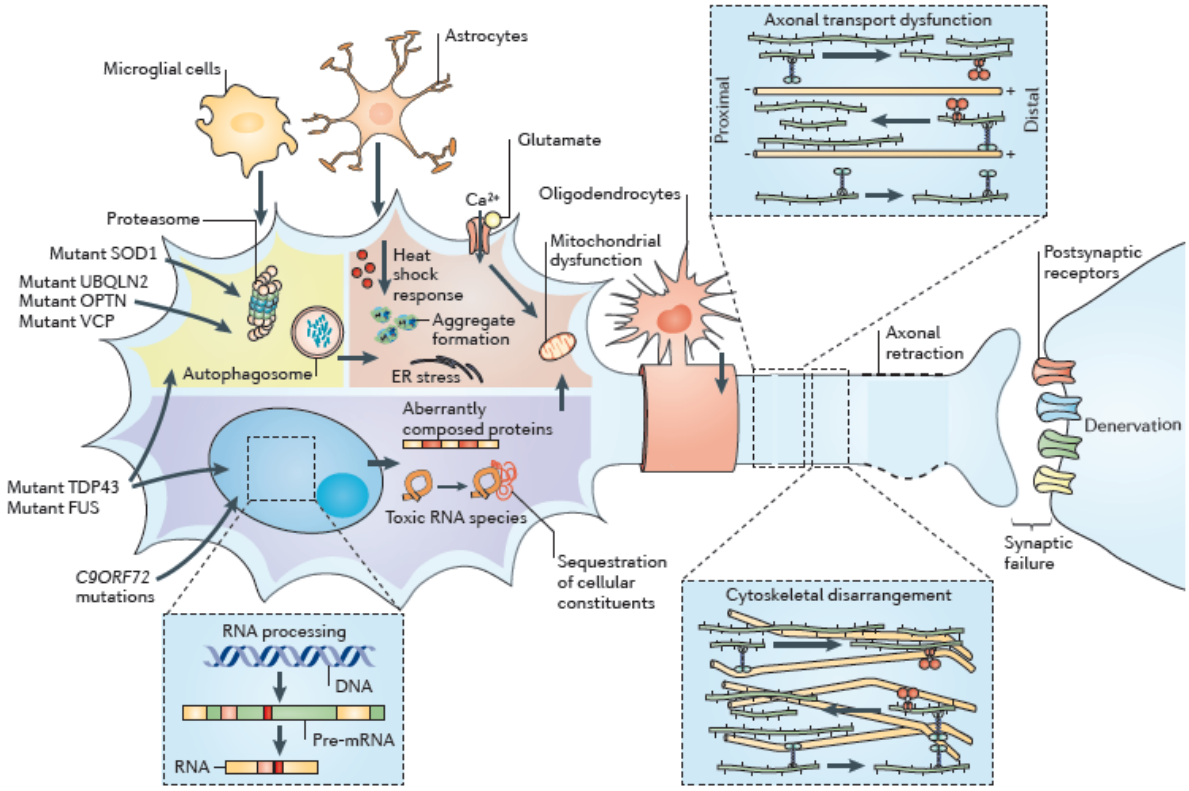

Figure 1.11 Overview of events in the pathogenesis of amyotrophic lateral sclerosis. Proteasomal and autophagic degradation of protein is caused by mutations in superoxide dismutase 1 (*SOD1*), ubiquilin 2 (*UBQLN2*), optineurin (*OPTN*), vasolin-containing protein (*VCP*) and potentially *TARDBP* (encoding TAR-binding protein 43 (TDP43)) and fused in sarcoma (*FUS*) (yellow). Mutations in chromosome 9 open reading frame 72 (*C9ORF72*), *TARDBP* and *FUS* cause aberrant RNA processing and structurally abnormal proteins (purple). This leads to aggregate formation, endoplasmic reticulum (ER) stress and mitochondrial dysfunction (orange). Cytoskeletal structures are misformed and axonal function fails leading to denervation and retraction. Non-neuronal cells affect this process either through loss of normal function or gain of toxic effect. Stress response capacity and susceptibility to excitotoxicity (for example, through the permeability characteristics of the glutamate receptor) are factors of vulnerability making neurons sensitive to these processes. (Adapted from Robberecht and Philips, 2013).

overcome. Following this axonal dysfunction and retraction, animal models have shown that the neuron cell bodies become visibly abnormal and die (Saxena and Caroni, 2011; Fischer et al., 2004).

In the following sections proteins that have been found to be mutated in ALS are discussed.

Superoxide dismutase 1 (SOD1) and oxidative stress

Understanding ALS at the molecular and genetic levels began with the identification of mutations in *SOD1*, which account for 15-20% of fALS cases (Dion et al, 2009). SOD1 is a cytosolic free-radical scavenger. More than 150 mutations have been reported to be pathogenic (Andersen and Al-Chalabi, 2011), of which nearly all are dominant. The discovery of a gene linked to ALS with an antioxidative role was not a surprise as there is a strong link between oxidative stress and neurodegenerative diseases (Barber and Shaw, 2010). Oxidative stress was shown to affect the release of presynaptic transmitters at neuromuscular junctions (Pollari et al., 2014). The amount of ROS in cells increases with age and is thought to be due to an increased leakage from the electron transport chain within mitochondria (Genova et al., 2004). Given that neuronal cells must function for long periods and have an extremely high energy demand provided through mitochondria, it is to be expected that they have an increased risk of ROS production and subsequently succumb to diseases such as ALS in which most cases are diagnosed past age 50. Whilst it remains unclear whether oxidative stress is an initial driver of degeneration or a consequence of other pathogenic factors, there is clear evidence of elevated oxidative stress in ALS patient neuronal cells. Several post-mortem studies have shown an increase in oxidative stress markers compared to controls (Ferrante et al., 1997; Beal et al., 1995; Shibata et al., 2001) and the extraction of cerebrospinal fluid from

ALS patients confirmed these increases at earlier stages of the disease (Bogdanov et al., 2000; Ihara et al., 2005).

The discovery of ALS patients with SOD1 mutations reinforced the link between oxidative stress and ALS. Mutant SOD1 animal models showed elevated levels of ROS with mutant SOD1 being one of the most highly oxidised proteins in the cell (Liu et al., 1998; Andrus et al., 1998). However, recent evidence suggests that loss of SOD1's dismutase activity is not critical for pathogenesis. Whilst some ALS patient SOD1 mutations do lead to decreased activity as a free-radical scavenger (e.g. A4V and G85R) leading to increased ROS accumulation, there are also many others that do not (e.g. G37R and G93A) (Borchelt et al., 1994; Yim et al., 1996). Additionally, SOD1 knockout mice did not develop ALS (Reaume et al., 1996), whilst manipulating wild-type levels of SOD1 in mutant SOD1-related ALS cells had no effect (Bruijn et al., 1998). Instead many SOD1 mutations cause misfolding and despite targeting for degradation through ubiquitylation, the proteins escape this process forming polymers and subsequently larger aggregates (Robberecht and Philips, 2013). Therefore, it appears that protein aggregation is critical in driving disease pathogenesis in SOD1 mutant patients. Interestingly, wild-type SOD1 proteins, that have undergone oxidation, have also been found in aggregates of sALS patients lacking SOD1 mutations (Brotherton et al., 2012).

Impaired protein degradation

The generation of cytoplasmic aggregates can occur due to interference with proteasomal and autophagic protein degradation caused by mutations in superoxide dismutase 1 (*SOD1*), vasolin-containing protein (*VCP*), ubiquilin 2 (*UBQLN2*) and optineurin (*OPTN*) (Figure 1.11) (Robberecht and Philips, 2012).

Transactive response element DNA/RNA binding protein of 43 kDa (TDP43)

TDP43, an RNA processing protein, is found in neuronal inclusions of 97% of ALS patients (Laferriére and Polymenidou, 2015). *TARDBP*, the encoding gene of TDP43, has been shown to have more than 35 dominant mutations causing ALS. Mutations were found to be predominantly located in the C-terminal region required for ribonucleoprotein binding and splicing (Sreedharan et al., 2008). The protein is part of the heterogeneous ribonucleoprotein family, which functions in transcription, RNA splicing and transport (see section *1.3.1*). Whilst predominantly located in the nucleus, during times of cell stress TDP43 largely resides in the cytoplasm and is recruited to stress granules. It functions to hold nonessential mRNA within an inactive state whilst the cell prioritises synthesis of proteins which can respond to the stressor, such as heat shock proteins (Robberecht and Philips, 2013). When stress resolves, TDP43 is released and relocates to the nucleus. A recent study showed TDP43 mutations to shift this nucleus-cytoplasmic balance in favour of the latter and it is thought that its presence within stress granules provides a pro-aggregation environment and consequently its inclusion within ALS aggregates (Johnson et al., 2008; Dewey et al., 2012).

Fused in sarcoma (FUS)

FUS is another RNA-processing protein with mutations linked to ALS. Like TDP43, FUS is predominantly nuclear, but is shuttled between nucleus and cytoplasm via transportin. The majority of ALS-causing mutations are missense and located within the C-terminal region, which, like *TARDBP*, contains a RNA-binding domain, as well as a nuclear localisation sequence (NLS). Disruption of nuclear import leads to cytoplasmic accumulation, recruitment to stress granules and continued aggregation (Dormann et al., 2010). Like TDP43,

FUS mutations are linked with FTD patients providing strong evidence that ALS and FTD are phenotypic variants of common pathological processes (Lee et al, 2013).

Chromosome 9 open reading frame 72 (C9ORF72)

Aetiological similarities between ALS and FTD subsequently led to genetic linkage studies and the identification of a locus on chromosome 9p21 in familial ALS-FTD (Vance et al., 2006) and genome-wide association studies in sporadic ALS and FTD (Shatunov et al., 2010; Lee at al., 2013). Further investigation revealed a GGGGCC (G_4C_2) repeat expansion within intron 1 of *C9ORF72* (DeJesus-Hernandez et al., 2011; Renton et al., 2011). It has proved to be a major breakthrough within the genetic analysis of ALS and it is now recognised as the most common genetic cause of both ALS and FTD. Repeats are found in over 40% of fALS, 20% of sALS cases, 25% of familial FTD cases and up to 90% of families with concurrent ALS and FTD (Renton et al., 2014; Majounie et al., 2012). Normal individuals typically have less than 25 G_4C_2 repeats (Majounie et al., 2012). Southern blotting studies have shown the repeats to number from 700-4400 in ALS and FTD patients (DeJesus-Hernandez et al., 2011; Gijselinck et al., 2012). C9ORF72 has a proposed role in endosomal and autophagy-lysosomal vesicle trafficking, suggesting a role in protein degradation (Farg et al., 2014). Interestingly, several patients with C90RF72 mutations have also been found to have mutations in a secondary gene, such as *TARDBP* (Van Blitterswijk et al., 2012). This suggests possible oligogenic aetiology of ALS and could provide a possible explanation for the phenotypic variation seen with C9ORF72 mutations, as well as their presence in both ALS and FTD patients (Robberecht and Philips, 2013).

1.4.2 RNA processing and ALS

In recent years, an irrefutable link has been made between RNA metabolism dysfunction and neurodegenerative diseases, including ALS and FTD (Xu et al., 2013). The emergence of this theme in ALS began with the identification of disease-associated mutations in the RNA-binding proteins, TDP43 and FUS. Both have extensive roles in RNA-processing, including RNA transcription, splicing, transport, translation and microRNA production. G_4C_2 hexanucleotide repeat expansions in *C9ORF72*, the most common known cause of fALS and sALS, have been shown to sequester RNA-binding proteins in nuclear foci including the direct binding of hnRNP-H to the RNA repeat nucleotides (Lee et al., 2013). Therefore, it appears that these major players are beginning to unravel a common link of dysfunction of RNA dynamics as a critical pathogenic mechanism in ALS. In addition, mutations in the RNA-binding proteins Ewing sarcoma breakpoint region 1 (EWSR1; Couthouis et al., 2012), TATA-box binding protein-associated factor 15 (TAF15; Couthouis et al., 2011), ataxin-2 (Elden et al., 2010), and more recently, hnRNP-A1 and hnRNP-A2/B1 (Kim et al., 2013) have all been associated with ALS. The various aspects of aberrant RNA processing leading to ALS pathogenesis are currently being elucidated and are discussed briefly below.

Mutations in TDP43 and FUS lead to mis-localisation away from the nucleus to the cytoplasm and may lead to cytotoxicity by a number of mechanisms. Both TDP43 and FUS regulate thousands of RNA targets (Polymenidou et al., 2011; Lagier-Tourenne et al., 2012). The dysregulation of such important proteins is likely to have severe downstream consequences. Whilst studies have shown that the overlap between the RNAs that the two proteins regulate is not very extensive, the 86 that they do have in common are enriched in very long intron sequences; these are known to have specific roles in neuronal cells suggesting an explanation for neuronal cell susceptibility (Lagier-Tourenne et al., 2012).

TDP43 and FUS depletion has been shown to result in the down-regulation of neuroglins and neurexins, proteins essential for effective neuronal function (Lagier-Tourenne et al., 2012). Studies investigating TDP43 and FUS knockdown effects have also shown complex alterations in splicing regulation depending on the specific binding location relative to exon-intron boundaries, causing enhanced or reduced exon splicing in hundreds of different genes (Tollervey et al., 2012; Polymenidou et al., 2011; Lagier-Tourenne et al., 2012).

RNA-processing proteins play important roles in protecting the cell during times of cellular stress, which include DNA damage, heat stress, and chemical exposures (Li et al., 2013). The priority in cells during this time is to conserve energy and divert cellular resources toward actions that will enable survival and recovery. Limiting translation of mRNAs to only those producing proteins required at that time is one way to conserve resources. This is achieved by assembling non-essential mRNAs and their associated RNA-processing proteins in to structures such as nuclear paraspeckles and cytoplasmic stress granules (SGs) where translation is stalled; later this may be reinitiated once the stress is cleared. Processing bodies (P-bodies) are separate sites at which mRNA may be degraded (Kedersha et al., 2005). Many RNA-processing proteins, including TDP43 and FUS, play important roles in SGs under conditions of cellular stress (Robberecht and Philips, 2013). An extended presence of TDP43 and FUS at SGs may sequester other RNA-binding proteins (RBPs) as both bind a diverse set of RNA-processing proteins, including several hnRNPs; however, no evidence of hnRNP-UL1 sequestration has been shown thus far (Freibaum et al., 2010; Chi et al., 2011). Extended periods of cellular stress suggest a potential mechanism for sALS initiation in which stress granule-mediated sequestration, rather than mutations, leads to dysfunction of RNA-processing proteins (Xu et al., 2013). Whilst considering these pathological pathways, perhaps most striking is that numerous studies have shown that deletion of the RNA-binding

domains in TDP43 and FUS prevents their aggregation and reduces cytotoxicity, confirming RNA-binding as a crucial factor in their ALS pathogenesis (Voigt et al., 2010; Ihara et al., 2013; Daigle et al., 2012).

C9orf72 RNA transcripts with G_4C_2 repeats form unique G-quadruplex secondary structures and DNA-RNA hybrids, which also sequester RBPs (Reddy et al., 2014; Lee et al., 2013). Subsequent depletion of RNA-processing proteins may cause ALS toxicity through RNA misprocessing. Despite the hexanucleotide repeat of *C9orf72* being within the first intron it is translated into polypeptides by a unique pathway known as repeat-associated non-AUG dependent (RAN) translation (Barmada, 2015) (Figure 1.12). Defective splicing and stalling of the ribosomal machinery results in translation in all reading frames of both the sense and anti-sense strands (Mori et al, 2013). This produces dipeptide repeats, such as poly-(Gly-Ala), poly-(Gly-Pro) and poly-(Gly-Arg), which induce aggregation, disrupt RNA processing within nucleoli (Kwon et al., 2014) and alter the function of Unc119, a protein required for axon development (May et al., 2014; Knobel et al., 2001). Recently, C9ORF72 has been proposed to have a role in endosomal and autophagy-lysosomal vesicle trafficking (Farg et al., 2014). A role in protein degradation like that of ubiquilin-2 may be another mechanism leading to the protein accumulation seen in ALS.

In addition to RNA expression, RNA splicing and sequestration, aberrant TDP43 and FUS function interferes with the biogenesis and processing of noncoding regulatory RNAs, such as microRNA (miRNA). Both proteins have been shown to bind directly to a number of miRNAs, as well as to interact with the miRNA processing complexes Drosha and Dicer (Gregory et al., 2004; Kawahara and Mieda-Sato, 2012). ALS patient cells exhibit abnormal miRNA levels and TDP43 depletion has been shown to significantly reduce levels of miR-132-5p, miR-143-5p/3p and miR-574-3p (Freischmidt et al., 2013). Interestingly, miRNA

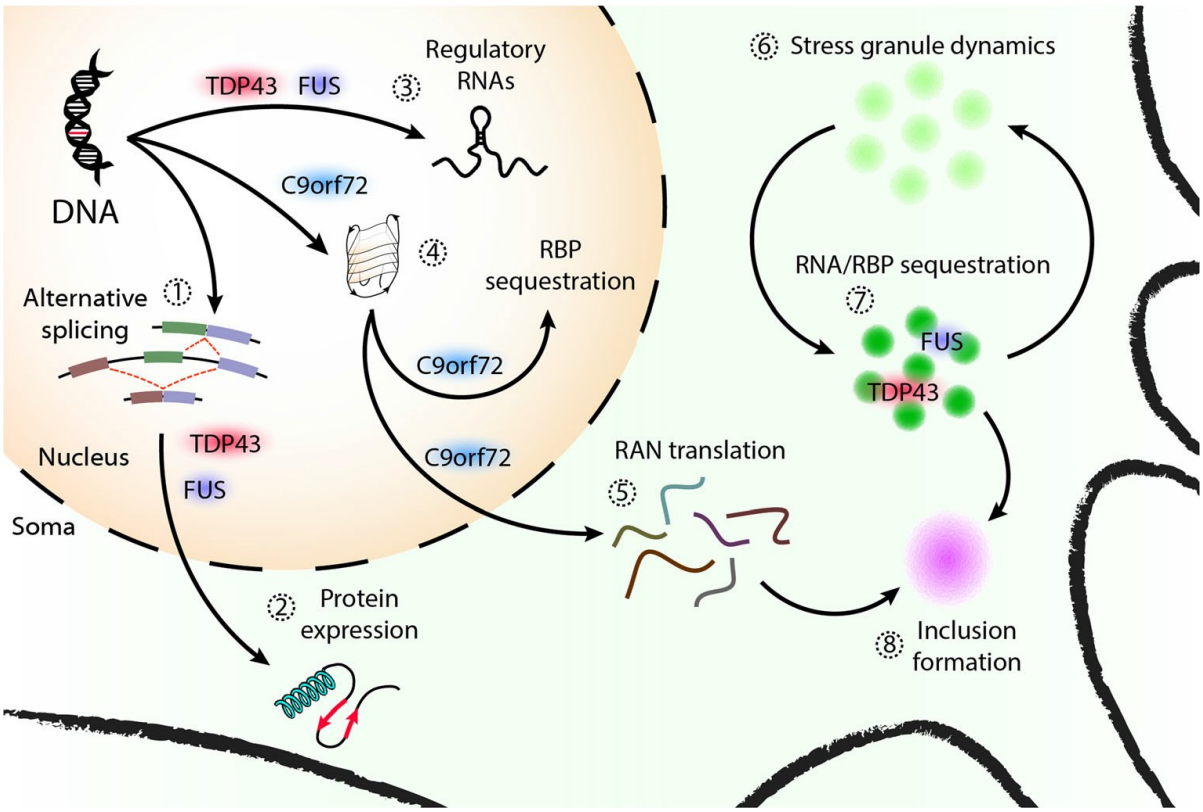

Figure 1.12 RNA dysfunction in ALS. Abnormal levels or localisation of transactive response element DNA/RNA binding protein of 43 kDa (TDP43) and fused in sarcoma (FUS) can alter (1) RNA splicing, (2) protein expression and (3) regulation by noncoding RNAs. (4) C9orf72 G_4C_2 repeats can sequester RNA-binding proteins (RBPs) and (5) expression through repeat-associated non-AUG dependent (RAN) translation causes further toxicity. (6) TDP43 and FUS participate in stress granule formation and abnormal dynamics may result in (7) RNA/RBP sequestration leading to (8) the formation of classical ALS protein aggregates (Barmada, 2015).

levels are tissue type-specific and very important to neuronal health. Their depletion has been shown to lead to neurodegeneration and provides further evidence for the selective vulnerability of motor neurons in ALS (Kawara and Mieda-Sato, 2012; Haramati et al., 2010).

1.4.3 Prion-like domain (PrLD) proteins and ALS

Prion proteins contain primary sequences which enable folding in to a number of different conformations. In addition, the 'prion form' can self-replicate by converting the native isoform to its own and seeding aggregation. The effects can be extensive as the new conformation typically alters protein function and diminishes the population of the native isoform. This behaviour is perhaps best known in prions causing transmissible brain wasting diseases, such as bovine spongiform encephalopathy (BSE) and Creutzfeldt-Jakob disease (CJD) (Colby and Prusiner, 2011). However, prion proteins are not all transmissible pathogens and are advantageously utilised in yeast (*Saccharomyces cerevisiae*) to pass specific heritable phenotypes from mother to daughter cell (Shorter and Lindquist, 2005). In addition, a prion-like behaviour of human proteins underpinning the pathogenesis of neurodegenerative diseases has begun to be elucidated in recent years (King et al., 2012). Due to the protein misfolding and aggregation seen in Parkinson's disease (PD), Alzheimer's disease (AD) and tauopathies (neurodegenerative diseases associated with an aggregation of tau protein) they have been termed proteinopathies, with α-synuclein in PD, β-amyloid in AD, and tau protein in various forms of dementia being the major proteins responsible by emulating prion behaviour (Grad et al., 2015).

ALS is also considered a proteinopathy as protein aggregation defines the disease. The focal start and contiguous, progressive spread of affected neurons in ALS is typical of the

seeded aggregation of prion proteins and has formed the basis of a prion-based theory of pathogenesis (Grad et al., 2015). The theory has gained momentum with the discovery of more and more proteins involved in ALS that have prion-like domains (PrLDs) and propensities. Yeast prion domains were originally thought of as 60 amino acids or more in length and enriched in asparagine (N) and glutamine (Q). Tyrosine (Y) and glycine (G) are now also recognised as relatively important residues for prion propensity. These amino acids generate a sequence of low complexity allowing flexibility in their intrinsic folding (Alberti et al., 2009; Toombs et al., 2010). Increasingly sophisticated algorithms have been designed in recent years which have allowed the identification of domains with possible prion-like behaviour. Among the 246 of 21,873 human genes analysed showing PrLDs there was a ~12-fold enrichment for RNA-binding proteins containing an RNA-recognition motif (RRM) domain (Couthouis et al., 2011). Another study showed of the 210 human RRM-bearing proteins, 29 have a PrLD, and 12 of these score in the top 60 prion candidates in the entire genome (King et al., 2012). Considering the importance of RNA-binding proteins in ALS this is a striking and interesting discovery. Of the RRM-containing proteins with PrLDs, the ALS-linked FUS, TAF15, EWSR1, and TDP43 were ranked 1st, 2nd, 3rd and 10th respectively, for prion propensity (King et al. 2012; Couthouis et al., 2011). FUS contains an N-terminal (amino acids 1-239) and TDP43 a C-terminal (amino acids 274-414) PrLD (Maniecka and Polymenidou, 2015). The domains make the proteins aggregation-prone and a prolonged presence in the cytoplasm may be enough to stimulate permanent aggregation. Furthermore, the majority of ALS-linked missense mutations occur within this domain of TDP43 increasing aggregation propensity and neurotoxicity (Johnson et al., 2009; Guo et al., 2011). Whilst the majority of ALS-causing FUS mutations were initially discovered in the nuclear localisation sequence, a large number have now been identified in the N-terminal PrLD (Da Cruz

and Cleveland, 2011). In contrast to TDP43 and FUS, wild-type SOD1 is structurally very stable and it is the ALS-linked mutations that confer an aggregation propensity (Chia et al., 2010; Prudencio et al., 2009).

There is a growing body of evidence for a crucial role of prion-like behaviour of ALS-linked proteins. Small amounts of aggregated SOD1 (Chia et al., 2010), TDP43 (Furukawa et al., 2011) and FUS (Nomura et al., 2014) were shown to induce mis-folding of their corresponding natively folded counterparts *in vitro*, suggesting template-dependent propagation like that of prions. Increased expression of TDP43's PrLD induced aggregation and cytotoxicity (Furukawa et al., 2011), whilst deletion of the domains in TDP43 and FUS prevented aggregation, providing strong evidence of their requirement for efficient seeding (Furukawa et al., 2011; Sun et al., 2011). TDP43 aggregates isolated from brain tissues of ALS patients have been shown to seed protein misfolding and accumulation when introduced to cultured cells, and the aggregates persisted within cells when the original pathogenic seed was removed showing a prion-like seeding capability (Nonaka et al., 2013).

In vivo studies have also shown supportive evidence for prion-like behaviour of SOD1 and TDP43. Co-expression of wild-type human SOD1 ($hSOD1^{WT}$) and $hSOD1^{A4V}$ (the most aggressive SOD1 mutant in humans) in transgenic mice resulted in an ALS-like phenotype (Deng et al., 2006). Even the simple overexpression of $hSOD1^{WT}$ or $hTDP43^{WT}$ in transgenic mice caused aggregation, neurotoxicity and shortened lifespan (Graffmo et al., 2013; Xu et al., 2010). Transmissibility between mice by injection of homogenates from terminally sick ALS mice has proved very inefficient and appears to reflect the non-transmissible nature of human neurodegenerative diseases, despite strong evidence for prion-like behaviour in the causative proteins (Maniecka and Polymenidou, 2015).

Studies are now beginning to show the functional/clinical relevance of many RNA-binding proteins possessing PrLDs. These domains allow the proteins to rapidly self-associate in to aggregate-like structures including the complexes required to carry out normal RNA metabolism, as well as the stress-related paraspeckles (Hennig et al., 2015), SG and P-body structures (Li et al., 2013) discussed in section *1.4.2*. The rapid self-aggregation, made possible by the PrLDs, allows the RNA-binding domains to recruit mRNAs and accumulate them in these stress granules until the cellular stress subsides. The reversibility of the prion-like aggregation subsequently allows the granules to disassociate and translation to resume as normal (Li et al., 2013). It appears that the proteins involved in forming these aggregate-like structures do so by a process called liquid-to-solid phase transition (Patel et al., 2015). This is achieved by extruding water resulting in the formation of a mesh-like structure described as a hydro-gel. This is different from the amyloid fibres formed by disease-causing prion proteins and is thought of as a functional alternative in eukaryotic cells (Hennig et al., 2015). However, these liquid-to-solid phase transitions have been shown to increase in speed in models using FUS proteins with ALS-associated mutations compared to WT protein (Patel et al., 2015). It appears that mutations in the PrLDs of ALS-associated RNA-processing proteins increase the risk of permanent aggregation in cells over time. The protein interactions move from being flexible hydrogels to forming solid fibrous structures and this may underlie a large part of the disease's pathogenesis (Lin et al., 2015).

As mentioned earlier, studies employing the use of mathematical models and algorithms had found a striking number of RRM containing proteins to also have PrLDs (Couthouis et al., 2011; King et al., 2012). Li et al. (2013), used the algorithm detailed in Alberti et al. (2009) to assess prion score in all human RNA-binding proteins, including those with RRMs and those with other types of RNA-binding motifs. This included RGG

domains, like that of hnRNP-UL1, and subsequently hnRNP-UL1 was found to score 10th for all human RNA-binding proteins and 37th for all human proteins (hnRNP-U also scored 15th amongst RNA-binding proteins).

PrLD prediction software programmes are also available online. Using PLAAC (prion-like amino acid composition), hnRNP-UL1 and –U are both shown to form PrLDs in their C-terminal regions. hnRNP-UL1's PrLD is larger and extends 242 amino acids from residue 615 to 856, whilst hnRNP-U's is 131 amino acids from residue 695 to 825 (Figure 1.13). A second sequence in hnRNP-U (aa168-188) and one in hnRNP-UL2 (aa642-691) are also prion-like in composition, but as they fall short of the widely considered 60 amino acid length minimum requirement for proper PrLD formation these are much less likely to affect aggregate formation (Figure 1.13). Given the role of hnRNP-UL1 in RNA-processing, its predicted PrLD and the discovery of hnRNP-A1 and –A2 mutations in ALS patients, hnRNP-UL1 is a strong ALS-associated gene candidate.

1.4.4 ALS and the DDR

Defective DNA damage responses have been strongly linked to cancer for many years, and more recently to aging and neurological disorders. Many of these disorders are congenital, such as ataxia telangiectasia (A-T), ataxia with occulomotor apraxia-1 (AOA1) and Cockayne syndrome (CS) (Madabhushi et al., 2014). However, growing evidence suggests that aberrant DNA damage responses and accumulated DNA damage correlate with neurodegeneration in AD, PD and ALS (Coppedé and Migliore, 2009; Banerjee et al., 2009; Coppedé and Migliore, 2015). An accumulation of DNA damage in neurons is unsurprising given that they are generally post-mitotic, can function for a whole life time and have a high

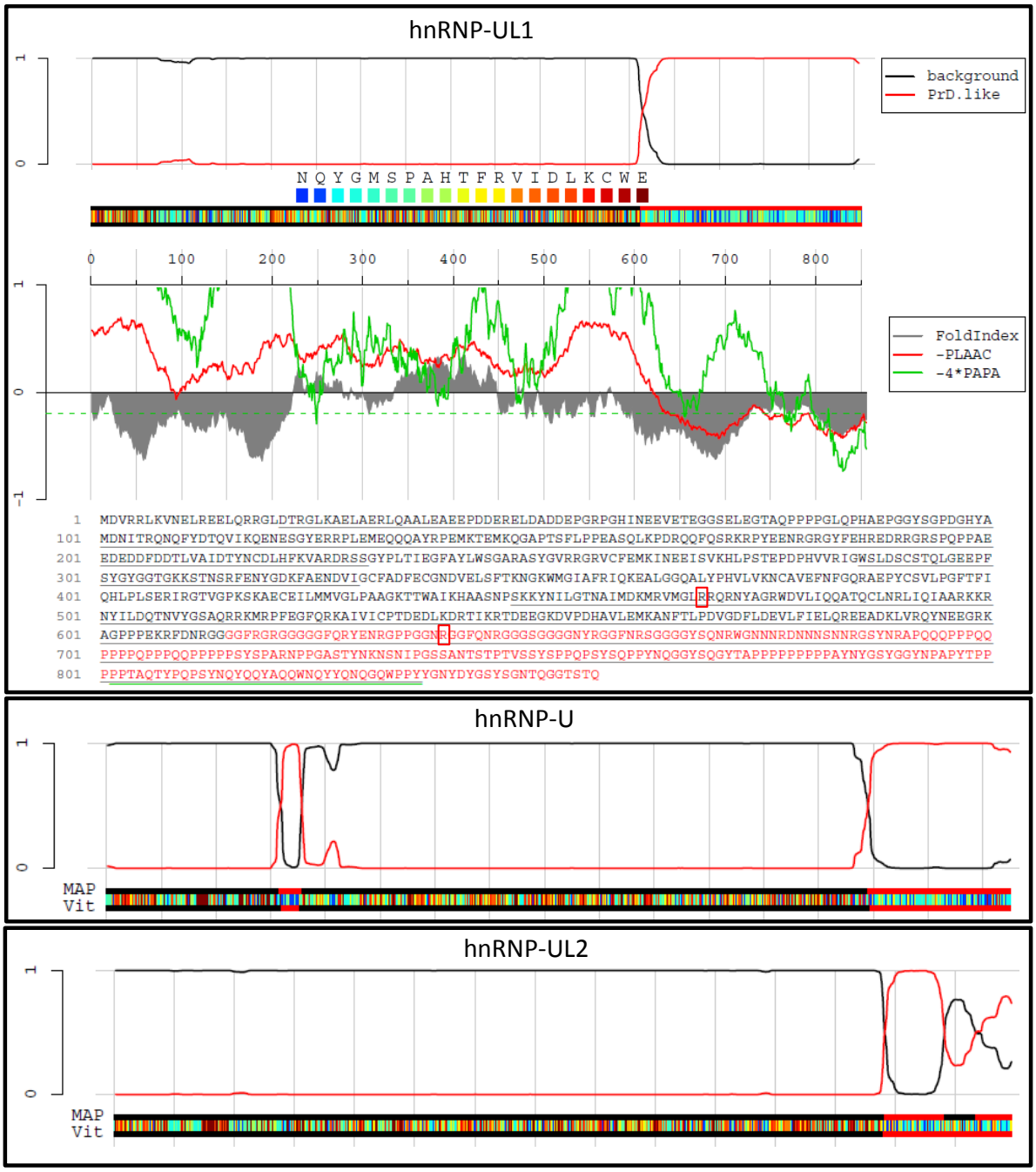

Figure 1.13 PrLD assessment of hnRNP-UL1, -U and –UL2 using PLAAC. Protein sequences were inputted in to PLAAC (prion-like amino acid composition; an algorithm-based prion-prediction web application) and graphical visualisation of data is shown. Each amino acid contributes to a hidden Markov model on a sliding scale within the protein to predict regions which are background (black line close to 1) or prion domain like (red line close to 1). hnRNP-UL1 is predicted to have a 292 aa prion-like region at its C-terminus, hnRNP-U has a 130 aa prion-like region at its C-terminus and hnRNP-UL2 a prion-like

region of less than 60 aa's. Each AA is colour-coded by its enrichment log-likelihood ratio. Further scores are generated by different algorithms all used to predict prion-like regions with the use of varying criteria; FoldIndex predicts intrinsically unfolded regions (grey curve less than zero); -PLAAC (red curve less than zero) and -4*PAPA (green curve less below the green dashed line) incorporates hydrophobic residue influence on amyloid formation. See Lancaster et al. (2014) for full details.

metabolic rate resulting in high levels of reactive oxygen species (ROS). Mitochondrial DNA (mtDNA) is particularly susceptible to oxidative damage due to its proximity to the mitochondria's inner membrane, which produces oxidative species during cellular respiration (Coppedé and Migliore, 2015).

The most common DNA lesion caused by ROS is 8-oxoguanine. Increased levels of 8-oxoguanine were observed in the neuronal cells of both sALS and fALS patients (Ferrante et al., 1997). Levels were also raised in the plasma, cerebrospinal fluid (CSF) and urine of ALS patients, with levels in urine correlating to disease severity (Bogdanov et al., 2000). Studies using a $SOD1^{C93A}$ transgenic fALS mouse model revealed oxidative nuclear and mtDNA damage in spinal motor neurons at very early stages of the disease (Aguirre et al., 2005; Warita et al., 2001). A further study showed a progressive increase of DNA damage with development of the disease, with SSBs occurring earlier than DSBs (Martin et al., 2007). Such evidence suggests that an accumulation of DNA damage, particularly in mitochondrial DNA contributes to mitochondrial dysfunction and motor neuron death as the cells have high metabolic requirements.

FUS has been shown to have a critical role in the DNA damage response itself. FUS is rapidly recruited to DSB sites in a PARP-1 dependent manner and depletion significantly reduced repair by both HR and NHEJ mechanisms (Mastracola et al., 2013; Rulten et al., 2013). FUS also forms a complex with HDAC-1 in response to DSBs, a protein critical to DNA repair in post-mitotic neurons (Wang et al., 2013). Moreover, ALS patient mutations of FUS (R521G, R521C, R224C and R514S) diminished recruitment to DSB sites and caused defective damage responses (Rulten et al., 2013; Wang et al., 2013; Qiu et al., 2014). This suggests that such mutations would affect efficient repair in neuronal cells of ALS patients causing further cellular dysfunction and toxicity.

Many parallels exist between FUS and hnRNP-UL1 including the presence of PrLDs, RGG motifs and major roles in RNA processing. In fact, both proteins bind U7 snRNP, but with different effects on transcriptional regulation. FUS stimulates the upregulation of histone gene expression (Raczynska et al., 2015), whereas hnRNP-UL1 downregulates the expression outside of S phase (Ideue et al., 2012). Both proteins also have roles in the DDR in the response to DSBs and both are rapidly recruited in a PARP-1 dependent manner (Mastracola et al., 2013; Hong et al., 2013). Other hnRNPs have also been found to have a role in ALS aetiology. hnRNP-A1 and hnRNP-A2B1 mutations were found to cause ALS in one family with the mutations occurring in the proteins' PrLDs stimulating aggregation by fibril formation (Kim et al., 2013). hnRNP-A2 and hnRNP-C1/C2 were found to be mis-localised to inclusion bodies in the muscle biopsies of ALS and FTD patients compared to controls (Cortese et al., 2014). Such sequestration of RNA processing proteins affects RNA transcription, expression and splicing as discussed in section *1.4.2*, whilst sequestration of FUS and theoretically hnRNP-UL1, although this has not been shown, would also lead to defective DNA damage repair. In addition, hnRNP-U (the homolog of hnRNP-UL1) deletions were identified in patients suffering from a neurological condition characterised by intellectual disability (ID), microcephaly, craniofacial anomalies, seizures, limb anomalies, and corpus callosum abnormalities (Thierry et al., 2012). Taken together results from all these studies generated our interest to study hnRNP-UL1's role in the DDR from an 'ALS viewpoint'.

1.5 Aims

Based on the identification of the putative kinase domain in hnRNP-UL1 and the discovery of ALS patients with hnRNP-UL1 mutations this study will have two principle aims. Firstly, to investigate the nucleotide binding and kinase activity of hnRNP-UL1 and, secondly, to investigate the DNA damage response in cells harbouring mutations in hnRNP-UL1. In order to determine this, a number of objectives will be addressed:

1. To confirm the ability of hnRNP-UL1 to bind ATP via interaction at its Walker A loop motif.
2. To determine whether hnRNP-UL1 exhibits kinase activity.
3. To determine whether ALS patient derived lymphoblastoid cell lines harbouring hnRNP-UL1 mutations exhibit defective DNA damage responses in response to various damaging agents.
4. To investigate any defects in the normal processes and characteristics of mutant forms of hnRNP-UL1 in comparison to wild-type. This includes:
   a) DNA damage responses.
   b) Protein-protein interactions.
   c) DNA interactions.

   This will be achieved by siRNA knockdown of endogenous hnRNP-UL1 and the transfection of mutated variants allowing the transient expression of only the variant protein forms in cells before treatments/experiments.

CHAPTER II

MATERIALS AND METHODS

2.1 CELL BIOLOGY TECHNIQUES

2.1.1 Cell Lines

All cell lines used during this study were of human origin. Individual lines are listed in Table 2.1.

Table 2.1 - Cell lines used in this study.

Cell Line	Cell Type	Source	Culture Medium
HeLa	Epithelial	Cervical carcinoma	DMEM
HeLa Flp-In	Epithelial	Cervical carcinoma	DMEM
A549	Epithelial	Small cell lung carcinoma	DMEM
293FT	Epithelial	Embryonic kidney	DMEM
ALS patient cell lines*	Lymphoblasts	ALS patient blood samples provided by Professor Jochen Weischaupt (University of Ulm, Germany)	RPMI

* For further details see section *4.2.1.*

2.1.2 Cell culture media

Cell lines were maintained in Dulbecco's Modified Eagle's Medium (DMEM, Sigma) or Roswell Park Memorial Institute (RPMI) 1640 medium (Sigma), supplemented with 8% Foetal Calf Serum (FCS) (Sigma). Antibiotics were not used.

2.1.3 Maintenance and passage of cell lines

Cells were cultured in humidified incubators at 37 °C with a supply of 5 % CO_2. Lymphoblastoid cell lines (LCLs) are non-adherent and grow in suspension. LCLs were

passaged by removal of cells to required dilution and addition of fresh media. All other cell lines were adherent, grown in monolayers and passaged as follows. Media was removed and cells washed with pre-warmed (to 37 °C) phosphate-buffered saline (PBS) (Gibco). Trypsin (Gibco) was added and incubated at 37 °C until cells had detached. The trypsin was deactivated by the addition of fresh media, and cells pelleted by centrifugation at 430 g for 5 minutes (mins). Pellets were subsequently resuspended in fresh medium, and re-plated at the appropriate dilution.

2.1.4 Cryopreservation of cell lines

Cells were trypsinised and pelleted as above, followed by re-suspension in medium containing 20 % FCS and 10 % DMSO (Sigma). Aliquots of 1ml were cooled to -80 °C at a controlled rate of 1°C/min via the utilisation of isopropanol. Samples were transferred to liquid nitrogen storage tanks for long term storage at -180 °C. Cells were rapidly thawed in medium at 37 °C, pelleted by centrifugation, and re-suspended in fresh medium before plating, as required.

2.1.5 IR and UV irradiation

Employing a 137 Cs source (irradiator model CIS IBL 437), cells were treated or mock-treated with ionising γ-rays at a dose-rate of 2.5 Gy/min. Prior to UV irradiation, medium was removed and cells washed with PBS. Cells were subsequently irradiated or mock-irradiated with UV radiation before replacement of medium. UV radiation (0.7 $J/m^2/sec$) with a wavelength of 254 nm was delivered in a single pulse using a Blak-Ray XX15S UV Bench Lamp (UVP).

2.1.6. Drug treatments

2.1.6.1 Camptothecin

Camptothecin (CPT) is a cytotoxic quinolone alkaloid, which inhibits DNA topoisomerase I. Non-adherent LCLs had CPT added directly to the media at a final concentration of 400 nM. The drug was left in the media and a proportion of the medium/cells harvested at the appropriate time points (*Section 2.3.1*). Adherent cells had media removed and fresh media containing 1 μM CPT added. Cells were harvested at appropriate time points (Section *2.3.1*).

2.1.6.2 Kinase inhibitors

During γ-^{32}P-ATP kinase assays cells were treated with various kinase inhibitors prior to cell harvesting. Stock concentrations were diluted in fresh media to the indicated concentrations in Table 2.2, before addition to cells. Inhibitors were also included in the reaction buffer during the kinase assays to the indicated concentrations in Table 2.2.

Table 2.2 – Kinase inhibitors used in kinase assays.

Name	Target	Stock concentration	Concentration used in media	Concentration used in kinase assays
VE-821	ATR	10 mM	5 μM	5 μM
KU55933	ATM	250 mM	25 μM	25 μM
NU7441	DNA-PK	5 mM	25 μM	25 μM
Roscovitine	CDK I/II	10 mM	20 μM	20 μM
SP600125	JNK	25 mM	25 μM	25 μM
Rapamycin	Mtor (p70S6K)	100 mM	20 μM	20 μM

V0126	ERK/MEK	10 mM	10 μM	10 μM
GSKIWH	GSK α/β	5 mM	5 μM	5 μM
SB203580	p38 α, β, γ, δ	10 mM	10 μM	10 μM
Plk1i (BI 2536)	PLK1	100 μM	20 μM	20 μM
Cdk1/2i III	CDK1 and CDK2	2.5 mM	20 μM	20 μM
Chk1i (Gö6976)	Chk1	1.32 mM	20 μM	20 μM

2.1.6.3 Tert-butylhydroquinone

Tert-butylhydroquinone (TBHQ) is an anti-oxidant, which also stimulates oxidative stress. HeLa cells were exposed TBHQ at differing concentrations and cells harvested at appropriate time points following treatment.

2.1.7 RNA interference (RNAi)

Control small interfering RNAs (siRNAs) and siRNAs targeting hnRNPUL1 are shown in Table 2.3.

Table 2.3 - siRNAs used in this study.

Target	**siRNA**	**Sense sequence**	**Company**
Non-silencing	MISSION siRNA universal negative control	5’ CGU ACG CGG AAU ACU UCG A dT dT 3’	Sigma

hnRNPUL1	Custom	5’ GCA GUG GAA CCA GUA CUA U dT dT 3’	Sigma
hnRNPUL2	SMART pool	5’ CAG AUU GCU UCC CGG ACA A 3’ 5’ CGG GGU AAA UGG UGG CGA A 3’ 5’ GUA AAG AGA CAG CGG GAU G 3’ 5’ CGG ACA AAU CGC CGA AAC A 3’	Thermo Scientific

Transfection of siRNA in to cells was carried out as follows. Cells were plated into 6 cm dishes 24 hours prior to transfection ensuring 80 % (±20) confluency the following day. Oligofectamine (OF) reagent (Invitrogen) was used to deliver siRNA duplexes into cells. 20 µl OF was added to 80 µl Opti-MEM, mixed and left for 5 mins at room temperature (RT). 17 µl of the appropriate siRNA (20 nM) was then added to 333 µl Opti-MEM, mixed and left for 5 mins at room temperature (RT). The OF mix and siRNA mix were then combined, vortexed and left for 20 mins at room temperature (RT). Cells were washed with Opti-MEM, 1 ml of Opti-MEM added per 6 cm dish and OF-siRNA liposome complexes added to the appropriate dishes. After 4-6 hour incubation at 37 °C the mixture was removed and replaced with fresh media. Transfections were repeated 24 hours after initial treatment.

Occasionally the second siRNA treatment was combined with DNA plasmid transfection. When doing so, Lipofectamine (LF) reagent (Invitrogen) was used instead of OF and the siRNA was combined with the plasmid DNA and the protocol described in *2.1.8* followed.

2.1.8 Transfection of plasmid DNA

DNA plasmids encoding a protein of interest were transfected into cells allowing subsequent expression of the protein for the following 72 hour period. Transfection of plasmid DNA in to

cells was carried out as follows. Cells were plated into 6 cm dishes 24 hours prior to transfection ensuring 80 % (±20) confluency the following day. LF reagent (Invitrogen) was used to deliver cDNAs into cells. 5 µl LF was added to 200 µl Opti-MEM, mixed and left for 5 mins at RT. 1 µg of plasmid DNA was added to200 µl Opti-MEM, mixed and left for 5 mins at RT. The LF mixture and plasmid DNA mixture were then combined, vortexed and left for 20 mins at RT. The LF-plasmid mixture was then added drop-wise to the media covering the cells and placed back in the 37 °C incubator.

2.2 MOLECULAR BIOLOGY TECHNIQUES

2.2.1 Preparation of media and plates

Luria broth (LB) was prepared with 10 g/l NaCl, 10 g/l bacto-tryptone and 5 g/l yeast extract in water, and sterilised by autoclaving at 120 °C and 100 kPa for 30 mins. LB-agar was prepared by adding 15 g/l agar to LB, and sterilising the solution by autoclaving as above. After cooling, ampicillin was added to a final concentration of 100 µg/ml. Before solidifying, aliquots of LB-agar were poured on to plates and left to cool inside a sterile fume hood. LB-agar plates were stored at 4 °C until used for bacterial transformations.

2.2.2 Bacterial transformations

Transformations of plasmids were carried out using competent α-Select Competent Cells (Bioline). Up to 100 ng of DNA was added to 10 µl of competent cells and incubated on ice for 20 mins, before being heat-shocked at 42 °C for 45 seconds. Cells were placed back on ice for 5 mins, before addition of 200 µl of LB and incubation at 37 °C for 1 hour. Cells were

then spread evenly on to LB-agar plates containing ampicillin, and incubated at 37 °C overnight.

2.2.3 Large scale preparation of DNA plasmids

Plasmids used in this study and the proteins they encode are detailed in Table 2.4.

Inoculation loops were used to pick colonies, and used to inoculate 5 ml cultures of LB containing 100 μg/ml ampicillin. Small cultures were incubated at 37 °C in an orbital shaker at 0.9 g overnight. 1 or 2 ml of these cultures were then transferred to large flasks containing 300 ml LB supplemented with 100 μg/ml ampicillin , and left to grow overnight at 37 °C in an orbital shaker at 0.9 g. The cells were then pelleted by centrifugation at 4000 g for 10 mins at 4 °C. Plasmid DNA was extracted from bacterial pellets using HiPure Plasmid Filter Maxiprep Kit (Invitrogen), according to the manufacturer's instructions. Final DNA pellets were resuspended in an appropriate volume of sterile nuclease-free water (Promega). DNA concentration was measured using a NanoDrop 2000 Spectrophotometer (Thermo Scientific).

Table 2.4 – Plasmids used in this study.

Plasmid	**Vector**	**Product**	**Tag**	**Amino acid mutation**	**Source**
hnRNPUL1-WT	pcDNA3	hnRNP-UL1	HA	None	R. Grand
hnRNPUL1-MWA	pcDNA3	hnRNP-UL1	HA	GKT433ARA	MDS*
hnRNPUL1-639	pcDNA3	hnRNP-UL1	HA	R639C	MDS*

hnRNPUL1-WT-siRES	pcDNA5/FRT/TO	hnRNP-UL1	HA	None	MDS*
hnRNPUL1-MWA-siRES	pcDNA5/FRT/TO	hnRNP-UL1	HA	GKT433ARA	MDS*
hnRNPUL1-639-siRES	pcDNA5/FRT/TO	hnRNP-UL1	HA	R639C	MDS*
hnRNPUL1-468-siRES	pcDNA5/FRT/TO	hnRNP-UL1	HA	R468C	MDS*
Flp-F70L	pOG44	Flp recombinase	n/a	n/a	Fisher Scientific

*MDS = Made during study. WT = wild-type, MWA = mutated Walker A, siRES = siRNA resistant.

2.2.4 Agarose gel electrophoresis

Agarose gels were prepared by dissolving agarose in TBE (100 mM Tris-HCl, 100 mM boric acid, 2 mM EDTA, pH 8) buffer to a final concentration of 1 %. The agarose was dissolved by heating to boiling point, before cooling and subsequent addition of ethidium bromide (Fisher Scientific) to a final concentration of 0.5 μg/ml. Before setting, the mixture was poured in to gel electrophoresis apparatus casts. DNA samples were diluted with 6X loading buffer (0.25 % bromophenol blue, 50 % glycerol in a 10 mM Tris-HCl, 1 mM EDTA, pH 8). Electrophoresis was carried out at 40 V in TBE running buffer for an appropriate time period. DNA was visualised with a UV transilluminator.

2.2.5 Site-directed mutagenesis PCR

Oligonucleotide primers were designed to mutate hnRNPUL1 either to cause amino acid substitutions or to provide resistance to siRNA. Primers used are detailed in Table 2.5 and were all purchased from Sigma-Aldrich.

Table 2.5 – Primer sequences used to generate mutated forms of HA-hnRNP-UL1.

Mutated Residues	**Primer Sequence**
GKT433ARA	**FWD**: 5' GCC TGC CTG CTG CTG CCA GGG CCA CAT GGG CCA TCA AAC ATG C 3' **REV**: 5' GCA TGT TTG ATG GCC CAT GTG GCC CTG GCA GCA GCA GGC AGG C 3'
R639C	**FWD**: 5' CCT GGA GGC AAC TGT GGC GGC TTC 3' **REV**: 5' GAA GCC GCC ACA GTT GCC TCC AGG 3'
R468C	**FWD**: 5' GTG ATG GGC CTA TGC CGG CAG CGG AAC 3' **REV**: 5' GTT CCG CTG CCG GCA TAG GCC CAT CAC 3'
None (siRNA resistance mutagenesis)	**FWD**: 5' GCA GTA TGC CCA GCA GTG GAA TCA ATA TTA TCA GAA CCA GGG CCA GTG G 3' **REV**: 5'-CCA CTG GCC CTG GTT CTG ATA ATA TTG ATT CCA CTG CTG GGC ATA CTG C 3'

Site-directed mutagenesis was carried out using reagents from Phusion unless otherwise stated. Briefly, the reaction mix was assembled as follows: 10 µl of 10X Phusion buffer, 3 µl

of 10 mM dNTPs (Promega), 150 ng of plasmid DNA template, 2 µl of 10µM primers (forward and reverse), 1.5 µl of Phusion DNA polymerase, and made up to a volume of 50 µl with nuclease-free water in PCR tubes. The reaction was performed in a PCR 2720 ThermoCycler (Applied Biosystems) according to the following phases:

98 °C => 2 mins

98 °C => 30 seconds
62 °C => 30 seconds
72 °C => 10 mins
} 35 cycles

72 °C => 10 mins

4 °C => hold

5 µl of PCR products were subjected to agarose gel electrophoresis to check efficiency of the PCR. Subsequently, the parental un-mutated plasmid DNA was removed by treatment with 1 µl of Dpn1 (New England BioLabs) at 37 °C for 3-5 hours. DNA was then ready for bacterial transformation.

2.2.6 DNA sequencing

Between 100-500 ng of plasmid DNA, along with 3.2 picomoles of a suitable sequencing primer was diluted in 10 µl of nuclease-free water. Samples were then taken to the DNA sequencing services laboratory at the University of Birmingham for processing, before analysis using Chromas Lite and EBI Emboss Needle software.

2.2.7 Cloning

Cloning of hnRNPUL1 DNA constructs between plasmids was achieved via the design of primers with overhangs containing restriction enzyme sites. This allowed cutting-out and subsequent ligation in to plasmids with the same restriction sites. The cloning primers used are detailed in Table 2.6 and were provided by Sigma-Aldrich.

Table 2.6 – Cloning primers used in this study.

Direction	**Encoded restriction enzyme site**	**Primer sequence**
Forward	EcoRV	5' GCT CAG ATA TCA TGG CTT ACC CAT ACG ATG 3'
Reverse	NotI	5' CGT ATA GCG GCC GCC TAC TGT GTA CTT GTG C 3'

PCR reaction mixes were assembled as follows: 10 µl of 10X Phusion buffer, 3 µl of 10 mM dNTPs, 100 ng of plasmid DNA template, 2 µl of 10µM primers (forward and reverse), 1 µl of Phusion DNA polymerase, and made up to a volume of 50 µl with nuclease-free water in PCR tubes. The reaction was performed in a PCR 2720 ThermoCycler according to the following phases:

98 °C => 5 mins

98 °C => 30 seconds
62 °C => 30 seconds
72 °C => 4 mins
} 32 cycles

72 °C => 4 mins

4 °C => hold

5 µl of PCR products were subjected to agarose gel electrophoresis to check efficiency of the PCR. 3µl of each restriction enzyme (NotI-HF and EcoRV-HF) (New England BioLabs) were added to 30 µl of PCR product (or 2 µl of plasmid vector DNA and 28 µl nuclease-free water), along with 10X CutSmart Buffer (New England BioLabs) and incubated at 37 °C for 2 hours.

Subsequently, the parental un-mutated plasmid DNA was removed by treatment with 1 µl of Dpn1 at 37 °C for 3-5 hours. 7.5 µl of 6X loading buffer was added to each sample and subjected to agarose gel electrophoresis. Bands were excised from the gel and DNA extraction performed using QIAquick Gel Extraction Kit Spin Columns (Qiagen) in accordance with the manufacturer's instructions. DNA was eluted in nuclease-free water at the final step.

2.3 PROTEIN AND DNA BIOCHEMISTRY TECHNIQUES

2.3.1 Preparation of total cell lysates

Adherent cells were harvested by removing media, washing twice in cold PBS, scraping the cells and resuspending them in cold PBS. Non-adherent LCLs were harvested by centrifugation at 430 g for 5 mins at 4 °C to pellet cells, removal of the supernatant and resuspension of the cell pellet in cold PBS. Cell suspensions in cold PBS were subsequently centrifuged at 430 g for 5 mins at 4 °C. Supernatant was removed and cell pellets resuspended in denaturing buffer (9 M Urea (Sigma-Aldrich), 150 mM β-mercaptoethanol (Sigma-Aldrich), 50 mM Tris-HCl, pH 7.5 (Melford Biolaboratories)). Cell lysates were

sonicated twice for 15 seconds with a 1 minute gap period on ice and centrifuged at 13000 g for 5 mins to clear cell debris. Cell lysates were stored at -80 °C until required.

2.3.2. Preparation of lysates from cells for co-immunoprecipitation

Adherent cells had media removed, were washed twice in cold PBS, scraped and resuspended in cold PBS. Non-adherent LCLs were centrifuged at 430 g for 4 mins at 4 °C to pellet cells, supernatant removed and resuspended in cold PBS. Cell suspensions were centrifuged at 430 g for 4 mins at 4 °C, and cell pellets resuspended in NETN buffer (0.5 % NP-40 (Sigma-Aldrich) 150 mM NaCl (Sigma-Aldrich), 50 mM Tris-HCl pH 7.5, 0.5 mM EDTA (Sigma-Aldrich)). Cells were lysed by sonication or using a Wheaton-Dounce hand homogeniser and centrifuged at 1700 g at 4 °C for 5 mins. The supernatant was collected and subjected to further centrifugations at 13250 g for 5 mins, and 113000 g for 30 mins (both at 4 °C). The supernatant was retained and pellets discarded.

2.3.3 Determination of protein concentration

Protein concentrations of cell lysates were determined by employment of a standard curve produced using known concentrations of bovine serum albumin (BSA, VWR) in 200 µl of Bradford 10 µl of cell lysate was diluted in 90 µl of sterile water, and 10 µl of this diluted cell lysate was added to 200 µl of Bradford. Three repeat protein concentrations for each sample were read by spectrophotometry at a wavelength of 595 nm using a microplate reader (Bio-Rad model 680).

2.3.4 SDS-polyacrylamide gel electrophoresis (SDS-PAGE)

Proteins were separated according to their molecular size by SDS-PAGE on 8 %, 10 % or 12 % polyacrylamide gels consisting of 30 % w/v acrylamide (37:5:1 BIS-acrylamide,

Severn Biotech), 0.1 % SDS (Severn Biotech), 0.1 M Tris (Melford Biolaboratories)/ 0.1 M Bicine (pH 8.3) (Severn Biotech), 0.25 % ammonium persulphate (APS, Sigma-Aldrich) and 0.25 % N, N, N', N'-Tetramethylethylenediamine (TEMED, Severn Biotech). Gels were poured in to pre-assembled apparatus from Hoeffer Scientific according to supplier instructions, well-combs set in place and the gel left to polymerise. Following polymerisation, well-combs were removed, wells washed twice with sterile water and then filled with running buffer (0.1 M Tris/ 0.1 M Bicine (pH 8.3) and 0.1 % w/v SDS) ready for sample loading. Sample buffer (5 % SDS, 5 M urea, 50 mM Tris-HCl pH 7.4, 0.15 M β-mercaptoethanol, 0.01% bromophenol blue (BDH Laboratories)) was added to protein samples, heated at 80 °C for 5 mins, centrifuged at 700 g for 10 seconds, and loaded in to gel wells alongside pre-stained molecular weight markers. The apparatus was run between 8-16 hours at a constant speed between 10-25 mA depending on the size of the proteins of interest.

2.3.5 Urea-polyacrylamide gel electrophoresis (Urea-PAGE)

DNA oligonucleotides were separated according to their molecular size by Urea-PAGE on 12 % polyacrylamide gels consisting of 45 % w/v urea (Sigma-Aldrich), 30% w/v acrylamide, 0.25 % APS and 0.25 % TEMED in TBE buffer. The gel pouring, apparatus and running was the same as in Section *2.3.4*.

2.3.6 Visualisation of proteins on nitrocellulose membranes

Proteins transferred on to nitrocellulose membranes were visualised by staining with Ponceau-S Stain consisting of 0.1 % Ponceau-S (Sigma-Aldrich) and 3 % trichloroacetic acid (TCA) (BDH Laboratories) for 30 seconds. Membranes were then washed 3-6 times with deionised water allowing visualisation of stained proteins.

2.3.7 Detection of radioactively labelled proteins and DNA by autoradiography

Gels were washed three times in 30 % v/v methanol (VWR)/ 10 % acetic acid (Fisher Scientific) in deionised water, before drying under a vacuum at 80 °C for 2 hours. Gels were then exposed to autoradiography film (GE Healthcare) for an appropriate time period.

2.3.8 ^{32}Phosphorous radioactive assays

2.3.8.1 α-^{32}P-ATP binding assay

Ox-ATP was prepared as follows: 5 µl of α-^{32}P-ATP (Perkin Elmer) was added to 0.5 mM HCl/0.5 mM sodium periodate (Sigma-Aldrich) and incubated at room temperature in the dark for 20 mins. 20 µl of 50 % glycerol was added and incubated for a further 20 mins in the dark. Then 5 µl of 2 M Tris HCl (pH 7.2), 1 µl of 1 M $MgCl_2$ and 13 µl of sodium cyanoborohydride ($NaCNBH_3$) (Sigma-Aldrich) was added.

Protein lysates were prepared as in Section *2.3.2*, but with the employment of an altered buffer (1 % NP-40 (Sigma-Aldrich), 500 mM NaCl (Sigma-Aldrich), 5 mM $MgCl_2$ (Sigma-Aldrich), 50 mM Tris-HCl pH 7.4, 2 mM EDTA (Sigma-Aldrich)). Immunoprecipitations were performed by incubation of primary antibody (typically 5-10 µl) (Table 2.7) or no antibody as a control at 4 °C overnight on rotation with the lysate. Samples were subsequently centrifuged at 113000 g at 4 °C for 5 mins and the pellet discarded. 50 µl of Protein G-agarose beads (KPL) suspended in an equal volume of the above buffer were added to each sample and rotated at 4 °C for 1 hour. Samples were then centrifuged at 700 g for 1 min at 4 °C and the supernatant discarded. Samples were washed four times in 1 ml of the above buffer by centrifugation at 700 g for 1 min at 4 °C and discarding the supernatant each time. 200 µl of the above buffer were added to each sample along with 15 µl of Ox-ATP and incubated at 4 °C on rotation overnight.

Samples were washed three times with buffer A (0.5 M KCl (BDH Laboratories), 5 mM $MgCl_2$, 1 mM EGTA, 5 mM $NaCNBH_3$, 0.5 % NP-40, 0.1 M Tris-HCl, pH 7.6) and three times with buffer B (5 mM MgCl2, 1 mM EGTA, 5 mM $NaCNBH_3$, 70 mM Tris-HCl, pH 6.8), before adding 50 µl of SDS sample buffer, heating at 80 °C for 5 mins, centrifuging at 700 g for 10 seconds, and fractionating by SDS-PAGE.

2.3.8.2 γ-^{32}P-ATP kinase assay

Protein samples were prepared as in Section *2.3.2* and the immunoprecipitation procedure followed as in Section *2.4.2* until the washing of the beads. Three washes were carried out with NETN buffer, two with NEN buffer and one with 1X reaction buffer (RB) (25 mM Tris HCl pH7.4, 130 mM KCl, 10 mM $MgCl_2$). To each sample 20 µl of a master mix was added, containing 1X RB (plus 5 mM dithiothreitol-DTT), 20 µCi γ-^{32}P-ATP, 5 µg protein substrate (myelin basic protein (MBP) or myosin phosphorylatable light chain (PLC)) or 100 nM DNA substrate (Table 2.7). Kinase inhibitors were added to samples as required (see Table 2.2 for details). Samples were incubated in a water bath at 30 °C for 30 mins. In the determination of oligonucleotide phosphorylation the reaction was stopped by adding 7 µl of termination buffer (95 % v/v formamide, 0.05 % w/v bromophenol blue), heating at 80 °C for 5 mins and centrifugation at 700 g for 10 seconds. For the protein determination experiments the reactions were stopped by adding SDS sample buffer. Experiments employing protein substrates were loaded on to a SDS-PAGE gel and those with DNA substrates on to a urea-acrylamide gel.

Table 2.7 – DNA substrates used for γ-^{32}P-ATP kinase assay.

Substrate	Single or double stranded	Overhang	Sequence
1	Single	None	5'-CCGTTTCGCTCAAGTTAGTATGTCAAAGCAGGC-3'
2	Double	5'	5'-(P)-CCGTTTCGCTCAAGTTAGTATGTCAAAG-3' 3'-GGCAAAGCGAGTTCAATCATACAGTTTCGTCCG-5'
3	Double	3'	5'-(P)- CCGTTTCGCTCAAGTTAGTATGTCAAAGCAGGC-3' 3'-GGCAAAGCGAGTTCAATCATACAGTTTC-5'
4	Double	None	5'-(P)- CCGTTTCGCTCAAGTTAGTATGTCAAAGCAGGC-3' 3'-GGCAAAGCGAGTTCAATCATACAGTTTCGTCCG-5'

2.3.9 Preparation of samples for mass spectrometry

Following the 30 minute incubation at 30 °C of a protein kinase assay in which 50 mM ATP was added instead of radioactively-labelled γ-^{32}P-ATP (see *2.3.8.2*), 0.5 ml of 9 M urea/50 mM ammonium bicarbonate (ABC) was added to each sample and incubated for 1 hour under gentle agitation. Following centrifugation, supernatant was removed, 50 mM DTT added and incubated at 56 °C for 30 mins. 100 mM iodoacetamide was added and incubated in the dark for 30 mins at RT. Samples were then added to FASP (filter-aided sample preparation) filters (Millipore), centrifuged and flow-through discarded. Filters were washed four times with 50 mM ABC and placed in fresh collection tubes. Mass spectrometry-grade trypsin (1 µg/sample, Promega) in 50 mM ABC was added and left at 37 °C overnight. Samples were centrifuged and supernatant transferred to low-binding Eppendorfs. The filters were given an additional wash with 50 mM ABC and this supernatant added to the previous collection. The resulting peptides were dried by vacuum centrifugation and then fractionated using a Bruker amaZon

ion trap mass spectrometer and processed and analyzed using the ProteinScape central bioinformatic platform (Bruker).

2.3.10 ssDNA-binding assays

24 hours after DNA transfections, samples were prepared as in Section *2.3.2*, with the substitution for NETN buffer by the following buffer: 0.1 % NP-40, 0.1 % β-mercaptoethanol, 10 % glycerol, 10 mM $MgCl_2$, 200 mM NaCl, 50 mM Tris-HCl, pH 7.4. Lysates were then divided and adjusted for appropriate NaCl concentrations for the titration of binding experiment. Subsequently, 50 µl cellulose beads with covalently attached calf serum derived ssDNA (Sigma-Aldrich) (or cellulose beads as a control) in an equal volume of the above buffer were added to each sample and rotated at 4 °C for 2 hours. Samples were then centrifuged at 700 g for 1 min at 4 °C and supernatant discarded. Samples were washed three times in 1 ml of the above buffer by centrifugation at 700 g for 1 min at 4 °C and discarding the supernatant each time. A final wash was made in the 0.1 M NaCl for all samples. 50 µl of SDS sample buffer was added to each sample, heated at 80 °C for 5 mins, centrifuged at 700 g for 10 seconds and subjected to SDS-PAGE and visualised by western blotting.

2.3.11 ssRNA-binding assays

24 hours after DNA transfections, samples were prepared as in Section *2.3.2*, with the substitution for NETN buffer by the following buffer: 0.1 % NP-40, 0.1 % β-mercaptoethanol, 10 % glycerol, 10 mM $MgCl_2$, 100 mM NaCl, 50 mM Tris-HCl, pH 7.4. Lysates were then divided and adjusted for appropriate NaCl concentrations for the titration of binding experiment. Subsequently, samples were rotated with 50 µl of ribonucleotide homopolymers (50 molecules of A, U, G or C) bound to streptavidin beads through a biotin molecule linked to the ribonucleotide for 2 hours at 4 °C. Samples were then centrifuged

at 700 g for 1 min at 4 °C and supernatant discarded. Samples were washed three times in 1 ml of the above buffer (adjusted for NaCl concentration accordingly) by centrifugation at 700 g for 1 min at 4 °C and discarding the supernatant each time. A final wash was made in the 0.1 M NaCl for all samples. 50 µl of SDS sample buffer was added to each sample, heated at 80 °C for 5 mins, centrifuged at 700 g for 10 seconds and subjected to SDS-PAGE and visualised by western blotting. Relative amounts of protein were determined by densitometric scanning.

2.4 IMMUNOCHEMISTRY TECHNIQUES

2.4.1 Antibodies

All antibodies used in this study and their origins are shown in Table 2.8 and Table 2.9.

Table 2.8 – Primary antibodies used in this study.

Antibody	Antigen	Dilution	Use	Species	Company/Source
sc-8408	Chk1	1:1000	WB	Mouse	Santa Cruz
	GFP				
HA	HA	1:2000	WB, IP, IF	Mouse	In house
2595S	Histone H2AX	1:1000	WB	Rabbit	Cell Signalling
ab122906	hnRNP-U	1:1000	WB, IP	Rabbit	Abcam
960	hnRNP-UL1	1:2000	WB, IP, IF	Rabbit	In house
961	hnRNP-UL1	1:2000	WB	Rabbit	In house
hnRNP-UL2	hnRNP-UL2	1:1000	WB, IP	Rabbit	In house
sc-6217	Lamin B	1:1000	WB	Goat	Santa Cruz
1D7	NBS1	1:1000	WB	Mouse	Genetex
sc-722	Nrf2	1:1000	WB	Rabbit	Santa Cruz

DO1	p53	1:100	WB	Mouse	In house
sc-8418	p70-S6K	1:1000	WB, IP	Mouse	Santa Cruz
	PAR	1:1000	WB	Mouse	
9542S	PARP-1	1:1000	WB	Rabbit	Cell Signalling
2341S	Phospho-Chk1 (Ser-345)	1:1000	WB	Rabbit	Cell Signalling
ab47272	Phospho-NBS1 (Ser-343)	1:1000	WB	Rabbit	Abcam
A300-245A	Phospho-RPA32 (Ser-S4/S8)	1:1000	WB, IF	Rabbit	Bethyl
A300259A	PNK1	1:1000	IP	Rabbit	Bethyl
	RPA32	1:1000	WB, IF	Mouse	
sc-147	SV40 Large T antigen	1:1000	IP	Mouse	Santa Cruz
ab41972	TDP43	1:1000	WB	Rabbit	Abcam
144	XRCC1	1:1000	WB	Mouse	Pierce
AC-74	β-Actin	1:10000	WB	Mouse	Sigma
JBW301	γ-H2AX (Ser-139)	1:1000	IF	Mouse	Millipore
sc-101696	γ-H2AX (Ser-139)	1:1000	WB, IF	Rabbit	Santa Cruz

Table 2.9 – Secondary antibodies used in this study.

Antibody	**Antigen**	**Dilution**	**Use**	**Species**	**Company/Source**
P0447	Mouse IgG	1:2000	WB	Goat	Dako
P0399	Rabbit IgG	1:3000	WB	Swine	Dako
P0449	Goat IgG	1:2000	WB	Rabbit	Dako
A11001 Alexa Fluor 488	Mouse IgG	1:1000	IF	Goat	Life Technologies
A11012 Alexa Fluor 594	Rabbit IgG	1:1000	IF	Goat	Life Technologies

2.4.2 Co- Immunoprecipitation

Samples, as prepared in Section *2.3.2*, were incubated with primary antibody (typically 5-10 µl) (Table 2.7), or no antibody as a control, at 4 °C overnight on rotation. Samples were subsequently centrifuged at 113000 g at 4 °C for 5 mins and the pellet discarded. 50 µl of Protein G-agarose beads suspended in an equal volume of NETN buffer were added to each sample and rotated at 4 °C for 1 hour. Samples were then centrifuged at 700 g for 1 min at 4 °C and the supernatant discarded. Samples were washed three times in 1 ml of NETN buffer and twice in NEN buffer (NETN buffer minus NP-40) by centrifugation at 700 g for 1 min at 4 °C and discarding the supernatant each time. 50 µl of SDS sample buffer was added to each sample, heated at 80 °C for 5 mins, centrifuged at 700 g for 10 seconds and subjected to SDS-PAGE.

2.4.3 Western blotting

After SDS-PAGE, separated proteins were transferred on to nitrocellulose membrane using the following method. Gels were laid on to pre-wetted nitrocellulose membranes of corresponding size, sandwiched between two pieces of Whatman filter paper and blotting sponges, and held securely in plastic cassettes. The transfer cassette was then placed in a transfer tank filled with transfer buffer (20 % v/v methanol, 0.19 M glycine and 0.05 M Tris) for 6-8 hours at 280 milliAmps (mA). Subsequent visualisation of proteins on the nitrocellulose membrane was carried out before blocking in 5 % skimmed dried milk powder (Sainsburys) in TBST (Tris-Buffered Saline Tween-80, consisting of 1 % Tween-80 (Sigma-Adrich), 0.15 M NaCl, 50 mM Tris-HCl, pH 7.4) for 30 mins under gentle agitation.

Primary antibodies (Table 2.7) were diluted in 5 % skimmed dried milk powder or 3 % BSA in TBST and incubated with the nitrocellulose membrane at 4 °C on a rocking table overnight.

Membranes were then washed 3 times (15 mins each) in TBST. Secondary antibodies (Table 2.8) conjugated to horse-radish peroxidase (HRP) were diluted in 5 % skimmed dried milk in TBST and incubated with the nitrocellulose membrane at RT on a rocking table for 2-4 hours. A further 6 washes (5 mins each) in TBST were carried out. Specific antigens on the membranes were then visualised by incubation with enhanced chemiluminescence (ECL) reagents (Millipore or GE Healthcare) for 1 minute and exposure to autoradiography film for an appropriate time period.

2.4.4 Immunofluorescence Microscopy

Cells were seeded on to 13 mm diameter micro cover slips (Fisher Scientific) in a 24-well plate. After treatment or mock-treatment and at selected time-points, cells were washed in PBS, fixed in cold 4 % paraformaldehyde (PFA) (Sigma-Aldrich) in PBS for 10 mins, permeabilised with 0.5 % v/v Triton X-100 (Sigma-Aldrich) in PBS, and left in PBS at 4 °C. Cells were blocked in cold 10 % FCS in PBS for 30 mins. Primary antibodies (Table 2.7) were diluted to the appropriate concentration in cold 10 % FCS in PBS and incubated with cells at 4 °C for 1 hour. Cells were washed three times with cold 10 % FCS in PBS, before incubation with fluorescent secondary antibodies (Table 2.8) diluted 1:1000 in cold 10 % FCS in PBS at 4 °C for 1 hour. Cells were washed twice in PBS before staining with DAPI (Sigma-Aldrich) in PBS (1 μg/ml) for 5 mins at 4 °C. A final wash in PBS was carried out before mounting on to viewing slides using Immu-Mount Gel (Thermo Scientific). Fluorescence images were taken using a Nikon E600 Eclipse microscope 333 equipped with a 60X and 100X oil lens. Images were acquired and analysed using Volocity Software 334 v4.1 (Improvision).

CHAPTER III

HNRNP-UL1 AS A KINASE

3.1 INTRODUCTION

Previous studies and those conducted in conjunction with our group highlighted a putative kinase region harbouring a Walker A motif in hnRNP-UL1 (Gabler et al 1998; Polo et al., 2012). This consensus motif typically confers adenosine triphosphate (ATP)-binding, however, this has not been confirmed for hnRNP-UL1 at a practical level. Nucleotide binding can be utilised by proteins for various activities, including transfer of the gamma-phosphate to substrates (phosphorylation by kinases). The human genome encodes over 500 kinases and the phosphorylation of target proteins is a common and important post-translation modification of proteins in many cellular processes (Manning et al., 2002). Upon investigation, hnRNP-UL1 showed appreciable primary and secondary structure homology to the protein polynucleotide kinase phosphatase (PNKP). PNKP is responsible for the phosphorylation of the 5' ends of DNA to allow efficient repair following DNA damage (section *1.3.5*).

This has led to a hypothesis that hnRNP-UL1 binds ATP, possibly for activity as a kinase. The aims of the work described in this chapter were to investigate this hypothesis by using radioactively labelled forms of ATP allowing determination of ATP-binding capability and phosphorylation of DNA and protein substrates *in vitro*.

3.2 RESULTS

3.2.1 hnRNP-UL1 shares significant homology to human PNKP

hnRNP-U and the U-like proteins 1 and 2 contain a Walker A motif, and possibly a Walker B motif. When comparing homology to other kinases, the kinase region of PNKP showed good amino acid sequence homology. This was most obvious within the region of close proximity to the Walker-A loop (Figure 3.1). The amino acid homology to PNKP within the kinase region was not extensive (21.57% for hnRNP-UL1); however, it was the most homologous of any kinase encoded by the human genome included in the Expasy and University College London PSIPRED protein sequence analysis software. Despite homology of primary structures being limited, there was significant secondary structure homology. The use of Expasy software Swiss-Pdb Viewer allowed secondary structure modelling of hnRNP-UL1's putative kinase domain based on the known structure of PNKP. The two proteins appear to share significant secondary structure similarity; most significantly downstream of the Walker A loop (Figure 3.2). This suggested that hnRNP-UL1, and possibly hnRNP-UL2, may contain a DNA kinase activity like that of PNKP, or alternatively a protein kinase activity.

In addition to the Walker A loop many nucleotide-binding proteins have a Walker B motif. This consists of a conserved aspartic acid or glutamic acid at the C-terminal end of a β-strand and is often preceded by a stretch of four hydrophobic residues (i.e. hhhhD/E). The acidic residue aids interaction with the Mg^{2+} ion and can be essential for catalysis (Matte and Delbaere, 2010). A Walker B motif is present in hnRNP-UL1 roughly 70 amino acids C-terminal of the Walker A loop (Figure 3.2). The Walker B motif is also conserved in hnRNP-U and –UL2 at a similar position. It is thought that NTPases can be differentiated from

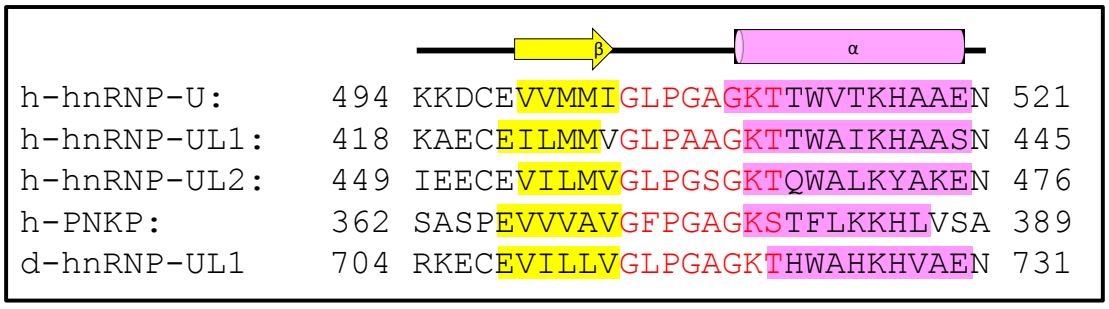

Figure 3.1 Sequence comparison of human hnRNP-U, -UL1, -UL2, PNKP and *drosophila* hnRNP-UL1. The amino acid residues constituting the Walker-A loop are red in colour, whilst those composing of the beta sheet are highlighted in yellow and those composing of the alpha helix are highlighted in pink.

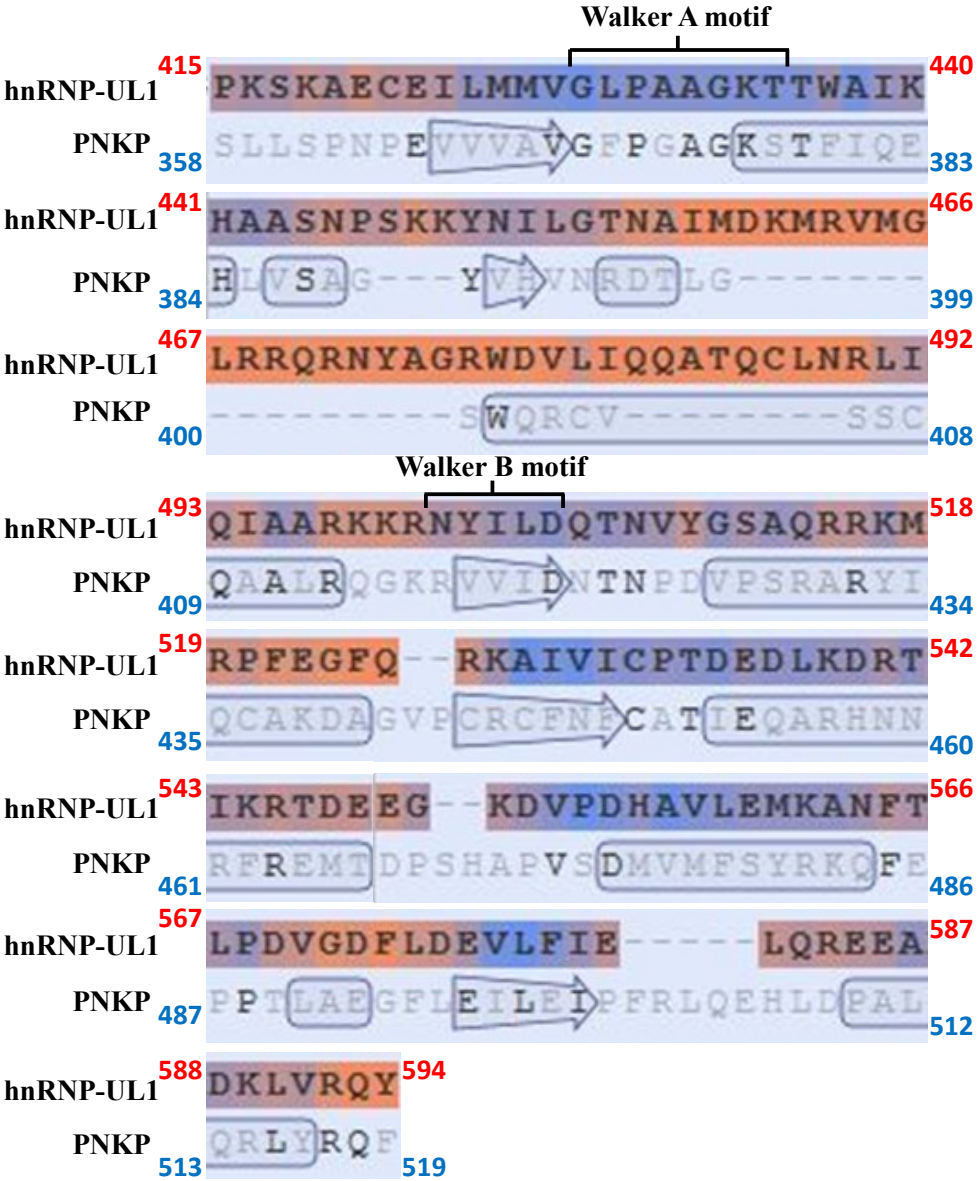

Figure 3.2 A secondary structure prediction of human hnRNP-UL1 based on the known structure of mouse PNKP. Analysis by Swiss-Pdb Viewer software (expasy.org) allowed secondary structure modelling of hnRNP-UL1 based on the known structure of PNKP. The amino acid sequences of the kinase domain and proposed kinase region of PNKP and hnRNP-UL1, respectively, are shown with corresponding areas of amino acid homology aligned. Alpha helices (boxed) and beta sheets (arrows) of PNKP are indicated. Areas of hnRNP-UL1 which are strongly predicted to form the same secondary structures are highlighted in blue directly above the corresponding PNKP sequence. Areas of red indicate regions which are less likely to form the same secondary structures. -, indicates where gaps have been introduced in the sequence to allow maximum homology.

kinases by an additional glutamic acid at the C-terminal end of the motif (Leipe et al., 2003). As this is not present in hnRNP-UL1, it also indicates hnRNP-UL1 possesses kinase activity.

3.2.2 ATP-binding by hnRNP-UL1

To determine whether the predicted Walker A loop of hnRNP-UL1 facilitated ATP-binding the protein was incubated with a non-hydrolysable form of ATP which irreversibly binds to any interacting species and contains a ^{32}P radioactive label for detection via autoradiography. SV40 large T antigen was used a positive control as it was readily available from 293FT cells and is known to bind ATP (Dean et al., 1987). Repeated experiments showed binding of ATP to immunoprecipitated SV40 large T antigen and hnRNP-UL1, but not to hnRNP-UL2 (Figure 3.3).

3.2.3 hnRNP-UL1 shows no activity as a DNA kinase

In the knowledge that hnRNP-UL1 bound ATP, we next investigated its capability as a DNA kinase. Bernstein et al. (2005) showed mammalian PNKP to have a preference for DNA substrates of at least 8 nucleotides in length and with a 3' overhang of 3-5 nucleotides. If hnRNP-UL1 was to possess DNA kinase activity, it was unknown whether it would exhibit a preference for a particular type of DNA end. Therefore, four oligonucleotides with different structures were used as potential substrates (Figure 3.4A). Once again, proteins were obtained by immunoprecipitation and then incubated with the substrates in the presence of γ-^{32}P-ATP. Recombinant PNKP was employed as a positive control. The recombinant PNKP was able to phosphorylate each of the 4 DNA substrates (Figure 3.4B). However, immunoprecipitated PNKP and hnRNP-UL1 failed to phosphorylate any of the substrates with repeated assays (Figure 3.4B).

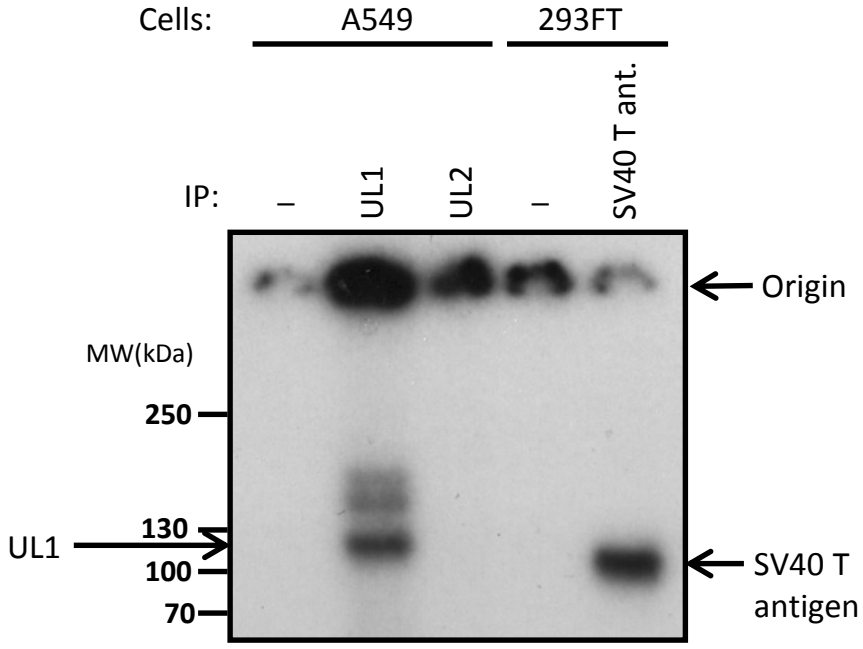

Figure 3.3 hnRNP-UL1 binds ATP. A549 and 293FT cells were lysed and immunoprecipitations performed using the indicated antibodies. Immunoprecipitated proteins were incubated with ox-α-^{32}P-ATP and subjected to SDS-PAGE. The dried gel was analysed by autoradiography.

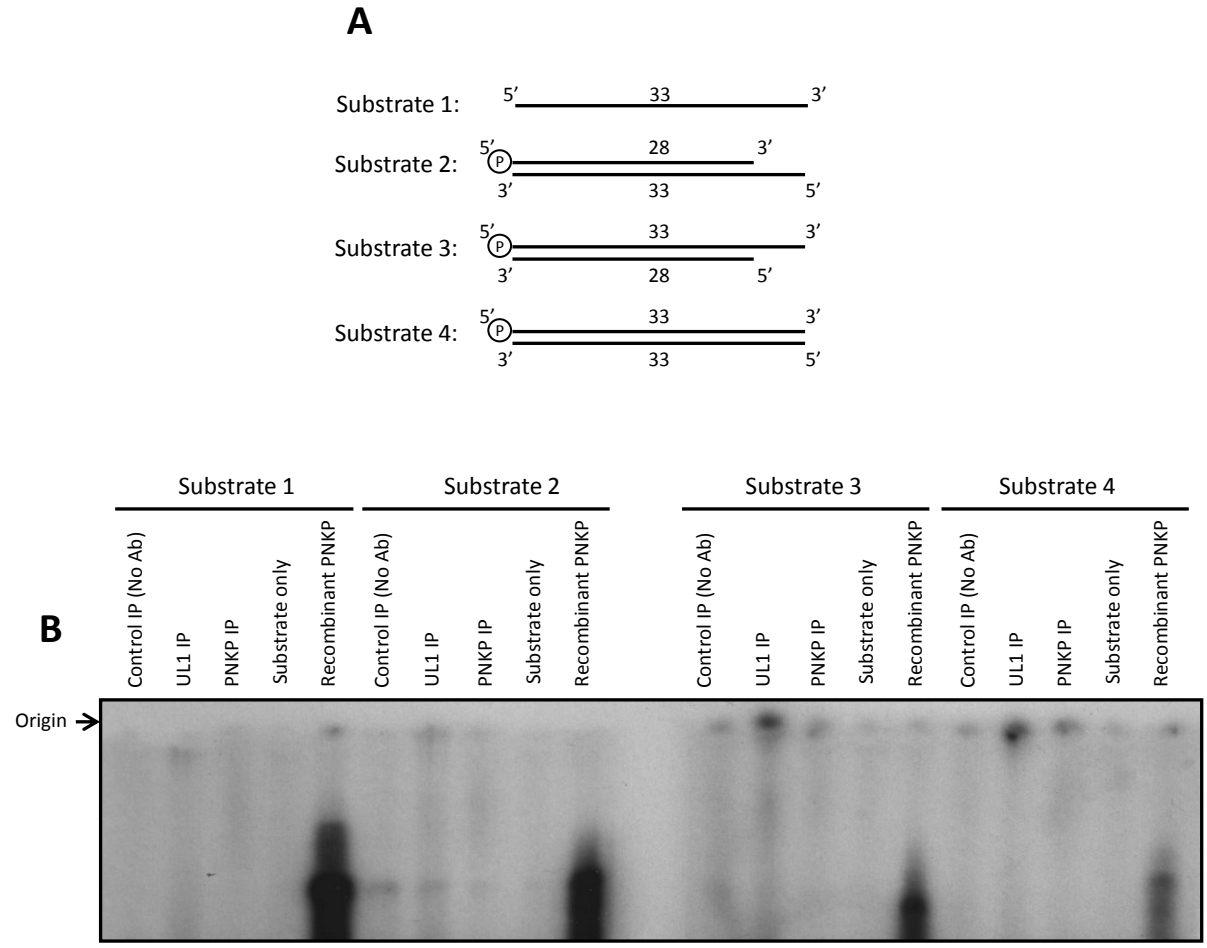

Figure 3.4 hnRNP-UL1 does not exhibit activity as a DNA kinase. A) Schematic of the DNA oligonucleotide substrates used to test hnRNP-UL1's activity as a DNA kinase. Sequences are shown in Table 2.6. B) HeLa cells were lysed and immunoprecipitations performed for hnRNP-UL1 or PNKP. The immunoprecipitated protein or recombinant PNKP protein was incubated with a reaction mixture containing the various DNA substrates and γ-^{32}P-ATP. After 1 hour the reaction was stopped, samples heated and run on a urea-polyacrylamide gel, before drying and analysis by autoradiography.

3.2.4 hnRNP-UL1 shows activity as a protein kinase

As hnRNP-UL1 appeared to lack DNA kinase activity, the possibility of its activity as a protein kinase was addressed. Several promiscuously phosphorylatable substrates were employed to test this, including MBP (myelin basic protein), PLC (myosin phosphorylatable light chain) and a number of histones (Figure 3.5A). Incubation of γ-^{32}P-ATP, immunoprecipitated hnRNP-UL1 and substrates resulted in each of the substrates being phosphorylated (Figure 3.5B). MBP and PLC exhibited the strongest phosphorylation and these were used for subsequent experiments.

Using proteomic mass spectrometry analysis two phosphorylated MBP peptides were identified after incubation with immunoprecipitated hnRNP-UL1. These were R.DTGILDS^{174}IGR.F and K.NIVTPRT^{232}PPPSQGK.G (phosphorylated amino acids are numbered; the full stops show where the actual peptide begins and ends). The second of these has a phosphorylation site similar to that suggested for MAP/ERK kinases (-P-X-S/T-P-) (Lewis et al., 1998) but the first does not appear to resemble a phosphorylation site for any of the well characterised commonly occurring serine/threonine kinases.

Levels of substrate phosphorylation increased with duration of reaction time, with a near maximum level reached after 30 minutes (Figure 3.5C). This reaction time was employed for subsequent experiments. Varying the amount of hnRNP-UL1 antibody used for the immunoprecipitation prior to the kinase assay also affected the intensity of phosphorylation observed. Phosphorylation also increased with greater volume of antibody used (Figure 3.5D), as would be expected due to more hnRNP-UL1 protein being obtained from cell lysates. A band was also observed in these experiments at 120 kDa, the position of migration of hnRNP-UL1 following SDS-PAGE, suggesting possible autophosphorylation of hnRNP-UL1.

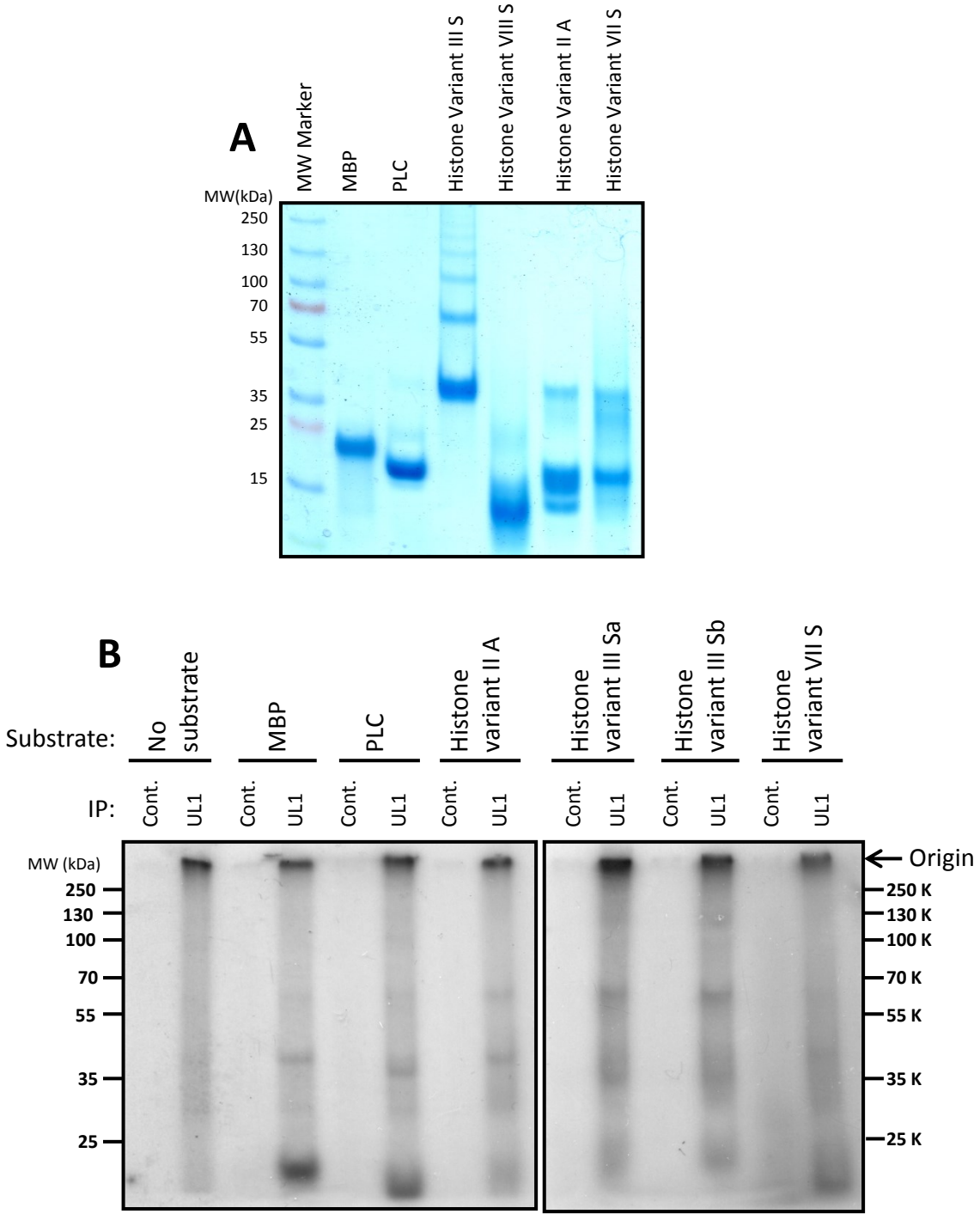
A
MW Marker
MBP
PLC
Histone Variant III S
Histone Variant VIII S
Histone Variant II A
Histone Variant VII S
MW(kDa)
250
130
100
70
55
35
25
15
B
Substrate:
No substrate
MBP
PLC
Histone variant II A
Histone variant III Sa
Histone variant III Sb
Histone variant VII S
IP:
Cont.
UL1
MW (kDa)
250
130
100
70
55
35
25
Origin
250 K
130 K
100 K
70 K
55 K
35 K
25 K

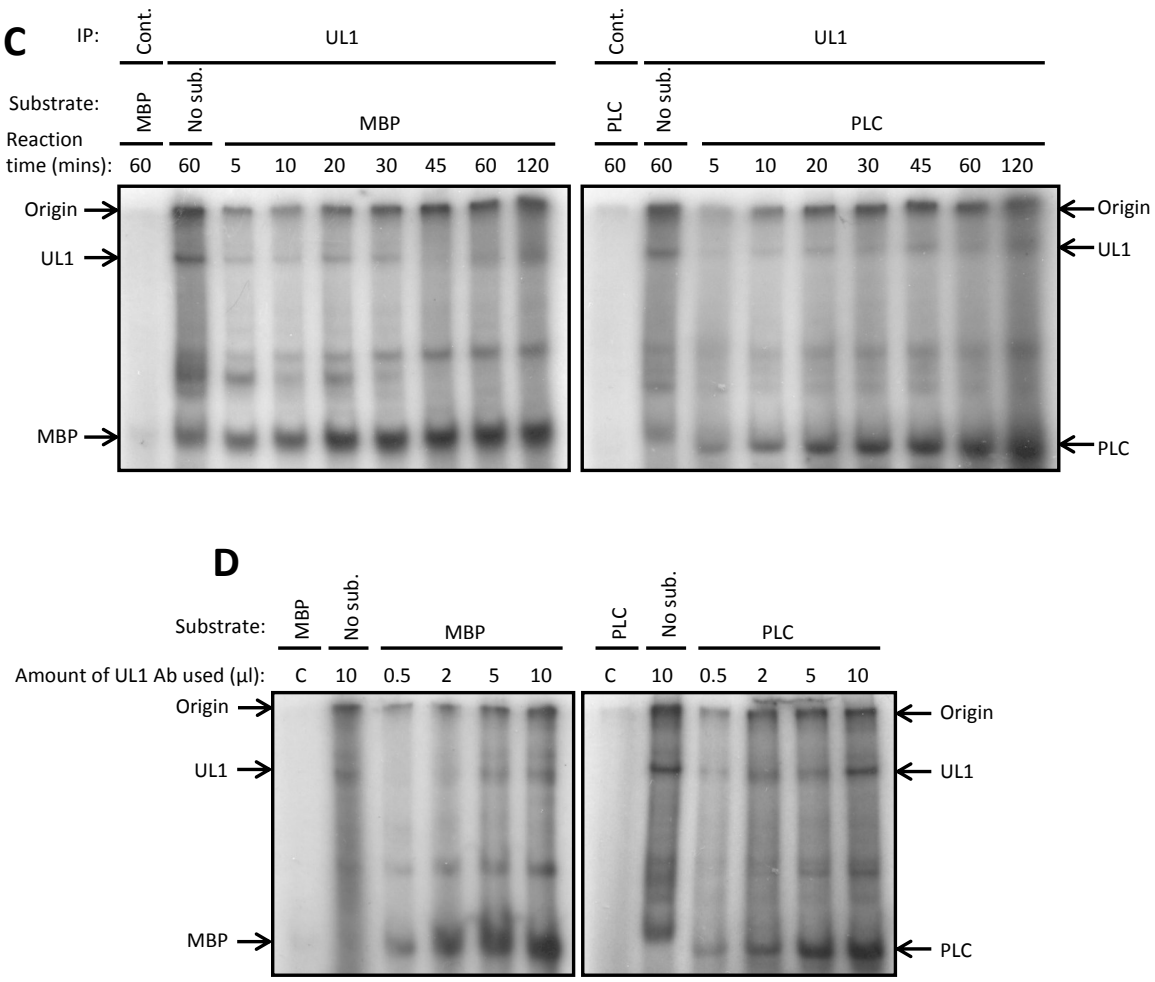

Figure 3.5 hnRNP-UL1 possesses activity as a protein kinase. A) Coomassie Blue staining of the various proteins used as substrates to test hnRNP-UL1's activity as a protein kinase. B) HeLa cells were lysed and immunoprecipitations performed. The immunoprecipitated protein was incubated with a reaction mixture containing the various indicated protein substrates and γ-^{32}P-ATP. After 1 hour the reaction was stopped, samples heated and run on a SDS-PAGE gel, before drying and analysis by autoradiography. C) HeLa cells were lysed and immunoprecipitations performed. The immunoprecipitated protein was incubated with a reaction mixture containing the indicated protein substrates and γ-^{32}P-ATP for varying time periods. The reaction was stopped, samples heated and run on a SDS-PAGE gel, before drying and analysis by autoradiography. D) HeLa cells were lysed and immunoprecipitations performed using different amounts of α-hnRNP-UL1 antibody. The immunoprecipitated protein was incubated with a reaction mixture containing the indicated protein substrates and γ-^{32}P-ATP. After 1 hour the reaction was stopped, samples heated and run on a SDS-PAGE gel, before drying and analysis by autoradiography.

3.2.5 hnRNP-U and –UL2 ATP-binding and kinase activity

Similar to hnRNP-UL1, both hnRNP-U and –UL2 contain Walker A motifs (Figure 3.1) and Walker B motifs. Additionally, their flanking regions are highly conserved and show some primary and secondary homology to PNKP, however it is less than hnRNP-UL1 (data not shown). Despite the presence of the Walker A motifs and highly conserved flanking regions the hnRNP-U and –UL2 proteins did not exhibit ATP-binding like hnRNP-UL1 (Figure 3.6A). Surprisingly, repeat kinase assays after immunoprecipitation of proteins showed hnRNP-U and –UL2 able to phosphorylate MBP and PLC (Figure 3.6B). The reason for this is unknown. The three proteins are expected to interact with one another and co-immunoprecipitation (co-IP) of hnRNP-UL1 and –UL2 was confirmed in Polo et al. (2012), as well as during this study by mass spectrometry following immunoprecipitation (Figure 3.7). The co-IP of hnRNP-UL1 may explain the substrate phosphorylation observed; however, by this argument it would be expected that ATP-bound protein would also be seen.

3.2.6 Validation of hnRNP-UL1 kinase activity by the use of kinase inhibitors

The isolation of hnRNP-UL1 by immunoprecipitation from cell lysates provides the possibility that the phosphorylation observed is not, in fact, attributable to hnRNP-UL1. Instead, an interacting partner of hnRNP-UL1 could co-immunoprecipitate and its kinase activity be the cause for the phosphorylation observed. This is conceivable, given the quite extensive list of known interacting partners of hnRNP-UL1, especially ATR indirectly through ATRIP (Blackford et al., 2008). Therefore, kinase inhibitors were used to treat cells prior to performing immunoprecipitation and during the kinase reaction. Firstly, inhibitors of all three PI3Ks, ATR, ATM and DNA-PK, were used. No reduction was seen in phosphorylation levels of the two substrates (Figure 3.8), suggesting the protein kinase

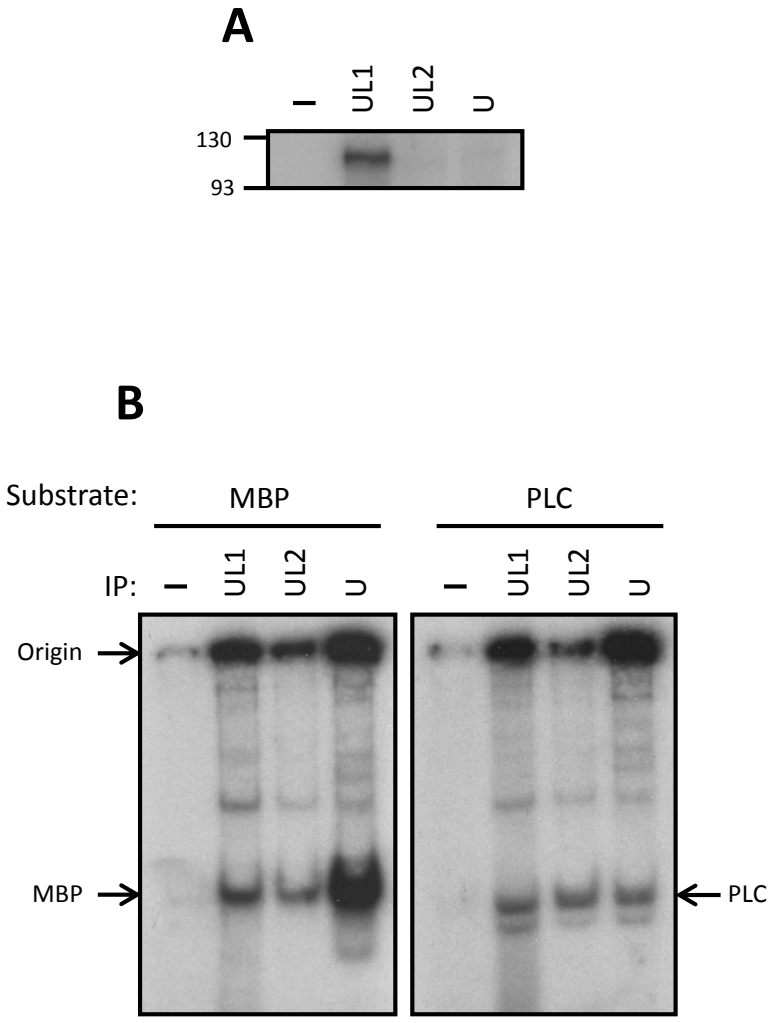

Figure 3.6 hnRNP-UL2 and hnRNP-U fail to bind ATP, but when immunoprecipitated exhibit protein kinase activity. A) HeLa cells were lysed and immunoprecipitations performed for the indicated proteins. Proteins were incubated with ox-α-^{32}P-ATP and subjected to SDS-PAGE. The dried gel was analysed by autoradiography. B) HeLa cells were lysed and immunoprecipitations performed. The immunoprecipitated protein was incubated with a reaction mixture containing the various indicated protein substrates and γ-^{32}P-ATP. After 30 minutes the reaction was stopped, samples heated and run on a SDS-PAGE gel, before drying and analysis by autoradiography.

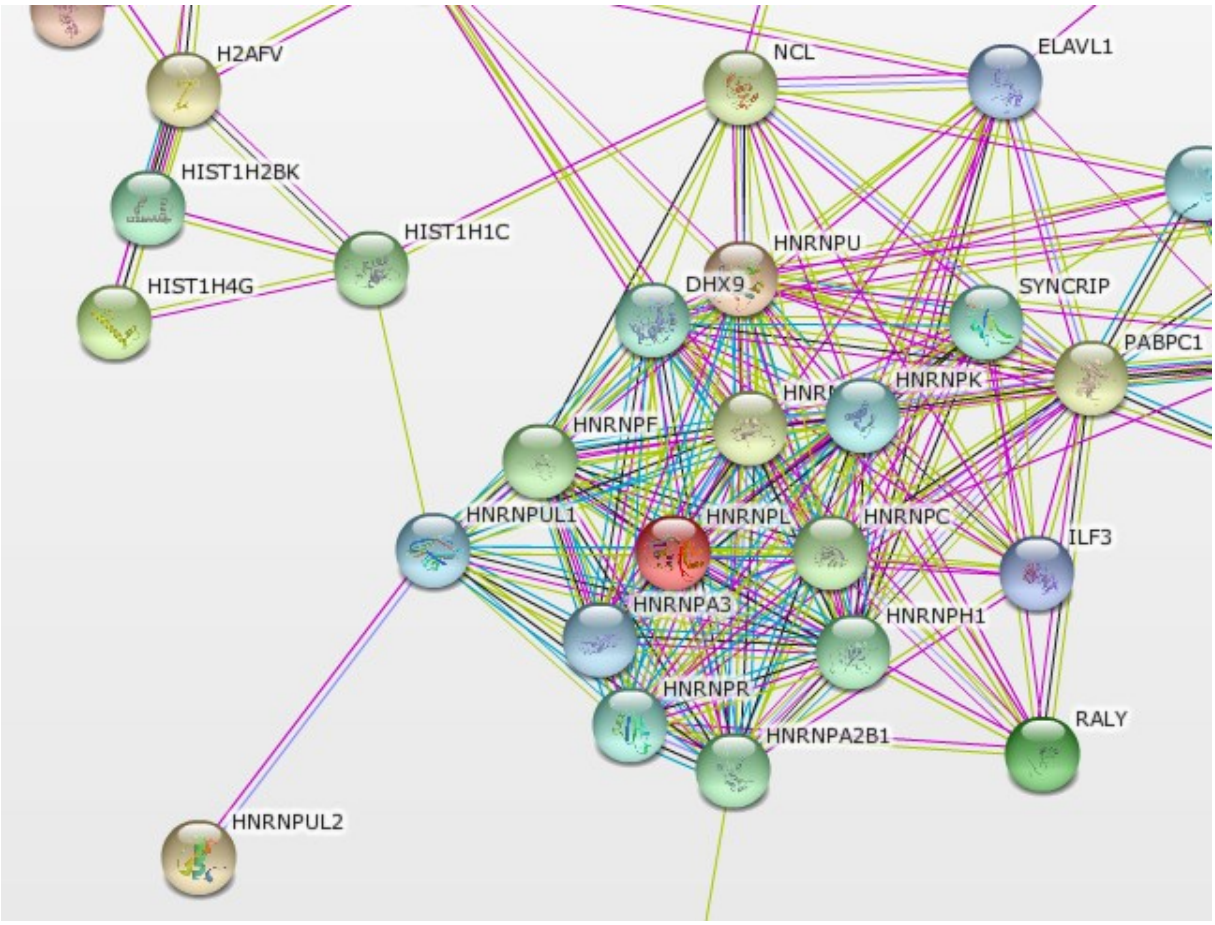

Figure 3.7 An interaction network for hnRNP-UL1 based on mass spectrometry data following co-immunoprecipitation. Hela cells were lysed and an immunoprecipitation performed using α-hnRNP-UL1 Ab. Co-immunoprecipitating proteins were identified using mass spectrometry and using websource 'string-db.org' an interaction network was generated. This shows the co-immunoprecipitating proteins identified by the mass spectrometry analysis linked by a string network. The connecting lines/strings represent different forms of evidence for the interaction of the two connected proteins, which are generated using varying data sources (see Szklarczyk et al., 2015 for further information). The string colours represent the following forms of evidence; pink = experiments; bright blue = databases; green = textmining (large collections of scientific texts are searched for statistically relevant co-occurrences of gene names); navy blue = coexpression; violet = homology (Szklarczyk et al., 2015).

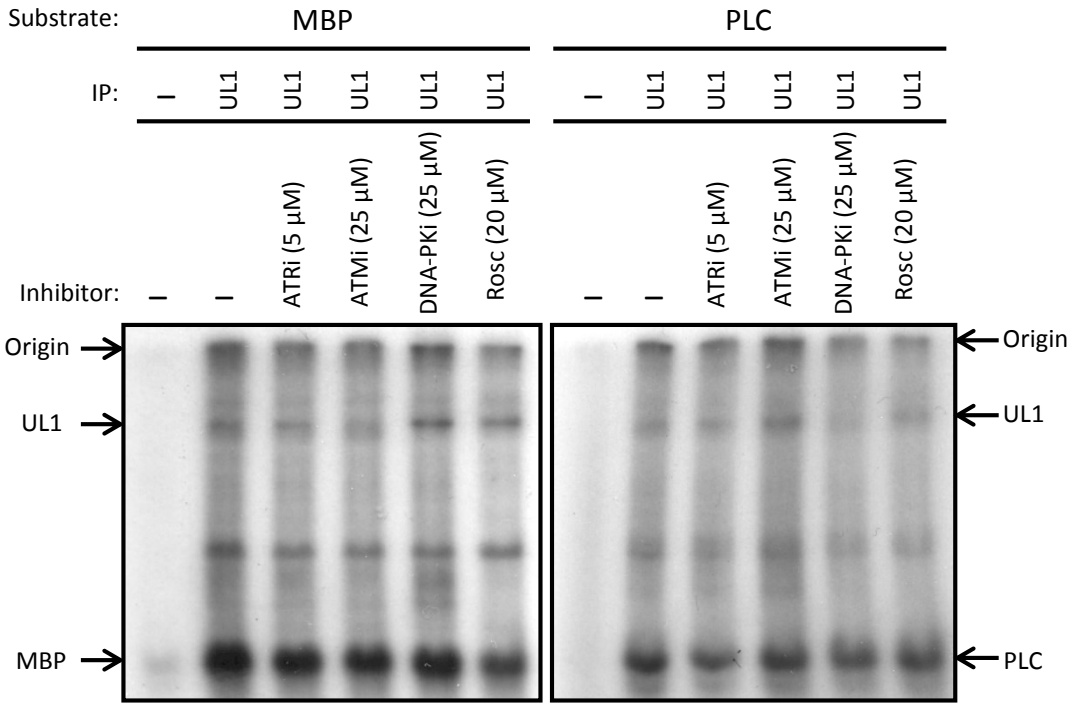

Figure 3.8 Phosphorylation of the MBP and PLC substrates is not due to the presence of PI3Ks. HeLa cells were exposed to the indicated concentrations of inhibitor compounds for 24 hours before being lysed and immunoprecipitations performed for the indicated proteins. The immunoprecipitated protein was incubated with a reaction mixture containing the various inhibitors, the indicated protein substrates and γ-^{32}P-ATP. After 30 minutes the reaction was stopped, samples heated and run on a SDS-PAGE gel, before drying and analysis by autoradiography.

activity observed is not due to these proteins. Roscovitine, an inhibitor of cyclin-dependent kinases (CDKs), was also used in the same manner with no reduction in phosphorylation of MBP and PLC (Figure 3.8).

The serine/threonine-protein kinase p70S6K (ribosomal protein S6 kinase) was found to co-immunoprecipitate with hnRNP-UL1 (Figure 3.9A). p70S6K acts downstream of mTOR signalling in response to growth factors to promote cell proliferation and cell cycle progression. The significance of the association of these two proteins is unknown and was not investigated during this study. However, its possible involvement in the phosphorylation observed in our kinase assays when immunoprecipitating hnRNP-UL1 needed to be eliminated. Immunoprecipitated p70S6K showed little to no kinase activity and a significant decrease in comparison to the phosphorylation seen with hnRNP-UL1 (Figure 3.9B and C). In addition, the use of rapamycin (an inhibitor of mTOR) to inhibit p70S6K did not decrease the level of phosphorylation observed when immunoprecipitating either p70S6K or hnRNP-UL1, suggesting any phosphorylation observed was not attributable to p70S6K.

A panel of other kinase inhibitors was also used to test if kinase activity shown by immunoprecipitated hnRNP-UL1 decreased in their presence. SP600125 (a c-Jun N-terminal kinase inhibitor) and PLK1i/BI 2536 (Polo-like kinase 1 inhibitor) showed the greatest effect in decreasing phosphorylation (Figure 3.9B and C). No interaction between hnRNP-UL1 and these two proteins has been shown previously. JNK is involved in responses to stress stimuli and stimulates inflammation, whilst PLK1 aids progression through the cell cycle suggesting no direct link between hnRNP-UL1 and these two proteins. The decreased phosphorylation seen in the presence of these inhibitors may be due to these small molecule inhibitors having some binding specificity to the active site of hnRNP-UL1, as well as their intended targets.

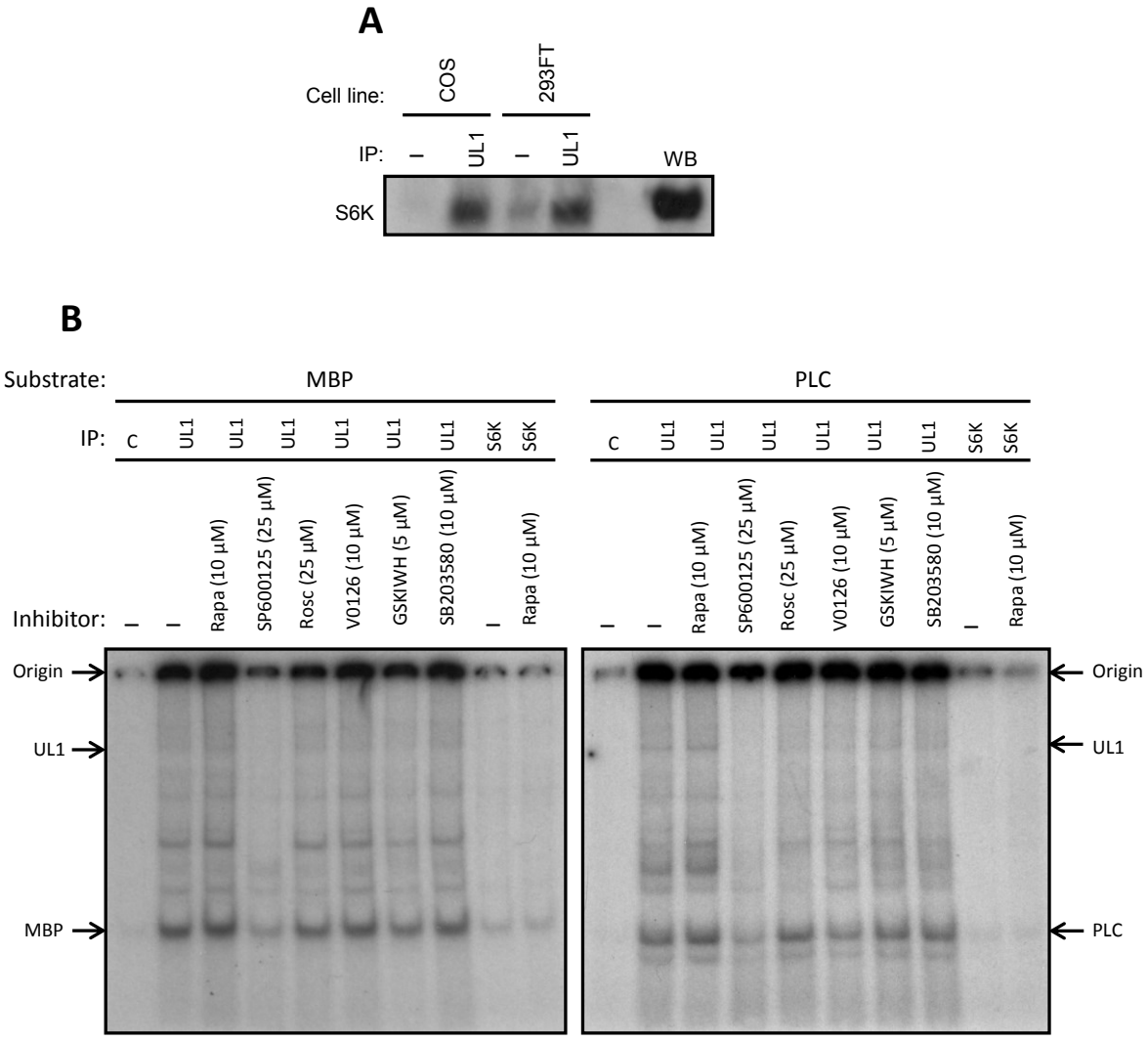
A
Cell line:
COS
293FT
IP:
–
UL1
–
UL1
WB
S6K
B
Substrate:
MBP
PLC
IP:
c
UL1
UL1
UL1
UL1
UL1
UL1
S6K
S6K
Inhibitor:
–
–
Rapa (10 μM)
SP600125 (25 μM)
Rosc (25 μM)
V0126 (10 μM)
GSKIWH (5 μM)
SB203580 (10 μM)
–
Rapa (10 μM)
Origin
UL1
MBP
PLC

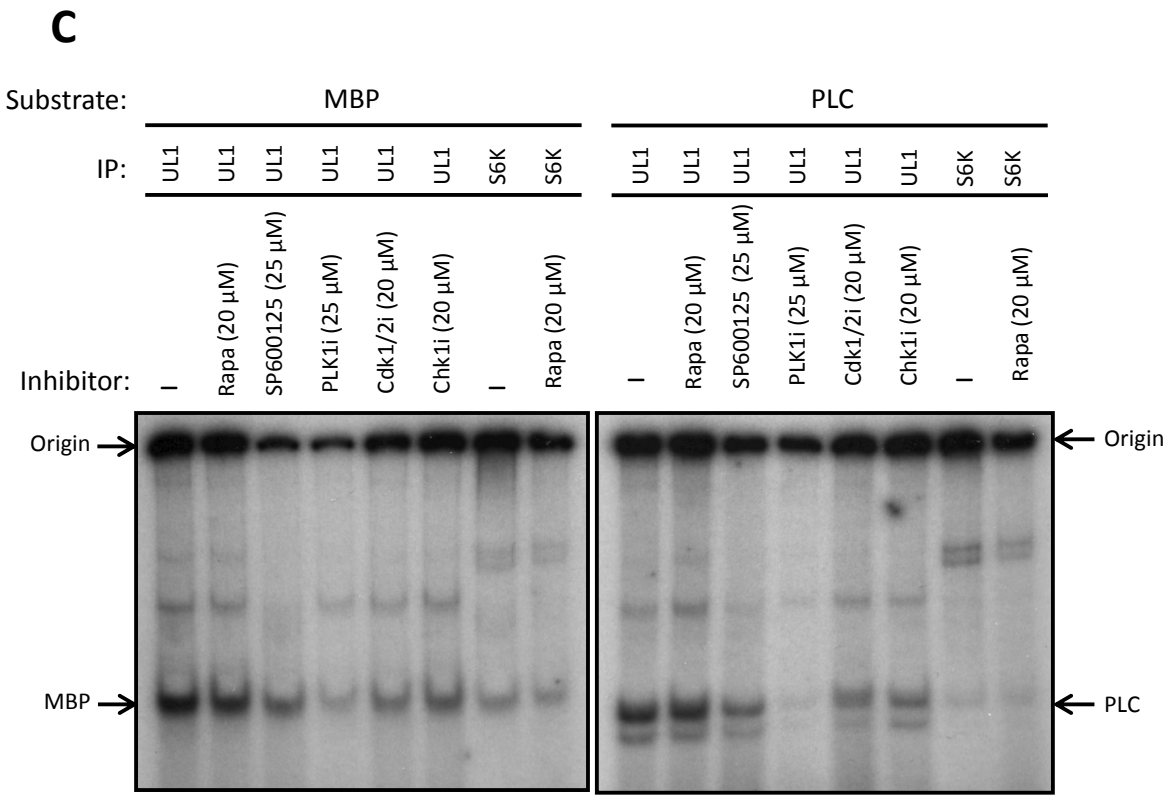

Figure 3.9 hnRNP-UL1 co-immunoprecipitates with p70S6K, although the observed phosphorylation is probably not due to p70S6K. A) COS and 293FT cells were lysed and immunoprecipitations performed for the hnRNP-UL1 or no antibody control. Samples were subjected to SDS-PAGE and western blots performed for p70S6K. B + C) HeLa cells were exposed to the indicated concentrations of inhibitor compounds for 24 hours before being lysed and immunoprecipitations performed for the indicated proteins. The immunoprecipitated protein was incubated with a reaction mixture containing the various inhibitors, the indicated protein substrates and γ-^{32}P-ATP. After 30 minutes the reaction was stopped, samples heated and run on a SDS-PAGE gel, before drying and analysis by autoradiography.

3.3 DISCUSSION

Within our group it has been known for many years that hnRNP-UL1 contained a putative kinase domain and shared structural homology to PNKP in this region. However, until now, no investigation had explored its nucleotide binding capability or kinase activity either as a DNA kinase or protein kinase at a practical level. The human genome encodes over 500 kinases the vast majority of which are protein kinases. PNKP is a DNA kinase and is essential to the DDR as 5' ends must be phosphorylated for ligation to occur after repair. Therefore, the novelty of investigating hnRNP-UL1 as a kinase, plus its greater homology to PNKP over any other kinase, made the study of potential DNA kinase activity very intriguing. However, no phosphorylation of DNA was observed in our experiments. As well as immunoprecipitated hnRNP-UL1, immunoprecipitated PNKP also failed to phosphorylate the DNA substrates used in our study and this may be due to a number of reasons. The PNKP antibody may not be particularly effective at immunoprecipitation and whilst the hnRNP-UL1 antibody is effective for immunoprecipitating the protein, sufficient levels of the protein may not have been obtained to observe phosphorylation. However, the DNA substrates used were effectively phosphorylated by recombinant mouse PNK suggesting that the lack of phosphorylation by immunoprecipitated human PNKP was not due to any problems with substrate specificity.

Whilst hnRNP-UL1 shared the most significant homology to PNKP in their respective kinase regions, hnRNP-UL1 also shared homology to a vast number of other kinases and these were all protein kinases. Once again the amino acid homology was limited, but many proteins showed a similar secondary structure and it would appear that the beta strands and alpha helices composing the kinase domains of many kinases are of a similar composition. Given this and the abundance of protein kinases compared to DNA kinases encoded by the

human genome, it is less surprising that protein and not DNA kinase activity was seen with hnRNP-UL1.

We repeatedly showed hnRNP-UL2 and hnRNP-U to lack ATP-binding, although both showed significant protein kinase activity. This anomaly is difficult to explain. Firstly, ATP-binding would be theoretically expected with all three proteins, especially after hnRNP-UL1 exhibited binding. All comprise a Walker A motif flanked by N-terminal residues predicted to form a beta-sheet and C-terminal residues predicted to form an alpha-helix, which is the stereotypical structure for a Walker A motif-containing, nucleotide-binding protein. In addition, the sequence homology between the three proteins across their entire predicted kinase regions is very high (62.8% between hnRNP-UL1 and –U / 50.6% between hnRNP-UL1 and –UL2). One possible explanation is the differences between their four interchangeable amino acid residues in the consensus motif (GXXXXGKT/S). Investigations made using the crystal structures of proteins with Walker A motifs in the Protein Data Bank showed that the four interchangeable XXXX residues have an influence on nucleotide-binding capability (Ramakrishnan et al., 2002). This is caused by differences in the Ramachandran angles of the proteins backbone and they must be of a certain range to permit the loop structure which surrounds the nucleotide during binding. The differences of these four residues in hnRNP-UL1 (LPAA), -U (LPGA) and –UL2 (LPGS) may be sufficient to alter the angles enough so hnRNP-U and –UL2 do not bind ATP.

Alternatively, the lack of ATP-binding could be due to a low efficiency of immunoprecipitation, although the kinase activity observed in γ-^{32}P-ATP experiments is strong when using the same antibodies. The antibodies show no cross reactivity upon western blotting suggesting antigen binding during immunoprecipitation should also be specific for each species. However, co-immunoprecipitation due to heterodimerisation is expected and

was confirmed between hnRNP-UL1 and –UL2 in Polo et al. (2012). Furthermore, recruitment of hnRNP-UL1 and -UL2 to DNA damage sites was interdependent (Polo et al., 2012). Considering this, hnRNP-UL2 and –U may co-immunoprecipitate hnRNP-UL1 and its activity may be responsible for the kinase activity observed. For this to be true lower levels of phosphorylation would be expected compared to the direct immunoprecipitation of hnRNP-UL1, however, it is greater with hnRNP-UL2 immunoprecipitation. There is also the possibility that hnRNP-UL1 binds ATP, but instead of direct phosphate transfer to the substrate it employs hnRNP-U for the kinase activity. However, this is unlikely given the functionality of other kinases being to bind triphosphate nucleotides and facilitate phosphoryl transfer themselves.

The band at 120 kDa visible in many of the protein kinase assays suggested possible autophosphorylation of hnRNP-UL1. Many kinases possess the capability to self-phosphorylate to regulate their activity; for example, ATM phosphorylates itself during DDRs to stimulate its own activity. In Figure 3.5 panels C and D, when kinase assays were carried out with hnRNP-UL1 in the absence of a substrate, the levels of autophosphorylation appear to increase. It is possible that in the absence of other substrates it is inclined to carry out more autophosphorylation. The autophosphorylation *in vivo* may occur to increase its own activity, as ATM does on serine 1981 in response to DNA damage. However, the site of this possible autophosphorylation and its biological relevance currently remains unclear.

The isolation of hnRNP-UL1 by immunoprecipitation from cell lysates and therefore the possibility of co-immunoprecipitating species being responsible for the phosphorylation seen in kinase assays was a major concern during the study. This could have been bypassed by the production of a recombinant form of hnRNP-UL1 but this unfortunately was never achieved mainly due to degradation of the protein. hnRNP-UL1 has a large number of

interacting partners both within RNA processing and DDR activities. It interacts directly with ATRIP, the binding partner of the ATR kinase, and ATR has been shown to co-immunoprecipitate with hnRNP-UL1 (Blackford et al., 2008). hnRNP-UL1 does not co-immunoprecipitate ATM (Blackford et al., 2008), but it is recruited to areas of DNA damage by interaction with NBS1 of the MRN complex, which in turn interacts with ATM. ATM and ATR are kinases with a wide variety of protein targets and their presence in reactions would most likely phosphorylate the promiscuous substrates MBP and PLC. The continued phosphorylation of the substrates in the presence of kinase inhibitors against the three PI3Ks (ATR, ATM and DNA-PK) provided greater confidence in hnRNP-UL1's kinase activity. The attribution of kinase activity to the interacting partner, p70S6K, was also found to be unlikely, providing further strength to hnRNP-UL1's proposed protein kinase activity.

There was a significant decrease in phosphorylation seen in the presence of two kinase inhibitors. These were SP600125 and PLK1i (BI 2536), which target c-Jun N-terminal kinase (JNK) and polo-like kinase 1 (PLK1), respectively. It is unknown whether either of these proteins is capable of co-immunoprecipitating with hnRNP-UL1. No study of their interaction has taken place and their involvement in cellular processes suggests no link between these two proteins and hnRNP-UL1. This should be tested in future work. Both SP600125 and BI2536 are small molecules which act by ATP competition at the binding site of their target protein (Bennett et al., 2001; Steegmaier et al., 2007). Like many other kinase inhibitors that act in a similar manner, they contain a nitrogen-ring system facilitating interaction with key residues of the active site of their target kinase (Bennett et al., 2001). It is the subtle chemical changes amongst these similar compounds that provide selectivity against specific kinases and not others. Both SP600125 and BI2536 were tested for activity against a panel of other kinases. SP600125 showed a 300-fold selectivity against the related MAPKs ERK1 and p38

(Bennett et al., 2001). BI 2536 showed more than a 1,000-fold selectivity relative to a panel of 63 other protein kinases (Steegmaier et al., 2007). However, hnRNP-UL1 was obviously not one of the protein kinases tested and it is possible that these small molecule inhibitors have some binding specificity to the active site of hnRNP-UL1, as well as their intended targets. Indeed, whilst BI 2536 showed good selectivity against many other kinases, it also affected the activities of PLK2 and PLK3 demonstrating binding can occur to other kinase active sites with similar structures (Steegmaier et al., 2007).

In conclusion, from the results shown in this chapter it appears likely that hnRNP-UL1 possesses some protein kinase activity, but no DNA kinase activity like that of PNKP to which it has the most significant primary and secondary structure homology within their kinase domains. To facilitate further investigation and to attempt to refute the possibility of a co-immunoprecipitating protein being responsible for the phosphorylation observed in kinase assays with immunoprecipitated hnRNP-UL1, a Walker A mutant (MWA)-hnRNP-UL1 construct was made by site-directed mutagenesis. Investigations with this construct are presented in chapter V.

CHAPTER IV

HNRNP-UL1 AND ALS

4.1 INTRODUCTION

Amyotrophic lateral sclerosis (ALS) is a relentlessly progressive neurodegenerative disease affecting the lower motor neurons (LMNs) in the brainstem and spinal cord, the upper motor neurons (UMNs) in the motor cortex and in some patients the prefrontal and temporal cortex of the brain (Robberecht and Philips, 2013). The aetiology and pathogenesis of the disease is complex with many associated mutated genes. In recent years, a number of genes with roles in RNA processing have been associated with ALS. Therefore, it was of great interest when Professor Weischaupt of the University of Ulm contacted us with details of four ALS patients with heterozygous, germline mutations in *hnRNP-UL1*.

As well as hnRNP-UL1's roles in RNA processing, it has been shown to have several roles in the DNA damage response (DDR). It was shown to interact with RPA70 and RPA32, which bind regions of single stranded DNA during repair (Blackford et al., 2008). Polo et al. (2012) showed it to be essential for the resection of the 5' strand during homologous recombination of double strand breaks (DSBs) by recruiting the endonuclease BLM. Hong et al. (2013) also showed a specific and rapid recruitment to DSBs through an interaction with PARP-1 catalysed PAR moieties. Given the known roles of hnRNP-UL1 in the DDR and growing evidence of accumulation of DNA damage in neuronal cells of patients with neurodegenerative disorders such as Parkinson's disease, Alzheimer's disease and ALS, we aimed to investigate the DDR in the lymphoblastoid cell lines derived from these patients with hnRNP-UL1 mutations (unfortunately fibroblasts from the patients were not available).

4.2 RESULTS

4.2.1 ALS patient mutations

ALS patients were discovered with heterozygous hnRNP-UL1 mutations by sequencing of the most common ALS mutated genes and the genes for the 150 most common RNA binding proteins. This was conducted on 252 German and Swedish families in which at least 2 individuals were affected. Lymphoblastoid cell lines (LCLs) were derived from blood samples of ALS patients sent from Professor Weischaupt. These included four hnRNP-UL1, one TDP43, and three FUS mutants (Table 4.1). The TDP43 and FUS mutants were included as they represented common mutations of these genes in ALS patients and their DNA damage response had not been investigated previously. Also included in the study were three patients with heterozygous microdeletions of the region 1q44, which includes the hnRNP-U gene (Table 4.1). These are not ALS patients, but have a neurological disorder manifesting in early childhood with intellectual disability (ID), microcephaly, craniofacial anomalies, seizures, limb anomalies, and corpus callosum abnormalities. This is detailed further in Thierry et al. (2012). The LCLs derived from patient blood samples are detailed in Table 4.1 and were investigated in this study for their DDR to both IR and camptothecin (CPT) treatment.

4.2.2 Protein expression levels are not affected by mutations

Mutations in all the cell lines were heterozygous meaning one wild-type allele was present. To check that expression levels of each of the proteins under investigation were 'normal', cell lysates were made and protein levels analysed by western blotting. Levels of hnRNP-UL1 are similar in the hnRNP-UL1 mutant cell lines to lab donor controls, as are TDP43 levels in the TDP43 mutant cells (Figure 4.1). Unfortunately, antibodies were not

Table 4.1 Details of the patient derived lymphoblastoid cell lines.

LCL cell line	Affected/mutated gene	Mutation (all heterozygous)	Patient disease
P1	HnRNP-U	1q44 microdeletion (entire gene not present on one allele)	Unnamed disorder. (Symptoms include intellectual disability, epileptic seizures, craniofacial anomalies and brain abnormalities.)
P3	HnRNP-U	1q44 microdeletion (entire gene not present on one allele)	
P5	HnRNP-U	1q44 microdeletion (entire gene not present on one allele)	
V1200	TDP-43	N352S	ALS
V2029	FUS	R521H	ALS
V321	FUS	K510R	ALS
V2183	FUS	R521H	ALS
V2250*	HnRNP-UL1	R639C	ALS
V2219*	HnRNP-UL1	R639C	ALS
V2721	HnRNP-UL1	A 2bp insert mutation which occurs intronically for all but one hnRNPUL1 RNA transcript. The exception is a transcript where the insertion causes a frameshift mutation at aa212.	ALS
V2716	HnRNP-UL1	R468C	ALS

The table shows the name assigned to each LCL patient cell line, the gene mutated, details of each mutation and the patient disease. *Siblings.

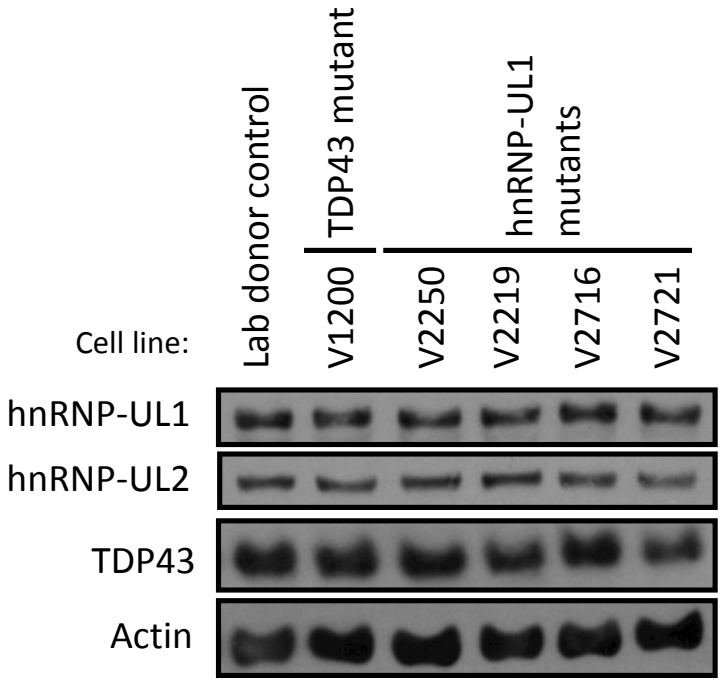

Figure 4.1 The expression levels of hnRNP-UL1, hnRNP-UL2 and TDP43 are normal in all the patient LCLs. Cell lysates were taken and proteins were separated by SDS-PAGE and subjected to western blotting with the indicated antibodies.

available for hnRNP-U or FUS at this time and therefore patient cell lines with these affected proteins were not investigated. Normal cellular protein levels suggest that any defects of the cells in their ability to execute DNA damage responses would not be due to haploinsufficiency.

4.2.3 The DNA damage response was unaffected in ALS LCLs

Patient LCLs were subjected to both IR and CPT treatment alongside LCLs derived from healthy individuals (lab donors). Both treatments induce DSBs and western blotting analysis for known markers of DSB DNA damage responses, including γH2AX (S139), pRPA (S4/S8) and pChk1 (S345), were used to analyse any discrepancies in responses. In response to IR and CPT all patient LCLs showed no repeatable defects in their DDR. Figures 4.2 and 4.3 show an example of the western blots obtained from V2219 and V2721 hnRNP-UL1 mutant cell lines in response to each treatment over a 24 hour time period. This was completed in triplicate for all the patient LCLs, but no repeatable and significant differences were observed between patients and controls. Some differences were observed, for example, the increased levels of γH2AX, pNBS1 and pChk1 in response to IR of the V2721 cell line compared to control. However, such differences were never repeatable and often variations reversed between control and patient cell lines upon repeat experiments. This is likely due to the variable nature of LCLs.

4.2.4 Localisation of hnRNPUL1 is unaffected by the mutations present in the ALS patient cells

Plasmid constructs encoding the HA-tagged R639C and R468C mutant hnRNP-UL1 proteins were made by site-directed mutagenesis. This allowed transfection in to HeLa cells and analysis of their cellular localisation by immunofluorescence. Localisation of both ALS

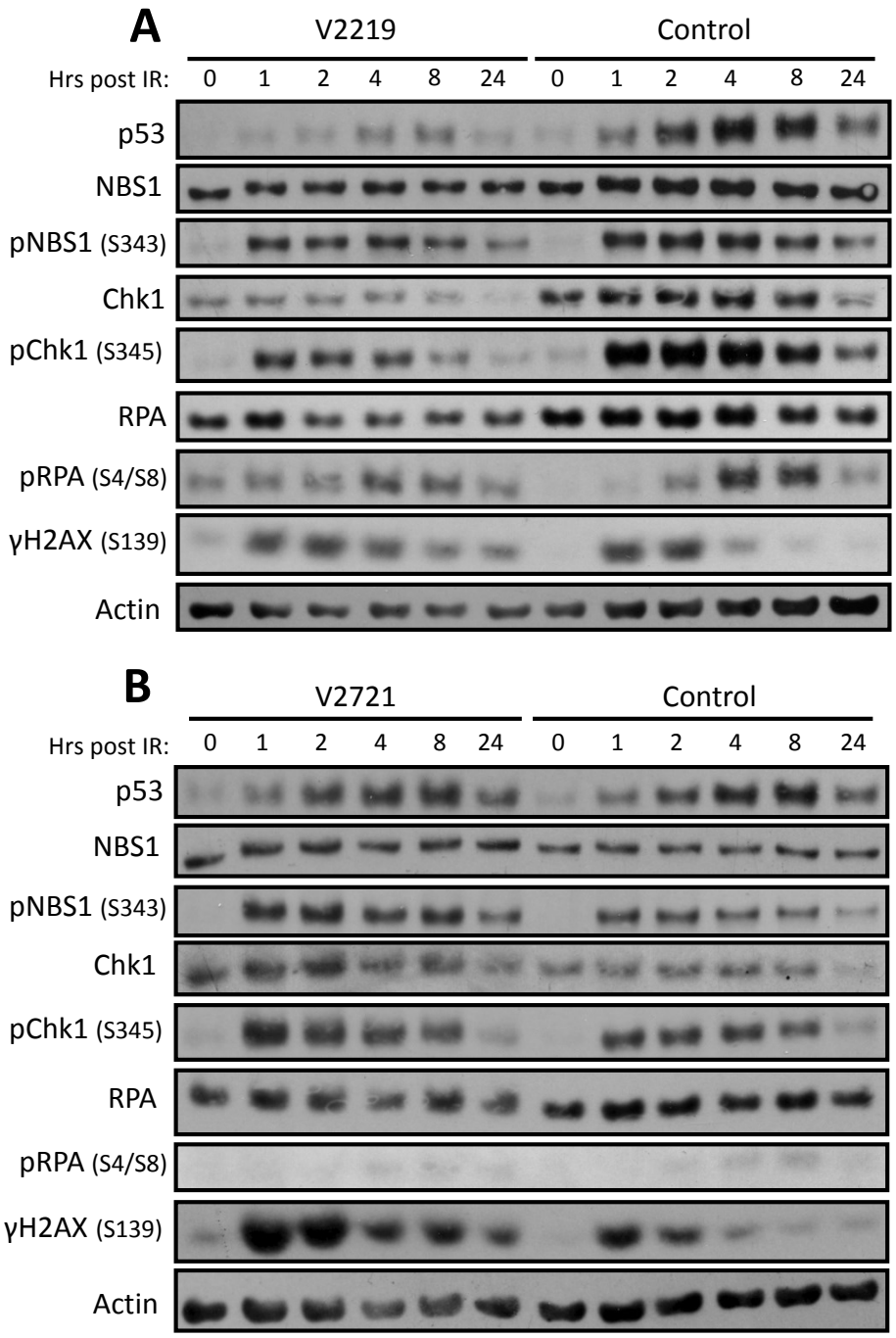

Figure 4.2 ALS patient cell lines exhibited no significant differences in their DDR to ionising radiation (IR) compared to non-patient controls. A and B) ALS and non-patient control LCLs were subjected to treatment with IR and lysates taken at 1, 2, 4, 8 and 24 hours post-treatment. Proteins were separated by SDS-PAGE and subjected to western blotting with the indicated antibodies.

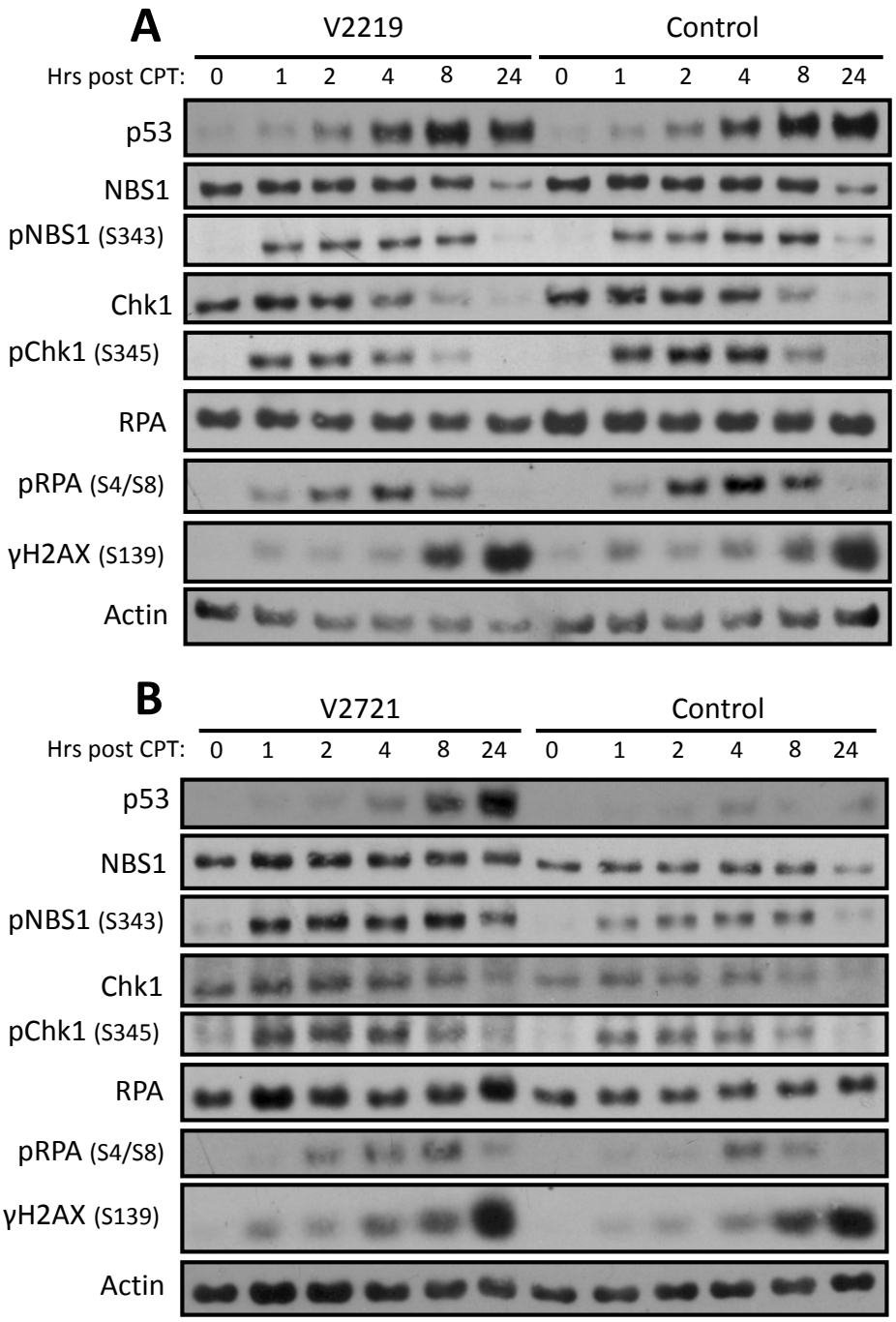

Figure 4.3 ALS patient cell lines exhibited no significant differences in their DDR to camptothecin (CPT) treatment compared to non-patient controls. A and B) ALS and non-patient control LCLs were subjected to treatment with CPT and lysates taken at 1, 2, 4, 8 and 24 hours post-treatment. Proteins were separated by SDS-PAGE and subjected to western blotting with the indicated antibodies.

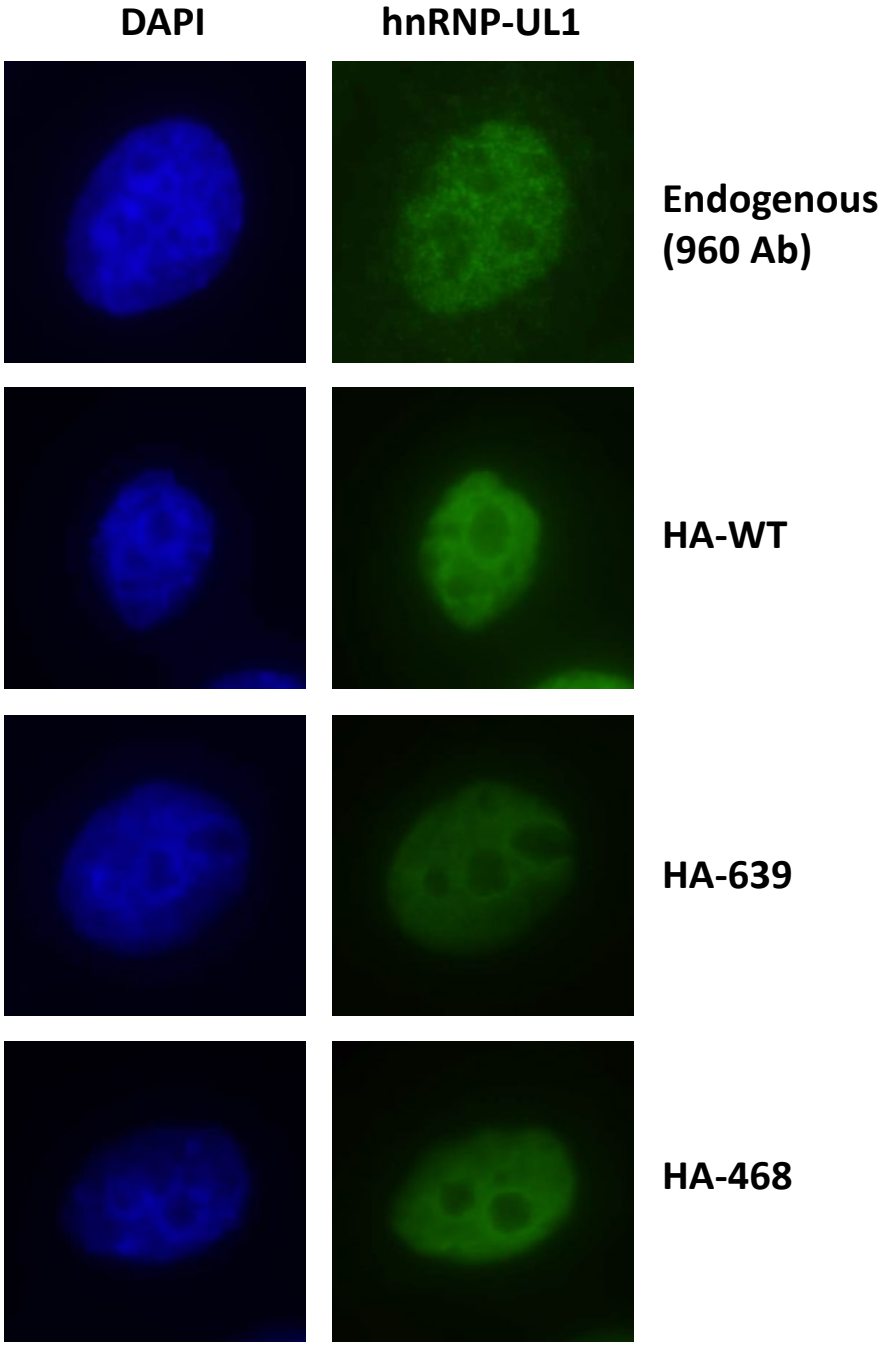

Figure 4.4 Localisation of hnRNP-UL1 is unaffected by the mutations present in the ALS patient cells. HeLa cells were transfected with the indicated hnRNP-UL1 expressing plasmid or left untreated. Cells were fixed and permeabilised 24 hours later, followed by staining with antibodies against hnRNP-UL1 (960) or HA. DNA was stained blue with DAPI. Microscope images were taken at X100 magnification.

mutant proteins was similar to WT, with the protein largely residing in the nucleus (Figure 4.4). When observing the HA-tagged proteins expressed transiently from the transfected plasmids the levels of fluorescence varied considerably between some cells and others (Figure 4.5). This is most probably a result of some cells transfecting more efficiently than others and therefore expressing more protein. The presence of cytoplasmic hnRNP-UL1 is visible, but the levels of the ALS mutant proteins are similar to that of WT (Figure 4.5). This suggests that these mutations do not directly result in a tendency for the protein to be sequestered in the cytoplasm as many ALS mutated proteins do (Robberecht and Philips, 2013), at least not after a 24 hour period following transfection.

4.2.5 Mutant hnRNP-UL1 proteins R639C and R468C do not induce oxidative stress

There is a strong link between oxidative stress and ALS (Barber and Shaw, 2010; Pollari et al., 2014). It was decided to investigate whether levels of oxidative stress increased when the two hnRNP-UL1 ALS patient mutants R639C and R468C were transfected in to HeLa cells. Nrf2 (nuclear erythroid 2-related factor 2) is a transcription factor, which acts on enhancer regions called AREs (*cis*-acting response elements) present in genes encoding drug metabolising enzymes, such as glutathione S transferase (GST) and NAD(P)H:quinone oxidoreductase 1 (NQO1). In response to antioxidants and electrophiles, Keap1 (Kelch-like ECH-associated protein 1) fails to ubiquitylate Nrf2 stabilising the protein and allowing greater upregulation of the above genes, helping the cell to combat the oxidative stress (Ma, 2013). Therefore, should the hnRNP-UL1 mutants stimulate oxidative stress an upregulation of Nrf2 would be expected. In the results shown in Figure 4.6 the effect of depletion of hnRNP-UL1 and the addition of the ALS mutant proteins is examined. Treatment with the antioxidant, TBHQ (*tert*-butylhydroquinone), used as a positive control, caused an increase in Nrf2 levels, especially at the 1 and 3 hour time points after use of the higher concentration of

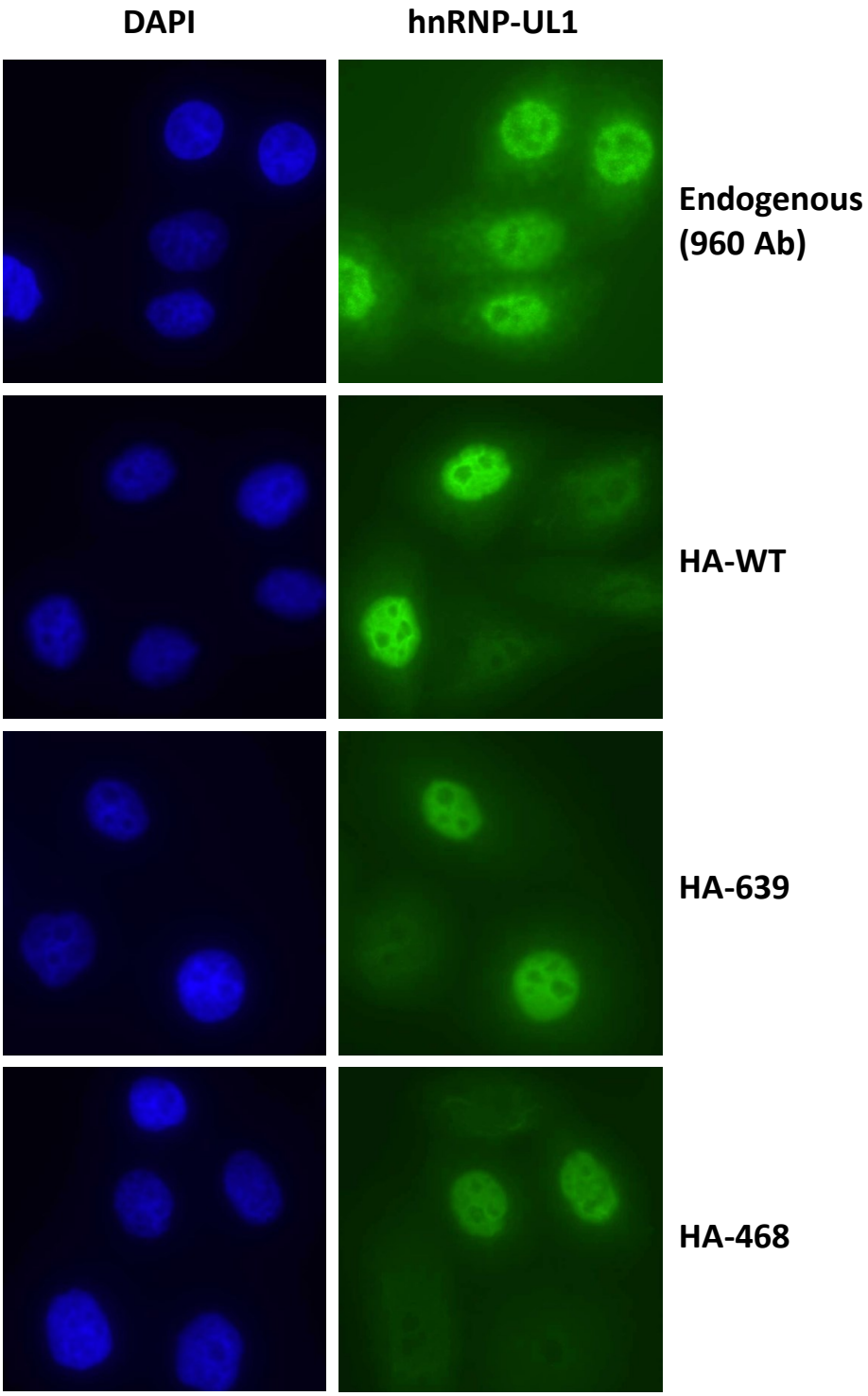

Figure 4.5 Localisation of hnRNP-UL1 is unaffected by the mutations present in the ALS patient cells. HeLa cells were transfected with the indicated hnRNP-UL1 expressing plasmid or left untreated. Cells were fixed and permeabilised 24 hours later, followed by staining with antibodies against hnRNP-UL1 (960) or HA. DNA was stained blue with DAPI. Microscope images were taken at X60 magnification.

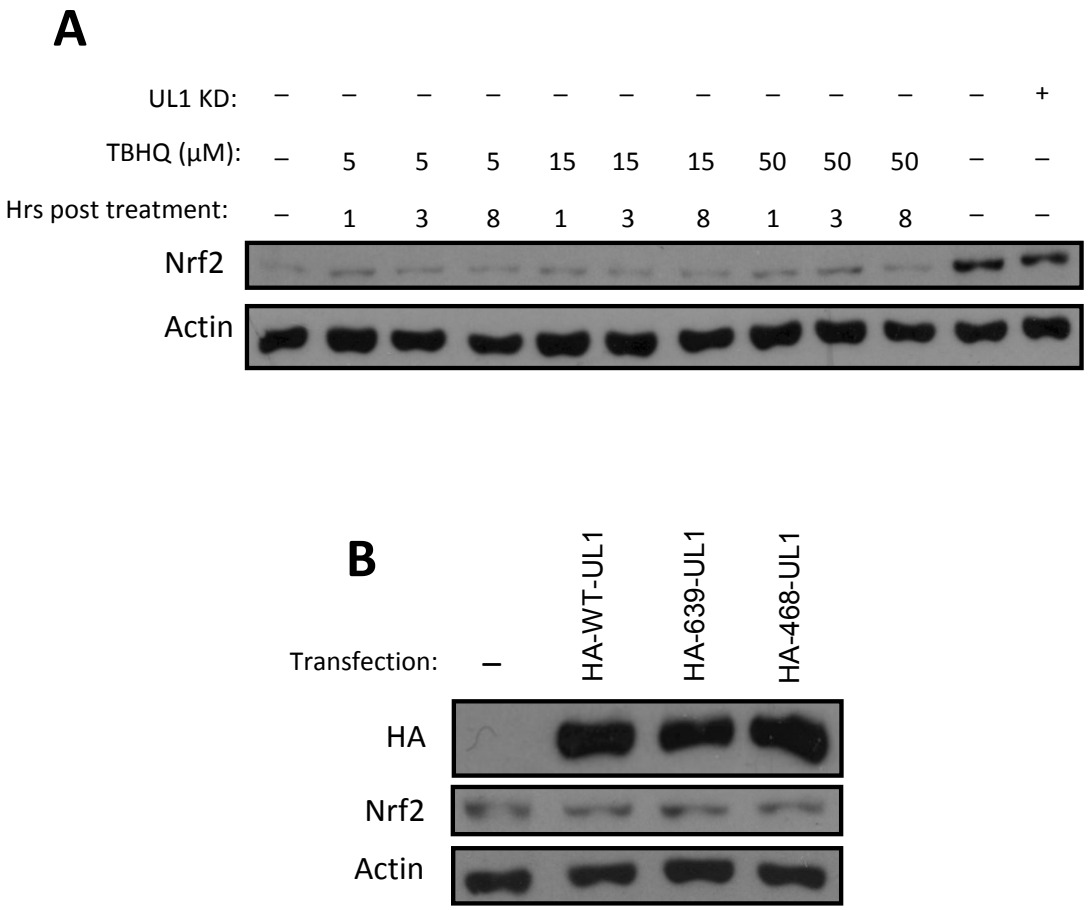

Figure 4.6 Expression of the ALS patient proteins harbouring the mutations R639C and R468C causes no increase in oxidative stress. A) U2OS cells were subjected to treatment with various concentrations of TBHQ and lysates taken at indicated time points. Proteins were separated by SDS-PAGE and subjected to western blotting with the indicated antibodies. B) HeLa cells were transfected with the indicated HA-tagged constructs of hnRNP-UL1. Lysates were subsequently taken 24 hours later, proteins separated by SDS-PAGE and subjected to western blotting with the indicated antibodies.

50 μM (Figure 4.6A) confirming Nrf2's response to oxidative stress. Expression of the hnRNP-UL1 mutants did not affect Nrf2 levels (Figure 4.6B) suggesting the base substitutions present in the mutants do not confer a gain or loss of function resulting in oxidative stress. Also, depletion of hnRNP-UL1 did not affect Nrf2 levels compared to control (Figure 4.6A) suggesting that hnRNP-UL1 has no significant role in regulating redox homeostasis in the cell.

4.3 DISCUSSION

In this chapter, the DDRs of ALS patient-derived LCLs were investigated. The importance of the DDR in neuronal development has long been recognised and is shown by the neurological disorders caused by mutations in genes encoding DDR proteins, such as ataxia telangiectasia (AT) and Seckel syndrome (SS) (for more details see section *1.2.6* and Table 1.1). In recent years, the DDR has been recognised for its importance in the proper functioning of the mature nervous system and a strong link has been established between DNA damage and neurodegenerative diseases, including ALS (Madabushi et al., 2014). Neuronal cells accumulate DNA damage over a long period of time and are at increased risk of oxidative stress due to their longevity and high oxygen demands. The use of this oxygen and production of ATP by the electron transport chain in mitochondria leaves the mtDNA particularly susceptible to oxidative damage (Coppedé and Migliore, 2015). Increased levels of oxidative damage have been observed in both ALS patient post-mortem studies of neuronal tissues and in the cerebrospinal fluid of ALS patients at early stages of the disease (Barber and Shaw, 2010). Levels of oxidative damage, as well as SSBs and DSBs, have been shown to correlate with disease severity (Bogdanov et al., 2000; Martin et al., 2007). However, the

degree to which DNA damage is a cause or consequence of neurodegeneration is still largely unclear, although it is likely that there is truth to both hypotheses (Coppedé and Migliore, 2015). Further evidence for DDR defects possibly having involvement in ALS comes from other neurodegenerative diseases caused by mutations in DDR genes, which is particularly evident in a subgroup of human autosomal recessive ataxias (Gueven et al., 2007). These include AT, ATLD, AOA1 and AOA2. In fact, AOA1 develops due to mutations in a gene encoding a DNA/RNA helicase (senataxin-SETX), which is also mutated in some fALS cases (Coppedé, 2011). AT and ATLD result from mutations in the genes encoding ATM and MRE11, respectively (Ciccia and Elledge, 2010). The progressive neurodegeneration seen in these diseases is due to the consequent DDR defects caused by dysfunction of the proteins, both of which play prominent roles in responses to DSBs. Therefore, the hnRNP-UL1 gene makes a reasonable gene candidate to be mutated in a neurodegenerative disease given its roles in DSB repair (Polo et al., 2012).

With an accumulation of DNA damage in ALS neuronal cells and a continuing exposure to damage, DDR defects could exacerbate disease progression by accelerating neuronal cell death. In fact, FUS has been shown to have roles in the DDR both through early phase PARP-1-dependent recruitment to DSBs, caused by laser-induced damage (Mastracola et al., 2013), and through interaction with HDAC-1 (Wang et al., 2013). Several FUS ALS patient mutations were shown to affect HDAC-1 binding causing DDR defects (Wang et al., 2013) and expression of FUS^{R521C} in an ALS mouse model caused accelerated disease progression (Qiu et al., 2014). Given what is known about the roles of hnRNP-UL1 in the DDR, its similarities with FUS discussed in section *1.4.4* and the growing evidence of DNA damage's role in ALS, we decided to explore the DDR in LCLs derived from ALS patient blood samples.

IR and CPT were used, as both agents induce DSBs, and hnRNP-UL1 has been shown to have roles in the DDR to DSBs. Polo et al. (2012) showed a reduction in phosphorylation of Chk1 and RPA in response to these damaging agents when hnRNP-UL1 was depleted. However, no consistent differences were observed in the DDRs of ALS patient cells and controls on examination of the levels of phosphorylation of these proteins. This was consistent for ALS patients with FUS and TDP43 mutations, as well as the non-ALS patients with deletions in the *hnRNP-U* gene. Two of the FUS mutants harboured base substitutions of the arginine residue 521. This is the same residue mutated in previous studies in which DSB repair defects were caused by diminished interaction with HDAC-1 both *in vitro* and *in vivo* (Wang et al., 2013; Qiu et al., 2014). Therefore, similar defects within the V2029 and V2183 LCLs harbouring a R521H FUS mutation would be expected, but were not seen (data not shown). Upon carrying out repeat experiments any differences between responses in patient cells and controls were slight and not reproducible and even reversed from one experiment to the next. This variability and lack of DDR defects in patient cells may be explained by the variable nature of EBV (Epstein Barr virus) immortalised LCLs.

LCLs are derived from primary blood B cells by infection with EBV stimulating high proliferation rates. This is thought to "immortalise" the cells; however, studies have shown that not all LCL strains become truly immortal and some undergo cellular crisis after an average of 40 passages due to low telomerase activity, low copy number of the EBV genome and decreased EBV expression (Jeon et al., 2003). The early senescence and eventual death of a number of the ALS patient LCLs occurred during this study. It is possible that the proliferation rates and different intracellular conditions affected the results obtained when conducting DDR experiments. This would explain the variation seen with repeated experiments as cellular states changed. The presence of EBV in the LCLs also directly affects

their DDRs. The EBV nuclear antigen 1 (EBNA-1) stimulates the production of ROS inducing chromosomal aberrations, including DSBs and is known to cause H2AX phosphorylation. The latent membrane protein 1 (LMP1) also inhibits DNA repair through downregulation of ATM (Gruhne et al., 2009a; Gruhne et al., 2009b). Depending on the copy number of the virus in different LCL strains and the expression levels of various viral proteins this could cause significant variations in any observed DDRs and possibly be responsible for the variations observed in our results.

A failure to detect significant DDR differences between controls and patient cells could also be due to the fact that the LCLs are derived from blood lymphocytes and may not reflect the intracellular metabolism of diseased ALS motor neuronal cells. The *hnRNP-UL1* mutations were discovered by sequencing conducted on blood samples. Therefore, the mutations are known to be germline, heterozygous mutations; however, there may be additional somatic mutations present in the diseased neuronal cells that would only be identifiable by isolation of those cells and sequencing of their DNA. It was known that the cells harbouring *hnRNP-UL1* germline mutations did not have any other mutations present in any of the known ALS-related genes. However, additional somatic mutations of these genes or of the other hnRNP-UL1 allele could also be present specifically in the neuronal cells. These could cause differences in the neuronal cells' DDRs, as well as influence other aspects of the disease's pathogenesis. This is a possibility worth mentioning considering that only 5-10 % of ALS cases are familial and the rest sporadic (Sreedharan, 2008). The pathogenicity, phenotypes and disease progression of sporadic cases are indistinguishable from familial cases and some sALS cases are known to harbour the same sporadic genetic aberrations as germline fALS cases (Andersen and Al-Chalabi, 2011). However, additional sporadic mutations in the neuronal cells of the patients in this study, which would not be present in the

B lymphocytes used to create our LCLs is a possibility worth considering. In addition, the increased exposure of motor neuronal cells of ALS patients to greater DNA damage stress than other cells (particularly oxidative damage), as already discussed, would influence responses to additional damaging agents such as IR and CPT. Therefore, ideally experiments looking at DDRs would have been conducted in a neuronal-like cell line or an ALS mouse model, but these were not possibilities available during our study. However, the creation of plasmid constructs encoding HA-tagged R639C and R468C hnRNP-UL1 proteins, which were also siRNA-resistant allows depletion of endogenous hnRNP-UL1 and transient expression of the mutant proteins in non-LCL cells. Such experiments are detailed in chapter V and circumvented the problem of the WT-hnRNP-UL1 being present due to heterogeneity in the LCLs. Investigations of the hnRNP-UL1 variants' capability to bind NBS1, XRCC1 and PARP-1, which influence its roles in the DDR, are also investigated in chapter V.

The pathogenic processes in ALS leading to neuronal cell death are complex and a combination of mechanisms including DNA damage defects, oxidative stress, mitochondrial dysfunction, protein aggregation, cytoskeletal dysfunction, RNA processing defects, glutamate excitotoxicity and endoplasmic reticulum stress may all play a part (Barber and Shaw, 2010). Therefore, despite no apparent DDR defects within the hnRNP-UL1 ALS patients it is still plausible that these mutations contribute to other pathogenic processes causing the neurodegeneration observed. Indeed, given that these mutations were found in familial cases of the disease and two siblings with the same mutation both developed the disease and no other ALS-related gene showed a germline mutation, it would suggest a pathogenic consequence to the hnRNP-UL1 mutations.

Perhaps the most obvious mechanism for hnRNP-UL1 mutations to contribute to ALS pathogenesis is through increased aggregation propensity as cytoplasmic inclusions remain as

the hallmark of the disease. The transfection of the R639C and R468C variants in HeLa cells did not lead to any observable increase in cytoplasmic levels of the protein or any aggregate formation (Figure 4.5). However, their expression over a time period of just 24 hours may be insufficient to generate large amounts of aggregation. The potential aggregation of hnRNP-UL1, including the R639C and R468C variants, as a contributing factor to ALS pathogenesis is further discussed in section *6.2*.

We considered the possibility of the mutants contributing to oxidative stress levels like that of some SOD1 mutations. However, the expression of Nrf2, a protein which increases with oxidative stress, failed to show an increase in expression when cells with either the R639C or R468C mutations were examined (Figure 4.6). The expression of the mutants in HeLa cells in this experiment was for a 24 hour period and it is possible that a prolonged presence of these mutant proteins may be required to stimulate oxidative stress. After all, familial cases of ALS typically take between 50 and 60 years to manifest symptoms meaning a more subtle and gradual increase could take place.

Given hnRNP-UL1's role in RNA processing and the firm establishment of RNA processing defects in ALS motor neuron cells as discussed in section *1.4.2*, a contribution to pathogenesis in this manner is very plausible. The RNA-binding of the hnRNP-UL1 variants is investigated and further discussion made in chapter V.

In conclusion, whilst our study showed no possible direct avenues for the patient mutations to contribute to ALS pathogenic mechanisms, there are many other possibilities for them to do so. Although our study had limitations, particularly in the type of cells in which the DDR experiments were conducted, it has gone some way to establishing that the effect of the hnRNPUL-1 mutations is on properties of the protein unrelated to its role in the DDR.

CHAPTER V

PROFILING THE HNRNP-UL1 MUTANTS

5.1 INTRODUCTION

During chapter IV two hnRNP-UL1 mutant plasmid constructs were produced by site-directed mutagenesis, which encoded base substitutions (R639C and R468C) the same as two of the ALS patient cell lines (V2250/V2219 and V2716 respectively). During this chapter, the creation of a Walker A mutant (MWA) by the same method was accomplished, which substituted key residues in the motif to investigate effects when the ATP-binding of hnRNP-UL1 was negated. These constructs were also made resistant to a siRNA targeting a single site at the C-terminus of hnRNP-UL1. Consequently, this allowed knockdown of endogenous hnRNP-UL1 and transfection of the mutant constructs followed by various experiments to investigate any affects.

The aims of the work in this chapter were to investigate any differences in the biological properties of the mutants compared to wild-type or defects in their cellular roles. This included the binding of ATP, single stranded-DNA and –RNA, DNA damage responses to various agents, their cellular localisation and the interaction with NBS1, XRCC1 and PARP-1.

5.2 RESULTS

5.2.1 The Walker A mutant does not bind ATP and lacks protein kinase activity

To verify the ATP-binding and protein kinase activity of hnRNP-UL1, a Walker A mutant (MWA) hnRNP-UL1 plasmid DNA construct was made by site-directed mutagenesis. The last three amino acids of the Walker A loop were changed as these were considered the most important for ATP-interaction and facilitating phosphorylation of substrates by kinases with Walker A loops (Deyrup et al., 1998). The glycine, lysine and threonine residues were substituted with alanine, arginine and alanine, respectively (GKT433ARA). Transfection of the construct in to HeLa cells and subsequent immunoprecipitation of the translated protein by its HA-tag allowed α- and γ-^{32}P radioactively labelled ATP experiments to be conducted.

As expected, MWA-hnRNP-UL1 was unable to bind ATP (Figure 5.1). It also showed significantly reduced phosphorylation of the protein substrate myelin basic protein (MBP) (Figure 5.2), strongly suggesting the activity observed in previous kinase assays was due to hnRNP-UL1 itself and not a co-immunoprecipitating protein. Despite what appears to be a complete inability to bind ATP by MWA-hnRNP-UL1 there was still some level of phosphorylation of MBP. However, this may be attributable to the homodimerising capabilities of hnRNP-UL1 such that upon immunoprecipitation of MWA-hnRNP-UL1 by its HA-tag, endogenous wild-type (WT) hnRNP-UL1 is co-immunoprecipitated. Co-immunoprecipitation of WT-hnRNP-UL1 and MWA-hnRNP-UL1 was confirmed by co-transfection of HA- and GFP-tagged constructs (Figure 5.3).

5.2.2 The R639C and R468C mutants exhibit normal ATP-binding and kinase activity

Using transfected constructs encoding the mutant hnRNP-UL1 variants, further α- and γ-^{32}P radioactively labelled ATP experiments showed no reduction in ATP-binding or protein

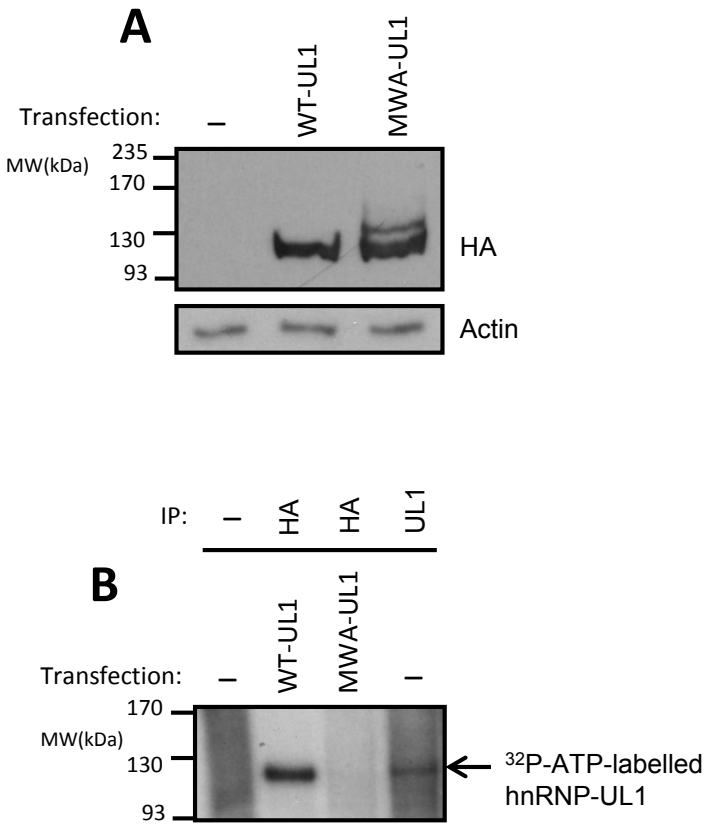

Figure 5.1 The Walker A mutant (MWA) does not bind ATP. A) HeLa cells were transfected with indicated HA-tagged constructs of hnRNP-UL1. Lysates show successful protein expression after blotting for the HA-tag. B) Following transfection of indicated constructs, cells were lysed and immunoprecipitations performed for the indicated proteins. Proteins were incubated with ox-α-^{32}P-ATP and subjected to SDS-PAGE. The dried gel was analysed by autoradiography.

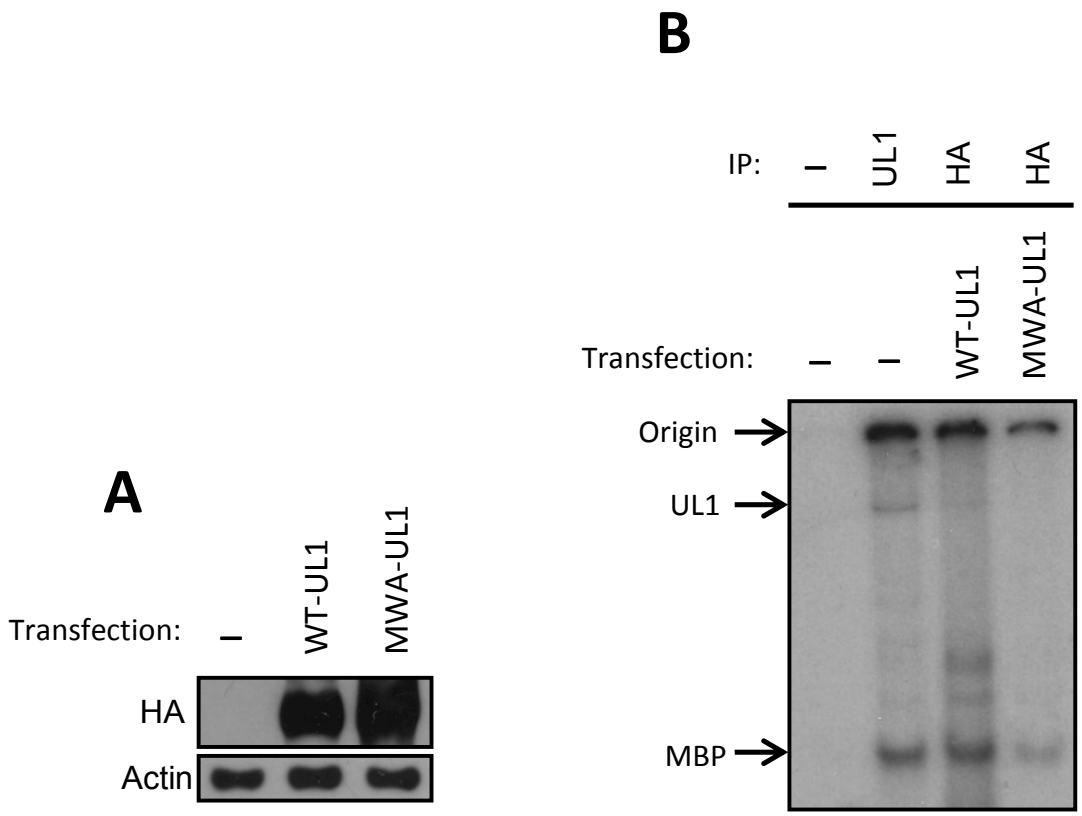

Figure 5.2 The Walker A mutant (MWA) has reduced kinase activity. A) HeLa cells were transfected with indicated HA-tagged constructs of hnRNP-UL1. Lysates show successful protein expression after blotting for the HA-tag. B) Following transfection of indicated constructs, cells were lysed and immunoprecipitations performed for the indicated proteins. Proteins were incubated with a reaction mixture containing the substrate MBP and γ-^{32}P-ATP. After 30 minutes the reaction was stopped, samples heated and run on a SDS-PAGE gel, before drying and analysis by autoradiography.

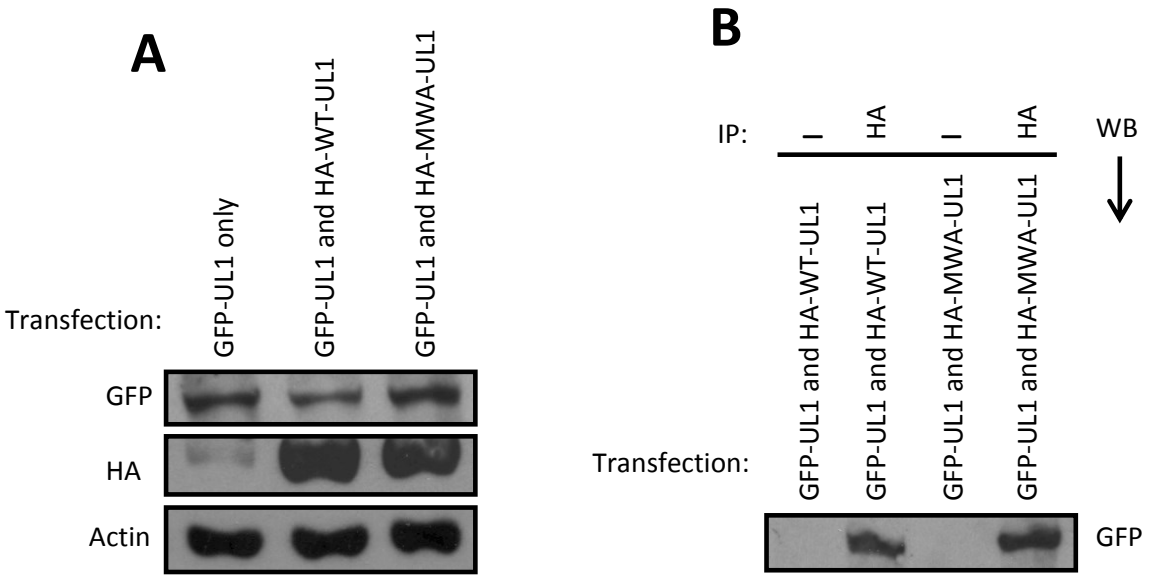

Figure 5.3 WT-WT and WT-MWA hnRNP-UL1 proteins homodimerise. A) HeLa cells were transfected with indicated HA- and GFP-tagged constructs of hnRNP-UL1. Lysates show successful protein expression. B) Following transfection of indicated constructs, cells were lysed and immunoprecipitations performed with the indicated antibodies. Proteins were separated by SDS-PAGE and subjected to western blotting to analyse the co-immunoprecipitation of GFP-tagged hnRNP-UL1.

kinase activity with the ALS patient R639C and R468C mutants (Figures 5.4 and 5.5). The residue 639 lays C-terminal to the proposed kinase domain and within the RGG domain making these results unsurprising. The 468 residue does fall within the kinase domain, just 33 residues C-terminal of the Walker A loop. However, it appears the mutation of this residue is unimportant to the protein's kinase activity.

5.2.3 Single stranded DNA-binding deficiencies of mutants

The ssDNA-binding capability of hnRNP-UL1 was observed by Gabler et al. (1998). Using a similar technique, it was found that the MWA-hnRNP-UL1 exhibited decreased ssDNA-binding, particularly at higher salt-concentrations where protein/DNA interactions are dissociated (Figure 5.6). This suggests that the ssDNA-binding capability of hnRNP-UL1 is dependent on ATP-binding to some degree, but the biological relevance of this remains unclear. It is possible that the three base substitutions of the MWA-hnRNP-UL1 mutant cause large conformational changes in the protein's structure on their own, which are sufficient to affect ssDNA-binding. The R639C and R468C mutants also showed decreased binding efficiency compared to that of wild-type, although it was only evident at the higher salt concentrations (Figure 5.6).

5.2.4 Single stranded RNA-binding deficiencies of mutants

Similar experiments were conducted in which cell lysates were incubated with biotin-labelled ribonucleotide homopolymers linked to streptavidin agarose to investigate the ssRNA-binding of each hnRNP-UL1 variant. As observed with ssDNA-binding, increasing salt concentrations dissociate protein/RNA interactions (Figure 5.7B) and all three variants reduce binding (Figure 5.7B, C and D). Gabler et al. (1998) showed hnRNP-UL1 to have ssRNA-binding preference for poly(G) followed by poly(C) and only very weak binding of

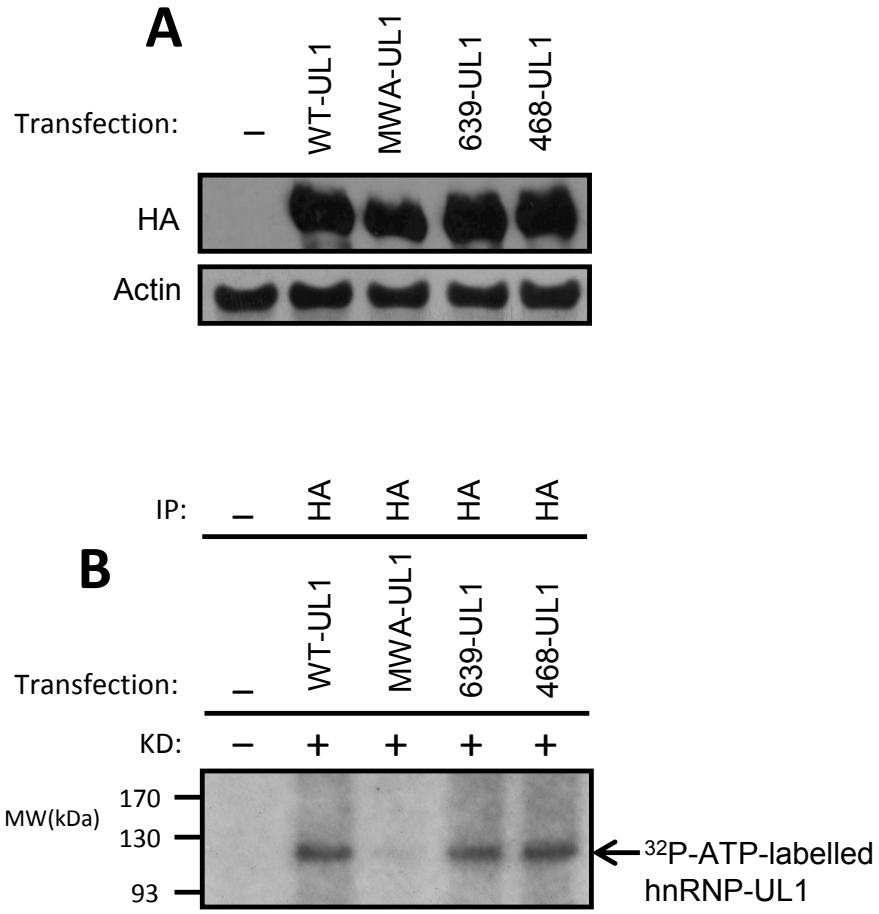

Figure 5.4 Binding of ATP by the hnRNP-UL1 mutants. A) HeLa cells were co-transfected with siRNA targeting endogenous hnRNP-UL1 and siRNA-resistant HA-tagged constructs of hnRNP-UL1 where indicated. Lysates show equal protein expression of the tagged proteins. B) Following transfection of indicated constructs, cells were lysed and immunoprecipitations performed for the indicated proteins. Proteins were incubated with ox-α-^{32}P-ATP and subjected to SDS-PAGE. The dried gel was analysed by autoradiography.

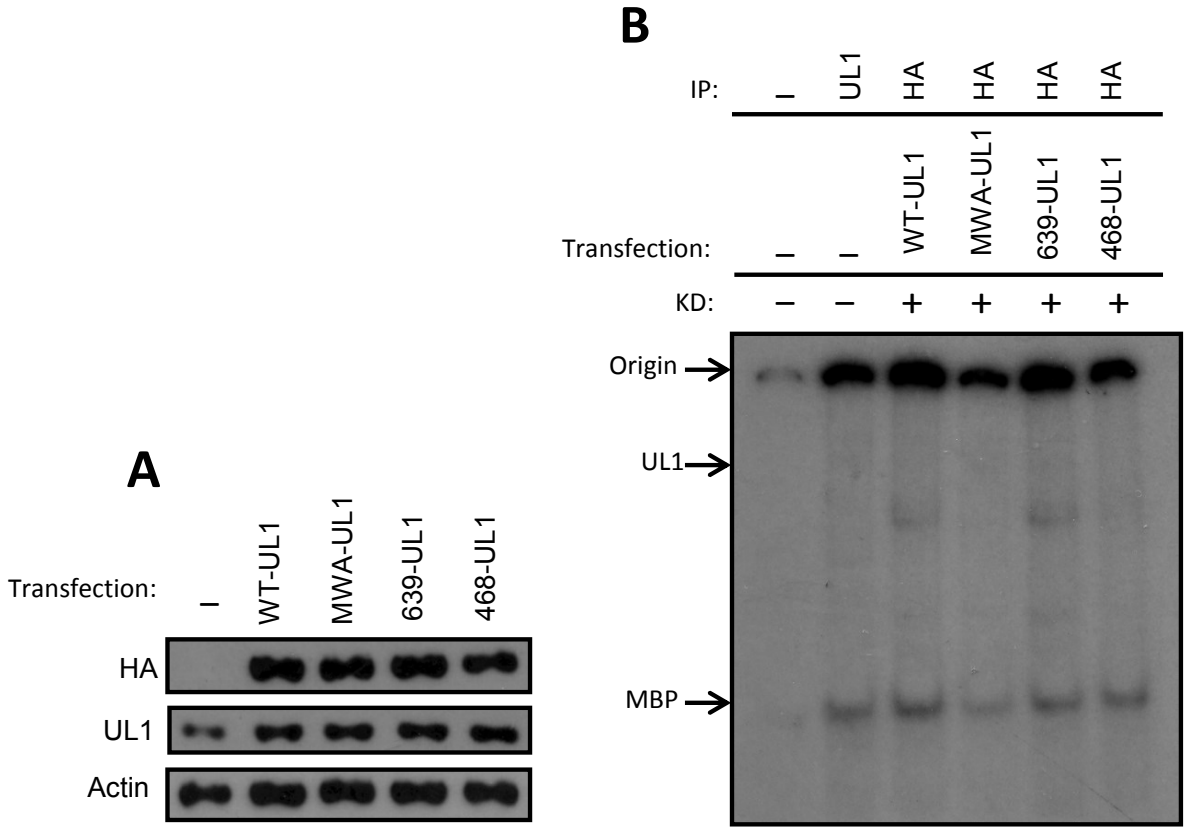

Figure 5.5 The R639C and R468C mutants exhibit kinase activity. A) HeLa cells were co-transfected with siRNA targeting endogenous hnRNP-UL1 and siRNA-resistant HA-tagged constructs of hnRNP-UL1 where indicated. Lysates show equal protein expression of the tagged proteins. B) Following transfection of indicated constructs, cells were lysed and immunoprecipitations performed for the indicated proteins. Proteins were incubated with a reaction mixture containing the substrate MBP and γ-^{32}P-ATP. After 30 minutes the reaction was stopped, samples heated and run on a SDS-PAGE gel, before drying and analysis by autoradiography.

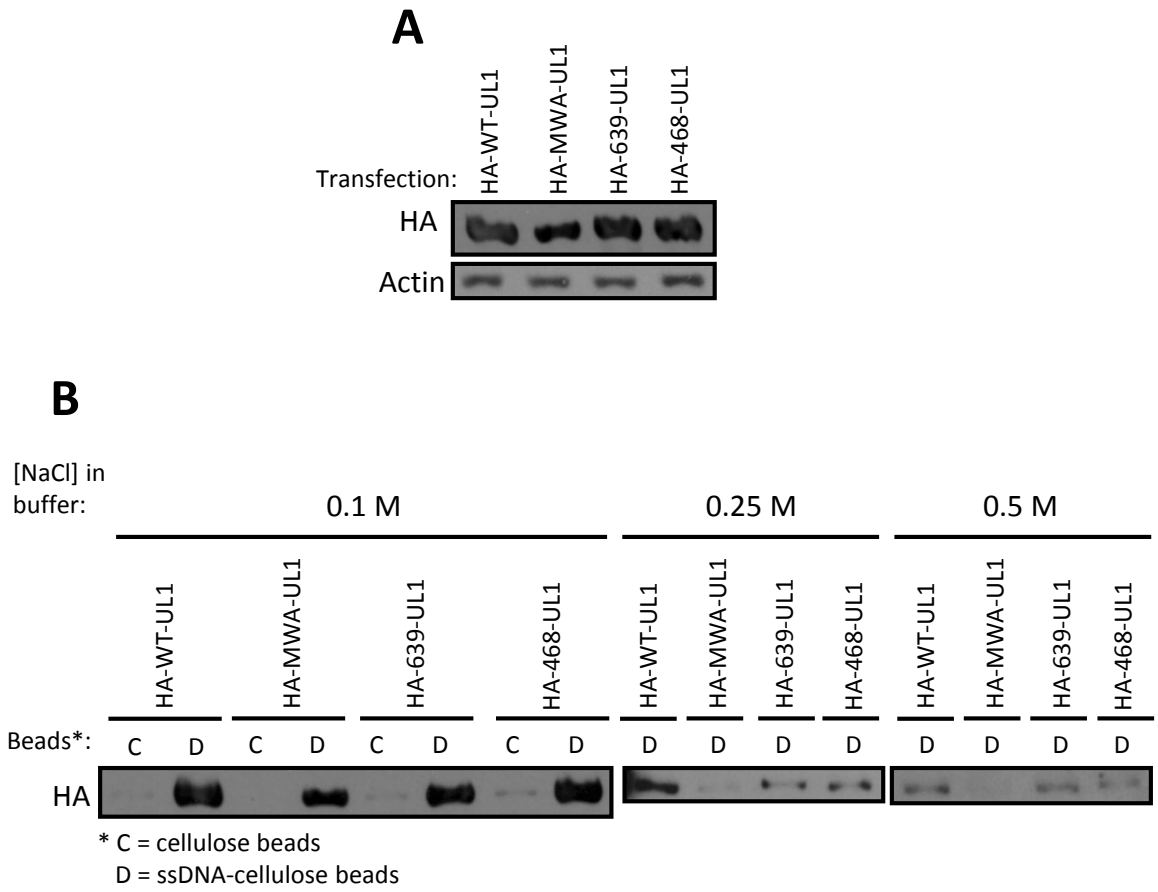

Figure 5.6 Reduced ssDNA-binding of hnRNP-UL1 mutants. A) HeLa cells were transfected with indicated HA-tagged constructs of hnRNP-UL1. Lysates show equal protein expression. B) Following transfection of indicated constructs, cells were lysed and incubated with the indicated beads (cellulose only or ssDNA-cellulose beads) for 2 hours at 4 °C in buffers with various NaCl concentrations. After beads were washed, SDS sample buffer was added, samples heated and run on a SDS-PAGE gel for analysis by western blotting.

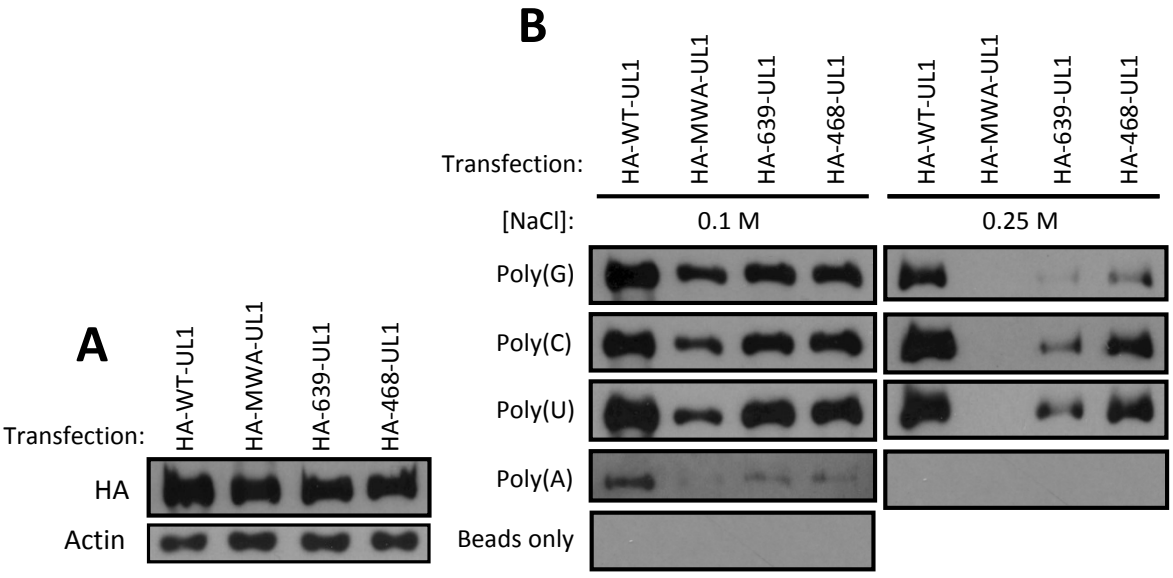
A
Transfection:
HA-WT-UL1
HA-MWA-UL1
HA-639-UL1
HA-468-UL1
HA
Actin
B
Transfection:
HA-WT-UL1
HA-MWA-UL1
HA-639-UL1
HA-468-UL1
HA-WT-UL1
HA-MWA-UL1
HA-639-UL1
HA-468-UL1
[NaCl]:
0.1 M
0.25 M
Poly(G)
Poly(C)
Poly(U)
Poly(A)
Beads only

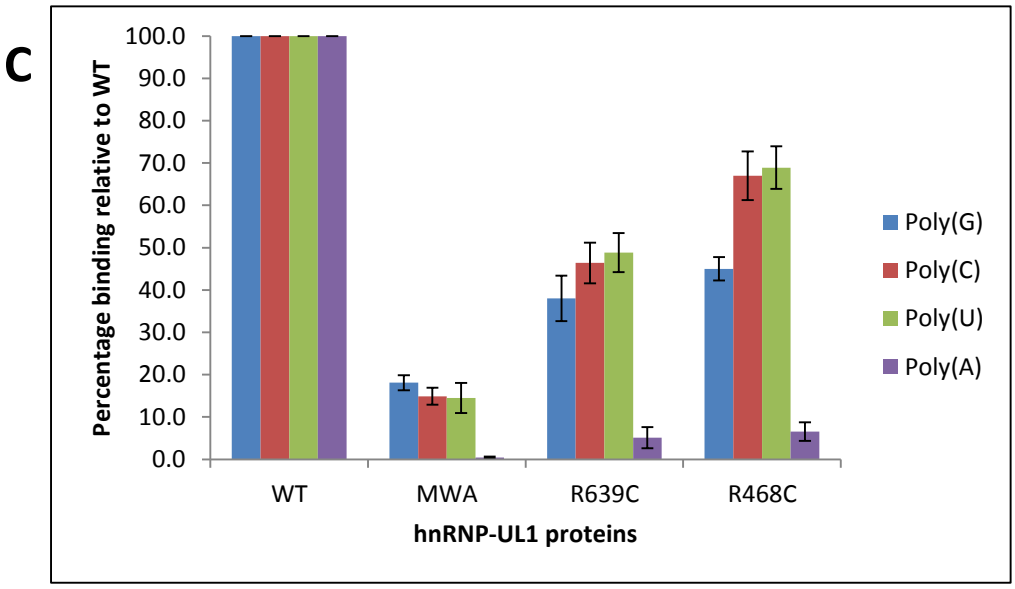
C
Percentage binding relative to WT
100.0
90.0
80.0
70.0
60.0
50.0
40.0
30.0
20.0
10.0
0.0
WT
MWA
R639C
R468C
hnRNP-UL1 proteins
Poly(G)
Poly(C)
Poly(U)
Poly(A)

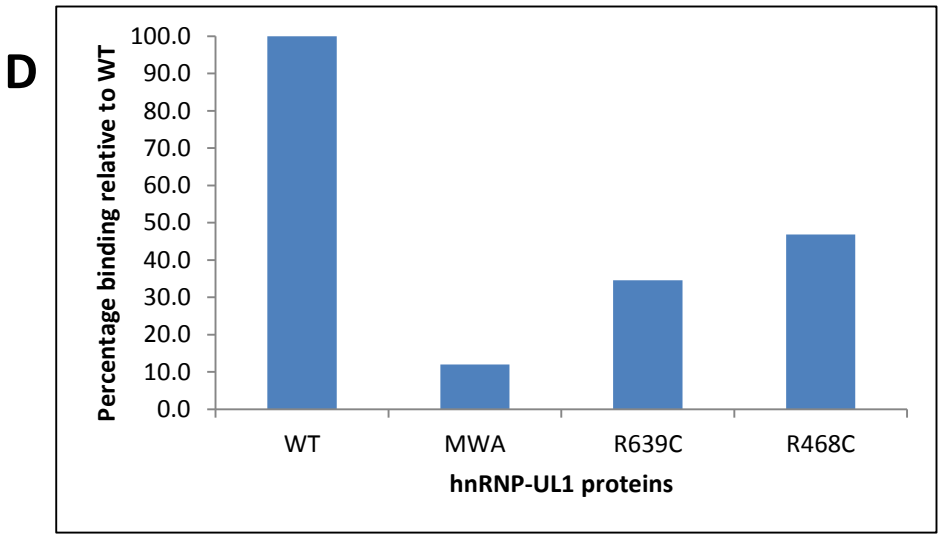
D
Percentage binding relative to WT
100.0
90.0
80.0
70.0
60.0
50.0
40.0
30.0
20.0
10.0
0.0
WT
MWA
R639C
R468C
hnRNP-UL1 proteins

Figure 5.7 Reduced ssRNA-binding of hnRNP-UL1 mutants. A) HeLa cells were transfected with indicated HA-tagged constructs of hnRNP-UL1. Lysates show equal protein expression. B) Following transfection of indicated constructs cells were lysed and incubated with the indicated beads (agarose-streptavidin only or ssRNA-agarose beads) for 2 hours at 4 °C in buffers with NaCl concentrations ranging from 0.1 M to 1 M (not all data shown). After beads were washed, Laemmli buffer was added, samples heated and run on a SDS-PAGE gel for analysis by western blotting. C) A bar graph showing the percentage binding of each hnRNP-UL1 mutant protein relative to WT after densitometry readings were made on the bands. Three repeat experiments were made and the averages of the readings from each NaCl concentration were used. D) A bar graph showing the average percentage binding of each hnRNP-UL1 mutant protein relative to WT across the four different ribonucleotides used.

poly(U) and poly(A). The very weak binding of poly(A) by either mutant or WT protein was confirmed by our results (Figure 5.7B and C). Poly(G) and poly(C) binding was similar to that shown in Gabler et al. (1998), however, poly(U) binding was significantly stronger in our experiments (Figure 5.7B and C); the reasons for this are not apparent at present. There was significant reduction in binding with all three mutant variants. The R639C substitution has a greater affect than R468C, which might be expected as the 639 residue is an arginine of a RGG tripeptide in the RGG domain known to be involved in RNA-binding. The MWA variant has the largest disruption of interaction relative to WT when densitometry readings were averaged for each polyribonucleotide (Figure 5.7D). This is possibly due to an overall disruption of protein structure caused by lack of ATP interaction or direct conformational changes caused by making three amino acid changes.

5.2.5 The DNA damage response of the mutants

Western blot analysis of DNA damage responses to ionising radiation (IR), camptothecin (CPT) and ultraviolet irradiation (UV) were undertaken. The depletion of hnRNP-UL1 by the use of siRNA caused DDR defects in response to IR and UV (Figures 5.8 and 5.10). These were a reduction in RPA phosphorylation at 24 hours in response to IR and a reduction in both the phosphorylation of RPA and H2AX in response to UV. These were similar to previous results, except for no reduction in Chk1 phosphorylation in response to IR or CPT was seen. Polo et al. (2012) also showed moderate reductions in pChk1 and large reductions in pRPA in response to CPT, which were not evident in our experiments (Figure 5.9). The production of siRNA resistant constructs for each of the WT, MWA and R639C variants allowed simultaneous knockdown of endogenous hnRNP-UL1 and expression of the HA-tagged construct of choice. Each of the hnRNP-UL1 variants restored the deficiencies in

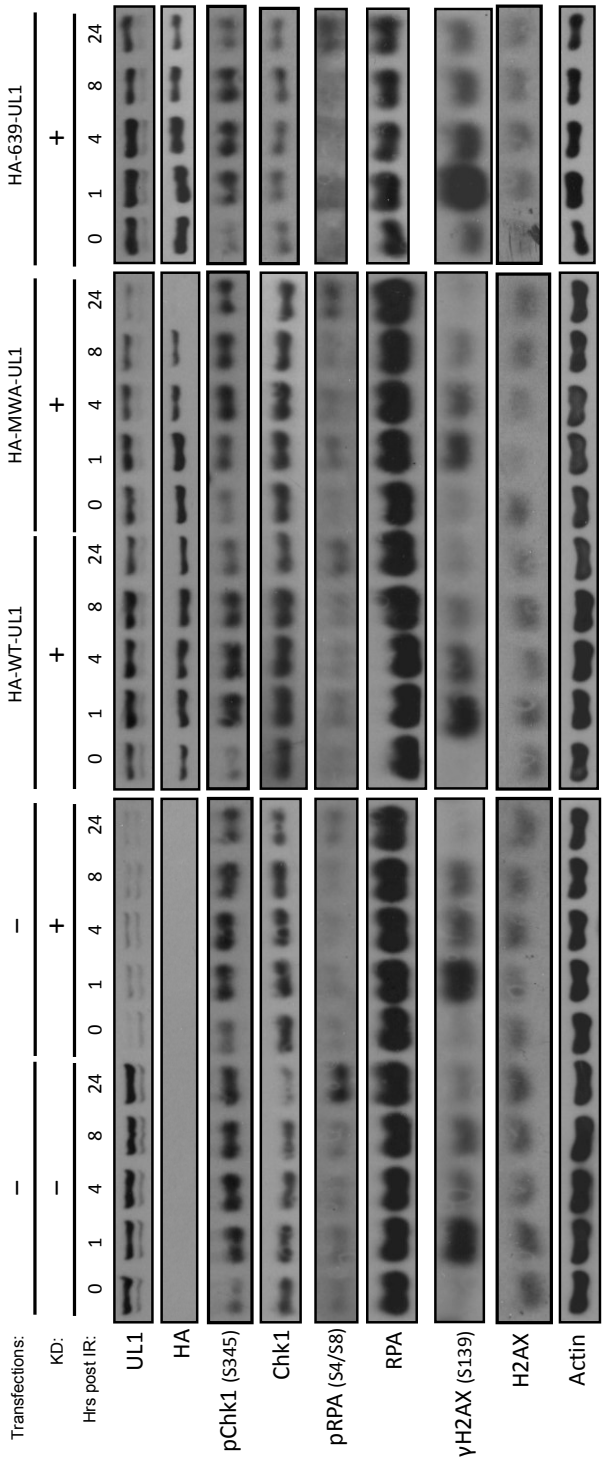

Figure 5.8 Wild-type and mutant proteins restore DDR defects seen in response to IR after knockdown of endogenous hnRNP-UL1. HeLa cells were co-transfected with siRNA targeting endogenous hnRNP-UL1 and siRNA-resistant HA-tagged constructs of hnRNP-UL1 where indicated. 24 hours later cells were subjected to 5 Gys of ionising radiation (IR) and lysates taken at 0, 1, 4, 8 and 24 hours post-treatment. Proteins were separated by SDS-PAGE and subjected to western blotting with the indicated antibodies.

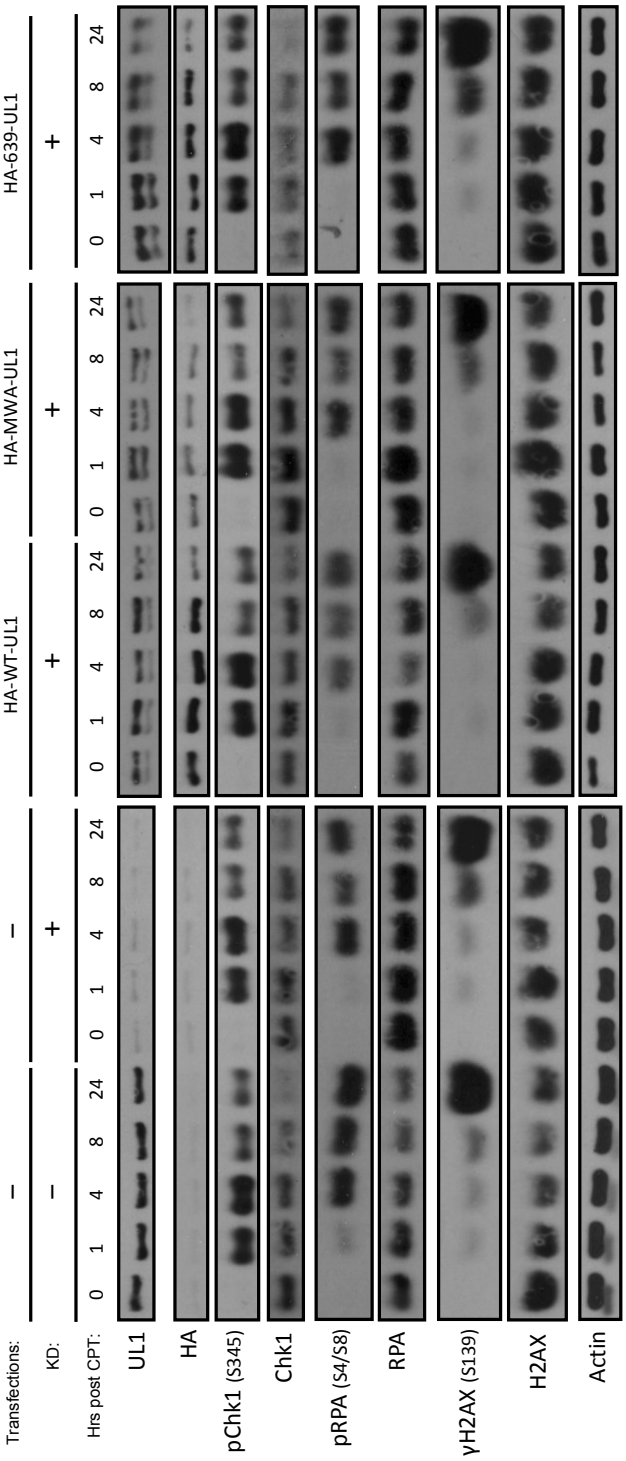

Figure 5.9 Wild-type and mutant proteins restore DDR defects seen in response to CPT after knockdown of endogenous hnRNP-UL1. HeLa cells were co-transfected with siRNA targeting endogenous hnRNP-UL1 and siRNA-resistant HA-tagged constructs of hnRNP-UL1 where indicated. 24 hours later cells were treated with 1 μM camptothecin (CPT) and lysates taken at 0, 1, 4, 8 and 24 hours post-treatment. Proteins were separated by SDS-PAGE and subjected to western blotting with the indicated antibodies.

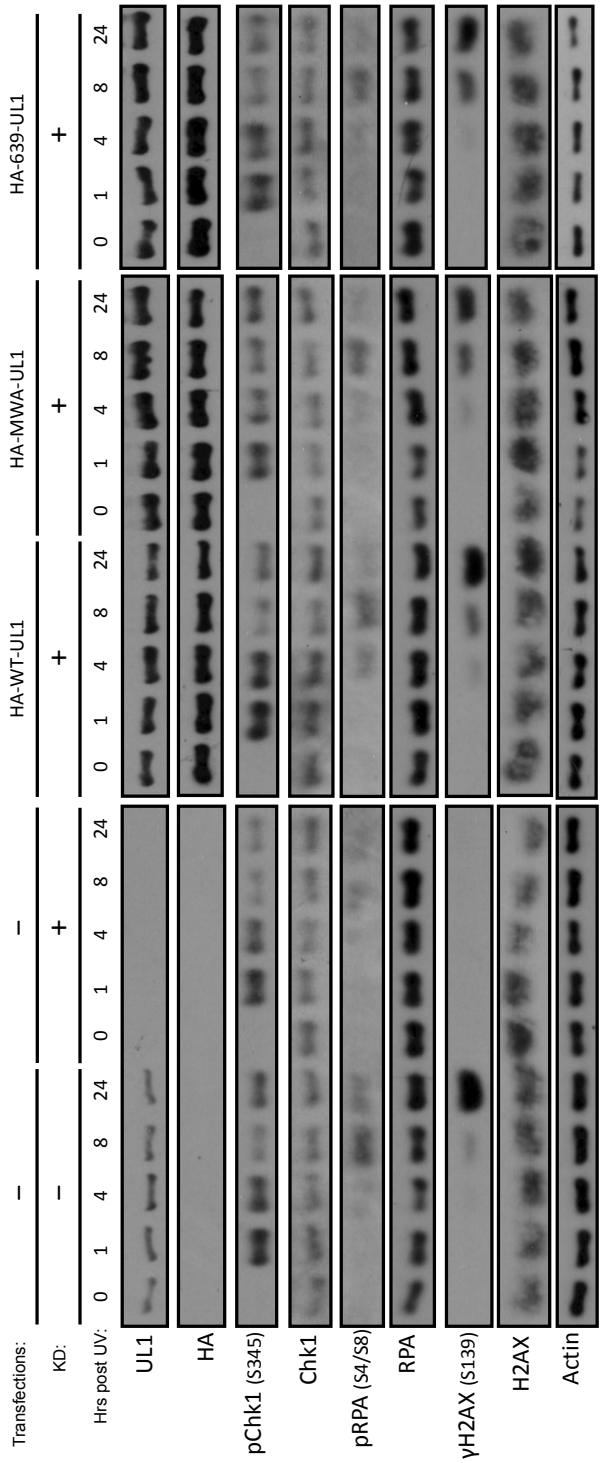

Figure 5.10 Wild-type and mutant proteins restore DDR defects seen in response to UV after knockdown of endogenous hnRNP-UL1. HeLa cells were co-transfected with siRNA targeting endogenous hnRNP-UL1 and siRNA-resistant HA-tagged constructs of hnRNP-UL1 where indicated. 24 hours later cells were subjected to 21 J/m^2 ultraviolet irradiation (UV) and lysates taken at 0, 1, 4, 8 and 24 hours post-treatment. Proteins were separated by SDS-PAGE and subjected to western blotting with the indicated antibodies.

DDRs seen with knockdown (Figures 5.8, 5.9 and 5.10) showing they have no influence on the DDR activities of the protein in response to these damaging agents.

In addition to western blots, immunofluorescence analysis was also performed. γH2AX foci were formed normally in the presence of each variant or when hnRNP-UL1 was depleted in response to IR (Figure 5.11). DSB repair foci indicated by 53BP1 staining were also cleared at a normal rate in hnRNP-UL1 depleted cells and in cells expressing hnRNP-UL1 mutants compared to WT-expressing cells (Figure 5.12). Consistent with the decreased phosphorylation of RPA in response to IR seen during western blot analysis (Figure 5.8), there was decreased pRPA foci formation with hnRNP-UL1 depletion compared to WT (Figure 5.13). Each variant was able to restore this phosphorylation (Figure 5.13), suggesting that they did not impair the role of hnRNP-UL1 in resection at DSBs.

5.2.6 Protein interactions of the mutants with XRCC1, NBS1 and PARP-1

During this study hnRNP-UL1 was found to co-immunoprecipitate with XRCC1, which plays a crucial role as a scaffold protein in the response to SSBs. None of the MWA, R639C or R468C mutations significantly affected this interaction of hnRNP-UL1 (Figure 5.14). This suggests the residues substituted in these mutants are not crucial for interaction with XRCC1 and therefore, a potential role in SSBR for hnRNP-UL1 would not be affected in these ALS patients.

NBS1 directly binds hnRNP-UL1 and thus recruits it to sites of laser-induced damage (Polo et al., 2012). This recruitment is important in facilitating hnRNP-UL1's promotion of ATR-dependent signalling in response to DSBs. The interaction of these two proteins is between the C-terminal of NBS1 and the middle/C-terminal region of hnRNP-UL1. Specifically, the BBS and RGG domains are required for this interaction *in vitro*, whilst the

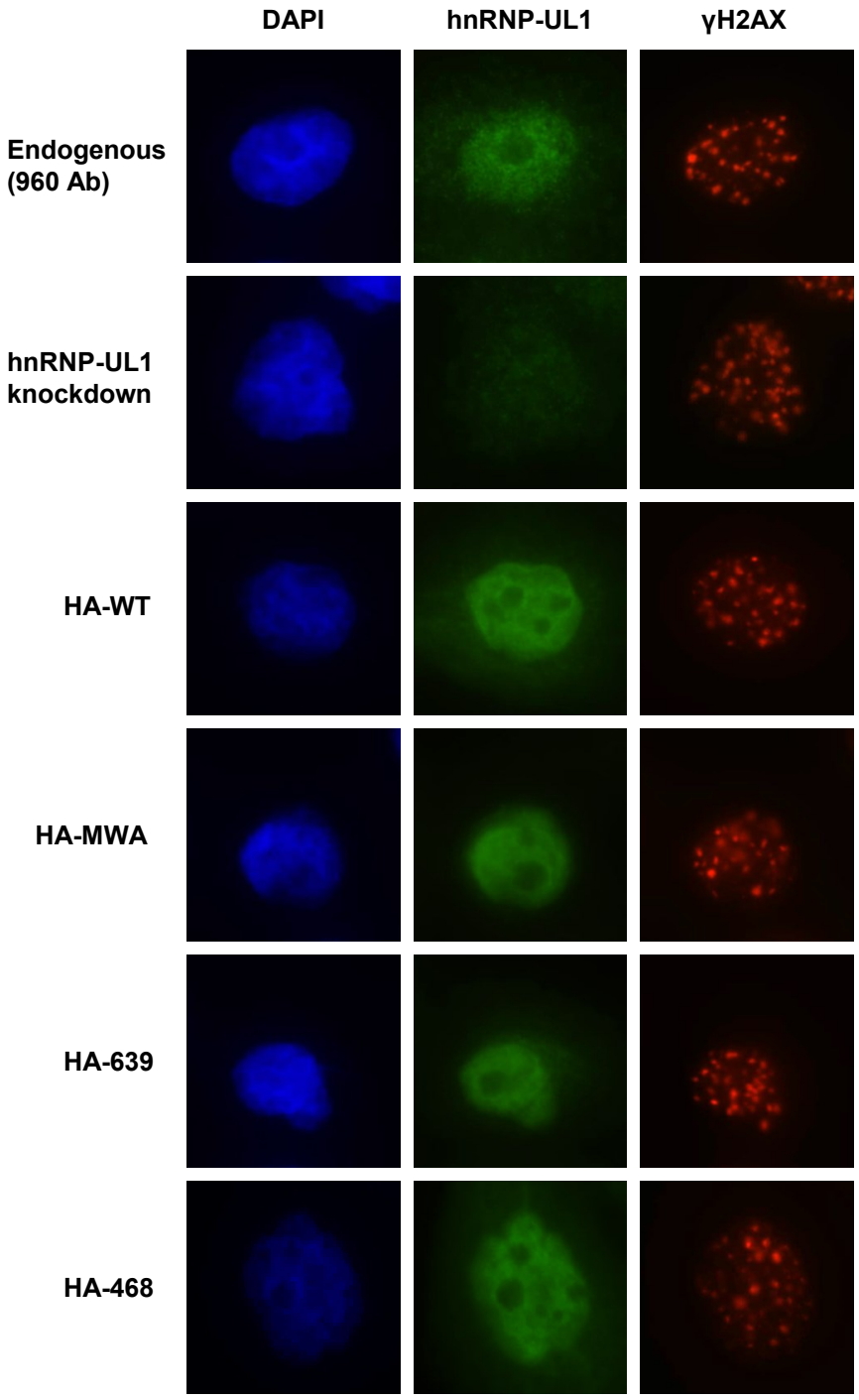

Figure 5.11 γH2AX foci form normally in response to IR in hnRNP-UL1 depleted cells and in cells expressing the various mutated forms. HeLa cells were simultaneously transfected with siRNA against endogenous hnRNP-UL1 and plasmids expressing the indicated hnRNP-UL1 constructs, or left untreated. After 24 hours, cells were exposed to 5 Gys of IR. Cells were fixed and permeabilised 6 hours later, followed by staining with antibodies against hnRNP-UL1 (960) or HA and γH2AX (S139). DNA was stained blue with DAPI.

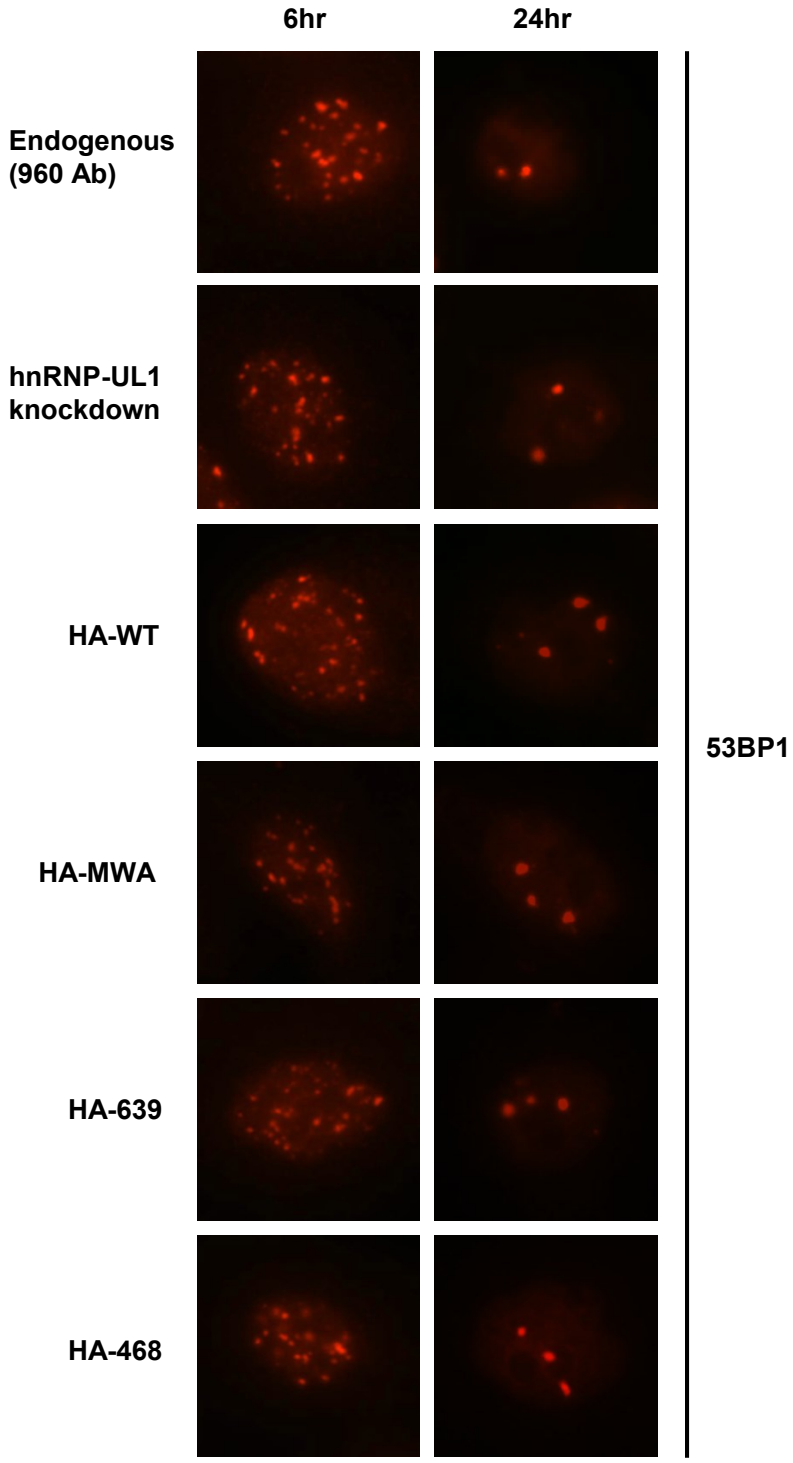

Figure 5.12 53BP1 foci are cleared at a normal rate in hnRNP-UL1 depleted cells and in cells expressing the various mutated forms. HeLa cells were simultaneously transfected with siRNA against endogenous hnRNP-UL1 and plasmids expressing the indicated hnRNP-UL1 constructs, or left untreated. After 24 hours, cells were exposed to 5 Gys of IR. Cells were fixed and permeabilised at indicated time points, followed by staining with antibodies against 53BP1. DNA was stained blue with DAPI.

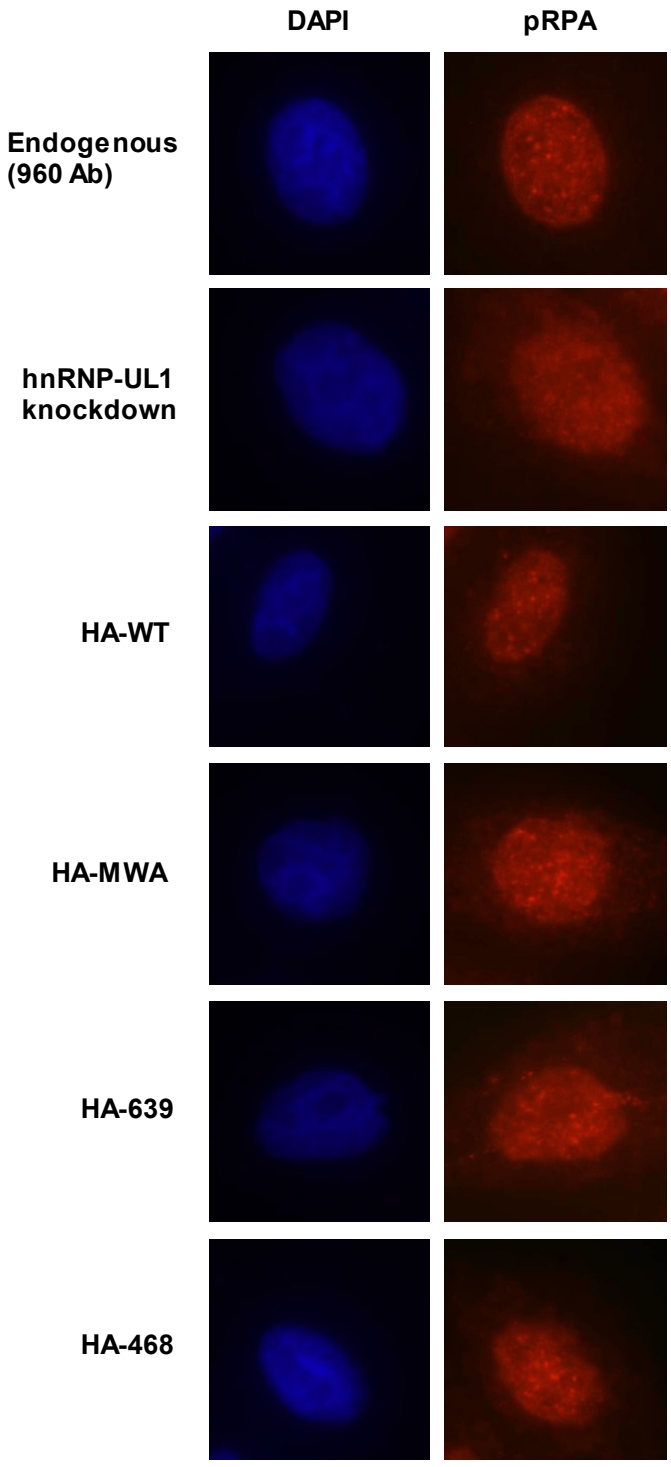

Figure 5.13 hnRNP-UL1 variants restored pRPA foci following endogenous protein depletion. HeLa cells were simultaneously transfected with siRNA against endogenous hnRNP-UL1 and plasmids expressing the indicated hnRNP-UL1 constructs, or left untreated. After 24 hours, cells were exposed to 5 Gys of IR. Cells were fixed and permeabilised 6 hours after treatment with IR, followed by staining with antibodies against pRPA (S4/S8). DNA was stained blue with DAPI.

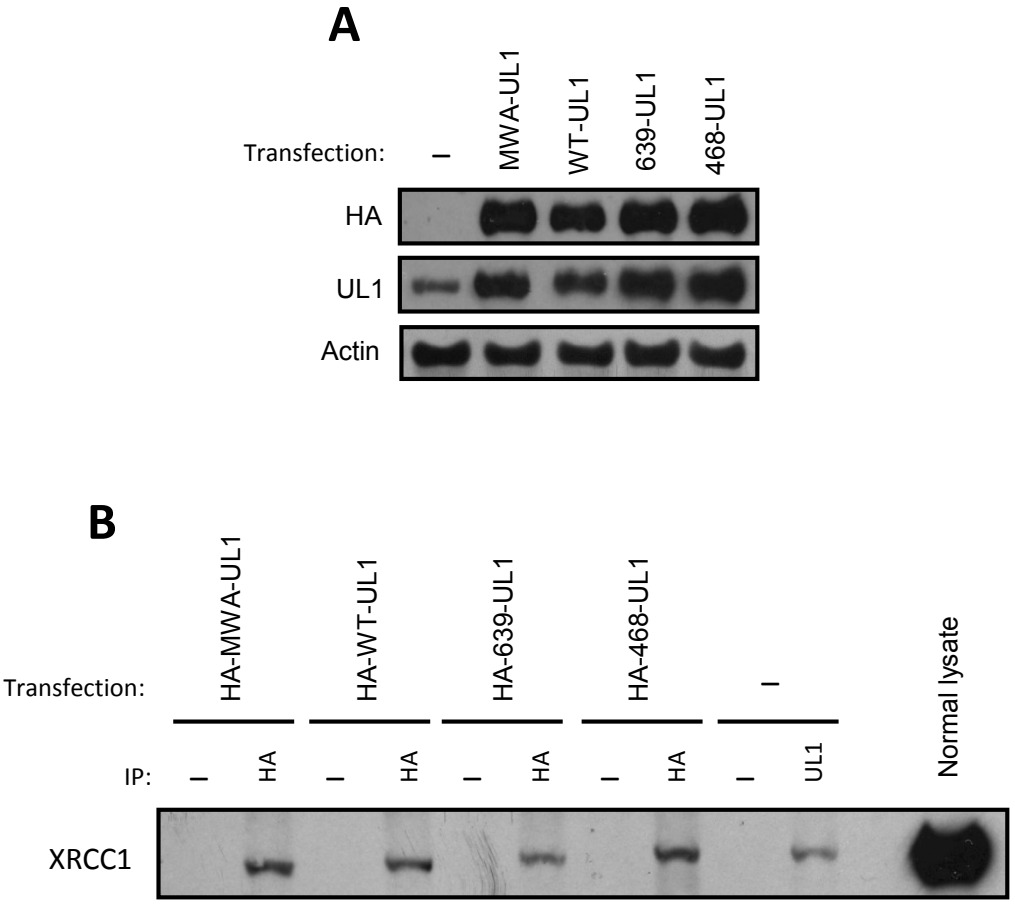

Figure 5.14 Interaction with XRCC1 is unaffected with mutant hnRNP-UL1 proteins. A) HeLa cells were transfected with indicated HA-tagged constructs of hnRNP-UL1. Lysates show successful protein expression. B) Following transfection of indicated constructs, cells were lysed and immunoprecipitations performed for the indicated proteins. Proteins were separated by SDS-PAGE and subjected to western blotting to analyse the co-immunoprecipitation of XRCC1.

RGG domain was shown to be critical for effective recruitment to damage sites *in vivo* (Polo et al., 2012). No significant reduction of interaction was observed during co-immunoprecipitation experiments conducted with each of the three hnRNP-UL1 mutants (Figure 5.15). The affected residues of the MWA mutant lie outside of the BBS and RGG domain and would therefore not be expected to have an impact on the interaction with NBS1. However, residue 468 lies within the BBS domain and the 639 residue lies at the centre of the RGG domain deemed critical for this interaction. Nonetheless, it appears that neither of these base substitutions are sufficient to affect NBS1 interaction. This is consistent with the restoration of RPA phosphorylation when WT-hnRNP-UL1 was complemented by the HA-tagged mutant variants, as any defect in the two proteins' interaction would cause a reduction in resection and exposure of ssDNA which is required for RPA-binding and subsequent phosphorylation.

The C-terminus (aa508-756) of hnRNP-UL1 mediates an interaction with PARP-1 and is recruited within seconds to sites of DNA damage in a PARP-1-dependent manner (Hong et al., 2013). The R468C and R639C variants did not affect the interaction despite the 639 residue falling within the interacting region; however, MWA-hnRNP-UL1 binding was reduced (Figure 5.16). This is surprising as the Walker A motif is upstream of the interacting region; however, this suggests that these substitutions can cause appreciable structural changes.

5.3 DISCUSSION

In Chapter III it was shown that hnRNP-UL1 binds ATP and these observations appeared to show protein kinase activity by phosphorylating the promiscuously

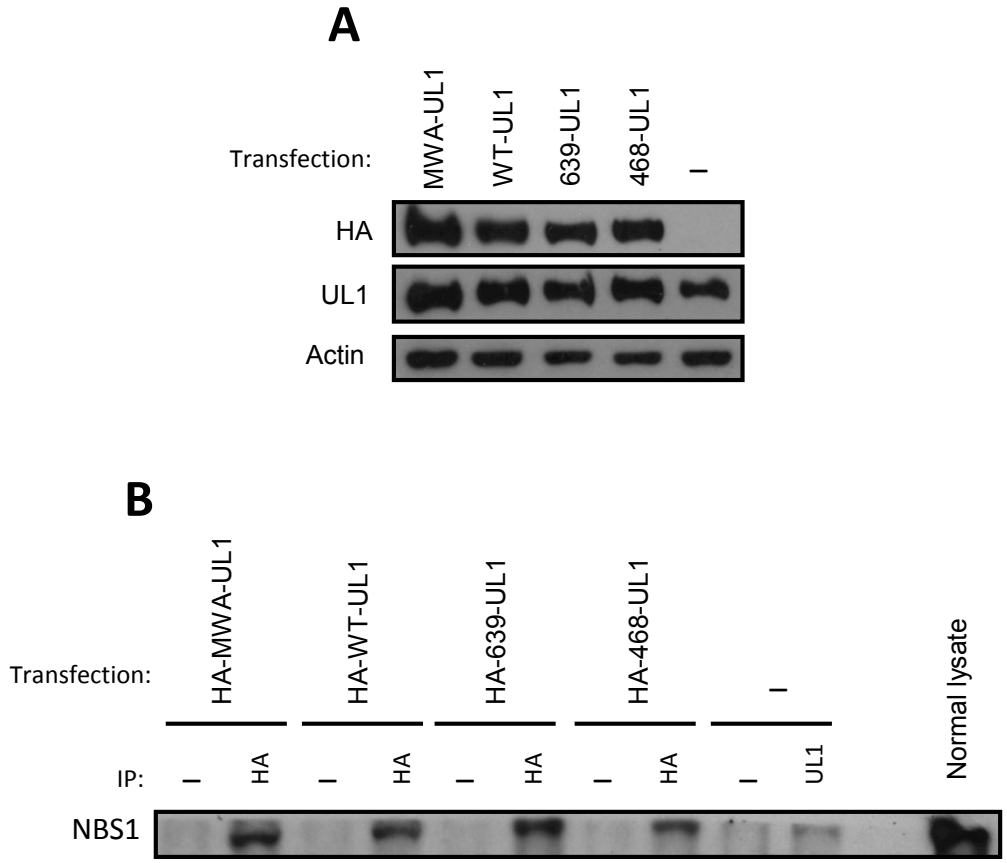

Figure 5.15 Binding of NBS1 is unaffected with mutant hnRNP-UL1 proteins. A) HeLa cells were transfected with indicated HA-tagged constructs of hnRNP-UL1. Lysates show successful protein expression. B) Following transfection of indicated constructs, cells were lysed and immunoprecipitations performed for the indicated proteins. Proteins were separated by SDS-PAGE and subjected to western blotting to analyse the co-immunoprecipitation of NBS1.

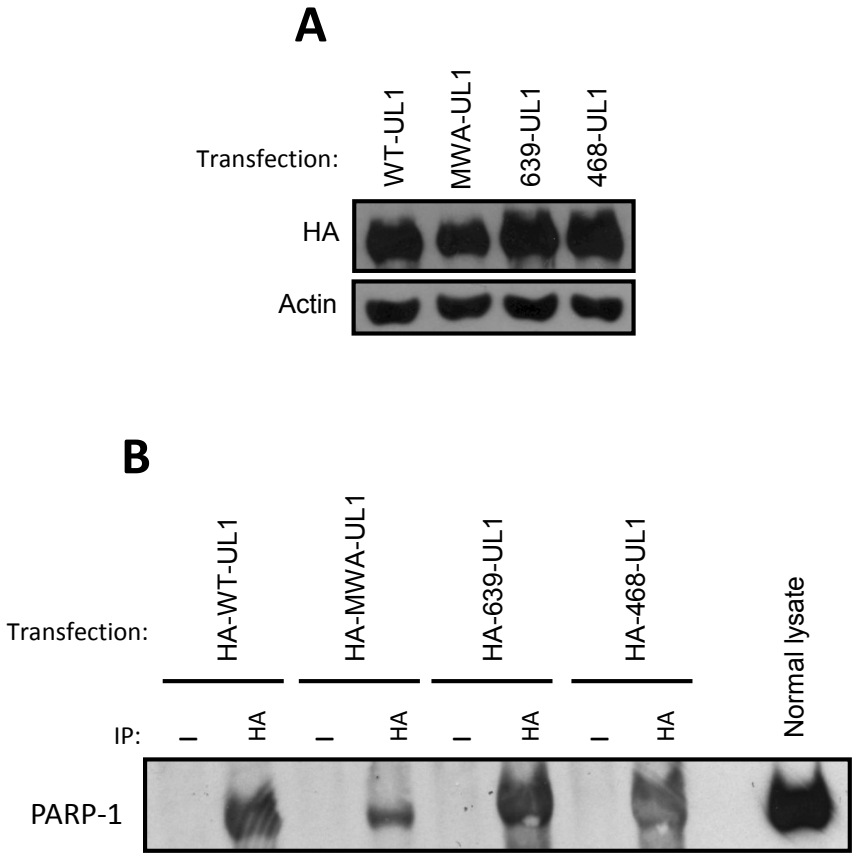

Figure 5.16 Interaction with PARP-1 is affected with the Walker A mutant but not the ALS variants. A) HeLa cells were transfected with indicated HA-tagged constructs of hnRNP-UL1. Lysates show successful protein expression. B) Following transfection of indicated constructs, cells were lysed and immunoprecipitations performed using an antibody against HA or a no antibody control. Proteins were separated by SDS-PAGE and subjected to western blotting to analyse the co-immunoprecipitation of PARP-1.

phosphorylatable substrates MBP and PLC. Due to the hnRNP-UL1 used in the kinase assays being immunoprecipitated from whole cell lysates it was possible that the phosphorylation seen was due to an interacting protein co-immunoprecipitating with hnRNP-UL1. A number of kinase inhibitors were employed in an attempt to rule out potential interacting proteins. However, it was still not conclusive that the phosphorylation seen was due to hnRNP-UL1. Therefore, the Walker A loop was mutated in an attempt to show that ATP-binding was indeed at the Walker A loop and that the kinase activity seen in the assays was attributable to hnRNP-UL1.

Within the Walker A loop the two glycine residues give an important flexibility to the loop and permit hydrogen-bonding with the phosphoryl groups of the nucleotide. The threonine binds to the essential Mg^{2+} cofactor ion and the lysine is necessary for phosphoryl transfer to the substrate. Within the work presented by Deyrup et al. (1998) several mutations were made by site-directed mutagenesis of the Walker A loop in the murine ATP-sulphurase/adenosine 5'-phosphosulphate kinase enzyme. Substituting the lysine for the similarly sized and charged arginine almost completely ablates kinase activity. A change of the threonine to alanine significantly reduces kinase activity but not to the same degree as the K→R substitution. Meanwhile, changing the most C-terminal glycine (adjacent to K) to alanine once again almost completely ablates kinase activity. Given that none of these changes completely removed the enzyme's kinase activity all three of the corresponding residues in hnRNP-UL1 were changed resulting in a GKT433ARA substitution. The changes prevented ATP-binding and also significantly reduced the phosphorylation of the MBP substrate. This strongly suggests that the phosphorylation observed is attributable to hnRNP-UL1.

Some phosphorylation is still evident when using immunoprecipitated HA-MWA-hnRNP-UL1 for the kinase assays and this would not be expected given that the mutations appear to ablate ATP-binding completely. There are a number of potential reasons for the small amount of activity seen. It is very possible that the phosphorylation is attributable to endogenous wild type-UL1 that was shown to co-immunoprecipitate with MWA-hnRNP-UL1. As discussed earlier, it is possible that other proteins are being co-immunoprecipitated with hnRNP-UL1 and are responsible for this phosphorylation, but the large reduction caused by the mutation of the Walker A loop would suggest any phosphorylation by co-immunoprecipitating proteins is minimal. Although unlikely, it should be considered that a conformational change caused by the substitutions may reduce the interaction with a co-immunoprecipitating protein which is solely responsible for the phosphorylation observed. In conclusion, whilst it is not absolutely conclusive that the protein kinase activity observed in our kinase assays is that of hnRNP-UL1, the use of the Walker A mutant strongly suggests so.

The kinase activity of the ALS patient mutants, R639C and R468C, were like that of wild-type. The 639 mutation is more than 40 amino acid residues C-terminal of the kinase domain and in the middle of the RGG domain. Therefore, this mutation would not be expected to influence kinase activity, unless the activity was dependent on RNA- or DNA-binding. The 468 mutation does lie within the kinase domain just 33 residues C-terminal of the Walker A loop and therefore might be expected to influence kinase activity. However, the secondary structure prediction based on PNKP using Swiss-Pdb Viewer software shows this residue to be in the middle of a section that shows no amino acid homology to PNKP or strong secondary structure prediction (Figure 3.2). Therefore, it is unlikely to be a critical residue in the secondary structure of hnRNP-UL1's kinase domain and subsequently does not affect kinase activity.

Analysis of the ssDNA- and ssRNA-binding capabilities of the mutants showed the MWA mutant to exhibit the most severe reduction on comparison to WT. Given that the arginine substituted in the R639C variant is in the middle RGG tripeptide of 5 in the RGG domain, which is known for permitting RNA interaction, it is a surprise that this mutant does not have a more serious effect on binding. The R468C variant reduces ssDNA-binding to a similar level, despite it being located N–terminal of the RGG domain and was not shown to be important for ATP-binding or kinase activity. The greater effect seen with the MWA mutant may occur for a number of reasons. Firstly, the three amino acid substitutions may induce gross conformational changes in the protein severely reducing binding capabilities. Secondly, ATP-binding could stabilise the ssDNA/ssRNA-binding of hnRNP-UL1.

Polo et al. (2012) described hnRNP-UL1 to have an ATR-dependent response to DSBs in which it played a crucial role in stimulating resection by the recruitment of BLM. DNA damage responses to IR and CPT treatment after knockdown of hnRNP-UL1 had caused a reduction in the phosphorylation of Chk1, an ATR substrate (Polo et al., 2012). This could not be confirmed in our study, but a reduction in the phosphorylation of RPA, which binds to ssDNA in the response to damage, was shown after treatment with IR and UV. A subsequent reduced recruitment of the protein to damage foci was also consistent. Therefore, our results are consistent with the role of hnRNP-UL1 in stimulating resection following DSBs, because without resection, RPA cannot bind to ssDNA and be phosphorylated.

Treatment with UV following knockdown of hnRNP-UL1 also strongly reduced the levels of γH2AX and pRPA. IR and CPT cause DSBs, whilst UV results in SSBs. However, all three can involve the binding of RPA to ssDNA and stimulation of ATR signalling. Phosphoprylation of RPA and H2AX occurs late in response to UV damage, usually 8-24 hours after treatment (Figure 5.10). This is because it is only the SSBs that collapse in to

DSBs that will cause extensive RPA phosphorylation and subsequent H2AX phosphorylation by initiation of ATR signalling. When levels of hnRNP-UL1 are depleted, resection and further binding of RPA would be delayed. Subsequent RPA phosphorylation and ATR stimulation are diminished, which is required for phosphorylation of H2AX.

Interestingly, when the mutant constructs were cotransfected with siRNA to knockdown endogenous hnRNP-UL1, expression of the mutant proteins restored the normal DDR to all three agents. Immunofluorescence experiments following complementation with each of the three variants (MWA, R639C and R468C) after depletion of endogenous hnRNP-UL1 also showed they restored normal DDR responses to IR. This suggests that the kinase activity of the protein is not required during its role in response to DNA damage. It also shows that the ALS patient mutations do not affect the protein's functionality in response to DNA damage. Whether hnRNP-UL1's role(s) in the DDR are limited to protein interactions as a type of scaffolding protein or that it uses its kinase activity to affect the function of other proteins is not known. Mass spectrometry analysis revealed that one of the peptides in MBP that was phosphorylated by hnRNP-UL1 had the consensus motif P-X-S/T-P, which MAP/ERK kinases are suggested to have specificity for. Out of hnRNP-UL1's known interactors in the DDR, BLM, CtIP, XRCC1, NBS1 and hnRNP-UL1 itself all contain at least one of these motifs. This could potentially make them targets for phosphorylation by hnRNP-UL1 and subsequently affect their DDR roles. Experiments to find substrates for hnRNP-UL1's kinase activity were not carried out due to lack of purified protein, but such investigation would be very interesting and may uncover further information about the protein's roles in the DDR. However, analysis of its interactions with NBS1, XRCC1 and PARP-1 were investigated. Levels of interaction of the hnRNP-UL1 variants with these

proteins would suggest whether any DDR defect would occur due to lack of proper interaction relative to WT.

The middle region of hnRNP-UL1 containing the BBS and RGG domains directly interacts with the C-terminal region of NBS1. Furthermore, the RGG domain was shown to be critical for *in vivo* recruitment of hnRNP-UL1 to sites of laser-induced damage by NBS1 (Polo et al., 2010). Recently, Gurunathan et al. (2015) were able to show that hnRNP-UL1 is methylated within its RGG motif by PRMT1 (protein arginine methyltransferase 1) and this methylation is required for NBS1 interaction. PRMT1 is the main arginine methyltransferase in mammalian cells and has a preference for RGG motifs (Thandapani et al., 2013). Mass spectrometry failed to show any methylation of the R639 residue in U20S cells, whilst a short GST-tagged region from amino acid 635 to 652 was methylated *in vitro* (Gurunathan et al., 2015). However, whether the methylation occurs at R639 or R645 or both is not known. The knockdown of PRMT1 significantly reduced the interaction between NBS1 and hnRNP-UL1. The substitution of all seven arginines that occur as part of a RG dipeptide or RGG tripeptide for lysine also caused large reductions in NBS1-hnRNP-UL1 interactions (Gurunathan et al., 2015). Our experiments showed no detectable decrease in interaction of the proteins when cells expressed the R639C mutant. The 639 arginine residue may or may not be methylated by PRMT1, but it appears mutation of this residue alone is not enough to reduce binding of NBS1. The R468C and MWA mutants also showed no decrease in NBS1 interaction. This coincides with the effective rescue of DNA damage responses with simultaneous knockdown of endogenous hnRNP-UL1 and expression of the transfected mutants. With no defect in NBS1 binding hnRNP-UL1 would be recruited to sites of DSBs as normal. Therefore, any possible DDR dysfunction in ALS patient neuronal cells with R639C or R468C mutations would not be due to reduced NBS1 interaction and failure to recruit to damage foci.

There were no defects in the binding of XRCC1 or PARP-1 by the two ALS patient variants either suggesting any potential role of hnRNP-UL1 in SSB repair would not be directly affected by these mutations. There was a reduction in the binding of MWA-hnRNP-UL1 to PARP-1. This is surprising as it was the C-terminus (aa561-756) of hnRNP-UL1 that was reported to interact with PARP-1 (Hong et al., 2013) and this excludes the Walker A motif. Once again, there is the possibility that conformational changes in the proteins structure caused by the base substitutions in the MWA variant may account for this change in binding. Or perhaps the interaction with PARP-1 is dependent upon nucleotide binding. Despite the decreased binding of the MWA variant to PARP-1 during co-immunoprecipitation, complementation of this variant for depleted endogenous hnRNP-UL1, restored all DDR defects to both DSB and SSB inducing agents. This suggests the amount of reduced interaction of the two proteins was not sufficient to cause any DDR defects.

Finally, no information is available yet on the site on hnRNP-UL1 for XRCC1 interaction. It is possible that hnRNP-UL1's interaction with XRCC1 may occur through PARP-1 as part of a complex. XRCC1 interacts directly with PARP-1 through a BRCT1 (BRCA1 C terminus) domain (Masson et al., 1998). Meanwhile, negatively charged RGG motifs have been proposed to facilitate binding of the positively charged PAR chains (Altemeyer et al., 2015); such an interaction may occur between hnRNP-UL1 and the self PARylated PARP-1.

CHAPTER VI

FINAL DISCUSSION AND FUTURE WORK

6.1 NUCLEOTIDE-BINDING OF HNRNP-UL1

Many proteins bind to nucleotide triphosphates through a number of recognition sequences (Matte and Delbaere, 2010). The most common of these is the Walker A motif, which is present along with a conserved Walker B motif in hnRNP-UL1, -UL2 and –U. During this study hnRNP-UL1 was shown to exhibit strong binding of ATP through its Walker A motif. However, a lack of ATP-binding by hnRNP-UL2 and –U was observed. This was a little surprising as the two motifs and their flanking regions are so highly conserved across the three proteins. One possible explanation is the differences of their Walker A motifs. Investigations made using the crystal structures of proteins with Walker A motifs in the Protein Data Bank showed that the four interchangeable XXXX residues in the consensus motif (GXXXXGKT/S) have an influence on nucleotide-binding capability (Ramakrishnan et al., 2002). Whilst these four amino acid residues in the motif do vary considerably among the nucleotide-binding proteins, their Ramachandran angles remain fairly consistent allowing the motif to form the critically important loop structure around the nucleotide (Ramakrishnan et al., 2002). The Ramachandran angles of the four interchangeable residues in hnRNP-UL1 (LPAA), -U (LPGA) and –UL2 (LPGS) were not investigated by Ramakrishnan et al. (2002) and although the amino acid changes are not extensive it is possible that the differences between them prevent hnRNP-U and hnRNP-UL2 binding ATP. Very conservative changes are also present in their Walker B motifs as well. The influence of these changes could be investigated by using site-directed mutagenesis PCR to substitute the different residues in the hnRNP-UL2 and hnRNP-U proteins to match those in hnRNP-UL1 and performing ATP-binding experiments.

None of the other 20-plus hnRNP family members possess a Walker A motif suggesting that any activity related to nucleotide binding is unique to these three proteins. As

other hnRNPs lack the Walker A motif and no binding of nucleotide triphosphates has been reported, it suggests that the binding by hnRNP-UL1 would not be related to any of its roles in RNA-processing. A potential function of hnRNP-UL1 nucleotide-binding outside of possible protein kinase activity is highlighted by another Walker A motif containing protein which functions in the DDR, Rad50 (Hopfner et al., 2000). Rad50 is part of the MRN complex discussed in *1.2.5*. It has an ATPase domain which is split N- and C-terminal of a 600-900 amino acid long heptad repeat insertion. The interaction of the N-terminal Walker A motif and C-terminal Walker B motif to ATP causes a conformational switch allowing the binding of DNA (Hopfner et al., 2000). This allows it to regulate the exonuclease activity of Mre11 by repositioning DNA ends in to the Mre11 active site (Hopfner et al., 2001). hnRNP-UL1 is known to stimulate DNA resection during HR by recruitment of BLM (Polo et al., 2012), as well as to interact with CtIP (Bruton et al., 2007). During the study presented here ablation of ATP-binding by mutation of hnRNP-UL1's Walker A motif was shown to significantly decrease the protein's DNA-binding capabilities. Therefore, it is possible that like Rad50, ATP-binding influences hnRNP-UL1's DNA-binding allowing the protein to regulate BLM and CtIP's DNA end resection activity. However, no DDR defects were detected with the MWA variant during this study and pRPA levels were restored to normal with complementation of the MWA variant for depleted wild-type hnRNP-UL1 following DSB induction by IR. Despite this it would be interesting to undertake experiments investigating this theory. A purified source of hnRNP-UL1 protein would allow structural studies by x-ray crystallography allowing the observation of conformational changes initiated by ATP-binding. Thus far, the production of a purified source of hnRNP-UL1 has not been possible due to the protein's instability, but may be possible with improved methods of bacterial or insect cell expression.

6.2 KINASE ACTIVITY OF HNRNP-UL1

During the investigations conducted in chapter III hnRNP-UL1 was shown to possess protein kinase activity, as were hnRNP-U and -UL2. The observed kinase activity for hnRNP-U and –UL2 was unexpected given the lack of ATP-binding seen. The possible reasons for this anomaly were discussed in section *3.3*. Also, the interest in studying the potential kinase activity of hnRNP-UL1 was generated by its amino acid and secondary structure homology to PNKP, a DNA kinase (Schellenberg and Williams, 2011). However, no DNA kinase activity was observed with immunoprecipitated hnRNP-UL1. No activity was observed for immunoprecipitated PNKP either, but only with recombinant protein, suggesting the procedure may have not been sensitive enough or suitable for detection of DNA phosphorylation. Therefore, repeated DNA kinase experiments with a purified and highly concentrated source of hnRNP-UL1 would be ideal before dismissing any hnRNP-UL1 DNA kinase activity.

During this study many efforts were made to eliminate the possibility of the protein kinase activity observed being that of a bound protein and not integral to hnRNP-UL1. The significant decrease in activity seen with the Walker A mutant (MWA) variant was the most significant evidence that the activity was integral to hnRNP-UL1. A number of protein kinase inhibitors did reduce the activity observed with immunoprecipitated hnRNP-UL1; however, none of these had been tested previously for specificity against hnRNP-UL1 (discussed further in *3.2.6*). The two which caused greatest reduction in activity were SP600125 and BI 2536, JNK and PLK1 inhibitors, respectively. To eliminate the possibility of JNK and/or PLK1 being the bound protein(s) responsible for the protein kinase activity, their interaction with hnRNP-UL1 should be investigated by immunoprecipitation in future experiments.

The novel interaction with p70S6K1 was also demonstrated during this study. It did not appear to be the bound protein responsible for the observed protein kinase activity either as direct immunoprecipitation of p70S6K1 resulted in less phosphorylation than was the case for hnRNP-UL1. However, the functional significance for the interaction of these two proteins is not yet known providing another exciting avenue for potential future work. The S6Ks (p70S6K1 and p54S6K2) are serine/threonine kinases which function downstream of mTOR in mTOR signalling pathways to stimulate cell growth and proliferation. A number of hnRNPs, including hnRNP-U, -F, -E1, and –C1/C2 have previously been shown to interact with p54S6K2 by mass spectrometry analysis of nuclear fractions and an interaction with hnRNP-F/H was also shown by co-immunoprecipitation. A p54S6K2, hnRNP-F and mTOR complex was shown to form in the nucleus and stimulate cell growth and proliferation in response to serum stimulation (Goh et al., 2010). Meanwhile, p70S6K1 has been shown to be involved in RNA processing following stimulation of mTOR signalling to enhance translation efficiency of spliced mRNA over non-spliced (Ma et al., 2008). Within our study, it was the 70 kDa p70S6K1 that was shown to immunoprecipitate with hnRNP-UL1. This suggests a potential functional purpose for the interaction between p70S6K1 and hnRNP-UL1 in mRNA splicing and an avenue for further investigation.

In chapter V the MWA variant was shown to reduce binding of both ssDNA and oligoribonucleotides. This may be simply due to the three amino acid substitutions inducing gross conformational changes in the protein, severely reducing binding capabilities. To test this, an hnRNP-UL1 construct could be produced by site-directed mutagenesis in which only one encoded amino acid of the Walker A motif is changed (instead of three). This would have less chance of inducing large conformational changes in the protein and ssDNA/RNA experiments could be repeated to see if the reduction in binding is the same. Another possible

explanation of the reduced binding is that ATP-binding could stabilise the ssDNA/RNA-binding of hnRNP-UL1. Accordingly, the protein's ATP-binding may well affect its roles in RNA-processing. To investigate which mRNAs hnRNP-UL1 processes RNA and protein expression studies could be investigated with and without depletion of the protein. Subsequently, the expression of those mRNAs and proteins could be observed in cells expressing wild-type and MWA-hnRNP-UL1. A further possibility is that hnRNP-UL1's kinase activity may occur when bound to ssDNA or RNA. Given hnRNP-UL1's involvement in resection during HR, the protein may bind the exposed 3' tail stimulating its kinase activity. hnRNP-UL1 may also have an unknown substrate for phosphorylation during its PARP-1-dependent recruitment in the early phase response to DNA damage. hnRNP-UL1 does possess kinase activity but the functional significance *in vivo* is currently unknown.

hnRNP-UL1's biological substrate is unknown and if revealed would probably give large clues to its functional role and significance. Mass spectrometry revealed two peptides phosphorylated in MBP and one of those fitted the consensus motif P-X-S/T-P, which MAP/ERK kinases are suggested to have specificity for. BLM, CtIP, XRCC1, NBS1 and hnRNP-UL1 itself all contain at least one of these motifs and could potentially be substrates for hnRNP-UL1's kinase activity. However, MBP was employed in the kinase assays due to its promiscuous nature as a phosphorylatable substrate and therefore using the motif at which it was phosphorylated to try and identify possible substrates for hnRNP-UL1 is mere speculation. To identify a substrate the production of a purified source of hnRNP-UL1 would be needed, which has thus far been unattainable. If produced, *in vivo* experiments could be conducted with ATP and selected protein substrate candidates, such as those mentioned above. However, hnRNP-UL1's kinase activity may not be a function of its role in the DDR, but instead as part of another cellular process. This is feasible due to the protein's multi-

functional nature in the cell. An involvement in a completely novel pathway may also be possible.

6.3 ALS AND HNRNP-UL1

ALS is an adult-onset neurodegenerative disorder with a complex aetiology and pathogenesis. Data discussed in chapter IV showed that LCLs derived from ALS patients with hnRNP-UL1 heterozygous mutations showed no defects in their responses to various DNA damaging agents. Similarly, no defects were shown when the patient variant proteins were complemented for WT hnRNP-UL1 and HeLa cells damaged by the same agents. The R639C and R468C variants did show defects in ssDNA-binding and ssRNA-binding however, which may potentially affect the processing of mRNAs with important roles in neuronal cells although there is no current evidence of this. Nucleotide-binding and protein-binding were not affected by the R639C and R468C variants and therefore the study failed to find evidence directly suggesting that these mutations lead to or contribute to the disease by any mechanism involving the 'DDR functions' of the protein. However, there are many other potential mechanisms that the mutations may affect, not least, the aggregation of the cytoplasmic ubiquitylated inclusions within the motor neurons and glial cells which continue to be the hallmark of ALS (Robberecht and Philips, 2013).

The protein composition of the cytoplasmic inclusions differs in the various types of ALS; however, 97% of patients have TDP43-positive inclusions (Laferriére and Polymenidou, 2015). RGG methylation has been shown to be important for the aggregation of TDP43 in forming these inclusions. RGG methylation was shown to stimulate ubiquitylation which increases its oligomerisation (Dammer et al., 2012). Following overexpression of

TDP43 in HEK-293 cells, mass spectrometry allowed analysis of the other proteins localised to these inclusions, many of them were hnRNPs, including hnRNP-U but not hnRNP-UL1 (Dammer et al., 2012). Many of the hnRNPs and other RNA-processing proteins also had peptides with methylated RGGs. hnRNP-UL1 has recently been shown to be methylated heavily within its RGG domain (Gurunathan et al., 2015), suggesting a possible similar mechanism to TDP43 of being ubiquitylated and having a presence in these inclusions. When the lysine residues required for ubiquitylation in the RGG domain of TDP43 were mutated this significantly decreased the aggregation of the protein and resultant inclusions (Dammer et al., 2012). This provides a possible mechanism by which hnRNP-UL1 is recruited to ALS inclusions and also potential avenues for treatment of ALS. hnRNP-UL1 is currently not known to be ubiquitylated, although it would be interesting to investigate ALS patient neuronal cell lysates for ubiquitylated hnRNP-UL1. If ubiquitylation did occur, the residues ubiquitylated could be identified by mass spectrometry and subsequent mutation of the residues to investigate alterations in aggregation propensity could be made.

hnRNP-UL1 may also have the ability to directly contribute to the formation of inclusions. The patient mutations investigated in this study may confer an increased susceptibility of the protein to aggregation. In recent years, the theory that neurodegenerative proteinopathies, such as PD, AD and ALS, have a prion-like mechanism underlying their protein aggregation (which remains a core aspect of their pathogenesis) has grown. As discussed in section *1.4.3*, many of the proteins associated with ALS have prion-like domains (PrLDs), including FUS, TDP43, SOD1, TAF15, EWSR1, hnRNP-A2 and hnRNP-A1 (King et al., 2012). hnRNP-UL1 also has a PrLD at its C-terminus extending from aa residue 614 to 856 (Figure 1.13) and was shown to score 10th for all human RNA-binding proteins and 37th for all human proteins on a scale for prion capacity based on its amino acid sequence and

composition (Li et al., 2013). In chapter IV, experiments in which the hnRNP-UL1 ALS variants were transiently expressed in HeLa cells showed no increased cytoplasmic localisation or aggregation. However, short-term transient expression may not be sufficient to induce detectable changes in the proteins localisation. The likelihood of the R639C and R468C base substitutions increasing aggregation propensity can be analysed by algorithm based software. ZipperDB calculates the potential of each 6-amino-acid stretch in the protein to form amyloid-like fibrils, which consist of β-sheets that stack in a cross-like fashion (Nelson et al., 2005). The R468C substitution makes little difference to the calculated Rosetta energy required to form a fibril (Figure 6.1A). However, the R639C substitution, which does reside in the predicted PrLD of hnRNP-UL1 (Figure 1.13) causes a significant change and brings the Rosetta energy of the GNCGGF hexapeptide very close to the -23 kcal/mol threshold (Figure 6.1B). This suggests that the R639C mutation may contribute to ALS pathogenesis by increasing the aggregation propensity of the protein leading to the formation of disease-causing aggregates. In addition, whilst no defects in DDRs were observed within this study with the mutated variants of hnRNP-UL1, if the variants caused cytoplasmic aggregation, depleting the nuclear pool of hnRNP-UL1 protein, effective responses to DNA damage in neuronal cells could be affected.

Sequestration of hnRNP-UL1, rather than self-stimulated aggregation, could also contribute to ALS pathogenesis. The mutation of other proteins, for example FUS and TDP43, causes mislocalisation to the cytoplasm or increased aggregation propensity resulting in the formation of inclusions affecting their own RNA-processing abilities but also other RNA-processing proteins trapped within the inclusions (Robberecht and Philips, 2013). The recently discovered C9ORF72 hexanucleotide repeat expansions are the single most common cause of ALS and give rise to nuclear as well as cytoplasmic aggregates (Donnelly et al.,

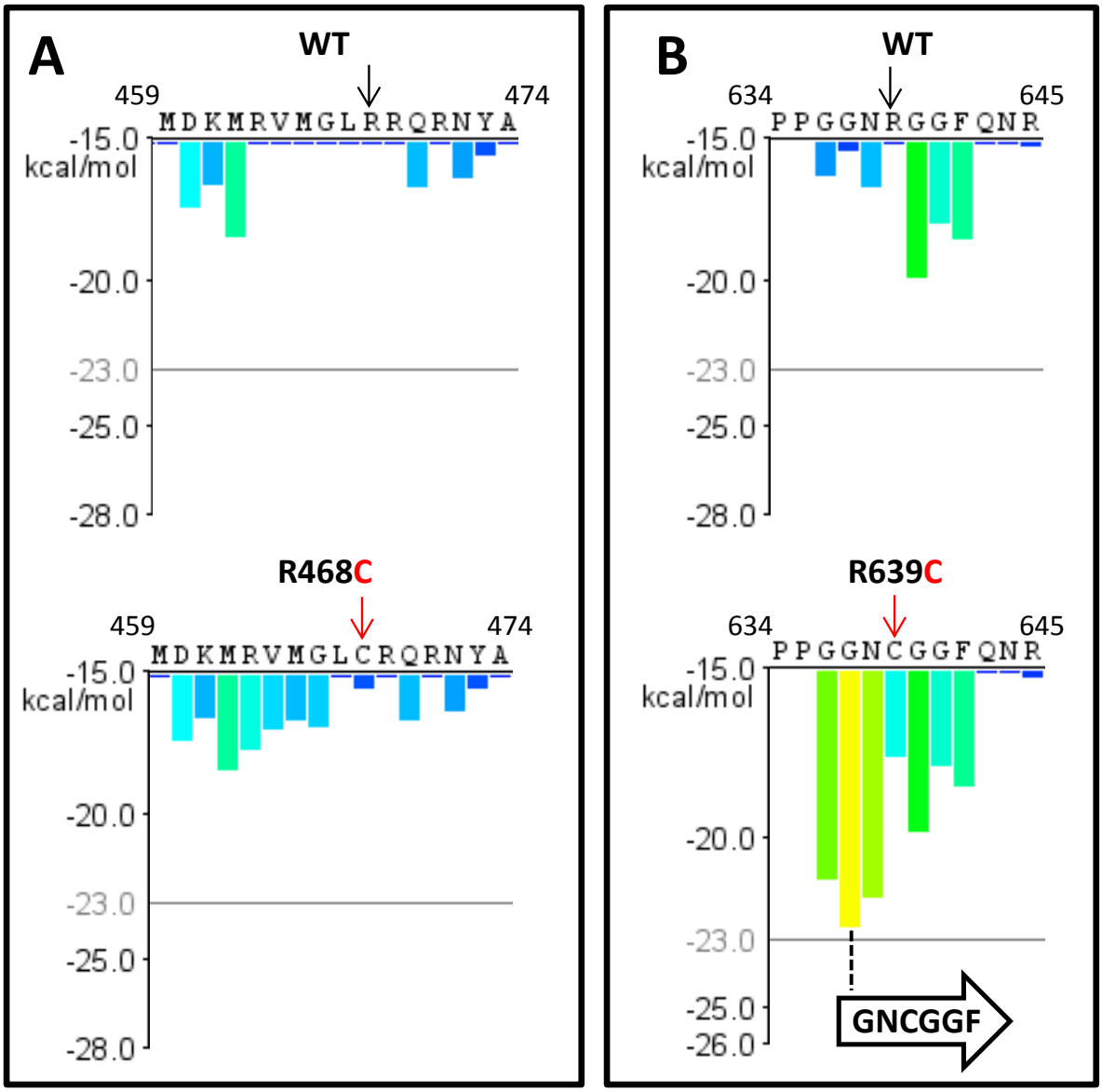

Figure 6.1 The effect of the hnRNP-UL1 patient mutations on potential steric zipper formation. ZipperDB (software available at http://services.mbi.ucla.edu/zipperdb/) calculates the predicted amyloid fibril-forming potential of each 6-amino-acid stretch. The residue sequence is plotted along the x-axis and each histogram bar represents one hexapeptide started at the amino acid above. Hexapeptides with a Rosetta energy below the indicated threshold of -23kcal/mol are predicted to form fibrils. A) The R648C substitution has little effect on predicted fibril formation. B) The R639C substitution has a significant effect on Rosetta energy scores bringing the hexapeptide GNCGGF very close to the threshold energy score.

2013). These aggregates trap a large number of RNA-processing proteins. hnRNP-UL1 could potentially be drawn in to these aggregates affecting the regular function of the protein and RNA metabolism in the cell, possibly leading to neurodegeneration (Lee et al., 2013).

Of the two ALS patient mutations characterised in this study, the R639C variant was the more likely to have deficiencies in RNA-binding due to the substitution of the arginine residue belonging to an RGG tripeptide in the middle of the RRG domain, which is known to be responsible for RNA interaction. This was confirmed during the RNA-binding investigations detailed in chapter V. Decreased RNA-binding would obviously influence the ability of hnRNP-UL1 to interact with mRNA molecules and correctly process them. hnRNP-UL1 is most likely involved in the regulation of thousands of mRNAs and any dysregulation of this role would likely have downstream effects that are detrimental to the cell. FUS and TDP43 were found to share regulation of mRNAs enriched in very long intron sequences, which are known to have specific roles in neuronal cells (Lagier-Tourenne et al., 2012). Little is known about the mRNAs that hnRNP-UL1 regulates, but a similar pattern would fit with the theory that dysregulation would cause neuronal cell susceptibility. Discovery of hnRNP-UL1-regulated mRNAs would allow the investigation of interaction between them and wild-type versus ALS-patient mutation proteins. Aberrant binding may give insights to the protein's contribution to ALS pathogenesis, particularly if the mRNAs and their translated proteins are neuronal cell specific.

Interestingly, the formation of many intracellular compartments which are not bound by membranes, such as nucleoli (Brangwynne et al., 2011), Cajal bodies (Strzelecka et al., 2010), germ granules (Brangwynne et al., 2009), stress granules (SGs; Wippich et al., 2013), processing bodies (P-bodies; Kerdesha et al., 2005) and DDR sites (Altmeyer et al., 2015), form by the same mechanism, a process called 'liquid demixing'. It is thought that proteins

containing the low-sequence complexity of PrLDs are essential for this process. Liquid demixing forms a defined and condensed spherical-shaped liquid-like droplet permitting close proximity and rapid internal rearrangement of the components within it (Patel et al., 2015). This allows the required complex biochemistry to occur in a confined and more organised location in time and space. Due to the vast and complex regulation required around DNA and RNA, the PrLDs are particularly abundant and have been conserved across evolution in DNA- and RNA-binding proteins (King et al., 2013). Thus, the continually expanding trend of RNA-binding domains and PrLDs within proteins linked to ALS has now been strengthened by a functional role for the two domains existing in the same protein.

SGs and P-bodies are good examples of how RNA-binding proteins with PrLDs (e.g. TDP43 and FUS) utilise their self-association properties to form these structures within minutes of the cell becoming stressed. The RNA-binding domains of these proteins recruit specifically targeted mRNAs, whilst their PrLDs allow the formation of the granular structures which protect them from potential damage. The reversibility of the aggregation then allows the granules to dissociate when the stress factor has been dealt with, releasing the sequestered mRNA and translation machinery to resume normal functions (Li et al., 2013). Studies have shown WT FUS forms droplets *in vivo* and overexpression causes the protein to form more viscous gel-like structures as opposed to its usual liquid-like droplet state. In this study, deletion of the PrLD in FUS ablated its droplet formation entirely, showing this region is responsible for this phenomenon (Patel et al., 2015). *In vitro* experiments showed that with increased time droplets would become fibrous and the fibrils grow in length in “sea-urchin-like” patterns. Furthermore, ALS patient variants, G156E and R244C of FUS, significantly accelerated the conversion of droplets to fibrous structures (Patel et al., 2015). With hnRNP-UL1 it would firstly need to be shown that hnRNP-UL1 was capable of forming liquid

droplets by phase separation. This would require good imaging equipment such as a detection of light diffraction through bright-field or phase-contrast microscopy (Altmeyer et al., 2015), or alternatively digital light-sheet microscopy (DLSM) allowing 3D imaging of dynamic subcellular objects (Patel et al., 2015). Hopefully, hnRNP-UL1 would show formation of liquid droplets through overexpression *in vivo*, which either did not occur in our short-term expression experiments or were undetectable by simple immunofluorescence microscopy techniques. Subsequently, experiments could be performed in which the PrLD of hnRNP-UL1 is deleted and liquid droplet formation observed. Then experiments could be conducted with the ALS-patient variants to investigate possible faster progression from droplets to fibrous structures with time compared to wild-type.

It appears that PrLDs within proteins confer the ability to form liquid-like compartments, which provide an essential and critically important functional environment in response to DNA damage (Altmeyer et al., 2015), various other cell stresses (Li et al., 2013) and even routine non-stress RNA regulation processes (Weber and Brangwynne, 2012). These PrLDs and subsequent intracellular compartments come with a caveat of an increased risk of aggregation. Cells possess regulatory mechanisms to control the formation and release of these liquid-like compartments, but with age these mechanisms may fail or become overwhelmed by mutations increasing the aggregation propensity of involved proteins. This could lead to the balance being tipped towards chronic aggregation providing a reasonable explanation for the late-onset of ALS. Indeed, a large number of ALS-causing mutations have been found in PrLDs and experiments are now showing that the mutations speed up the liquid-to-phase transition of the proteins (Patel et al., 2015). Stress-induced pathways of SG formation and progressively aberrant liquid-to-solid phase transitions may be central to the pathogenesis of the disease. Given the known domains, RNA-processing functions (which

are so similar to those of other ALS-linked proteins, e.g. FUS and TDP43), plus the novel ALS patients with hnRNP-UL1 mutations here, it is reasonable to suggest that hnRNP-UL1 is a very strong candidate for involvement in ALS pathogenesis. Studies with transgenic mice expressing hnRNP-UL1 ALS-patient variations would provide the ideal environment for investigation of long-term aggregation of the proteins. Furthermore, these mutated forms of the protein could be targeted to neuronal tissue to see if ALS-like symptoms could be generated.

6.4 THE ROLE OF HNRNP-UL1 IN THE EARLY RESPONSE TO DNA DAMAGE

Another aspect of cellular biology which requires rapid and controlled compartmentalisation is areas around DNA damage sites (DNA damage foci). Poly(ADP-ribose) (PAR) levels are rapidly and significantly increased at sites of DNA damage. Recent studies show that the electrostatic interactions between positively charged RGG repeats and negatively charged PAR cause the liquid demixing observed at DNA damage sites, which is further amplified by the aggregation-prone PrLDs (Altmeyer et al., 2015). Recent evidence suggests these compartments then function to provide a specific localised area in which the controlled recruitment of repair factors and exclusion of other proteins can occur (Altmeyer et al., 2015; Sharma et al., 2015). A number of proteins with both RGG repeats and PrLDs have been shown to be recruited to these sites, such as the three FET proteins (TAF15, EWS and FUS) (Altmeyer et al., 2015). This was shown by mutating varying numbers of the RGG repeats in the three FET proteins (TAF15, EWS and FUS) which were shown to be rapidly recruited to laser-induced DSB sites in a PAR-dependent manner. Decreasing the number of RGG repeats caused a correlative decrease in recruitment; mutation of all eight arginines in

FUS completely ablated its recruitment. The isolated PrLDs of the three FET proteins formed spherical hydrogel-like structures when expressed in human cells (Altmeyer et al., 2015).

Whilst hnRNP-UL1's role in early phase responses to DNA damage remains unclear and was not specifically investigated during this study, the recent evidence for proteins containing RGG motifs and PrLDs in liquid demixing provides a possible function for the protein during this stage of the DDR. hnRNP-UL1 has been shown to be recruited to laser-induced DSB sites in a PARP-1-dependent manner as part of the very early response to DNA damage (Polo et al, 2012; Hong et al., 2013). Additionally, hnRNP-UL1 was shown to associate physically with PARP-1 by immunoprecipitation and be PARylated by PARP-1. Live cell imaging showed that a GFP-tagged RGG motif alone was sufficient for recruitment, however, the PrLD domain minus the RGG motif showed significantly improved recruitment and both regions together were responsible for yet stronger recruitment (Hong et al., 2013). This would fit with the proposed theory of RGG repeats and PAR causing liquid demixing, but the PrLDs allow significant amplification of the accumulation. This evidence suggests hnRNP-UL1 may play a very important role in helping to create an initial controlled compartment around the damage site which would then facilitate assembly of other repair factors. Investigation of hnRNP-UL1's recruitment to laser-induced DSBs could be made by decreasing the number of RGG repeats by mutation of the arginine residues and observing whether recruitment decreases as with FUS in Altmeyer et al. (2015).

During this study, the interaction between hnRNP-UL1 and PARP-1 was investigated with the various constructs made (the Walker A mutant/MWA and the ALS-patient mutations R639C and R468C). Results in chapter V showed the MWA variant to reduce binding to PARP-1. As explained in section *5.3*, this could be due to gross conformational changes induced by the three amino acid changes of this variant or that the PARP-1 interaction is

dependent upon nucleotide binding of hnRNP-UL1. Alternatively, mutation in the Walker A motif could lead to specific changes in the PARP binding site. To investigate this, an alternative Walker A mutant could be created with just one of the three critical GKT residues being mutated and the immunoprecipitation experiments repeated. Furthermore, the hnRNP-UL1 R639C variant protein was shown to have no reduced binding to PARP-1. This mutation of a single arginine residue within one of the protein's seven RG or RGG repeats was evidently not enough to effect the interaction with PARP-1. It would be interesting to conduct PARP-1 immunoprecipitation studies with an RGG deletion hnRNP-UL1 protein and also with a construct in which all the arginines of the RGG motif were mutated. Similarly, as XRCC1 is recruited to damage sites by an association with PARP-1 (Masson et al., 1998), carrying out immunoprecipitation studies with the same hnRNP-UL1 variants would also be interesting. It is conceivable that hnRNP-UL1, PARP-1 and XRCC1 exist as a complex which is dependent on PARylation following DNA damage.

The link between RGG domains, PrLDs and liquid demixing was further explored in Altmeyer et al. (2015). Interestingly, overexpression of the FUS PrLD region alone stimulated the self-assembly of heterogeneous liquid droplets containing endogenous wild-type FET proteins as well as hnRNP-UL1 (Altmeyer et al., 2015). Fusion of the FUS PrLD (aa1-211) to its RGG repeats (aa468-526) led to more significant accumulation at laser-irradiated sites, suggesting the PrLD domains can further drive phase separation by recruiting other similarly structured proteins. The initial *in vivo* stimulus of this protein assembly was shown to be driven by PARylation as depleting the PAR-degrading enzyme PAR glycohydrolase (PARG) caused more pronounced and prolonged liquid droplet formations in response to DNA damage as detected by light diffraction through both bright-field and phase-contrast microscopy. PARP inhibitors also completely abolished droplet formation. Furthermore, the

presence of PAR and purified RGG/PrLD-containing synthetic peptides alone were sufficient enough to form aggregates *in vitro*, showing this ability is intrinsic to these domains under stimulation from PAR (Altmeyer et al., 2015). Investigations in to the hnRNP-UL1's ability to cause liquid demixing using detection of light diffraction would be very interesting. Expressing a purified source of the protein (or even just the C-terminus RGG/PrLD region) *in vitro* in the presence of PAR and observing liquid droplet formation would give an insight in to whether the protein possesses an intrinsic ability to perform this process or whether the protein is recruited to these compartments as a contributing factor but of less importance as other proteins such as the FET family members. *In vivo* experiments could also be conducted in which hnRNP-UL1 is overexpressed and liquid droplet formation is observed. Additionally, similar experiments following depletion of endogenous hnRNP-UL1 and expression of various mutated constructs (e.g. RGG motif deletion, PrLD deletion, RGG arginine substituted) could be carried out.

As mentioned above, these liquid droplet compartments serve to control the recruitment of certain proteins. A good example of another membrane-less liquid-droplet compartment is the nucleolus, which permits access to ribosomal RNA and RNA-binding proteins, but not other nuclear components such as DDR factors (Altmeyer et al., 2015). Fully-folded globular DDR proteins, such as NBS1, MDC1 and 53BP1, were excluded from the PrLD-protein liquid droplets under normal conditions. However, following DNA damage stress MDC1 was permitted access to the droplets whilst 53BP1 was excluded (Altmeyer et al., 2015). This is very interesting as MDC1 has a proximal role in DDR as an attachment factor for other repair proteins (Bekker-Jensen and Mailand, 2010), whereas 53BP1 has a late-phase role particularly in guiding DSB repair pathway choice towards NHEJ (Panier and Boulton, 2014). This suggests that the rapid PAR-seeded liquid droplet formation around

break sites functions to selectively permit access to repair factors needed for early-phase responses whilst excluding late-phase response proteins.

Recent evidence suggests hnRNP-UL1 is involved in the inclusion and exclusion of DDR proteins as shown by Sharma et al. (2015) during investigation of the roles of long non-coding RNAs (lncRNAs) in the DDR. A novel lncRNA, named *DDSR1* (DNA damage-sensitive RNA1), was upregulated in response to treatment with various DNA damaging agents. Mass spectrometry showed *DDSR1* to interact with hnRNP-UL1. Their relationship was further strengthened when depletion of *DDSR1* was shown to compromise HR by decreasing DNA end resection (Sharma et al., 2015), similarly hnRNP-UL1 depletion has the same effect (Polo et al., 2012). Furthermore, BRCA1/RAP80 complex accumulation at damage sites increased with *DDSR1* depletion (Sharma et al., 2015). The BRCA1/RAP80 complex is known to restrict DNA end resection (Coleman and Greenber, 2011). This leads to the proposal that links the early phase role of hnRNP-UL1 to the late phase role of stimulating DNA end resection and subsequently repair by HR. hnRNP-UL1 interacts with *DDSR1*, and along with many other PAR stimulated RGG/PrLD-containing proteins, forms liquid droplets which function to selectively exclude or include access to specific proteins. Preventing the accumulation of DNA resection-inhibitory BRCA1/RAP80 complexes helps the selection of repair pathway choice towards HR (Sharma et al., 2015; Lukas and Altmeyer, 2015). hnRNP-UL1 later recruits factors such as BLM to stimulate the resection required for HR (Polo et al., 2012). Sharma et al. (2015) used the more sensitive technique of live cell imaging to measure a significant increase in the recruitment kinetics of BRCA1 and RAP80 to laser-induced DSBs following *DDSR1* depletion. Polo et al. (2012) was not able to detect an increase in BRCA1 recruitment following whole cell irradiation to induce DSBs following hnRNP-UL1 depletion. Therefore, it would be of interest to conduct studies with live cell imaging

following laser-induced irradiation treatment to see whether the BRCA1/RAP80 recruitment increases following hnRNP-UL1 depletion as it does with *DDSR1* depletion. This would help to confirm the proposed role of hnRNP-UL1 in guiding DSB repair pathway choice towards HR by its control of exclusion and inclusion of specific proteins as part of the early phase liquid demixing machinery.

The FET family proteins, FUS, EWS and TAF15, have all been shown to be mutated leading to ALS. Of great interest to furthering the understanding of ALS pathogenesis the three proteins were shown to be significantly involved in the PAR-dependent formation of the liquid droplet structures around DNA damage breaks. Mass spectrometry analysis identified TAF15 and FUS among the top ten proteins to be PARylated following DNA damage (Jungmichel et al., 2013). EWS and FUS, like hnRNP-UL1, have been shown to localise rapidly and transiently to sites of DNA damage (Mastrocola et al., 2013; Wang et al., 2013). GFP-tagged TAF15 truncations of only its RGG domain or its PrLD domain were sufficient to be recruited to damage sites (Izhar et al., 2015) providing further evidence for the importance of each of the two domains in the recruitment to these sites. Additionally, co-depletion of the three proteins abolished liquid droplet formation in response to DNA damage, whilst the over expression of individual members greatly enhanced the process (Altmeyer et al., 2015). The three FET proteins share an important role in initiating rapid liquid droplet formation around DNA damage sites. All three are also strongly linked to ALS and ALS patient mutations have been shown to cause DDR defects (Qiu et al., 2014). Therefore, the potential for defective DNA damage repair to have a significant role in ALS pathogenesis is still very plausible. hnRNP-UL1 fits with the trends of these proteins and despite no evidence of the ALS hnRNP-UL1 patient mutations showing DDR defects during this study it should not be ruled out that they do cause DDR defects. In the study by Qiu et al. (2014), transgenic

mice expressing the ALS patient mutation FUS-R521C showed evidence of DNA damage in spinal motor neurons and cortical neurons causing severe dendritic and synaptic defects. This was caused by defective repair of oxidation damage in the 5' noncoding exons of the *Bdnf* (brain derived neurotrophic factor) gene. BDNF protein is a neuronal cell growth factor helping to promote the survival of existing neurons and growth and differentiation of new ones (Hyman et al., 1991). The ineffective repair was compounded by the mutant FUS protein binding *Bdnf* RNA more strongly than wild-type, resulting in splicing defects (Qiu et al., 2014). The transgenic mouse model expressing an ALS patient mutated protein allowed the direct link between DNA damage defects and disease pathogenesis to be made. A similar investigation conducted with hnRNP-UL1 would be very interesting. It would eliminate the problems seen in this study with heterogeneous mutations in lymphoid cells, the variability of LCL responses to DNA damage and would potentially enable the identification of unique ALS-related pathogenesis in patients with hnRNP-UL1 mutations.

To conclude, it is quite feasible that during times in which the cell is not stressed RNA-binding motif containing-PrLDs bind to cognate RNA or DNA targets as part of RNA granules. The formation of RNA granules was shown to be regulated by a combination of RNA-binding specificity and PrLDs *in vitro* (Kato et al. 2012; Lin et al., 2015). The PrLDs of numerous RNA-binding proteins, and also full-length hnRNP-A1 alone, were shown to phase separate *in vitro* to form liquid droplets. This was stimulated by low salt concentrations or RNA (Lin et al., 2015). This shows RNA is capable of stimulating liquid demixing by hnRNP proteins, which may occur naturally *in vivo* to form RNA granules. Therefore, rapid PAR formation in response to DNA damage within the nucleus may serve to out-compete these RNA interactions, stimulating the transient assembly around break sites (Altmeyer et al., 2015).

CHAPTER VI

REFERENCES

Aguirre N., Beal M.F., Matson W.R., et al.. Increased oxidative damage to DNA in an animal model of amyotrophic lateral sclerosis, *Free Radic Res.* 2005;35:383-388.

Alberti S., Halfmann R., King, O., et al.. A systematic survey identifies prions and illuminates sequence features of prionogenic proteins. *Cell*. 2009;137:146-158.

Allinson S.L.. DNA end-processing enzyme polynucleotide kinase as a potential target in the treatment of cancer. *Future Oncol*. 2010;6:1031-1042.

Altmeyer M., Neelsen K.J., Teloni F., et al. Liquid demixing of intrinsically disordered proteins is seeded by poly (ADP-ribose). *Nat Commun.* 2015;6:1-12.

Andersen P.M. and Al-Chalabi A.. Clinical genetics of amyotrophic lateral sclerosis: what do we really know? *Nature Rev Neurol.* 2011;7:603-615.

Andrus P.K., Fleck T.J., Gurney M.E., et al.. Protein oxidative damage in a transgenic mouse model of familial amyotrophic lateral sclerosis. *J Neurochem*. 1998;71:2041–2048.

Aravind L. And Koonin E.V.. SAP – a putative DNA-binding motif involved in chromosomal organization. *Trends Biochem Sci.* 2000;25:112-114.

Bachi A., Braun I.C., Rodrigues J.P., et al.. The C-terminal domain of TAP interacts with the nuclear pore complex and promotes export of specific CTE-bearing RNA substrates. *RNA*. 2000;6:136-158.

Banerjee R., Starkov A.A., Beal M.F., et al.. Mitochondrial dysfunction in the limelight of Parkinson's disease pathogenesis. *Biochim Biophys Acta.* 2009;1792:651-663.

Barber S.C. and Shaw P.J.. Oxidative stress in ALS: key role in motor neuron injury and therapeutic target. *Free Radical Bio Med.* 2010;48:629-641.

Barmada S.J.. Linking RNA dysfunction and neurodegeneration in amyotrophic lateral sclerosis. *Neurotherapeutics*. 2015;12:340-51.

Barral P.M., Rusch A., Turnell A.S., et al.. The interaction of the hnRNP family member E1B-AP5 with p53. *FEBS Letters*. 2005;579:2752-2758.

Beal M.F., Ferrante R.J., Browne S.E., et al.. Increased 3-nitrotyrosine in both sporadic and familial amyotrophic lateral sclerosis. *Ann Neurol*. 1997;42:644-654.

Bennett B.L., Sasaki D.T., Murray B.W., et al.. SP600125, an anthrapyrazolone inhibitor of Jun N-terminal kinase. *P Natl Acad Sci USA*. 2001;98:13681-13686.

Bensimon G., Lacomblez L. and Meininger, V.F.. A controlled trial of riluzole in amyotrophic lateral sclerosis. ALS/Riluzole Study Group. *N Engl J Med.* 1994;330:585-591.

Bekker-Jensen S. and Mailand N.. Assembly and function of DNA double-strand break repair foci in mammalian cells. *DNA Repair*. 2010;9:1219–1228.

Bernstein N.K., Williams R.S., Rakovszky M.L., et al.. The molecular architecture of the mammalian DNA repair rnzyme, polynucleotide kinase. *Mol Cell*. 2005;17:657-670.

Biton S., Barzilai A. and Shiloh, Y.. The neurological phenotype of ataxia-telangiectasia: solving a persistent puzzle. *DNA Repair*. 2008;7:1028-1038.

Blackford A.N., Bruton R.K., Dirlik O., et al.. A role for E1B-AP5 in ATR signalling pathways during adenovirus infection. *J Virol*. 2008;82:7640-7652.

Bogdanov M., Brown R.H, Matson W., et al.. Increased oxidative damage to DNA in ALS patients. *Free Radic Biol Med.* 2000;29:652-658.

Bohr V.A.. Rising from the RecQ-age: the role of human RecQ helicases in genome maintenance. *Trends Biochem Sci*. 2008;33:609-620.

Borchelt D. R., Lee M.K., Slunt H.S., et al.. Superoxide dismutase 1 with mutations linked to familial amyotrophic lateral sclerosis possesses significant activity. *P Natl Acad Sci USA*. 1994;91:8292-8296.

Brangwynne C.P., Eckmann C.R., Courson D.S., et al.. Germline P granules are liquid droplets that localize by controlled dissolution/condensation. *Science*. 2009;324:1729-1732.

Brangwynne C.P., Mitchison T.J., and Hyman A.A.. Active liquid-like behavior of nucleoli determines their size and shape in Xenopus laevis oocytes. *P Natl Acad Sci USA*. 2011;108:4334-4339.

Brotherton T.E. et al.. Localization of a toxic form of superoxide dismutase 1 protein to pathologically affected tissues in familial ALS. *P Natl Acad Sci USA*. 2012;109:5505-5510.

Bruijn L.I., Houseweart M.K., Kato S., et al.. Aggregation and motor neuron toxicity of an ALS-linked SOD1 mutant independent from wild-type SOD1. *Science*. 1998;281:1851-1854.

Bruton R.K., Rasti M., Mapp K.L., et al.. C-terminal-binding protein interacting protein binds directly to adenovirus early region 1A through its N-terminal region and conserved region 3. *Oncogene*. 2007;26:7467-7479.

Bryant H.E., Schultz N., Thomas H.D., et al.. Specific killing of *BRCA2*-deficient tumours with inhibitors of poly(ADP-ribose) polymerase. *Nature.* 2005;434:913-917.

Bugreev D.V., Yu X., Egelman E.H., et al.. Novel pro- and anti-recombination activites of the Bloom's syndrome helicase. *Genes Dev*. 2007;21:3085-3094.

Caldecott K.W.. Single-strand break repair and genetic disease. *Nat Rev Genet.* 2008;9:619-631.

Chapman J.R., Taylor M.R. and Boulton S.J.. Playing the end game: DNA double-strand break repair pathway choice. *Mol Cell*. 2012;47:497-510.

Chaudhury A., Chander C. and Howe P.H. Heterogeneous nuclear ribonucleoproteins (hnRNPs) in cellular processes: Focus on hnRNP E1's multifunctional regulatory roles. *RNA*. 2010;16:1449-1462.

Chen Y.I.G., Moore R.E., Helen Y.G., et al.. Proteomic analysis of in vivo-assembled pre-mRNA splicing complexes expands the catalog of participating factors. *Nucleic Acids Res*. 2007;35:3928-3944.

Chi Y-H., Semmes O.J. and Jeang K-T.. A proteomic study of TAR-RNA binding protein (TRBP)-associated factors. *Cell Biosci*. 2011;1:9.

Chia R., Tattum M.H., Jones S., et al.. Super-oxide dismutase 1 and tgSOD1 mouse spinal cord seed fibrils, suggesting a propagative cell death mechanism in amyotrophic lateral sclerosis. *PLoS ONE*. 2010;5:e10627.

Chu W.K. and Hickson I.D.. RecQ helicases: multifunctional genome caretakers. *Nat Rev Cancer*. 2009;9:644-654.

Ciccia A. and Elledge S.J.. The DNA damage response: making it safe to play with knives. *Mol Cell*. 2010;40:179-204.

Colby D.W. and Prusiner S.B.. De novo generation of prion strains. *Nat Rev Microbiol*. 2011;9:771-777.

Coleman K. A. and Greenberg R.A.. The BRCA1-RAP80 complex regulates DNA repair mechanism utilization by restricting end resection. *J Biol Chem*. 2011;286:13669-13680.

Cooper G.M., 2006. The cell: a molecular approach, Fourth Edition. Sinauer Associates, Inc. ISBN: 978-0-87893-219-1.

Coppedè, F.. An overview of DNA repair in amyotrophic lateral sclerosis. *Sci World J*. 2011;11:1679-1691.

Coppedè F., and Migliore L.. DNA damage and repair in Alzheimer's disease. *Curr Alzheimer Res*. 2009;6:36-47.

Coppedè F., and Migliore L.. DNA damage in neurodegenerative diseases. *Mut Res-Fund Molecular M*. 2015:776:84-97.

Coquelle N., Havali-Shahriari Z., Bernstein N., et al.. Structural basis for the phosphatase activity of polynucleotide kinase/phosphatase on singleand double-stranded DNA substrates. *P Natl Acad Sci USA*. 2011;108:21022–21027.

Corneo B., Wendland R.L., Deriano L., et al.. Rag mutations reveal robust alternative end joining. *Nature.* 2007;449:483-486.

Cortese A., Plagnol V., Brady S., et al.. Widespread RNA metabolism impairment in sporadic inclusion body myositis TDP43-proteinopathy. *Neurobiol Aging*. 2014;35:1491-1498.

Couthouis J., Hart M.P., Erion R., et al.. Evaluating the role of the FUS/TLS-related gene *EWSR1* in amyotrophic lateral sclerosis. *Hum Mol Genet.* 2012;21:2899–2911.

Couthouis J., Hart M.P., Shorter J., et al.. Feature article: a yeast functional screen predicts new candidate ALS disease genes. *P Natl Acad Sci USA*. 2011;108:20881-20890.

Da Cruz S. and Cleveland D.W.. Understanding the role of TDP-43 and FUS/TLS in ALS and beyond. *Curr Opin Neurobiol*. 2011;21:904-919.

Daigle J.G., Daigle J.G., Lanson N.A., et al.. RNA binding ability of FUS regulates neurodegeneration, cytoplasmic mislocalization and incorporation into stress granules associated with FUS carrying ALS-linked mutations. *Hum Mol Genet.* 2012;22:1193-1205.

Dammer E.B., Fallini C., Gozal Y.M., et al.. Coaggregation of RNA-binding proteins in a model of TDP-43 proteinopathy with selective RGG motif methylation and a role for RRM1 ubiquitination. *PLoS ONE.* 2012;7:e38658.

Dean F.B., Bullock P., Murakami Y., et al.. Simian virus 40 (SV40) DNA replication: SV40 large T antigen unwinds DNA containing the SV40 origin of replication. *P Natl Acad Sci USA*. 1987;84:16-20.

DeJesus-Hernandez M., Mackenzie I.R., Boeve B.F., et al.. Expanded GGGGCC hexanucleotide repeat in noncoding region of C9ORF72 causes chromosome 9p-linked FTD and ALS. *Neuron*. 2011;72:245-256.

Deng H.X., Shi Y., Furukawa Y., et al.. Conversion to the amyotrophic lateral sclerosis phenotype is associated with intermolecular linked insoluble aggregates of SOD1 in mitochondria. *P Natl Acad Sci USA*. 2006;103:7142-7147.

Dewey C.M. et al.. TDP-43 aggregation in neurodegeneration: are stress granules the key? *Brain Res.* 2012;1462:16-25.

Deyrup A.T., Krishnan S., Cockburn B.N., et al.. Deletion and site-directed mutagenesis of the ATP-binding motif (P-loop) in the bifunctional murine ATP-sulfurylase/adenosine 5'-phosphosulfate kinase enzyme. *J Biol Chem.* 1998;273:9450-9456.

Dion P.A., Daoud H. and Rouleau G.A.. Genetics of motor neuron disorders: new insights into pathogenic mechanisms. *Nat Rev Genet*. 2009;10:769-782.

Donnelly C.J., Zhang P.W., Pham J.T., et al.. RNA toxicity from the ALS/FTD C9ORF72 expansion is mitigated by antisense intervention. *Neuron.* 2013;80:415-428.

Dormann D. Rodde R., Edbauer D., et al.. ALS-associated fused in sarcoma (*FUS*) mutations disrupt Transportin-mediated nuclear import. *EMBO.* 2010;29:2841-2857.

Dreyfuss G., Matunis M.J., Pinol-Roma S., et al.. hnRNP proteins and the biogenesis of mRNA. *Annu Rev Biochem*. 2003;62:289-321.

Elden A.C., Kim H.J., Hart M.P., et al.. Ataxin-2 intermediate-length polyglutamine expansions are associated with increased risk for ALS. *Nature.* 2010;466:1069-1075.

Fan J., Yang X., Wang W., et al.. Global analysis of stress-regulated mRNA turnover by using cDNA arrays. *Proc Natl Acad Sci USA*. 2002;99:10611-6.

Farg M.A., Sundaramoorthy V., Sultana J.M., et al.. C9ORF72, implicated in amytrophic lateral sclerosis and frontotemporal dementia, regulates endosomal trafficking. *Hum Mol Genet*. 2014;23:3579-3595.

Ferrante R.J., Browne S.E., Shinobu L.A., et al.. Evidence of increased oxidative damage in both sporadic and familial amyotrophic lateral sclerosis, *J Neurochem.* 1997;69:2064-2074.

Filippo J.S., Sung P., and Klein H.. Mechanism of Eukaryotic Homologous Recombination. *Annu Rev Biochem*. 2008;77:229-257.

Fischer L.R., Culver D.G., Tennant P., et al.. Amyotrophic lateral sclerosis is a distal axonopathy: evidence in mice and man. *Exp Neurol.* 2004;185:232-240.

Freibaum B.D., Chitta R.K., High A.A., et al.. Global analysis of TDP-43 interacting proteins reveals strong association with RNA splicing and translation machinery. *J Proteome Res*. 2010;9:1104-1120.

Freischmidt A., Müller K., Ludolph A.C.,et al.. Systemic dysregulation of TDP-43 binding microRNAs in amyotrophic lateral sclerosis. *Acta Neuropathol Commun*. 2013;1:42.

Furukawa Y., Kaneko K., Watanabe S., et al.. A seeding reaction recapitulates intracellular formation of Sarkosyl-insoluble transactivation response element (TAR) DNA-binding protein-43 inclusions. *J Biol Chem.* 2011;286:18664-18672.

Gabler, S., Schutt, H., Groitl, P., et al.. E1B 55-kilodalton-associated protein: a cellular protein with RNA-binding activity implicated in nucleocytoplasmic transport of adenovirus and cellular mRNAs. *J Virol*. 1998;72;7960-7971.

Gamble S.C., Dunn M.J., Wheeler C.H., et al.. Expression of proteins coincident with inducible radioprotection in human lung epithelial cells. *Cancer Res*. 2000;60:2146-2151.

Gennery A.R.. Primary immunodeficiency syndromes associated with defective DNA double-strand break repair. *Br Med Bull*. 2006;77-78:71-85.

Genova M.L., Pich M.M., Bernacchia A., et al.. The mitochondrial production of reactive oxygen species in relation to aging and pathology. *Ann N. Y. Acad Sci.* 2004;1011:86-100.

Gijselinck I., Van Langenhove T., van der Zee J., et al.. A C9orf72 promoter repeat expansion in a Flanders-Belgian cohort with disorders of the frontotemporal lobar degenerationamyotrophic lateral sclerosis spectrum: a gene identification study. *Lancet Neurol*. 2012;11:54-65.

Goh E.T., Pardo O.E., Michael N., et al.. Involvement of heterogeneous ribonucleoprotein F in the regulation of cell proliferation via the mammalian target of rapamycin/S6 kinase 2 pathway. *J Biol Chem*. 2010;285:17065-17076.

Grad L.I., Fernando S.M. and Cashman N.R.. From molecule to molecule and cell to cell: Prion-like mechanisms in amyotrophic lateral sclerosis. *Neurobiol Dis.* 2015;77:257-265.

Graffmo K.S., Forsberg K., Bergh J., et al.. Expression of wild-type human superoxidedismutase-1 in mice causes amyotrophic lateral sclerosis. *Hum Mol Genet.* 2013;22:51-60.

Gregory R.I., Yan K-P., Amuthan G., et al. The microprocessor complex mediates the genesis of microRNAs. *Nature*. 2004;432:235-240.

Gruhne B., Sompallae R., Marescotti D., et al.. The Epstein–Barr virus nuclear antigen-1 promotes genomic instability via induction of reactive oxygen species. *Proc Natl Acad Sci USA*. 2009a;106:2313-2318.

Gruhne B., Sompallae R., and Masucci M.G.. Three Epstein–Barr virus latency proteins independently promote genomic instability by inducing DNA damage, inhibiting DNA repair and inactivating cell cycle checkpoints. *Oncogene*. 2009b;28:3997-4008.

Gueven N., Chen P., Nakamura J., et al.. A subgroup of spinocerebellar ataxias defective in DNA damage responses. *Neuroscience*. 2007;145:1418-1425.

Guo W., Chen Y., Zhou X., et al.. An ALS-associated mutation affecting TDP-43 enhances protein aggregation, fibril formation and neurotoxicity. *Nat Struct Mol Biol.* 2011;18:822-830.

Gurunathan G., Yu Z., Coulombe Y., et al.. Arginine methylation of hnRNPUL1 regulates interaction with NBS1 and recruitment to sites of DNA damage. *Sci Rep*. 2015;5:1-9.

Hanahan D. and Weinberg R.A.. Hallmarks of cancer: the next generation. *Cell*. 2011;144:646-674.

Haramati S., Chapnik E., Sztainberg Y., et al.. miRNA malfunction causes spinal motor neuron disease. *Proc Natl Acad Sci USA.* 2010;107:13111-13116.

Hartmuth K., Urlaub H., Vornlocher H.P., et al.. Protein composition of human prespliceosomes isolated by a tobramycin affinity-selection method. *Proc Natl Acad Sci USA*. 2002;99:16719-16724.

Haley B., Paunesku T., Protić M., et al.. Response of heterogeneous ribonuclear proteins (hnRNP) to ionising radiation and their involvement in DNA damage repair. *Int J Radiat Biol*. 2009;85:643-655.

Hennig S., Kong G., Mannen T., et al.. Prion-like domains in RNA binding proteins are essential for building subnuclear paraspeckles. *J Cell Biol.* 2015;210:529-539.

Hoeijmakers J.H.. DNA damage, aging, and cancer. *N Engl J Med*. 2009;361:1475-1485.

Hong Z., Jiang J., Ma J., et al.. The role of hnRPUL1 involved in DNA damage response is related to PARP1. *PLoS ONE*. 2013;8:1-10.

Hopfner K.P., Karcher A., Craig L., et al.. Structural biochemistry and interaction architecture of the DNA double-strand break repair Mre11 nuclease and Rad50-ATPase. *Cell*. 2001;105:473-485.

Hopfner K.P., Karcher A., Shin D. S., et al.. Structural biology of Rad50 ATPase: ATP-driven conformational control in DNA double-strand break repair and the ABC-ATPase superfamily. *Cell*. 2000;101:789-800.

Hyman C., Hofer M., Barde Y.A., et al.. BDNF is a neurotrophic factor for dopaminergic neurons of the substantia nigra. *Nature.* 1991;350:230-232.

Ideue T., Adachi S., Naganuma T., et al.. U7 small nuclear ribonucleoprotein represses histone gene transcription in cell cycle-arrested cells. *Proc Natl Acad Sci USA*. 2012;109:5693-5698.

Ihara R., Matsukawa K., Nagata Y., et al.. RNA binding mediates neurotoxicity in the transgenic Drosophila model of TDP-43 proteinopathy. *Hum Mol Genet*. 2013;22:4474-4484.

Ihara Y., Nobukuni K., Takata H., et al.. Oxidative stress and metal content in blood and cerebrospinal fluid of amyotrophic lateral sclerosis patients with and without a Cu,Zn-superoxide dismutase mutation. *Neurol Res*. 2005;27:105-108.

Iwanaga K., Sueoka N., Sato A., et al.. Heterogeneous nuclear ribonucleoprotein B1 protein impairs DNA repair mediated through the inhibition of DNA-dependent protein kinase activity. *Biochem Bioph Res Co*. 2005;333:888-895.

Izhar L., Adamson B., Ciccia A., et al.. A systematic analysis of factors localized to damaged chromatin reveals PARP-dependent recruitment of transcription factors. *Cell Rep.* 2015;11:1486-1500.

Jackman J., Alamo I. Jr., Fornace A.J. Jr., et al.. Genotoxic stress confers preferential and coordinate messenger RNA stability on the five gadd genes. *Cancer Res.* 1994; 54:5656-62.

Jackson S.P. and Bartek J.. The DNA-damage response in human biology and disease. *Nature*. 2009;461:1071-1078.

Jen K.Y. and Cheung V.G.. Transcriptional response of lymphoblastoid cells to ionizing radiation. *Genome Res*. 2003;13:2092–2100.

Jeon J.P., Nam H.Y., Shim S.M., et al.. Sustained viral activity of Epstein-Barr virus contributes to cellular immortalization of lymphoblastoid cell lines. *Mol Cell.* 2009;27:143-148.

Johnson B.S., Snead D., Lee J.J., et al.. TDP-43 is intrinsically aggregation-prone, and amyotrophic lateral sclerosis-linked mutations accelerate aggregation and increase toxicity. *J Biol Chem*. 2009;284:20329-20339.

Jungmichel S., Rosenthal F., Altmeyer M., et al.. Proteome-wide identification of poly (ADP-Ribosyl) ation targets in different genotoxic stress responses. *Mol Cell*. 2013;52:272-285.

Kato M., Han T.W., Xie S., et al.. Cell-free formation of RNA granules: low complexity sequence domains form dynamic fibers within hydrogels. *Cell*. 2012;149:753-767.

Katyal S. and McKinnon P.J.. DNA strand breaks, neurodegeneration and aging in the brain. *Mech Ageing Dev.* 2008;129:483-491.

Kastan M.B. and Bartek J.. Cell-cycle checkpoints and cancer. *Nature.* 2004;432:316-323.

Kawahara Y. and Mieda-Sato A.. TDP-43 promotes microRNA biogenesis as a component of the Drosha and Dicer complexes. *Proc Natl Acad Sci USA*. 2012;109:3347-3352.

Kedersha N., Stoecklin G., Ayodele M., et al.. Stress granules and processing bodies are dynamically linked sites of mRNP remodeling. *J Cell Biol*. 2005;169:871-884.

Kerzendorfer C. and O'Driscoll M.. Human DNA damage response and repair deficiency syndromes: linking genomic instability and cell cycle checkpoint proficiency. *DNA Repair*. 2009;8:1139-1152.

Kim H.J., Kim N.C., Wang Y-D., et al.. Mutations in prion-like domains in hnRNPA2B1 and hnRNPA1 cause multisystem proteinopathy and ALS. *Nature.* 2013;28;495:467-73.

King O.D., Gitler A.D. and Shorter J.. The tip of the iceberg: RNA-binding proteins with prion-like domains in neurodegenerative disease. *Brain Res*. 2012;1462:61-80.

Knobel K.M., Davis W.S., Jorgensen E.M., et al.. UNC-119 suppresses axon branching in C. elegans. *Development*. 2001;128:4079-4092.

Koch C.A., Agyei R., Galicia S., et al.. Xrcc4 physically links DNA end processing by polynucleotide kinase to DNA ligation by DNA ligase IV. *EMBO.* 2004;23:3874-3885.

Koonin E.V., Wolf Y.I. and Aravind L.. Protein fold recognition using sequence profiles and its application in structural genomics. *Adv Protein Chem*. 2000;54:245-275.

Krecic A.M. and Swanson M.S.. hnRNP complexes: composition, structure, and function. *Curr Opin Cell Biol*. 1999;11:363-371.

Krishnakumar R. and Kraus W.L.. The PARP side of the nucleus: molecular actions, physiological outcomes, and clinical targets. *Mol Cell*. 2010;39:8-24.

Kwon I., Xiang S., Kato M., et al.. Poly-dipeptides encoded by the C9orf72 repeats bind nucleoli, impede RNA biogenesis, and kill cells. *Science*. 2014;345:1139-1145.

Kzhyshkowska J., Rusch A., Wolf H., et al.. Regulation of transcription by the heterogenous nuclear ribonucleoprotein E1B-AP5 is mediated by complex formation with the novel bromodomain-containing protein BRD7. *Biochem J*. 2001;371:385-393.

Laferrière F. and Polymenidou M.. Advances and challenges in understanding the multifaceted pathogenesis of amyotrophic lateral sclerosis. *Swiss Med Wkly.* 2015;145:w14054.

Lagier-Tourenne C., Polymenidou M., Hutt K.R., et al.. Divergent roles of ALS-linked proteins FUS/TLS and TDP-43 intersect in processing long pre-mRNAs. *Nat Neurosci*. 2012;15:1488-1497.

Lee S.W., Lee M.H., Park J.H., et al.. SUMOylation of hnRNP-K is required for p53-mediated cell-cycle arrest in response to DNA damage. *EMBO*. 2012;31:4441-4452.

Lee Y.B., Chen H.J., Peres J.N., et al.. Hexanucleotide repeats in ALS/FTD form length-dependent RNA foci, sequester RNA binding proteins, and are neurotoxic. *Cell Rep*. 2013;5:11781186.

Leipe D.D., Koonin E.V. and Aravind L.. Evolution and classification of P-loop kinases and related proteins. *J Mol Biol*. 2003;333:781-815.

Lewis T.S., Shapiro P.S. and Ahn N.G. Signal transduction through MAP kinase cascades. *Adv Cancer Res*. 1998;74:49-114.

Li Y.R., King O.D., Shorter J., et al.. Stress granules as crucibles of ALS pathogenesis. *J Cell Biol*. 2013;201:361-372.

Lin Y., Protter D.S., Rosen M.K., et al.. Formation and maturation of phase-separated liquid droplets by RNA-binding proteins. *Mol Cell.* 2015;60:1-12.

Lindahl T. and Barnes D.E.. Repair of endogenous DNA damage. *Cold Spring Harb Symp Quant Biol.* 2000;65:127-133.

Liu R., Althaus J.S., Ellerbrock B. R., et al.. Enhanced oxygen radical production in a transgenic mouse model of familial amyotrophic lateral sclerosis. *Ann Neurol*. 1998;44:763-770.

Loizou J.I., El-Khamisy S.F., Zlatanou A., et al.. The protein kinase CK2 facilitates repair of chromosomal DNA single-strand breaks. *Cell*. 2004;117:17-28.

Lord C.J. and Ashworth A.. The DNA damage response and cancer therapy. *Nature.* 2012;481:287-294.

Lukas J., and Altmeyer M.. A lncRNA to repair DNA. *EMBO Rep*. 2015:e201541309.

Luo Q., Nieves E., Kzhyshkowska J., et al.. Endogenous transforming growth factor-β receptor-mediated Smad signaling complexes analyzed by mass spectrometry. *Mol Cell Proteomics*. 2006;5:1245-1260.

Ma Q.. Role of nrf2 in oxidative stress and toxicity. *Annu Rev Pharmacol Toxicol.* 2013;53:401-426.

Ma X.M., Yoon S.O., Richardson C.J., et al.. SKAR links pre-mRNA splicing to mTOR/S6K1-mediated enhanced translation efficiency of spliced mRNAs. *Cell*. 2008;133:303-313.

Madabhushi P., Pan L. and Tsai L-H.. DNA damage and its links to neurodegeneration. *Neuron*. 2014;83:266-282.

Majounie E., Renton A.E., Mok K., et al. Frequency of the C9orf72 hexanucleotide repeat expansion in patients with amyotrophic lateral sclerosis and frontotemporal dementia: a cross-sectional study. *Lancet Neurol*. 2012;11:323-330.

Maniecka Z. and Polymenidou M.. From nucleation to widespread propagation: A prion-like concept for ALS. *Virus Res*. 2015;ArticleInPress.

Manning G., Whyte D.B., Martinez R., et al.. The protein kinase complement of the human genome. *Science*. 2002;298:1912-1934.

Mao Z., Bozzella M., Seluanov A., et al.. DNA repair by nonhomologous end joining and homologous recombination during cell cycle in human cells. *Cell Cycle*. 2008;7: 2902-2906.

Martin L.J., Liu Z., Chen K., et al.. Motor neuron degeneration in amyotrophic lateral sclerosis mutant superoxidedismutase-1 transgenic mice: mechanisms of mitochondriopathy and cell death. *J Comp Neurol*. 2007;500:20-46.

Masson M., Niedergang C., Schreiber V., et al.. XRCC1 is specifically associated with poly (ADP-ribose) polymerase and negatively regulates its activity following DNA damage. *Mol Cell Biol.* 1998;18:3563-3571.

Mastrocola A.S., Kim S.H., Trinh A.T., et al.. The RNA binding protein Fused In Sarcoma (FUS) functions downstream of PARP in response to DNA damage. *J Biol Chem.* 2013;288:24731-24741.

Matsuoka S., Ballif B.A., Smogorzewska A., et al.. ATM and ATR substrate analysis reveals extensive protein networks responsive to DNA damage. *Science*. 2007;316:1160-6.

Matte A. and Delbaere L.T.J.. ATP-binding motifs. *ELS*. 2010.

Mattick J.S.. Challenging the dogma: the hidden layer of non-protein-coding RNAs in complex organisms. *Bio Essays.* 2003;25:930-939.

Matzuk M.M. and Lamb D.J.. The biology of infertility: research advances and clinical challenges. *Nat Med*. 2008;14:1197-1213.

May S., Hornburg D., Schludi M.H., et al.. C9orf72 FTLD/ALSassociated Gly-Ala dipeptide repeat proteins cause neuronal toxicity and Unc119 sequestration. *Acta Neuropathol.* 2014;128:485-503.

Maynard S., Schurman S.H., Harboe C.. et al.. Base excision repair of oxidative DNA damage and association with cancer and aging. *Carcinogenesis.* 2009;30:2-10.

McKinnon P.J.. DNA repair deficiency and neurological disease. *Nat Rev Neurosci*. 2009;10:100-112.

Meek K., Gupta S., Ramsden D.A., et al.. The DNA-dependent protein kinase: the director at the end. *Immunol Rev*.2004;200:132-141.

Melis J.P.M., van Steeg H. and Luijten M.. Oxidative DNA damage and nucleotide excision repair. *Antioxid Redox Sign*. 2012.

Mimetou E.P. and Symington L.S.. DNA end resection: Many nucleases make light work. *DNA Repair*. 2009;8:983-995.

Mladenov E. and Iliakis G.. Induction and repair of DNA double strand breaks: the increasing spectrum of non-homologous end joining pathways. *Mutat Res-Fund Molecular M.* 2011;711:61-72.

Mori K., Weng S.M., Arzberger T., et al.. The C9orf72 GGGGCC repeat is translated into aggregating dipeptide-repeat proteins in FTLD/ALS. *Science*. 2013;339:1335-1338.

Moumen A., Masterson P., O'Connor M.J., et al.. hnRNP K: An HDM2 target and transcriptional coactivator of p53 in response to DNA damage. *Cell*. 2005;123:1065-1078.

Nam E.A. and Cortez D.. ATR signalling: more than meeting at the fork. *Biochem J.* 2011;436:527-536.

Nelson R., Sawaya M.R., Balbirnie M., et al.. Structure of the cross-β spine of amyloid-like fibrils. *Nature*. 2005;435:773-778.

Nomura T., Watanabe S., Kaneko K., et al.. Intranuclear aggregation of mutant FUS/TLS as a molecular pathomechanism of amyotrophic lateral sclerosis. *J Biol Chem*. 2014;289:1192-1202.

Nonaka T., Masuda-Suzukake M., Arai T., et al.. Prion-like properties of pathological TDP-43 aggregates from diseased brains. *Cell Rep.* 2013;4:124-134.

O'Driscoll M. and Jeggo P.A.. The role of the DNA damage response pathways in brain development and microcephaly: insight from human disorders. *DNA Repair*. 2008;7:1039-1050.

Panier S. and Boulton S.J.. Double-strand break repair: 53BP1 comes into focus. *Nat Rev Mol Cell Biol.* 2014;15:7-18.

Patel A., Lee H.O., Jawerth L., et al.. A liquid-to-solid phase transition of the ALS protein FUS accelerated by disease mutation. *Cell.* 2015;162:1066-1077.

Paull T.T. and Gellert M.. The 3' to 5' exonuclease activity of Mre 11 facilitates repair of DNA double strand breaks. *Mol Cell.* 1998;1:969-979.

Paulsen R.D., Soni D.V., Wollman R., et al.. A genome-wide siRNA screen reveals diverse cellular processes and pathways that mediate genome stability. *Mol Cell*. 2009;35:228-39.

Pecorino L., 2008. Molecular biology of cancer. Mechanisms, targets and therapeutics. Oxford and New York: Oxford University Press. ISBN: 978-0-19-921148-7.

Pollari E., Goldsteins G., Bart G., et al.. The role of oxidative stress in degeneration of the neuromuscular junction in amyotrophic lateral sclerosis. *Front Cell Neurosci*. 2014;8:1-8.

Polo S., Blackford A., Chapman J. et al. Regulation of DNA-end resection by hnRNPU-like proteins promotes DNA double-strand break signaling and repair. *Mol Cell*. 2012;45:1-12.

Polymenidou M., Lagier-Tourenne C., Hutt K.R., et al.. Long pre-mRNA depletion and RNA mis-splicing contribute to neuronal vulnerability from loss of TDP-43. *Nat Neurosci.* 2011;1: 4459-468.

Pratt K.. Interaction properties of hnRNP-U family proteins and SIM:SUMO interaction of the deSUMOylation enzyme SENP7 and the SIMs role in protein functionality. *MRes Diss University of Birmingham*, 2012.

Prudencio M., Hart P.J., Borchelt D.R., et al.. Variation in aggregation propensities among ALS-associated variants of SOD1: correlation to human disease. *Hum Mol Genet.* 2009;18:3217-3226.

Qiu H, Lee S, Shang Y., et al.. ALS-associated mutation FUS-R521C causes DNA damage and RNA splicing defects. *J Clin Invest*. 2014;124:981-99.

Raczynska K.D., Ruepp M.D., Brzek A., et al.. FUS/TLS contributes to replication-dependent histone gene expression by interaction with U7 snRNPs and histone-specific transcription factors. *Nucleic Acids Res*. 2015:gkv794.

Ramakrishnan C., Dani V.S. and Ramasarma T.. A conformational analysis of Walker motif A [GXXXXGKT (S)] in nucleotide-binding and other proteins. *Protein Eng.* 2002;15:783-798.

Rappsilber J., Ryder U., Lamond A.I., et al.. Large-scale proteomic analysis of the human spliceosome. *Genome Res*. 2002;12:1231-1245.

Reaume A.G., Elliott J.L., Hoffman E.K., et al.. Motor neurons in Cu/Zn superoxide dismutase-deficient mice develop normally but exhibit enhanced cell death after axonal injury. *Nat Genet*. 1996;13:43-47.

Reddy K., Schmidt M.H.M., Geist J.M., et al.. Processing of double-R loops in (CAG)·(CTG) and C9orf72 (GGGGCC)·(GGCCCC) repeats causes instability. *Nucleic Acids Res*. 2014;42:10473-10487.

Renton A.E., Chio A. and Traynor B.J.. State of play in amyotrophic lateral sclerosis genetics. *Nat Neurosci*. 2014;17:17-23.

Reinhardt H.C. and Yaffe M.B.. Kinases that control the cell cycle in response to DNA damage: Chk1, Chk2, and MK2. *Curr Opin Cell Biol*. 2009;21:245-255.

Reinhardt H.C., Cannell I.G., Morandell S., et al.. Is post-transcriptional stabilization, splicing and translation of selective mRNAs a key to the DNA damage response? *Cell Cycle*. 2011;10:23-27.

Ringholz G.M., Appel S.H., Bradshaw M., et al.. Prevalence and patterns of cognitive impairment in sporadic ALS. *Neurology*. 2005;65:586-590.

Robberecht W. and Philips T.. The changing scene of amyotrophic lateral sclerosis. *Nat Rev Neurosci*. 2013;14:248-264.

Rockx D.A., Mason R., van Hoffen A., et al.. UV-induced inhibition of transcription involves repression of transcription initiation and phosphorylation of RNA polymerase II. *Proc Natl Acad Sci USA*. 2000;97:10503-10508.

Rosenfeld J. and Strong M.J.. Challenges in the understanding and treatment of amyotrophic lateral sclerosis/motor neuron disease. *Neurotherapeutics*. 2015;12:317-325.

Rouleau M., Patel A., Hendzel M.J., et al.. PARP inhibition: PARP1 and beyond. *Nat Rev Cancer*. 2010;10:293-301.

Rulten S.L., Rotheray A., Green R.L., et al.. PARP-1 dependent recruitment of the amyotrophic lateral sclerosis-associated protein FUS/TLS to sites of oxidative DNA damage. *Nucleic Acids Res*. 2013, 1–8.

Sartori A.A., Lukas C., Julia Coates J., et al.. Human CtIP promotes DNA end resection. *Nature*. 2007;450:509-515.

Saxena S. and Caroni P.. Selective neuronal vulnerability in neurodegenerative diseases: from stressor thresholds to degeneration. *Neuron*. 2011;71,:35-48.

Schärer O.D.. Nucleotide excision repair in eukaryotes. *CSH Perspect Biol*. 2013;5:a012609.

Schellenberg M.J. and Williams R.S.. DNA end processing by polynucleotide kinase/phosphatase. *Proc Natl Acad Sci USA*. 2011;58:20855-20856.

Segal-Raz H., Mass G., Baranes-Bachar K., et al.. ATM-mediated phosphorylation of polynucleotide kinase/phosphatase is required for effective DNA double-strand break repair. *EMBO Rep.* 2011;12:713-719.

Sharma V., Khurana S., Kubben N., et al.. A BRCA1-interacting lncRNA regulates homologous recombination. *EMBO Rep.* 2015:e201540437.

Shatunov A., Mok K., Newhouse S., et al.. Chromosome 9p21 in sporadic amyotrophic lateral sclerosis in the UK and seven other countries: a genome-wide association study. *Lancet Neurol*. 2010;9:986-994.

Shen J., Gilmore E.C., Marshall C.A., et al.. Mutations in PNKP cause microcephaly, seizures and defects in DNA repair. *Nat Genet.* 2010;42:245249.

Shibata N., Nagai R., Uchida, K., et al.. Morphological evidence for lipid peroxidation and protein glycoxidation in spinal cords from sporadic amyotrophic lateral sclerosis patients. *Brain Res*. 2001;917:97-104.

Shiffman D., Rowland C.M., Louie J.Z., et al.. Gene variants of VAMP8 and HNRPUL1 are associated with early-onset myocardial infarction. *Arterioscler Thromb Vasc Biol*. 2006;26:1613-1618.

Shorter J., and Lindquist S.. Prions as adaptive conduits of memory and inheritance. *Nat Rev Genet*. 2005;6:435-450.

Shrivastav M., De Haro L.P. and Nickoloff J.A.. Regulation of DNA double-strand break repair pathway choice. *Cell Res.* 2008;18:134-147.

Shuck S.C., Short E.A. and Turchi JJ. Eukaryotic nucleotide excision repair: from understanding mechanisms to influencing biology. *Cell Res.* 2008;18:64-72.

Singh R. and Valcárcel J.. Building specificity with nonspecific RNA-binding proteins. *Nat Struct Mol Biol*. 2005;12:645-653.

Sobacchi C., Marrella V., Rucci F., et al.. RAG dependent primary immunodeficiencies. *Hum Mutat*. 2006;27:1174-1184.

Spry M., Scott T., Pierce H., et al.. DNA repair pathways and hereditary cancer susceptibility syndromes. *Front Biosci*. 2007;12:4191-4207.

Sreedharan J., Blair I.P., Tripathi V.B., et al.. TDP-43 mutations in familial and sporadic amyotrophic lateral sclerosis. *Science.* 2008;319:1668-1672.

Steegmaier M., Hoffmann M., Baum A., et al.. BI 2536, a potent and selective inhibitor of polo-like kinase 1, inhibits tumor growth in vivo. *Curr Biol*. 2007;17:316-322.

Stewart G., Maser R.S., Stankovic T., et al.. The DNA double-strand break repair gene hMRE11 is mutated in individuals with an ataxia-telangiectasia-like disorder. *Cell*. 1999;99: 577-587.

Stewart G.S., Panier S., Townsend K., et al.. The RIDDLE syndrome protein mediates a ubiquitin-dependent signaling cascade at sites of DNA damage. *Cell*. 2009;136:420-434.

Stracker T.H. and, Petrini J.H.. The MRE11 complex: starting from the ends. *Nat Rev Mol Cell Biol.* 2011;12:90-103.

Strzelecka M., Trowitzsch S., Weber G., et al.. Coilin-dependent snRNP assembly is essential for zebrafish embryogenesis. *Nat Struct Mol Biol*. 2010;17:403-409.

Su Z., Zhang Y., Gendron T.F., et al.. Discovery of a biomarker and lead small molecules to target r(GGGGCC)-associated defects in c9FTD/ALS. *Neuron*. 2014;83:1043-1050.

Sun Z., Diaz Z., Fang X., et al.. Molecular determinants and genetic modifiers of aggregation and toxicity for the ALS disease protein FUS/TLS. *PLoS Biol*. 2011;9:e1000614

Symington L.S. and Gautier J.. Double-strand break end resection and repair pathway choice. *Annu Rev Genet.* 2011;45:247-271.

Szklarczyk D., Franceschini A., Wyder S., et al.. STRING v10: protein–protein interaction networks, integrated over the tree of life. *Nucleic Acids Res*. 2015;43:447-452.

Talbot K.. Motor neuron disease: the bare essentials. *Pract Neurol.* 2009; 9:303-309.

Thandapani P., O'Connor T.R., Bailey T.L., et al.. Defining the RGG/RG motif. *Mol Cell.* 2013;50:613-623.

Thierry G., Beneteau C., Pichon O., et al.. Molecular characterization of 1q44 microdeletion in 11 patients reveals three candidate genes for intellectual disability and seizures. *Am J Med Genet A*. 2012;158:1633-40.

Tollervey J.R., Curk T., Rogelj B., et al.. Characterizing the RNA targets and position-dependent splicing regulation by TDP-43. *Nat Neurosci*. 2011;14:452-458.

Toombs J.A., McCarty B.R. and Ross E.D.. Compositional determinants of prion formation in yeast. *Mol Cell Biol*. 2010;30:319-332.

Trujillo K.M., Yuan S.S., Lee E.Y., et al.. Nuclease activities in a complex of human recombination and DNA repair factors Rad50, Mre11, and p95. *J Biol Chem.* 1998;273:21447-21450.

van Blitterswijk M., van Es M.A., Hennekam E.A., et al.. Evidence for an oligogenic basis of amyotrophic lateral sclerosis. *Hum Mol Genet.* 2012;21:3776-3784.

van der Net J.B., Janssens A.C.J., Defesche J.C., et al.. Usefulness of genetic polymorphisms and conventional risk factors to predict coronary heart disease in patients with familial hypercholesterolemia. *American J Cardiol*. 2009;103:375-380.

Van Der Net J.B., Oosterveer D.M., Versmissen J., et al.. Replication study of 10 genetic polymorphisms associated with coronary heart disease in a specific high-risk population with familial hypercholesterolemia. *Eur Heart J*. 2008;29:2195-2201.

van Oordt W.V.D.H., Diaz-Meco M.T., Lozano J., et al.. The MKK3/6-p38-signaling cascade alters the subcellular distribution of hnRNP A1 and modulates alternative splicing regulation. *J Cell Biol.* 2000;149:307-316.

Vance C., Al-Chalabi A., Ruddy D., et al.. Familial amyotrophic lateral sclerosis with frontotemporal dementia is linked to a locus on chromosome 9p13.2-21.3. *Brain*. 2006;129:868-876.

Verma A. and Tandan R.. RNA quality control and protein aggregates in amyotrophic lateral sclerosis :A review. *Muscle Nerve.* 2013;47:330-338.

Vichi P., Coin F., Renaud J.P., et al.. Cisplatin- and UV-damaged DNA lure the basal transcription factor TFIID/TBP. *EMBO.* 1997;16:7444-7456.

Voigt A., Herholz D., Fiesel F.C., et al. TDP-43-mediated neuron loss in vivo requires RNA-binding activity. *PLoS ONE*. 2010;5:e12247.

Vucic S., Rothstein J.D., and Kiernan M.C.. Advances in treating amyotrophic lateral sclerosis: insights from pathophysiological studies. *Trends Neurosci.* 2014;37:433-442.

Walker J.E., Saraste M., Runswick M., et al.. Distantly related sequences in the alpha- and beta-subunits of ATP synthase, myosin, kinases and other ATP-requiring enzymes and a common nucleotide binding fold. *EMBO*. 1982;1:945-951.

Waltes R., Kalb R., Gatei M., et al.. Human RAD50 deficiency in a Nijmegen breakage syndrome-like disorder. *Am J Hum Genet*. 2009;84:605-616.

Wang W.Y., Pan L., Su S.C., et al.. Interaction of FUS and HDAC1 regulates DNA damage response and repair in neurons. *Nat Neurosci.* 2013;16:1383-1393.

Warita H., Hayashi T., Murakami T., et al.. Oxidative damage to mitochondrial DNA in spinal motor neurons of transgenic ALS mice. *Brain Res Mol Brain Res.* 2001;89:147-152.

Watson J.D., and Crick F.H.. Molecular structure of nucleic acids; a structure for deoxyribose nucleic acid. *Nature*. 1953;*171*:737-738.

Weber S.C. and Brangwynne C.P.. Getting RNA and protein in phase. *Cell*. 2012;149:1188-1191.

Weinfeld M., Mani R.S., Abdou I., et al.. Tidying up loose ends: the role of Polynucleotide kinase/phosphatase in DNA strand break repair. *Trends Biochem Sci.* 2011;36:262-271.

Wippich F., Bodenmiller B., Trajkovska M.G., et al.. Dual specificity kinase DYRK3 couples stress granule condensation/dissolution to mTORC1 signaling. *Cell*. 2013;152:791-805.

Woo J.S., Imm J.H., Min C.K., et al.. Structural and functional insights into the B30.2/SPRY domain. *EMBO*. 2006;25:1353-1363.

Wu L., Bachrati C.Z., Ou J., et al.. BLAP75/RMI1 promotes the BLM-dependent dissolution of homologous recombination intermediates. *Proc Natl Acad Sci USA*. 2006;103:4068-4073.

Xu Y.F., Gendron T.F., Zhang Y.J., et al.. Wild-type human TDP-43 expression causes TDP-43 phosphorylation, mitochondrial aggregation, motor deficits, and early mortality in transgenic mice. *J Neurosci.* 2010;30:10851-10859.

Yang C. and Carrier F.. The UV-inducible RNA-binding protein A18 (A18 hnRNP) plays a protective role in the genotoxic stress response. *J Biol Chem*. 2001;276:47277-47284.

Yim M.B., Kang J.H., Yim H.S., et al.. A gain of-function of an amyotrophic lateral sclerosis-associated Cu,Zn-superoxide dismutase mutant: an enhancement of free radical formation due to a decrease in Km for hydrogen peroxide. *Proc Natl Acad Sci USA*. 1996;93:5709-5714.

Yun M.H. and Hiom K. CtIP2BRCA1 modulates the choice of DNA double-strand-break repair pathway throughout the cell cycle. *Nature*. 2009;459:460-464.

Zhang S., Schlott B., Gorlach M., et al.. DNA-dependent protein kinase (DNA-PK) phosphorylates nuclear DNA helicase II/RNA helicase A and hnRNP proteins in an RNAdependent manner. *Nucleic Acids Res.* 2004;32:1-10.

Zhu Y., Hu J., Hu Y., et al.. Targeting DNA repair pathways: a novel approach to reduce cancer therapeutic resistance. *Cancer Treat Rev*. 2009;35:590-596.